A NEW METHOD FOR MODELING REINFORCEMENT AND BOND IN FINITE ELEMENT ANALYSIS OF REINFORCED CONCRETE

by

ABDULLAH AHMAD BAJARWAN, B.Sc., M.Sc.

A Doctoral Thesis Submitted in partial fulfilment of the requirements for the award of the Doctor of Philosophy of the Loughborough University of Technology

February, 1989

Declaration

The research in this thesis has not been submitted in support of an application for another degree or qualification at this or another institution of learning.

Acknowledgements

The author would like to express his sincere gratitude to his Supervisor Dr. R. J. Allwood for his friendly guidance, encouragement, and excellent supervision throughout the period of this research, without which this work would have not been possible.

The author would also like to thank his Director of Research Professor L. L. Jones and all members of the Civil Engineering department at Loughborough University of Technology.

SYNOPSIS

In conventional finite element analysis of reinforced concrete the steel bars are normally assumed to lie along the concrete element edges and very often the bond gripping the steel to the concrete is assumed to be infinitely stiff. The first assumption makes it difficult to model all steel bars leading to the inclusion of only a few representative bars. Shear reinforcement is usually ignored. Thin concrete cover also creates difficulty by causing long thin finite elements in that region. The second assumption does not reflect the true behaviour of the system.

In this research a new method for the modelling of steel in reinforced concrete by finite element analysis has been developed which allows all steel reinforcement to be included in the analysis. The method is based on modelling the steel and concrete separately, the two materials being interconnected by the bond forces between them. Thus, bond stiffness is naturally included in the analysis. Such interconnection of steel and concrete is achieved by an interface bond matrix which is derived from the relative displacements between the steel and the concrete at the steel nodes. A linear bond slip relation is assumed for the bond, and a linear stress strain relation is assumed for the concrete and the steel. The work has extended also to nonlinear bond stress-slip relation. Concrete is represented by 8-noded isoparametric quadrilateral elements, and the steel is represented by two noded bar elements. The bond is represented by springs joining each steel node to all 8-concrete nodes.

The solution of the resulting system of equations is achieved in an iterative manner which converges quite rapidly, and which requires less computation than the direct solution needs .

Three types of problems are analysed in two dimension to demonstrate the application of this new method. These are beam, cantilever and pullout problems. The first two, being real problems, demonstrate the ability of the method to handle complex steel arrangements, thin concrete covers and anchorage of steel, while the third problem shows the application of load to the steel rather than to the concrete. Concrete and steel deformations and stresses are calculated at their nodes. Bond stresses are given at all steel nodes. In the nonlinear bond analysis, deterioration of bond will be demonstrated in pullout and pushout tests at high loads.

TABLE OF CONTENTS

LIST OF FIGURES AND FLOWCHARTS

LIST OF TABLES

NOTATION

j	a node on a steel bar
U_{sj}	displacement of node j along the steel bar
U_{cj}	displacement of the concrete at node j in the direction of the steel bar.
u_{cj}	component of U_{cj} in the x-direction.
v_{cj}	component of U_{cj} in the y-direction.
Δ_j	relative displacement at node j.
Ω	bar priemeter.
ø	the angle of the bar to the x-axis.
N	a shape function of the concrete element.
N_{ij}	shape function relating U_{cj} to displacement at element node i.
p_{sj}	the bond force acting on the steel at node j.
p_{cj}	the bond force acting on the concrete at node j.
u_{ei}	concrete displacement in x-direction at element node i.
v_{ei}	concrete displacement in y-direction at element node i.
P_e	the vector of forces equivalent to p_{cj} acting on the nodes of one concrete element.
D_e	the vector of displacements of the nodes of one concrete element.
C_{ej}	the matrix giving U_{cj} in terms of D_e

K_{Be}	The assembled matrix of $C_{ej}^{t}\, b_j\, C_{ej}$ for all steel nodes in a concrete element.
K_{be}	Diagonal matrix of all b in a concrete element.
C_e	The assembled matrix of all C_{ej} in a concrete element.
D_{se}	Vector of steel nodes displacements in a concrete element.
P_{bce}	Bond forces at a concrete element degrees of freedom.
P_{bse}	Bond forces at steel nodes in a concrete element.
P_{bc}	Bond forces at all concrete element degrees of freedom.
P_{bs}	Bond forces at all steel nodes.
D_c	the vector of displacements of all concrete nodes
D_s	the vector of displacements of all steel nodes
P_c	the vector of loads applied to the concrete nodes.
P_s	the vector of loads applied to the steel nodes.
b	the stiffness of a bond spring.
K_b	the diagonal matrix of all b.
R_0	the bond stiffness.
C	the assembled matrix of all C_e
K_B	the assembled matrix of $C_e^{t}\, b\, C_e$ for all bond springs.
K_c	the assembled stiffness matrix for all concrete elements.
K_s	the assembled stiffness matrix for all steel elements.
a_s	cross-sectional area of steel.
l_d	length reqiured for anchorage of reinforcement.

f_{bs}	external force applied to steel to achieve anchorage
f_{bc}	external force applied to concrete to achieve anchorage
β_s	Accelerating factor applied to steel solution in first iterative method.
β_c	Accelerating factor applied to concrete solution in the first iterative method.
κ	A scaling factor applied to initial approximation of concrete solution in the first iterative method.
λ	Tolerance on concrete solution.
α	Damping factor for iterative scheme adopted.
ω	Scaling fator for iterative solution of anchorge.
σ_x	Normal concrete stresss in x direction.
σ_y	Normal concrete stresss in y direction.
τ_{xy}	Concrete shearing stress.
ε_x	Normal concrete strain in x direction.
ε_y	Normal concrete strain in y direction.
ν	Poisson's ratio.
E_c	Elasticity modulus for concrete.
E_s	Elasticity modulus for steel.
q_u	Local ultimate bond stress.
q_0	Initial bond stress due to shrinkage.
μ	Coeffiecient of friction.
P_r	Radial pressure at concrete steel interface.

σ_{rcon}	copressive radial pressure.
σ_{rbar}	Tensile radial pressure due to bar contraction.
σ_t	Concrete stress perpindicular to the bar axis.
Δ_u	Slip at ultimate bond stress.
q	Bond stress.
TDOF	total degrees of freedom.
TDOFC	total degrees of freedom of concrete.
TDOFS	total degrees of freedom of steel.
NCE	Number of concrete elements.

Chapter 1

1. INTRODUCTION

Finite element analysis of reinforced concrete structures has attracted many researchers as can be seen from the large number of published papers in this field. Modelling of concrete behaviour has received considerable attention in these investigations. However some of the important aspects which are necessary for accurate modelling of finite element analysis of reinforced concrete have received less attention and these are :

i) Modelling of bond holding the concrete and steel together is usually ignored in conventional methods by assuming perfect bond between the two materials.

ii) One finite element mesh is used to represent both the concrete and the steel with elements representing the steel at the edges of the concrete elements which leads to concrete elements whose size and shape is set by the geometry of the steel bars and also to the inclusion of only few representative bars in the analysis and not all the reinforcement which is usually present in a real structure.

iii) Modelling of thin concrete cover over reinforcement creates a problem because it influences the mesh representing the concrete.

Bond holding concrete and steel acts in the interface of the two materials. The nature of bond allows a certain "slip" to develop between concrete and steel at their interface before failure of bond occurs. Therefore, including bond stiffness is an essential requirement for an accurate analysis of reinforced concrete.

In finite element analysis of reinforced concrete the mesh used to model structure usually consists of adjacent finite elements representing concrete and steel and are set in a pattern that will reflect the relative location of the concrete and steel in the real structure. Because of the restriction imposed by the conventional method of analysis the finite elements representing the reinforcement bars are placed at the edges of the elements representing the concrete because finite elements representing steel and concrete can not intersect each other. This will result in selecting only a few representative bars. Otherwise, including all bars will result in an immense number of concrete elements. Concrete cover creates another difficulty in representing the finite element mesh for concrete because usually long and thin elements end up in this area leading to elements with aspect ratio 'height/base' much higher (or lower) than one, thus, reducing the accuracy of the solution. The above may be avoided when using finite element analysis with embedded or distributed representation of the steel.

In this research a new method is developed in which the concrete and steel are modelled quite separately. Forces are transferred between the two materials through bond acting at their interface. These forces are calculated using the bond stiffness value obtained from the bond stress-slip curve. Thus bond is included in the analysis. This proposed method of modelling is derived in chapter 3.

The separate analysis of the reinforcement leads to modelling of the reinforcing bars in the absence of the concrete. This will

allow the inclusion of all steel bars regardless of their location or orientation. Also, separate analysis of concrete will eliminate concrete cover problems because the concrete mesh is designed to match the expected stress pattern in the concrete in the absence of the reinforcement.

Further advantages of the method are that loads can be applied to either or both the concrete and the steel, and other details such as anchorage of bars can be modelled.

Efficiency of the method of solution in terms of the number of arithmetic operations required to carry out the solution will be examined since these have a direct influence on the computer time used for the solution. Standard methods of assembling one stiffness matrix for the whole structure and solving it directly may be quite inefficient specially when a large number of reinforcement bars are present. In this thesis a new approach is taken for the solution of the system equilibrium equations. Separate stiffness matrices are assembled. An iterative method of solution is adopted and compared to standard methods.

The aim of this thesis is to describe the development of this new method and to demonstrate its applicability to some real reinforced concrete structures. It is not the intention to present actual studies of the behaviour of the constituent materials of reinforced concrete. Therefore, the approach taken to achieve this is to use the simplest possible constitutive model for concrete and steel which can establish the basic characteristics of each material behaviour. Thus, the model will be described for a linear

elastic stress strain relationship for concrete and a linear elastic relationship for steel. A linear stress-slip relationship for bond is used initially, however, since this research is more concerned with modelling of bond, the model is extended to include a nonlinear bond stress-slip relationship. The method of solution is applicable to any bond model. In this thesis a bond model described by Allwood et al. (1984) is chosen. The selected bond model describes the nonlinear bond stress-slip relationship taking into account lateral pressure between concrete and steel.

A set of real reinforced concrete structures will be analysed by this method to demonstrate its applicability. Solution of plane stress modelling of three types of problems will be presented to illustrate the different advantages of this model. The problems are as follows: a beam problem, cantilever problem and pull-out test problems. Some of these problems will be solved using both linear and nonlinear bond models.

Chapter 2

2. LITERATURE REVIEW

2.1 Introduction

In a reinforced concrete structure the transfer of load between concrete and the reinforcing steel bars depends upon bond holding the two materials together. Experimental studies on bond shows that some "slip" develops in the interface of the two materials before complete failure of bond occurs. Bond stiffness values, obtained from measurements of this "slip" and the associated bond-stress, are to be be included in finite element analysis of reinforced concrete structures. Without representation of bond incorrect results may be obtained e.g. Allwood (1980).

There is a lot of research available on the finite element analysis of reinforced concrete which assumes perfect bond between concrete and steel ignoring the relative displacement between the two materials. The review in this chapter will be concerned with only those studies which include bond stiffness or which allow for bond in other forms. Also, finite element analysis of reinforced concrete with distributed or embedded reinforcement with and without including bond will be reviewed in this chapter.

Other reviews are done later in chapter 5 and include a brief review on nonlinear stress-strain relationship of concrete, a review of experimental work done on bond, and a brief review of nonlinear bond-stress slip relationship.

2.2 Review

2.2.1 Modelling of Bond in Finite Element Analysis

The earliest work done on modelling of bond in finite element analysis of reinforced concrete was that of Ngo and Scordelis (1967). They introduced a linkage element between concrete and steel to represent bond. According to Ngo and Scordelis " The linkage element can be thought of conceptually as consisting of two linear springs parallel to a set of orthogonal axes H and V ", figure (2.1). Also, " The linkage element has no physical dimensions at all and only its mechanical properties are of importance ". Each of the springs is assigned a stiffness value from which the stiffness matrix for the linkage element is obtained. If the springs in the H and V directions have stiffness k_h and k_v respectively then the stress strain relation is given by :

$$\begin{bmatrix} \sigma_h \\ \sigma_v \end{bmatrix} = \begin{bmatrix} K_h & 0 \\ 0 & K_v \end{bmatrix} \cdot \begin{bmatrix} \varepsilon_h \\ \varepsilon_v \end{bmatrix}$$

where. ε_h and ε_v are the relative displacements between points I and J in the H and V directions.

The bond linkage element as applied to the finite element idealisation of a single reinforced concrete beam is shown schematically in Figure (2.2).

The above work of Ngo and Scordelis assumes a linear relationship between bond slip and bond stress. Nilson (1968) pointed out that the relationship between bond stress and bond slip is strictly.

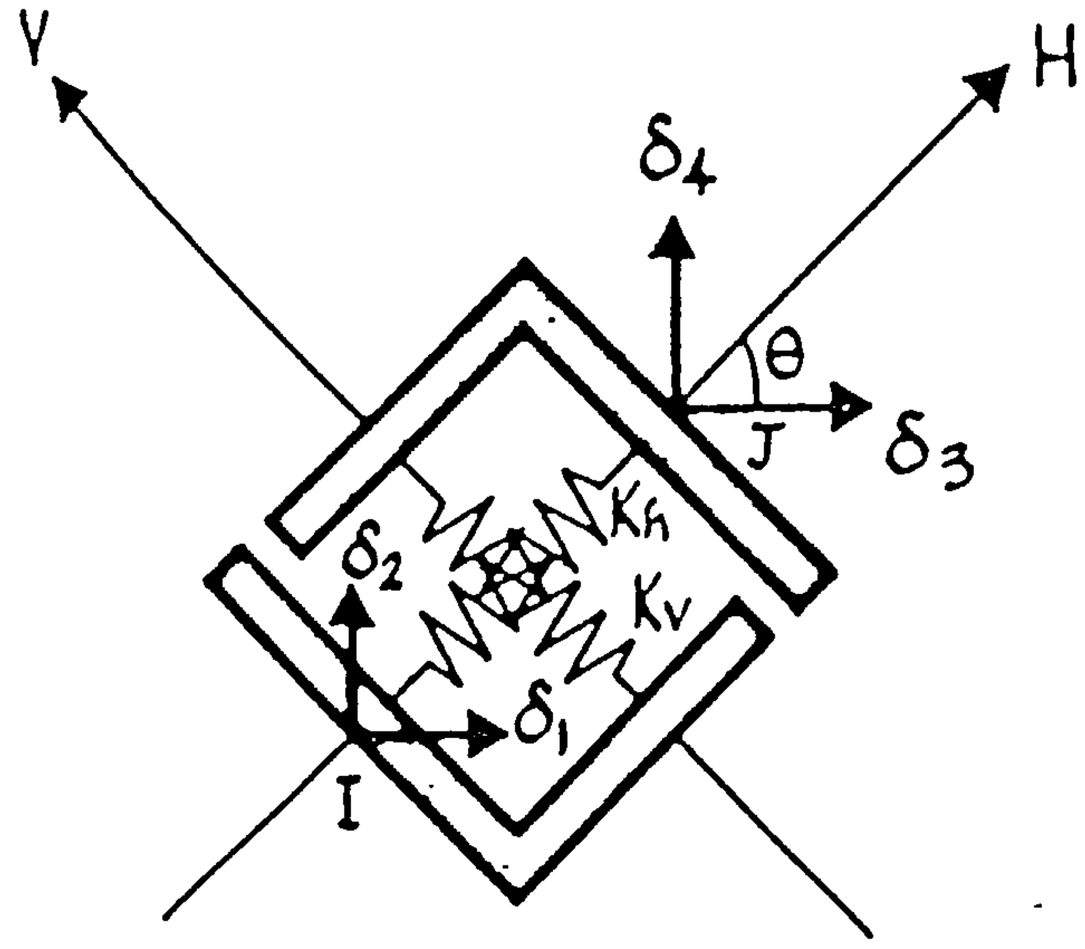

Figure(2.1) - Linkage Element to Represent Bond,
After Ngo and Scordelis (1967)

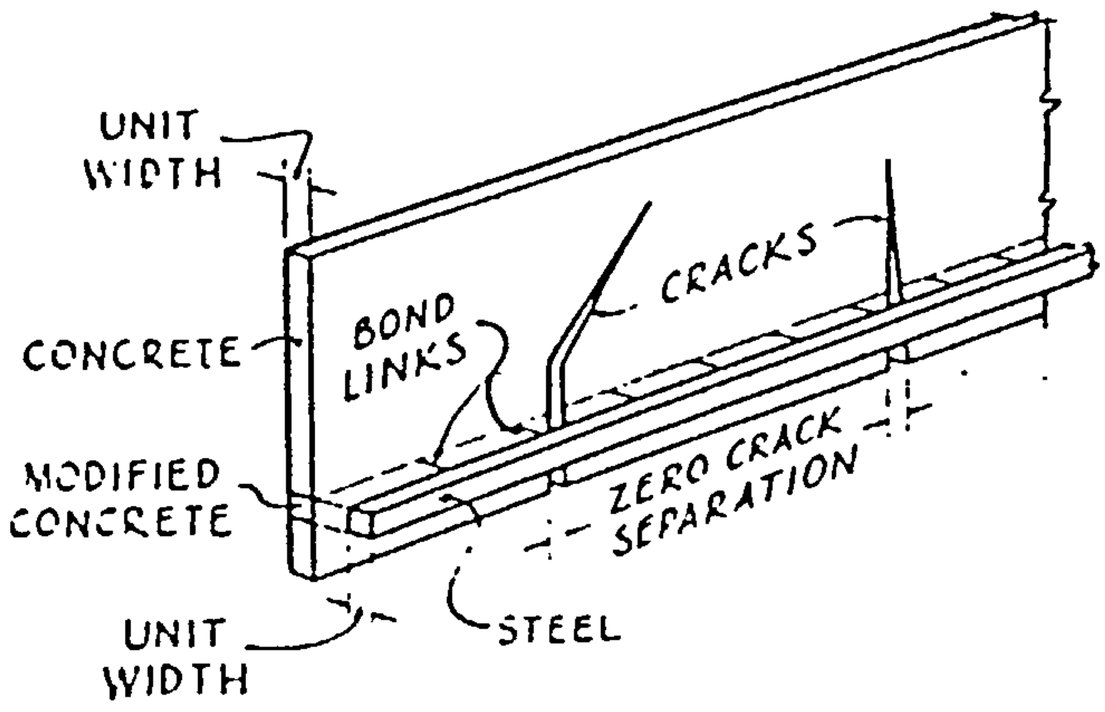

Figure(2.2) - Linkage Element within an Analytical Model,
After Ngo and Scordelis (1967)

nonlinear and that is based on experimental evidence. Thus he introduced a bond-slip equation which is derived indirectly from experiments reported by Bresler and Bertero (1966). Nilson introduced a third order degree polynomial relating local bond stress (μ) to local bond slip (d) which is given as :

$$\mu = 3606 \times 10^3 \, d - 5356 \times 10^6 \, d^2 + 1986 \times 10^9 \, d^3$$

The spring linkage stiffness is found by differentiating μ with respect to the displacement d. The application of the linkage element to a reinforced concrete member is shown in figure (2.3). One linkage element is specified at the top of a bar segment and one at the bottom as shown in figure (2.3).

Using spring linkage elements to represent bond in finite element analysis of reinforced concrete can be found in the work of many authors. Some examples are given now. Robins (1971) used spring linkage elements to simulate bond in the analysis of a reinforced concrete deep beam by finite element method. Labib and Edwards (1978) used a transverse linkage element to simulate bond. Again, spring linkage element is found in the work of Scordelis, Ngo and Franklin (1974). Imbabi and Cope (1984) used a linkage element with stiffness components parallel and normal to the reinforcement bar so as to simulate bond-slip and dowel action. Nagatomo and Kaka (1985) used linkage element to model the relative slippage along rib surface in the finite element study on bond.

Allwood (1980) used the spring connectors to represent bond in

the study of a reinforced concrete beam-column connection. He used nonlinear springs deduced from bond stress-slip relationship obtained from his experimental work. Also, he used nonlinear springs following the relationship from Edwards and Yannopoulus (1978) . For comparison with perfect bond he used also infinitely stiff springs. Figure (2.4) shows stresses in the reinforcement of the beam-column for the different stiffness values.

Allwood, Parsons and Robins (1984) have developed a bond model which allows for the effect of lateral pressures between concrete and steel. These lateral pressures are generated initially by the shrinkage of concrete as it cures but are modified by contraction of the reinforcing bars under load and by the stresses created in the concrete from applied loads also. The model predicts the bond stress-slip behaviour up to and beyond local failure. The basis of the bond model is to extend the concept of a local ultimate bond strength and to create a local bond stress-slip relationship depending on the radial interface pressure. The above model is adopted for the nonlinear bond model of this research and will therefore be explained in greater details later in chapter 5.

The bond element used in the above model of Allwood et al. was developed by Parsons (1984). It is a 6 noded shearing element figure (2.5). Quadratic variation in both the displacements and bond stress-slip moduli is assumed along the length of the element.

Reinhardt Blaauwendraed and Vos (1984) have modelled bond in a numerical way by making use of the shape of the steel bar and the properties of the concrete. They assumed that there is a concrete

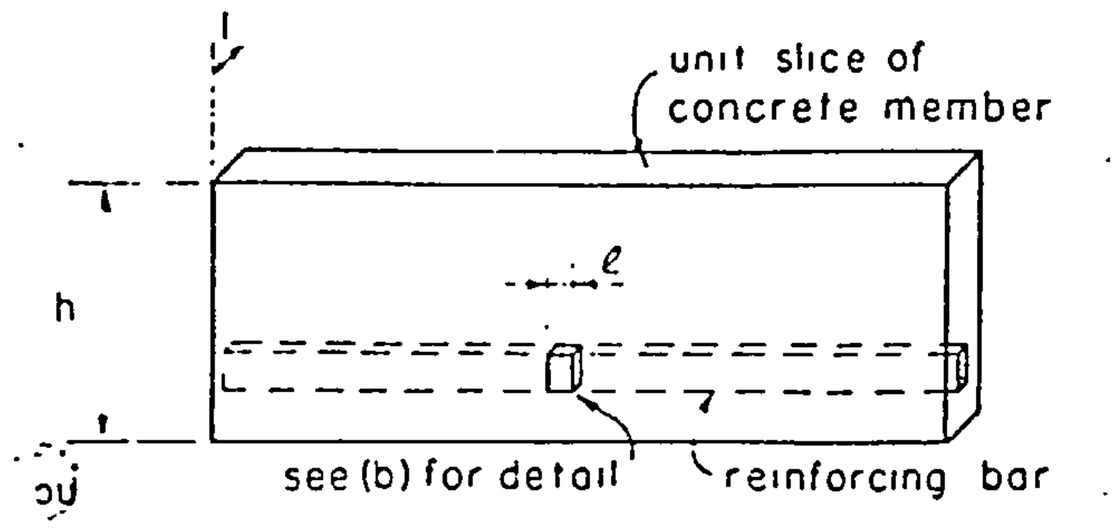

(a) Model of Reinforced .Concrete Member

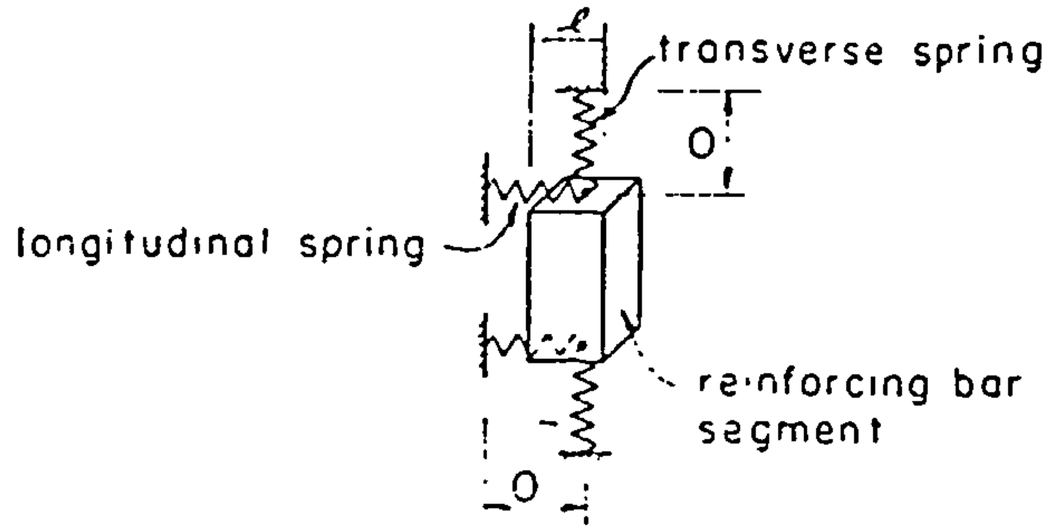

(b) Detail of Bond Linkage

Figure (2.3) - Representation of Bond, After Nilson (1968)

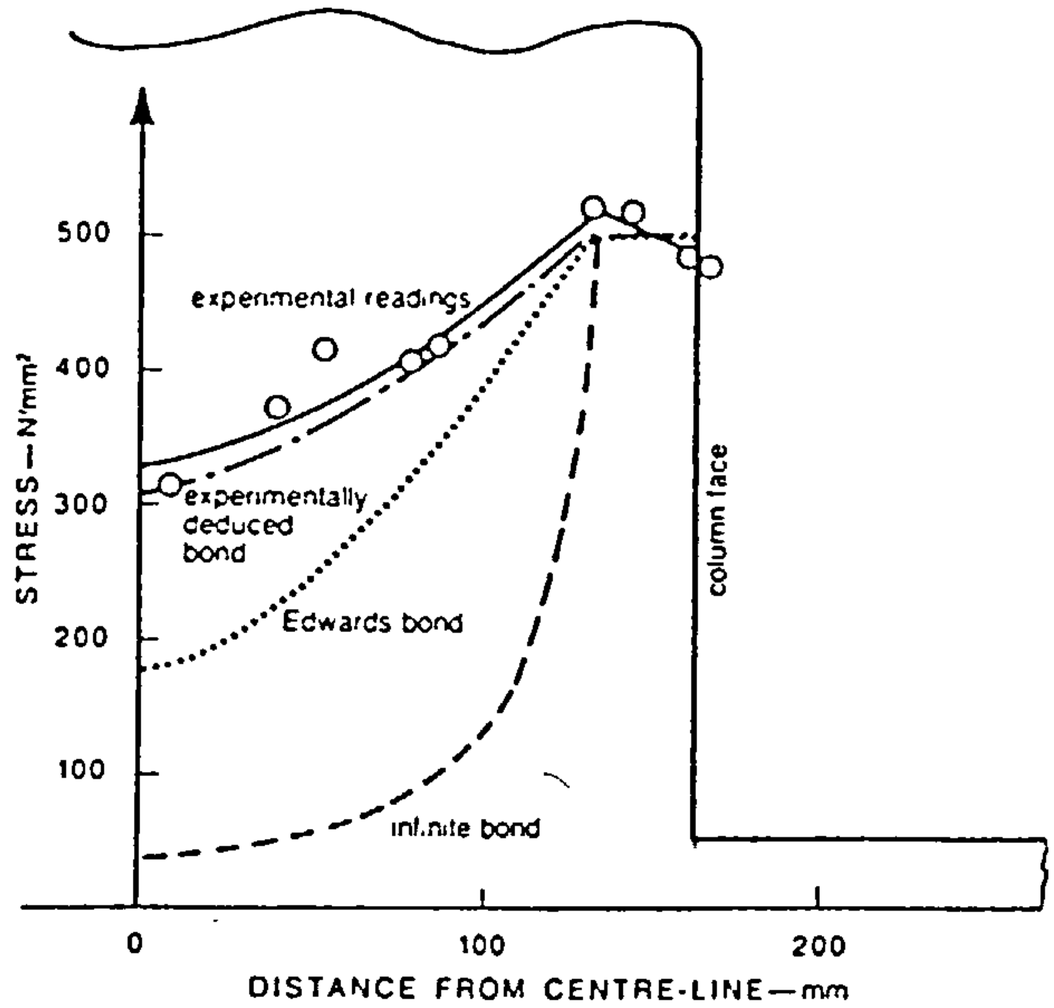

Figure (2.4) - Reinforcement Stresses in a Beam-Column Connection, After Allwood (1980)

layer "slip layer" around the bar which is stressed to a much higher extent than the remaining part of the structure. This layer is treated by non-linear finite element analysis. Figure (2.6) shows a deformed bar with a "slip layer" which is divided into sections according to the rib spacing. Once the behaviour of a slip layer section is known, it can be handled as a single element (interface element) in a finite element mesh with stresses and displacements along the boundary as shown in figure (2.6). The stresses and displacements can be used as input for a linear elastic analysis of the remainder of the concrete part.

Yankelevsky (1985) presented a one dimensional model which is based on equilibrium and a linear bond stress-slip law. An equilibrium between axial force in a bar element and the circumferential shear stress is obtained. Also, by ignoring concrete deformation as compared to steel deformation an equilibrium between steel strain and bond slip can be obtained. The relationship between axial force and slip at the element nodes is expressed through a stiffness matrix.

2.2.2 Modelling with Embedded Reinforcement

Finite element analysis of reinforced concrete with embedded reinforcement is found in the work of Phillips and Zienkiewicz (1976). Isoparametric elements are used to idealize the concrete and special elements embedded in the isoparametric elements are used to simulate the reinforcement. The formulation of the steel

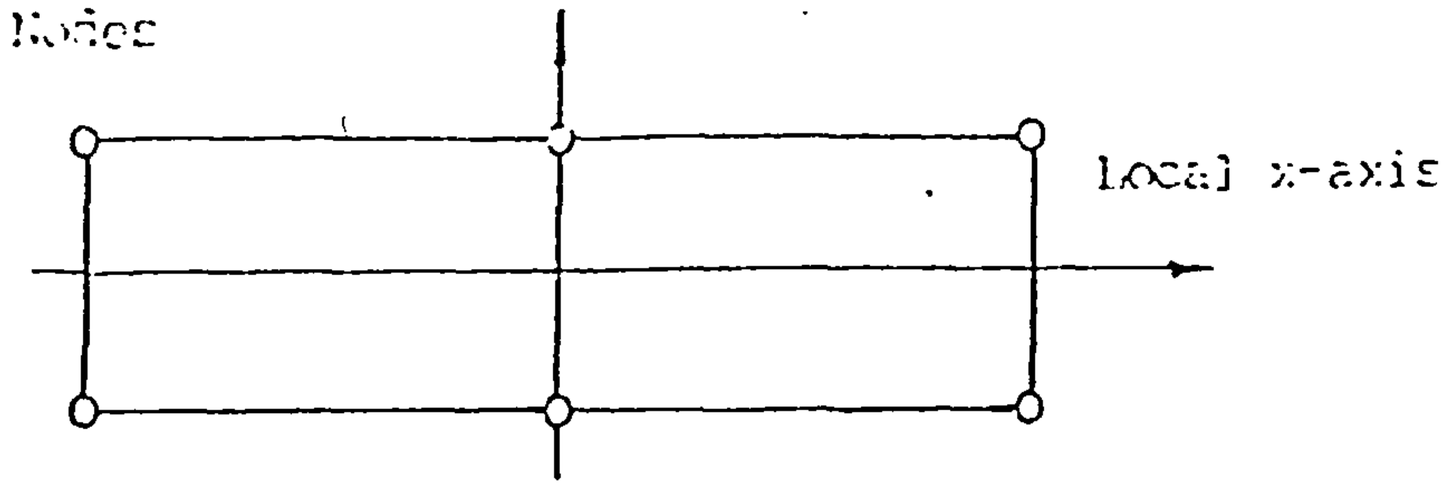

Figure (2.5) - 6 Noded Bond Element.

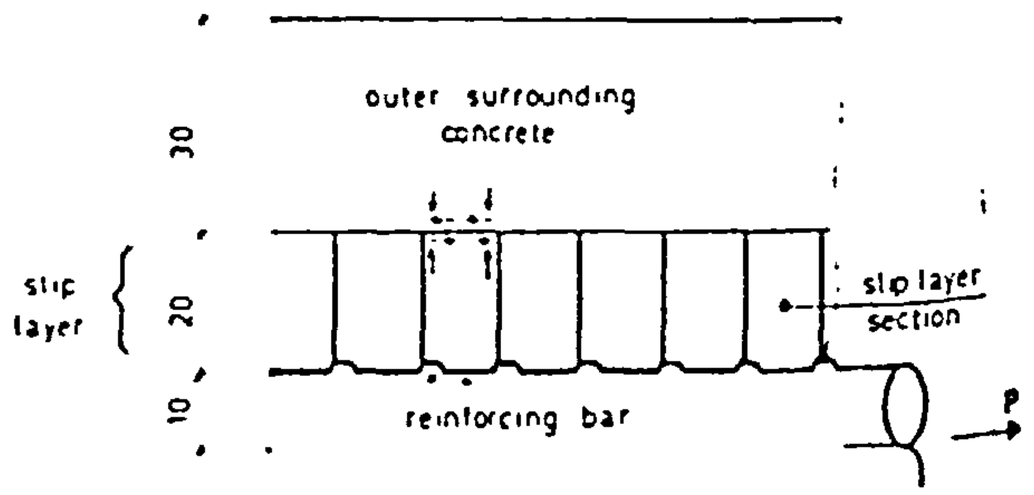

- Axisymmetrix representation of slip layer section approach

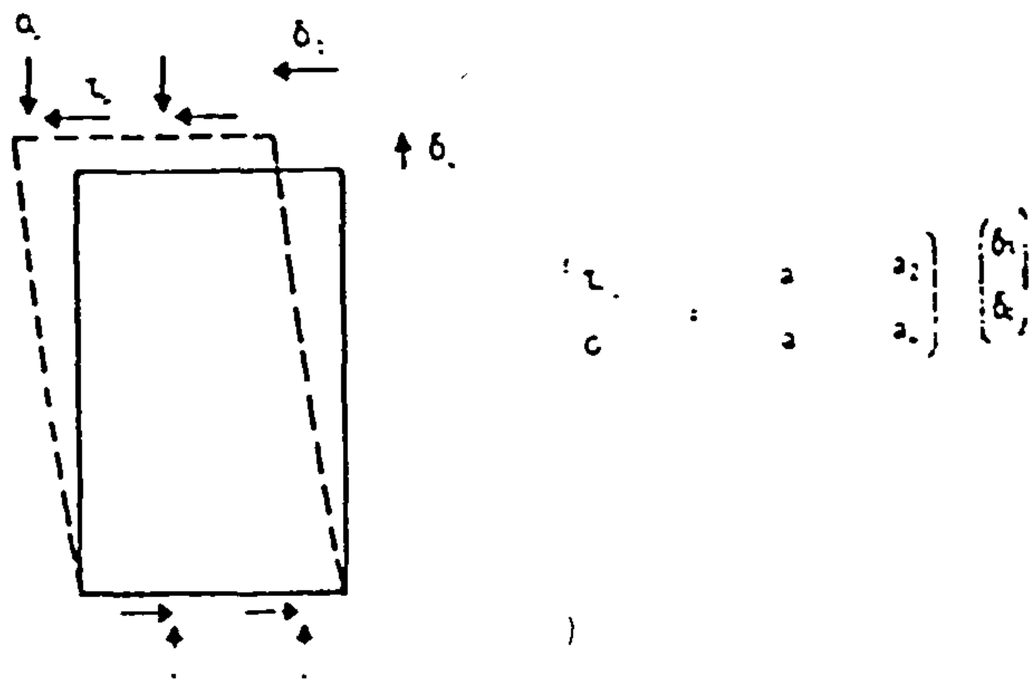

- Constitutive behaviour of a slip layer section for use in finite element programs.

Figure(2.6) - Slip Layer Section For Use in Finite Element Analysis, After Reinhardt et. al. (1984)

elements requires that the strain in the steel is equal to that in the surrounding isoparametric element. Thus perfect bond is assumed. The reinforcing bars are restricted to lie along the local co-ordinate lines of the basic element. The same shape functions are used for the bar as for the main concrete element. The displacements of the bar are obtained from the displacements of the basic element because full compatibility between the bar and the basic element is assumed.

Balkrishnan and Murray (1987) adopted a similar approach in which their embedded representation for reinforcement includes bond slip. A typical finite element of their model is composed of quadratic concrete elements, embedded reinforcing bars, and distributed bond elements selectively placed along the reinforcement. The bond slip at a given point on the steel bar is obtained from the contribution of the bond elements lying within the concrete element. If a number of p bond elements are selected then

$$w_b = \sum H_j U_{bj}$$

where

w_b the bond slip

U_{bj} is the degree of freedom of the p nodes on the reinforcement within the concrete element

H_j are the shape functions used to interpolate the bond slip at any point.

Bond slip at a certain point along the bar is related to the steel

displacement , w_s, and to the concrete displacement, w_c, at that point by the relation

$$w_b = w_s - w_c$$

The stiffness matrix of the concrete element is assembled in the standard manner. The stiffness matrix for the reinforcing element is formed and assembled in the standard manner and added to the stiffness matrix of the concrete element. Finally the stiffness matrix for the bond elements is assembled with the concrete and reinforcement element in the standard manner.

The method presented for the reinforcing element requires that the bar is placed parallel to a local coordinate axis. The bond elements require additional nodal points along the reinforcement. Thus, increasing both the number and the band width of the equations from those for the concrete mesh alone.

2.3 Discussion

From the literature review presented in the previous section it can be seen that the number of papers found on modelling of bond between concrete and steel in finite element analysis of reinforced concrete is quite few.

The review shows that the most common way of representing bond is by using the linkage element. Linkage element can be used to represent bond in the longitudinal direction for example Ngo and Scordelis (1967) or it can be used to represent both longitudinal direction and dowel action for example Imbabi and Cope (1984). The importance of including bond in the analysis and the effect of the stiffness values used in the linkage element has been demonstrated by Allwood (1980) figure (2.4)

Finite element analysis of reinforced concrete with Embedded reinforcement as outlined by Phillips and Zienkiewicz (1976) assumes perfect bond between concrete and steel. Also, the reinforcing bars are assumed to lie along the local coordinate lines of the concrete element so inclined bars to the element axis can not be included.

Balkrishnan and Murray's (1987) approach using embedded reinforcement is similar to Phillips and Zienkiewicz approach but allows for bond. Stiffness matrices for concrete reinforcement and bond elements are assembled in the standard manner. The resulting reinforcement and bond matrices are then added to the concrete matrices as in the conventional manner. This will result

in a consequence increase in the total number of degrees of freedom and band width for the resulting equations. Direct methods of solving a very large global stiffness matrix which usually results for the whole structure is expensive operation from computer point of view.

Another assumption made to simplify the derivation of the stiffness matrices is to place the reinforcing element parallel to the local axis of the concrete element. Thus inclined bars to the concrete element axis can not be included in the analysis.

Chapter 3

3. A NEW METHOD FOR MODELLING OF REINFORCED CONCRETE LINEAR CASE

3.1 Introduction

The purpose of this chapter is to develop the new method for modelling of reinforced concrete by the finite element method which removes some of the constraints imposed by the conventional method of analysis. Some of the difficulties faced when modelling reinforced concrete structures by the conventional method are demonstrated first by the following example.

3.1.1 A Conventional analysis

Figure (3-1) shows a cantilever which is to be analysed by the conventional finite element analysis. The cantilever is composed of two materials, namely concrete and steel. In the conventional analysis of this structure each of the two materials is represented by an appropriate type of finite element. Concrete is represented by 8-noded rectangular plane elements. The steel is represented by 3-noded bar elements to satisfy compatibility between the selected concrete elements and the steel bars elements. In the construction of the mesh two conditions are to be satisfied i) the selected elements and the overall mesh has to reflect the physical shape and the relative location of each material. ii) The elements representing each material can not cross each other so the steel is laid along the edges of the

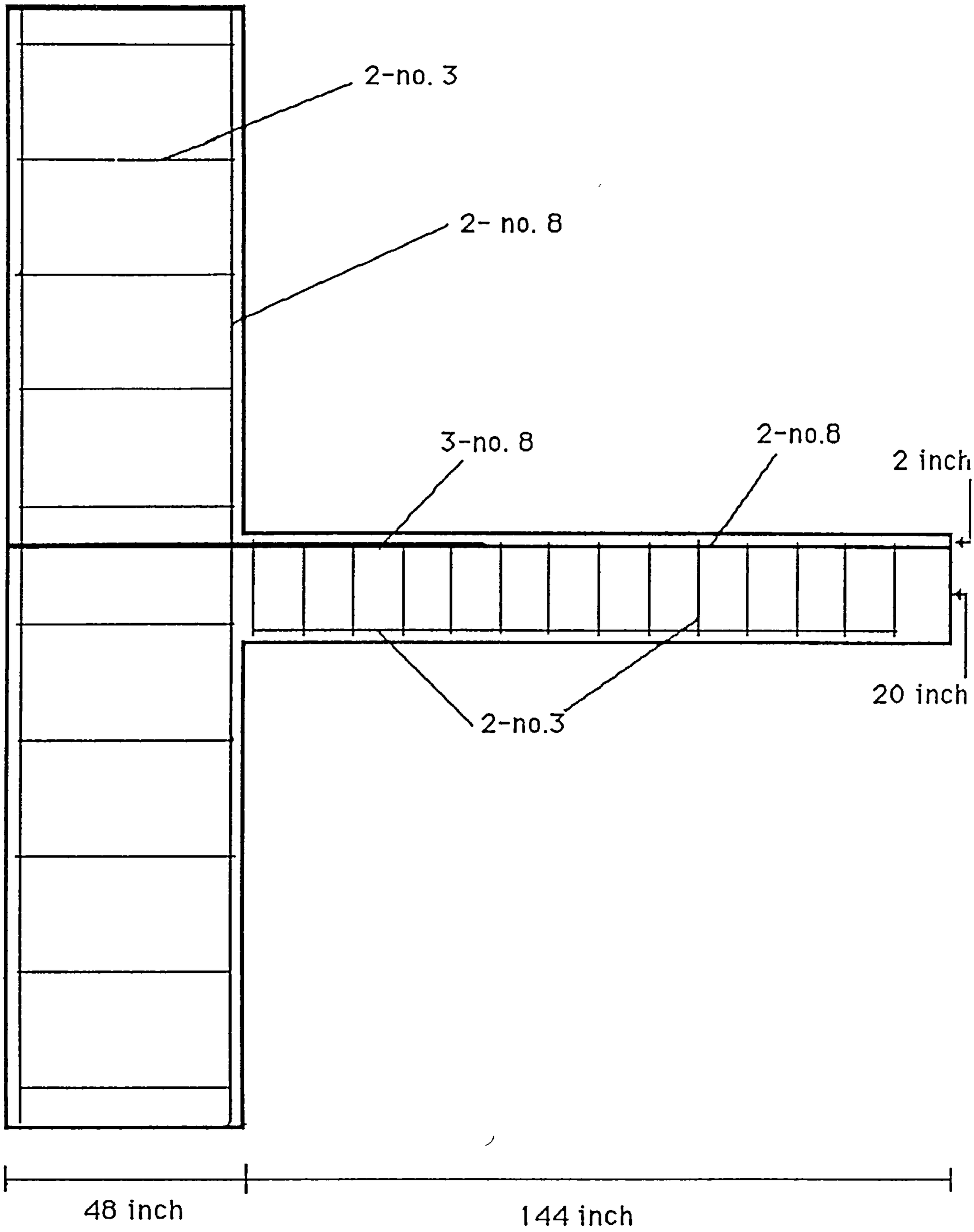

Figure (3.1) - Cantilever showing full detailed reinforcement

concrete elements leading to a mesh consisting of adjacent elements.

It is difficult to construct a mesh that will represent the concrete and all the steel shown in the cantilever of figure (3-1) based on the above conditions, because an immense number of concrete elements are required whose size and shape is set by the geometry of the reinforcement bars rather than by the need to model the stress flows in the concrete. Also it is expensive to solve for a mesh with large number of elements from computer point of view. As a result, the problem is usually simplified by including only the main reinforcements and ignoring the shear and other detailed reinforcement. In this cantilever case the tension reinforcement is the only reinforcement included. So the cantilever in figure (3-2) is now to be analysed instead of the original one. The finite element mesh of figure (3-3) is now constructed to represent the cantilever of figure (3-2).

Another problem arises which is the modelling of the shallow concrete cover on the main steel bars near the concrete surface. The problem faced in this region is the very high aspect ratio of the elements representing concrete. Thus, a finer mesh has to be constructed. Again this will create a similar problem in the concrete elements at the two ends of the column. In order to have elements of acceptable aspect ratio the appropriate mesh for this problem will need a very large number of concrete elements. The solution of the resulting system of equations greatly increase computer time needed to perform the calculations.

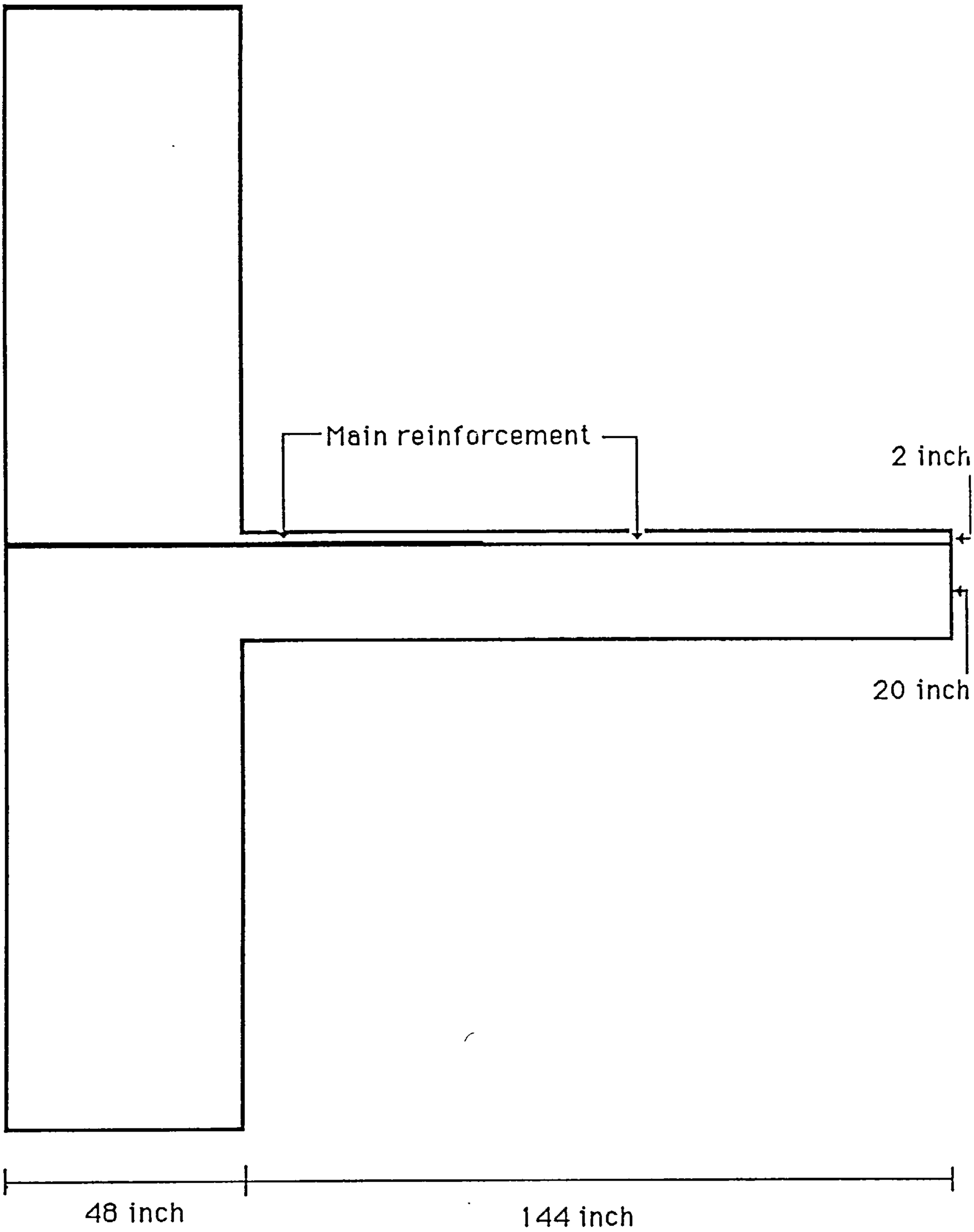

Figure (3.2) - Cantilever of figure (3.1) showing main reinforcement

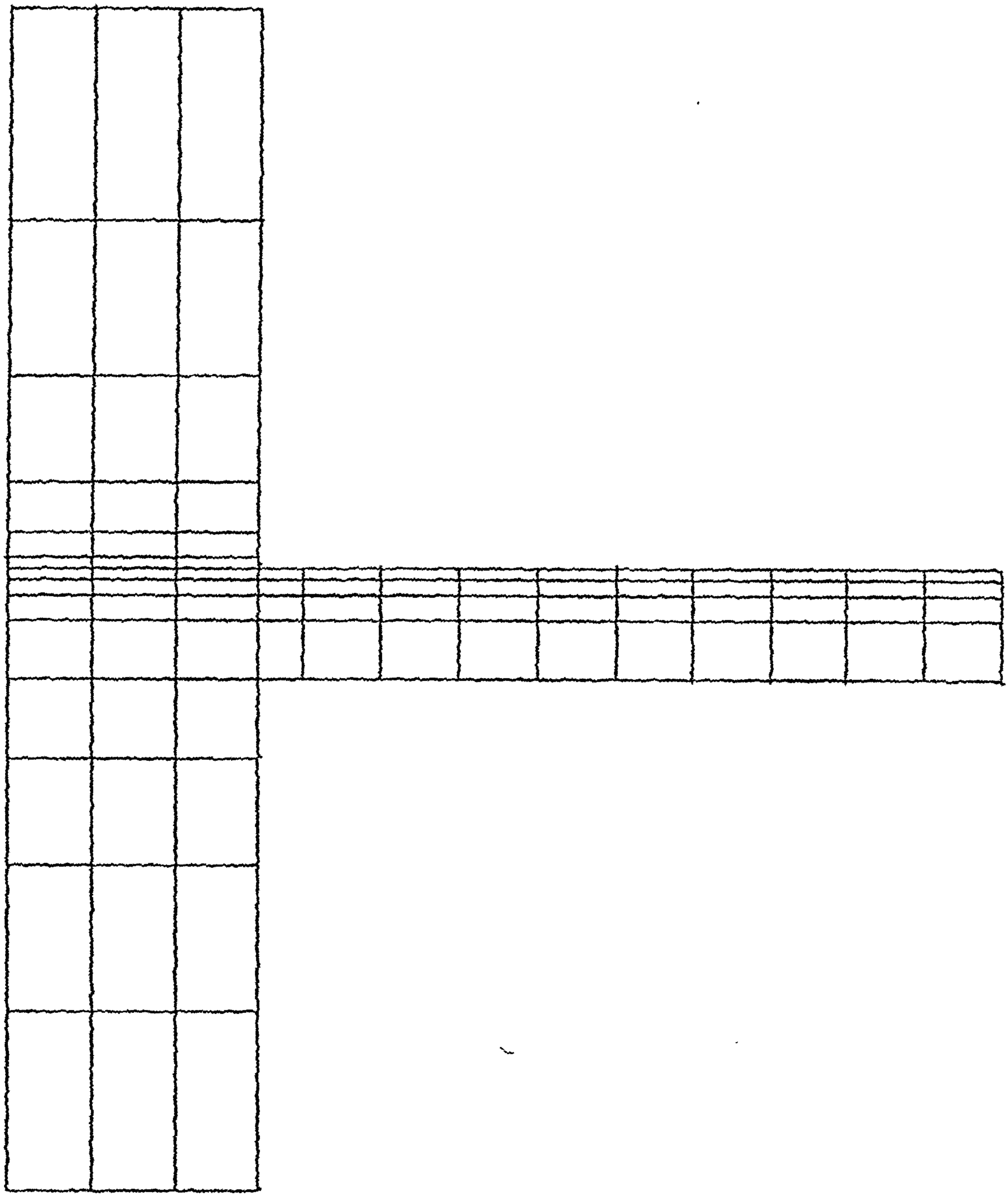

Figure (3.3) - Finite element mesh for the cantilever of figure (3.2) for the conventional method.

The above discussion of the cantilever by the conventional analysis represents only the difficulty involved in constructing the finite element mesh. Another very important point in the conventional method which is often assumed is that the analysis is based on assuming the bond between the steel and the concrete to be infinitely stiff. However, such an assumption does not reflect the true relation between the concrete and the steel. In the analysis of a beam column intersection by the finite element method, Allwood (1980) has shown the important effect on the stress distribution in the main reinforcement within the column when allowing for realistic bond stiffness value versus infinite bond figure (2.4). Thus the modelling of bond must be included for a more realistic analysis.

3.1.2. The new method of analysis

In this chapter a new method will be described for the analysis of reinforced concrete by finite element method and which uses bond between reinforcement and the surrounding concrete as the basis for the development of the theory. The steel and the concrete will each be modelled and analysed separately. Figure (3-4) illustrates the basic idea of separating the concrete and the reinforcement of the structure to be analysed. Such analysis does not require the concrete and the steel to have adjacent elements or common interconnecting nodes. The process of combining these into a mass of reinforced concrete is achieved by interconnecting the two materials through the bond forces acting between them. Thus bond, a basic requirement in reinforced concrete construction, is

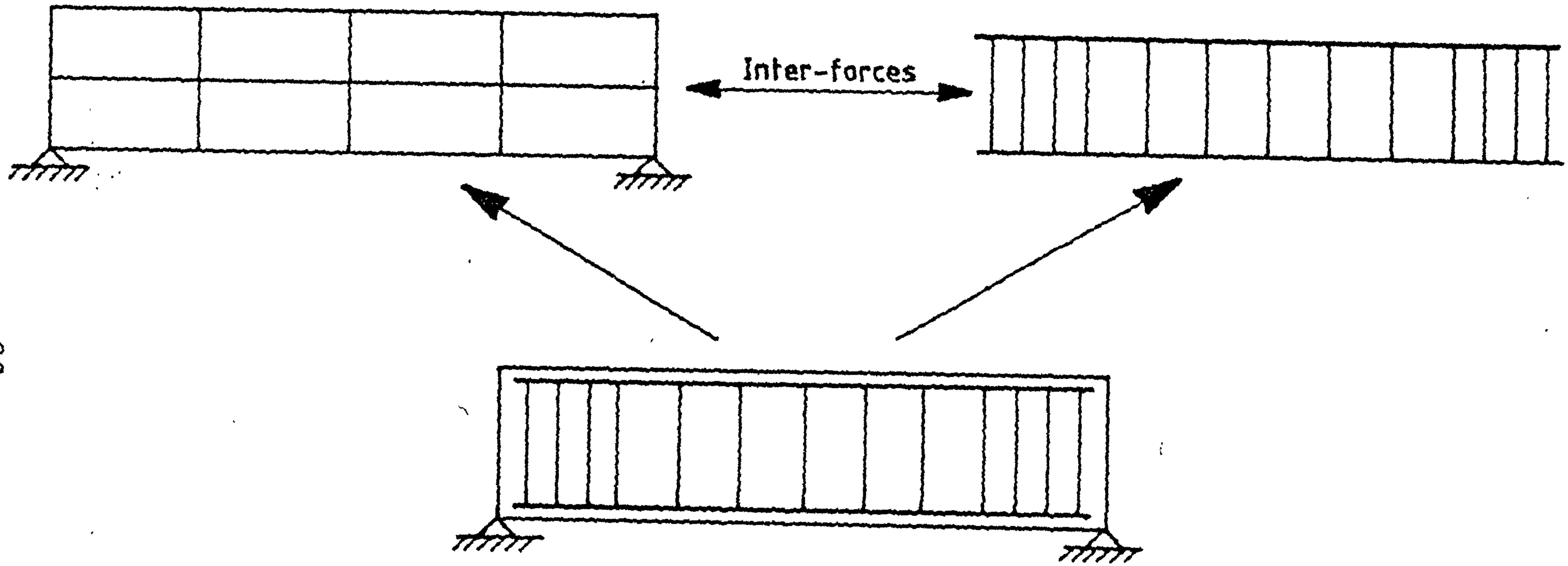

Figure (3.4) - Separate analysis of concrete and steel

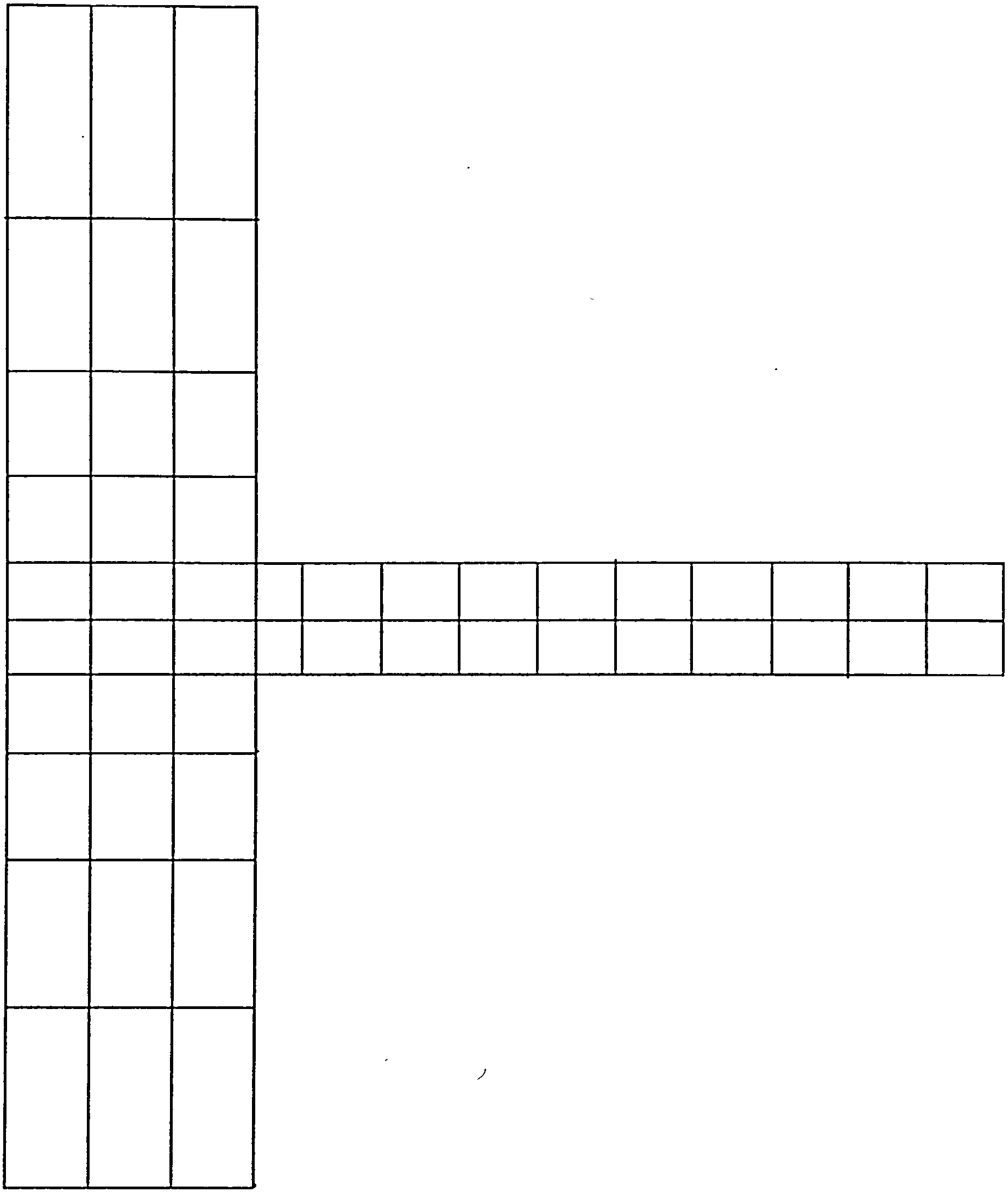

Figure (3.5) - Finite element mesh for the cantilever of figure (3.1) using the new method.

naturally included in the analysis. These bond forces are derived from the relative movement between the steel and the concrete

The analysis of the cantilever in figure (3.1) by this method can be carried out using the simple finite element mesh shown by figure (3.5). The mesh shown only matches the expected concrete stress patterns. Also, all the steel bars shown are included without affecting the concrete mesh and with very little impact on the computer time needed for the solution. Modelling of the concrete cover is no longer a problem. Modelling of bond is also included in the analysis. By this method some of the other details in reinforced concrete design can be achieved such as steel anchorage. In the case of the cantilever the tension steel is to be anchored in the column. It will be shown that steel anchorage can be easily modelled by this method.

In the details of the method given now, linear constitutive equations are assumed for the concrete, steel and bond and the concrete is assumed to carry tension. Although concrete may be represented by any convenient element shape, in the derivation of the method concrete is represented by two dimensional isoparametric quadrilateral elements, and the steel is represented by two noded bar elements. Bond may be conveniently represented here as springs joining the concrete and reinforcement nodes together.

3.2 Theory of the method

3.2.1 General

Consider a steel bar embedded in a mass of concrete as shown in figure (3-6), which may represent a small part of a reinforced concrete structure. Upon loading the structure both the concrete and the steel will experience some deformations although the load is applied to the concrete surface. Therefore, a transfer of forces between the concrete and the steel takes place. This transfer of forces between the concrete and the steel occurs through bond. Bond is the term used to describe the interaction between the embedded bar and the surrounding concrete which takes place in the interface of the two materials.

To model bond in finite element analysis, consider the previous bar of figure (3-6) to be represented by strings of two noded bar elements. Figure (3-6) shows one steel node s_j which is to be closely examined. The same figure also shows a concrete point c_j which is located next to steel node s_j, i.e. both have the same x and y coordinates. Naturally upon loading the structure, both the concrete point and the steel node will deform. The deformation of the concrete point c_j in the direction of the bar axis is given by U_{cj}. The deformation of the steel node s_j along the bar axis is given by U_{sj}. The relation between the two deformations can be classified into two types according to the bond phenomena between the concrete and the steel :

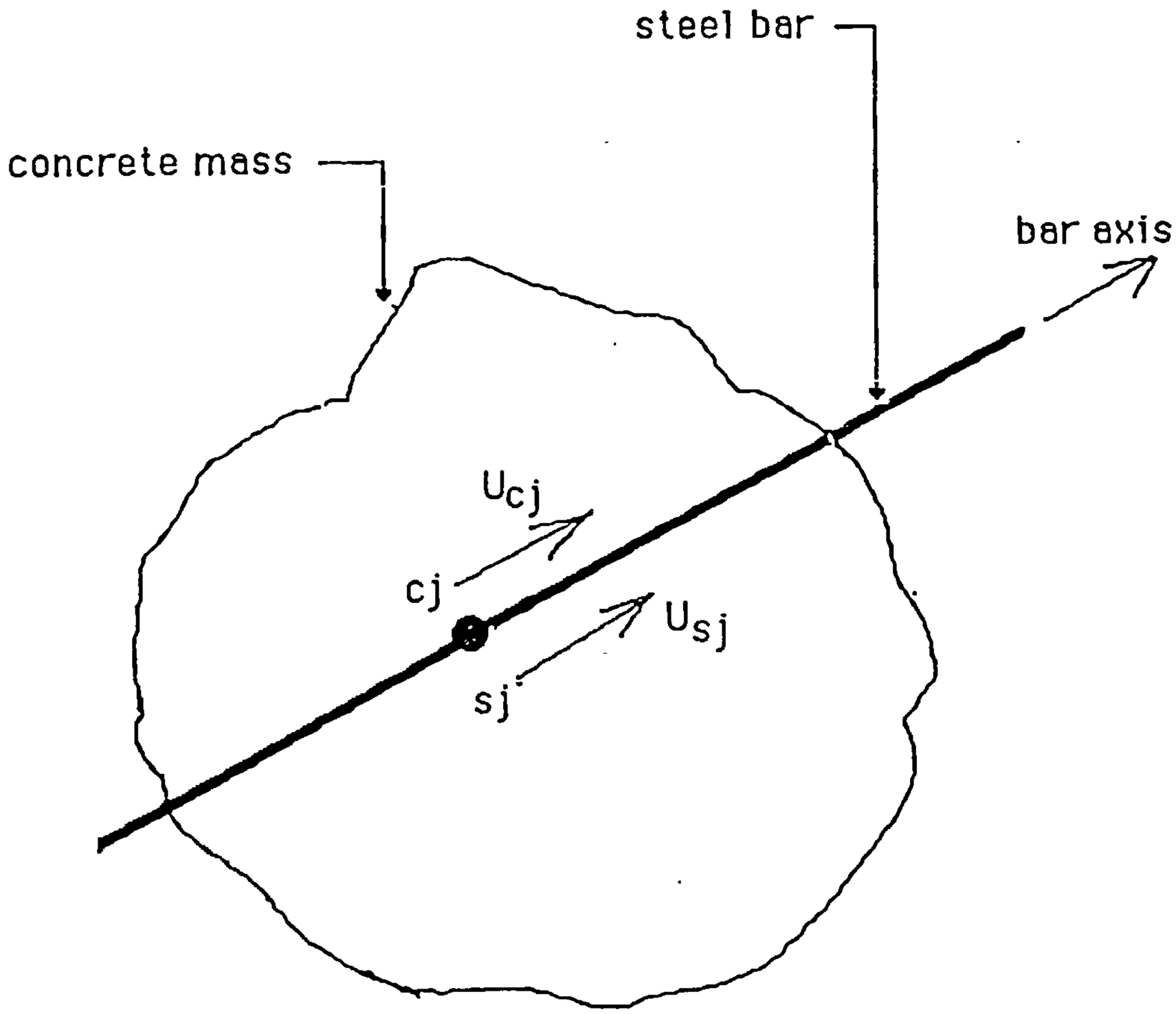

Figure (3.6) - Displacement of a steel node with respect to the surrounding concrete.

i) If the concrete and the steel are perfectly bonded together then the two deformations U_{cj} and U_{sj} are identical, or

$$U_{cj} - U_{sj} = 0 \qquad (3\text{-}1)$$

ii) If the bond between the concrete and the steel is not perfectly connecting the two materials i.e. bond allows for a "special" relation to exist between the concrete and the steel other than perfect bond of the two materials, then the concrete point deformation U_{cj} is different from the steel node deformation U_{sj}, leading to the following relation

$$U_{cj} - U_{sj} = \Delta_j \qquad (3\text{-}2)$$

where Δ_j is the relative displacement along the bar axis of the steel node sj with respect to the surrounding concrete which develops before failure of bond occurs. Δ is known as "slip". Thus the slip which is being included here in the theory is the recoverable slip not the permanent slip associated with the failure of bond near cracks as might be defined normally.

It is easier to model reinforced concrete based on equation (3-1) since modelling of bond is not required. However, since laboratory experiments (see chapter 5) have shown different deformations between concrete and steel, then equation (3-2) is valid. So a more realistic modelling of reinforced concrete should include bond. One of the difficulties faced in exact modelling of bond arises from the lack of complete understanding of the bond phenomena in transmitting forces between concrete and steel.

However bond behaviour can be closely modelled based on the bond stress slip obtained from experimental measurements (see section 5.4.2)

3.2.2 The bond spring

In this research bond modelling depends on the relative displacement Δ along the bar axis between concrete and steel given by equation (3-2).

The concrete point c_j and the steel node s_j are assumed to be connected by a linear spring. The spring has no physical dimensions but it has material properties described by its stiffness. The spring stiffness will be included in the analysis of reinforced concrete to transfer forces from concrete to steel or from steel to concrete. Modelling of bond by springs, or "bond springs", will not change the geometry of the structure since it does not have any physical dimensions. The bond spring is assumed to act only along the axis of the reinforcement so it idealizes longitudinal interaction between the bar and the surrounding concrete.

Bond is assumed to act at the whole surface area of the steel. For the derivation of the finite element analysis every bond spring will cover an area equal to one bar element interface area and its point of action is at the centre of the bar element. The steel nodes are chosen to represent the point of action of the bond springs.

3.2.3 Bond matrix at a steel node

If the reinforcement bar is divided into a number of elements equal to n, then, this results in n+1 steel nodes. Therefore, n+1 bond springs exist along the bar. Since steel nodes represent the point of action of bond springs then each spring will be effective over the interface area of one bar element which extends from one half the element on the left of the steel node to one half the element on the right of the node. Springs at the ends of the bar are effective for one half bar element, either to the right or to the left of the steel node. Therefore, the stiffness of one bond spring can be calculated as follows

$$b = R_0 \cdot \Omega \cdot 1/2 \sum \text{adjacent bar elements lengths} \qquad (3\text{-}3a)$$

where

b is the bond spring stiffness which expresses the stiffness of the bond over an area of one bar element and lumped at the steel node.

R_0 is the bond stiffness. This value is obtained from the initial tangent of the bond stress-slip curve. R_0 is further discussed in sections (5.4.2) and (5.4.3).

Ω is the perimeter of the bar

Consider again the steel node s_j. The bond force acting on the steel at the steel node s_j is given by p_{sj} and is calculated from the bond stiffness, R_0, and the relative displacement of the steel node with respect to the surrounding concrete point cj. p_{sj}

represents the bond force for one half the bar element to the left of the steel node and one half the bar element to the right of the steel node and by assuming ~~the~~ that the bar elements for the same bar are of equal lengths the following is obtained :

$$p_{sj} = \int_{-s/2}^{s/2} R_0 \,.\, \Omega \,.\, (U_{sj} - U_{cj})\, dx \qquad (3\text{-}3b)$$

where

s is the length of one bar element

$(U_{sj} - U_{cj})$ at node j is assumed to be the average value over the integral length leading to :

$$p_{sj} = R_0 \,.\, \Omega \,.\, s \,.\, (U_{sj} - U_{cj})$$

or $$p_{sj} = b \,.\, (U_{sj} - U_{cj})$$

Further, to go by the definition of Δ in equation (3-2) this can be rewritten as

$$p_{sj} = -b \,.\, (U_{cj} - U_{sj}) \qquad (3\text{-}4a)$$

To establish equilibrium with the surrounding concrete an opposite force in direction and equal in magnitude given by p_{cj} is to be acting on the surrounding concrete at the point c_j . This leads to

$$p_{cj} = b \,.\, (U_{cj} - U_{sj}) \qquad (3\text{-}4b)$$

Equations (3-4a) and (3-4b) can be expressed in matrix form leading to

$$\begin{bmatrix} b & -b \\ -b & b \end{bmatrix} \cdot \begin{bmatrix} U_{cj} \\ U_{sj} \end{bmatrix} = \begin{bmatrix} p_{cj} \\ p_{sj} \end{bmatrix} \qquad (3\text{-}5)$$

The stiffness matrix of equation (3-5) is the bond matrix describing the relation between one steel node and the surrounding concrete in the longitudinal direction of the reinforcement.

3.2.4 Transformation of bond matrix

3.2.4.1 General

In the previous section the bond interface matrix relating one steel node to one concrete point, which represents the surrounding concrete was derived. Since in the analysis of concrete by finite element method concrete is usually represented by elements of triangular or quadrilateral shapes, then the steel node s_j is to be related to concrete element nodes rather than the concrete point c_j.

Although the method applies for any element shape, quadrilateral concrete element will be used to illustrate the method. , The concrete is assumed to be represented by 8-noded, plane, quadrilateral, isoparametric element. The choice of this element will lead to quadratic shape functions describing the concrete displacement variation over the element and the element boundaries and so relating generic displacements within the element to nodal displacements of the element.

3.2.4.2 Transformation of displacements

Consider the previous concrete point cj to be located within the boundary of an isoparametric quadrilateral plane element figure (3.7). The displacement of this point in the x axis direction is given by u_{cj} and its displacement in the y axis direction is given by v_{cj}. So U_{cj} is a vector given by

$$[U_{cj}] = \begin{bmatrix} u_{cj} \\ \\ \\ v_{cj} \end{bmatrix}$$

Further U_{cj} can be related to the nodal displacements through the shape function $[N]$ see Zienkiewicz (1985)

$$U_{cj} = [N] \cdot [D_e] \qquad (3.6)$$

From the above two equations the following is obtained

$$[U_{cj}] = \begin{bmatrix} u_{cj} \\ \\ v_{cj} \end{bmatrix} = \begin{bmatrix} N_{1j} & 0 & N_{2j} & 0 & \ldots\ldots\ldots\ldots N_{8j} & 0 \\ \\ 0 & N_{1j} & 0 & N_{2j} & \ldots\ldots\ldots\ldots 0 & N_{8j} \end{bmatrix} \begin{bmatrix} u_{e1} \\ v_{e1} \\ u_{e2} \\ v_{e2} \\ . \\ . \\ . \\ u_{e8} \\ v_{e8} \end{bmatrix} \qquad (3\text{-}7)$$

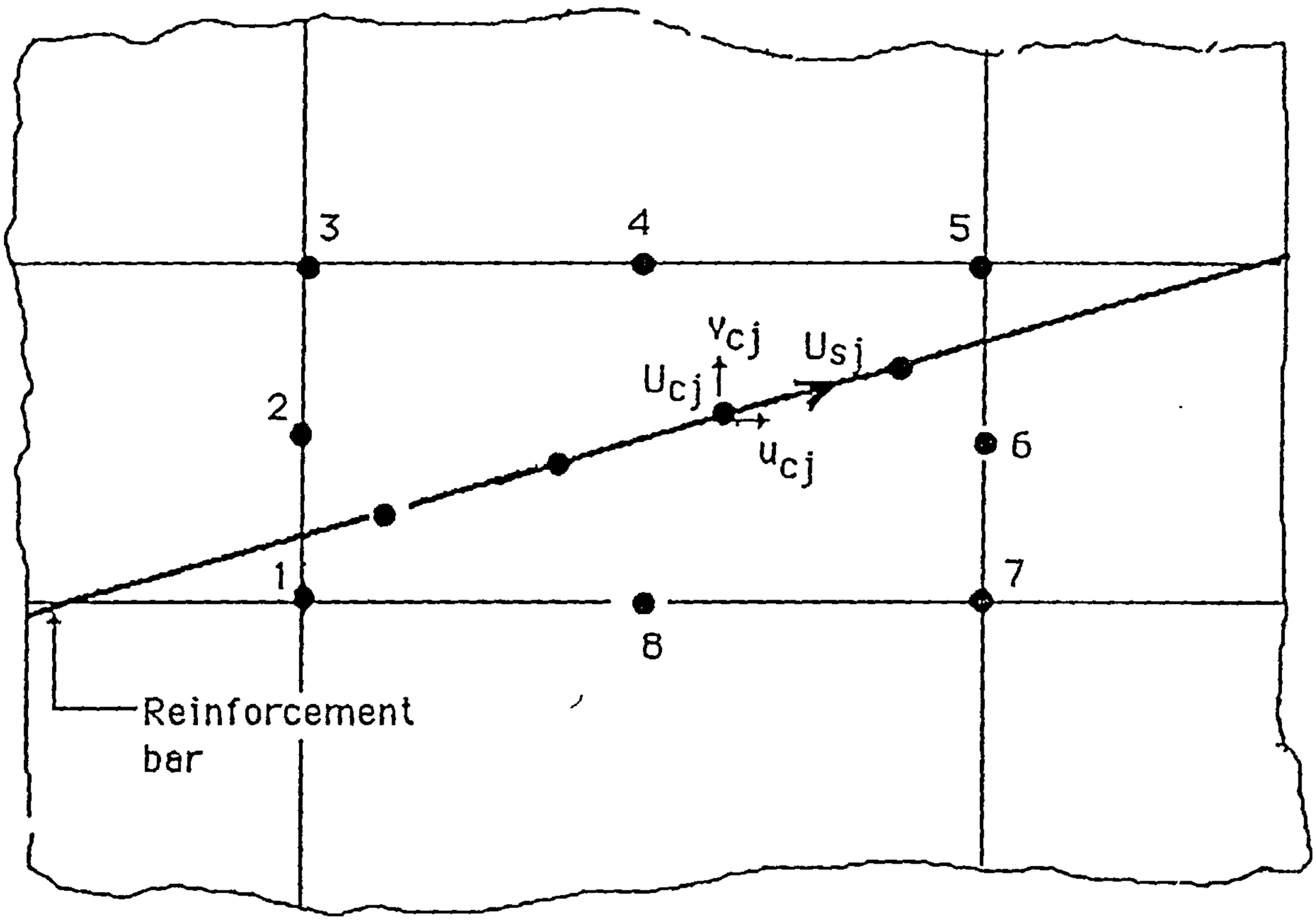

Figure (3.7) - A reinforcing steel bar crossing 8-noded iso-parametric concrete element

where

N_{ij} is the value of the shape function relating the concrete displacements at point j to concrete displacement at element node i.

u_{ei} is the concrete displacement at element node i in the x direction.

v_{ei} is the concrete displacement at element node i in the y direction.

The vector $[D_e]$ is defined as

$$[D_e] = \begin{bmatrix} u_{e1} \\ v_{e1} \\ u_{e2} \\ . \\ . \\ . \\ u_{e8} \\ v_{e8} \end{bmatrix} \qquad (3\text{-}8)$$

numbers refer to local numbering of the concrete element nodes. Recall that the concrete displacement of point c_j in the direction of the bar axis is given by U_{cj}. Thus if the bar is at angle ø to the local x-axis of the concrete element figure (3-7), then the magnitude of the displacement $[U_{cj}]$ is related to u_{cj} and v_{cj} by the following relation

$$U_{cj} = u_{cj}.\cos\text{ø} + v_{cj}.\sin\text{ø} \qquad (3\text{-}9)$$

Substituting equations (3-7) into equation (3-9)^{a} and re-arranging to obtain

$$[U_{cj}] = [\, N_{1j}.\cos\phi \quad N_{1j}.\sin\phi \quad N_{2j}.\cos\phi \quad \ldots\ldots\ldots\ldots\ldots\ldots] \begin{bmatrix} u_{e1} \\ v_{e1} \\ u_{e2} \\ \cdot \\ \cdot \\ \cdot \\ \cdot \\ \cdot \\ v_{e8} \end{bmatrix} \quad (3\text{-}9)^{b}$$

The matrix $[C_{ej}]$ is defined as

$$[C_{ej}] = [\, N_{1j}.\cos\phi \quad N_{1j}.\sin\phi \quad N_{2j}.\cos\phi \quad . \quad \ldots\ldots\ldots\ldots\ldots\ldots] \qquad (3\text{-}10)$$

Thus $[C_{ej}]$ is the transformation matrix which relates the displacement of the concrete point cj within the concrete element in the direction of the steel bar axis to the element nodal displacements.

Equation (3-9)^{b} can be rewritten in the form

$$U_{cj} = [\, C_{ej} \,] \cdot [D_e] \qquad (3\text{-}11)$$

The above equation transforms the concrete displacement U_{cj} acting at the point cj in the direction of the steel axis to the concrete degrees of freedom.

3.2.4.3 Transformation of bond forces

The deformation of the concrete point cj was related to the concrete element nodes by equation (3-11). In this section the bond force p_{cj} is to be related to the concrete element nodes. This is done using the well known transformation based on the equivalence of work done in either local or global axes. Thus since

$$U_{cj} = [\, C_{ej} \,] \cdot [D_e] \qquad (3\text{-}11)$$

then

$$[P_e] = [C_{ej}]^t \cdot [p_{cj}] \qquad (3\text{-}12)$$

where

$[P_e]$ is the vector of bond forces which is equivalent to p_{cj} and acting on the concrete element nodes.

3.2.4.4 The transformation matrix

In the previous two sections the displacement of the concrete in the direction of the steel axis for point cj which lies within the concrete element was found and expressed by equation (3-11). Also the equivalent nodal forces due to a force acting at the point cj within the concrete element is expressed by equation (3-12). In this section the transformation of the bond matrix given by equation (3-5) will be accomplished.

Substituting equation (3-11) into equation (3-4b) the following is obtained

$$[p_{cj}] = b \cdot ([C_{ej}] \cdot [D_e] - [U_{sj}])$$

By pre-multiplying the above equation by $[C_{ej}]^t$ the following relation is obtained

$$[C_{ej}]^t \cdot [p_{cj}] = [C_{ej}]^t .b. [C_{ej}] \cdot [D_e] - [C_{ej}]^t \cdot b \cdot [U_{sj}] \qquad (3\text{-}13)$$

Now substituting for $[C_{ej}]^t.[p_{cj}]$ from equation (3-12) to get

$$[P_e] = [C_{ej}]^t \cdot b \cdot [C_{ej}] \cdot [D_e] - [C_{ej}]^t \cdot b \cdot [U_{sj}] \qquad (3\text{-}14)$$

Similarly, by substituting equation (3-11) into equation (3-4a) will lead to

$$p_{sj} = -b \cdot ([C_{ej}] \cdot [D_e] - [U_{sj}])$$

or

$$p_{sj} = -b \cdot [C_{ej}] \cdot [D_e] + b \cdot [U_{sj}] \qquad (3\text{-}15)$$

Equations (3-14) and (3-15) can be expressed in matrix form as

$$\begin{bmatrix} [C_{ej}]^t.b.[C_{ej}] & -[C_{ej}]^t.b \\ -b.[C_{ej}] & b \end{bmatrix} \cdot \begin{bmatrix} [D_e] \\ U_{sj} \end{bmatrix} = \begin{bmatrix} [P_e] \\ p_{sj} \end{bmatrix} \qquad (3\text{-}16)$$

Equation (3-16) expresses the (17x17) bond matrix connecting one steel node whose deformation is specified along the bar axis to all degrees of freedom of the concrete element. Figure (3-8) illustrates the springs connecting a steel node to all degrees of freedom for the 8-noded quadrilateral element, implied in the transformations leading to (3-16). Note that in (3-16) U_{sj} and p_{sj} are scalars.

3.2.5 Element bond matrix

In the previous section the bond matrix was derived for one steel node within a quadrilateral concrete element . By applying equation (3-16) to all steel nodes located in the same concrete element, the element bond matrix can be established. This is accomplished by adding the contribution of the bond matrix of each steel node located in the same concrete element . In equation form this is expressed as

$$\begin{bmatrix} [K_{Be}] & -[C_e]^t . [K_{be}] \\ -[K_{be}].[C_e] & [K_{be}] \end{bmatrix} . \begin{bmatrix} [D_e] \\ [D_{se}] \end{bmatrix} = \begin{bmatrix} [P_{bce}] \\ [P_{bse}] \end{bmatrix} \quad (3\text{-}17)$$

where

$[K_{Be}]$ is the sum of the $[C_{ej}]^t.b_j.[C_{ej}]$ of all the steel nodes within the concrete element .

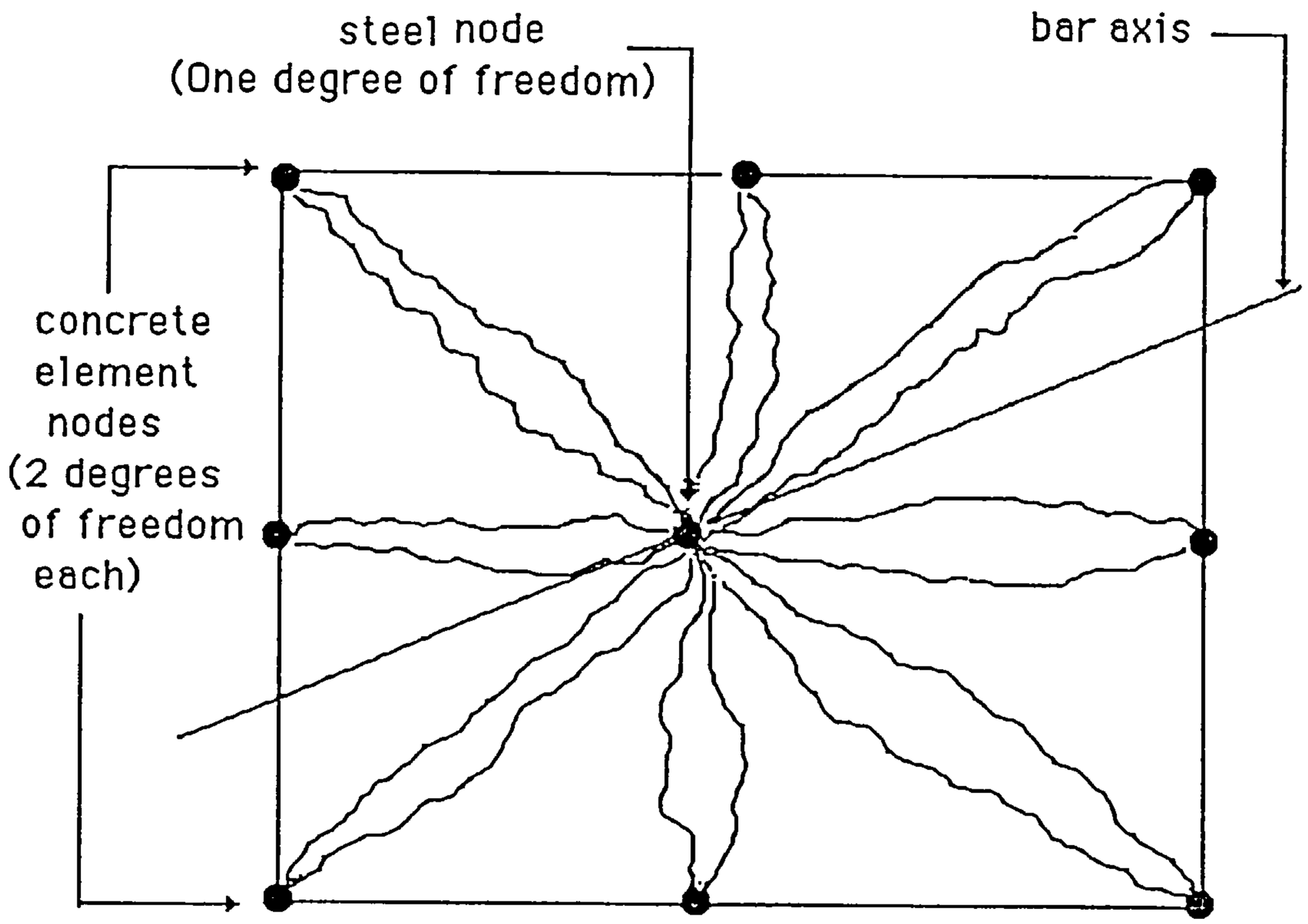

Figure (3.8) - Transformed bond stiffness connecting one steel node to element degrees of freedom.

$$\text{i.e.} \quad [K_{Be}] = \sum [C_{ej}]^t . b_j . [C_{ej}]$$

j= the steel node number

$[K_{be}]$ is a diagonal matrix of b values of the steel nodes within the concrete element

$$[K_{be}] = \begin{bmatrix} b_1 & 0 & \ldots\ldots & 0 \\ 0 & b_2 & \ldots\ldots & 0 \\ \ldots & \ldots & \ldots & \ldots \\ 0 & \ldots\ldots & \ldots\ldots & b_{nse} \end{bmatrix}$$

$[C_e]$ is a matrix containing all $[C_{ej}]$ of the steel nodes within the concrete element

$$\text{i.e.} \quad [C_e] = \begin{bmatrix} C_{e1} \\ C_{e2} \\ . \\ . \\ C_{e\ nse} \end{bmatrix}$$

nse is the number of steel nodes in the concrete element.

$[D_{se}]$ a vector containing displacements of all steel nodes within one concrete element.

$[P_{bce}]$ internal bond forces acting at the concrete element degrees of freedom.

$[P_{bse}]$ internal bond forces acting at the steel nodes within the concrete element.

Example:

Figure (3-9) shows 3 steel nodes lying within a 8-noded quadrilateral concrete element. The selected steel nodes are of different bars. Thus every steel node will have its own spring bond stiffness value b and the angle of inclination of the bar ø of which it is a part . To establish the bond matrix for this concrete element it is first necessary to establish the bond matrix for the first node which will be of the form

$$\begin{bmatrix} [C_{e1}]^t.b_1.[C_{e1}] & -[C_{e1}]^t.b_1 \\ -b_1.[C_{e1}] & b_1 \end{bmatrix} \times \begin{bmatrix} [D_e] \\ U_{s1} \end{bmatrix} = \begin{bmatrix} [P_e] \\ P_{s1} \end{bmatrix} \quad (3\text{-}18)$$

The subscript 1 refers to node number one. The same is carried out for the next two nodes numbers 2 and 3. Once this has been done the element bond matrix is now constructed as shown in figure (3-10).

3.2.6 Global bond matrix

The global bond matrix relating all the reinforcement bars to the concrete is assembled according to the following steps:

i) Divide all steel nodes up into groups, each of which lie over one concrete element.

ii) Construct the bond matrix for every node according to equation (3-16)

iii) Assemble in the element matrix for the node in step 2

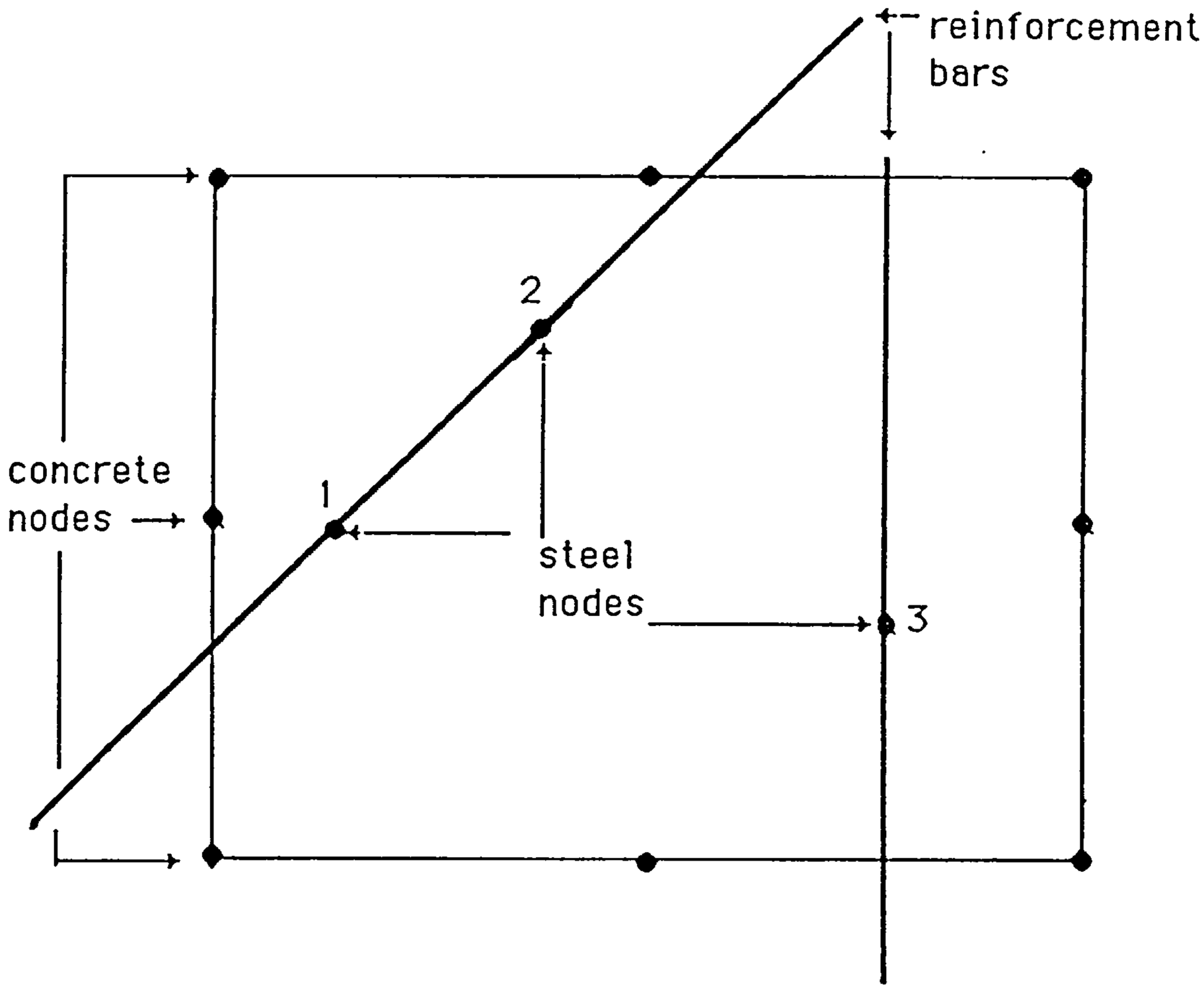

Figure (3-9) - Three steel nodes from two different bars
within 8-noded quadrilateral concrete element.

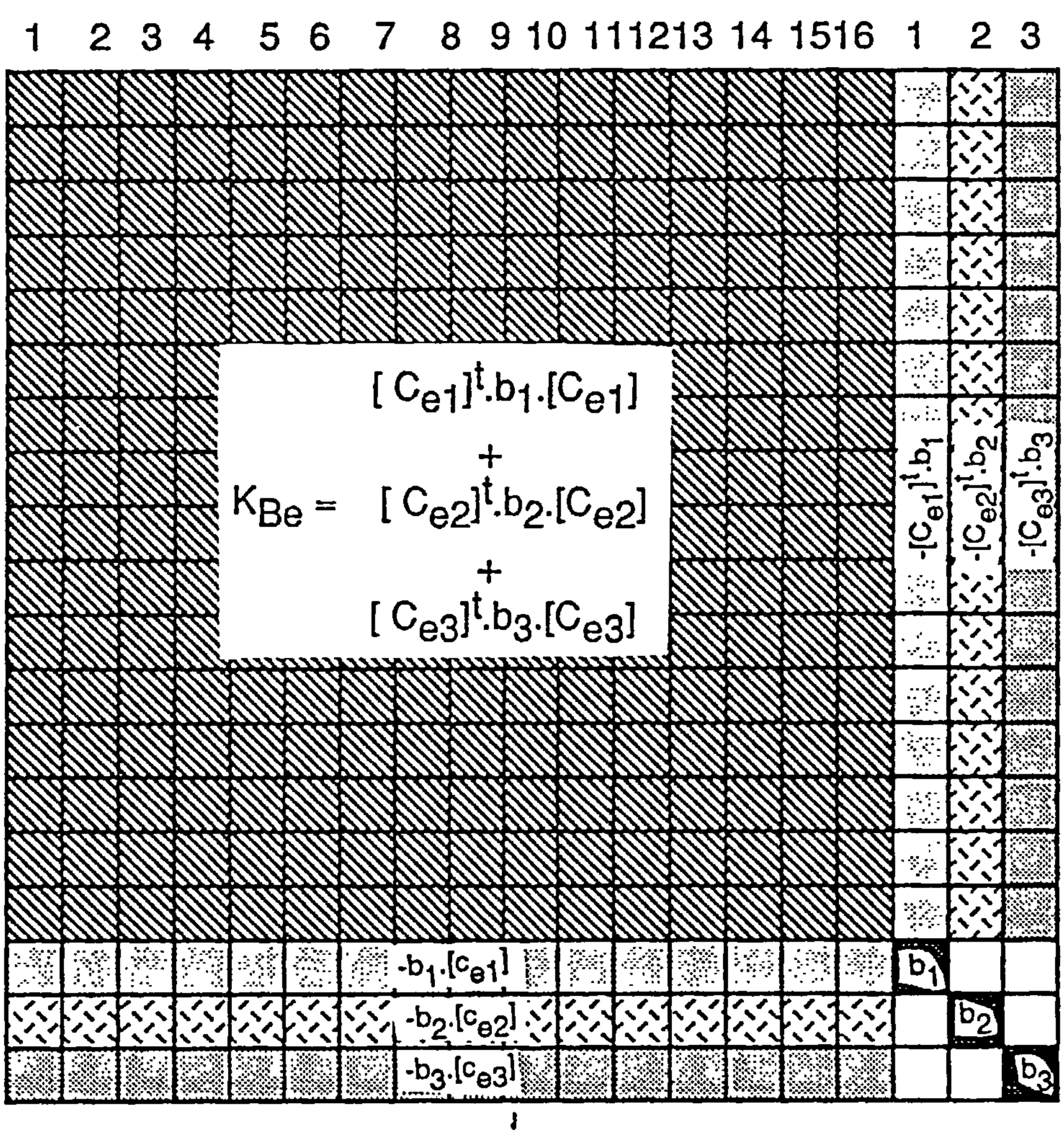

Figure (3-10) Element bond matrix for figure (3-9)

according to equation (3-17)

iv) Repeat step ii and iii for all steel nodes within the same element according to the grouping of step i as illustrated in figure (3-10).

v) assemble the element bond matrix into the global bond matrix. This assembly is achieved by adding the correct element contribution according to the global freedom numbering of the degrees of freedom of the concrete elements and the global numbering of the steel nodes . Once steps ii to iv have been repeated for all concrete elements which have steel nodes within their boundaries, the global bond matrix of all steel nodes can be established . The results can be expressed in matrix form as

$$\begin{bmatrix} [K_B] & -[C]^t.[K_b] \\ -[K_b].[C] & [K_b] \end{bmatrix} \cdot \begin{bmatrix} [D_c] \\ [D_s] \end{bmatrix} = \begin{bmatrix} [P_{bc}] \\ [P_{bs}] \end{bmatrix} \qquad (3\text{-}19)$$

The matrix [K_B] in equation (3-19) is assembled from the [K_{Be}] matrix of all the concrete elements . It is a banded matrix and its band width is controlled by the numbering of the concrete element nodes. Thus it is of the same band width as the concrete stiffness matrix (section (3.3))

The above global displacement vector contains concrete and reinforcement displacements which are separated in two vectors D_c and D_s such that D_c is a vector containing concrete displacements alone and D_s is a vector containing steel displacements alone.

Some short cuts are taken in the program to simplify these steps. For example the global K_B is not assembled instead the K_{Be} matrix for each element is assembled and saved so the calculation is done for one concrete element and its associated steel nodes at a time. This is further explained in chapter 4.

The matrix [K_b] is a diagonal matrix containing the spring stiffness of all the steel nodes in the order of the steel nodes global numbering.

$[D_c]$ is the vector of displacement of all degrees of freedom of concrete

$[D_s]$ is the vector of all steel nodes displacements for all the bars

$[P_{bc}]$ is the vector of all internal bond forces acting at the concrete degrees of freedom

$[P_{bs}]$ is the vector of all internal bond forces acting at the steel nodes

[C] is assembled from all $[C_e]$

Example:

Figure (3-11) shows a small mesh containing three 8-noded rectangular elements. One steel bar is passes through the elements at an angle ø. There are three steel nodes in every concrete element. The global bond matrix is established according to the steps shown above. The resulting global matrix is shown in figure (3-12)

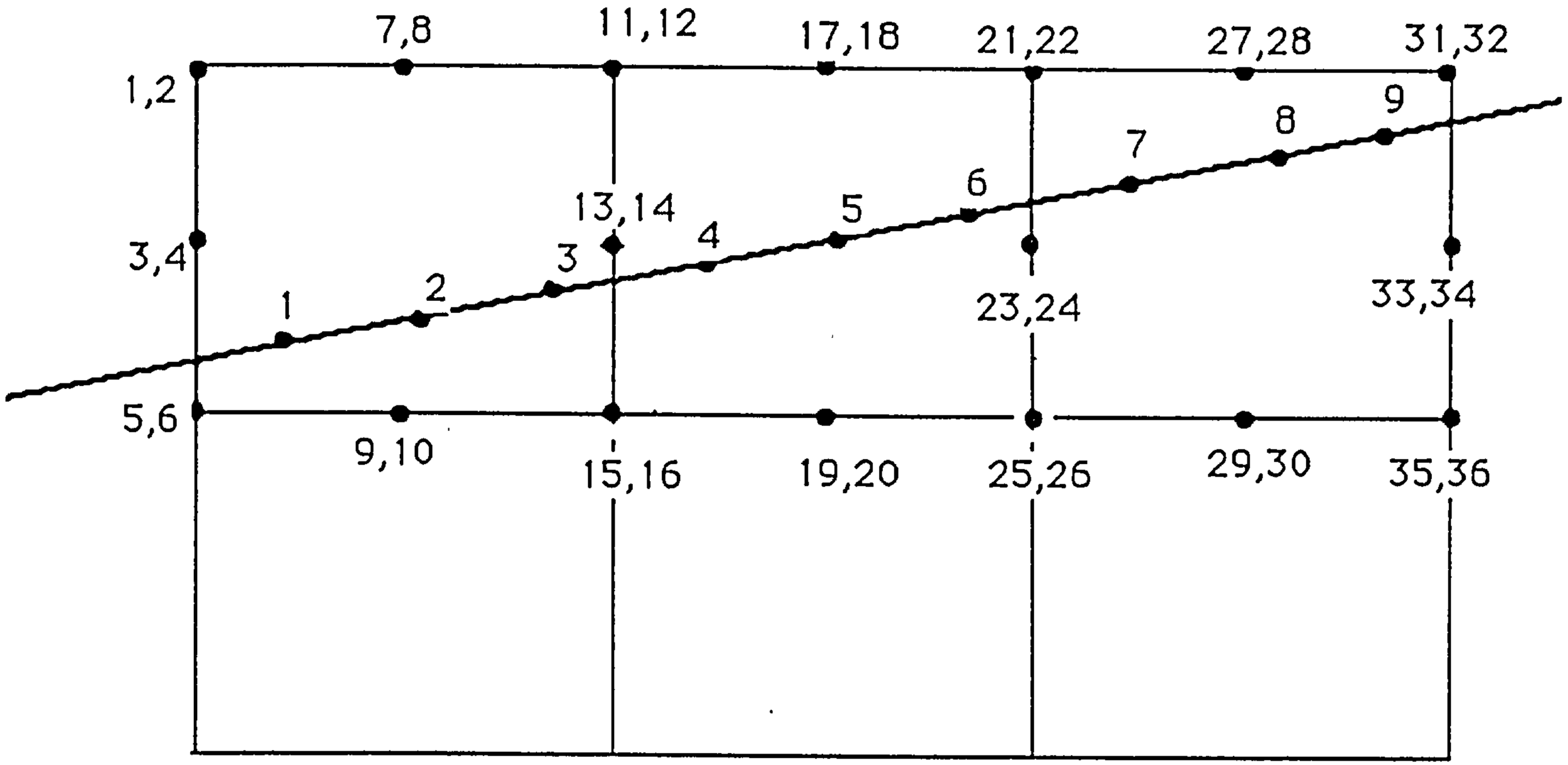

Figure (3-11) - A reinforcing bar passing through 3 concrete elements

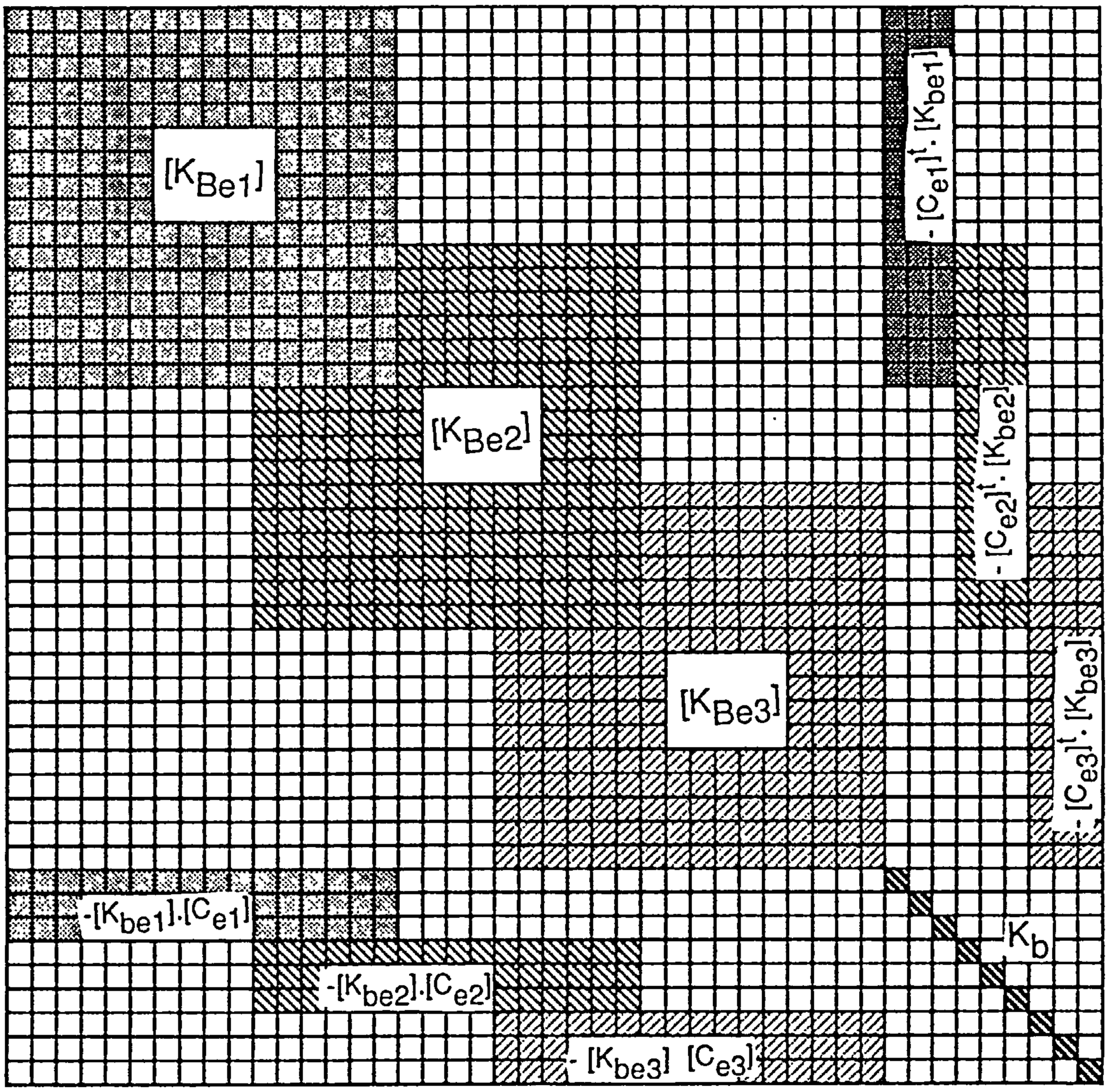

Figure (3-12) Global bond matrix for the mesh of figure (3-11)

3.3 Modelling of concrete

The concrete may be modelled by any type of finite element derived by the displacement approach but it should be noted that the shape functions are also used in transforming the bond interface matrix in section (3.2).

As the concrete mesh must accurately represent the concrete alone, it has to match the concrete distribution of forces and stresses regardless of the steel location . Two dimensional plane stress analysis assuming linear, elastic stress-strain relationship will be used see chapter 5 for more details. The formulation of the element stiffness matrix for concrete is based on the adopted constitutive laws and is done in the conventional manner. To be consistent with section (3.2) quadratic shape functions are used to approximate the element boundary and the displacement variation over the element. Therefore concrete is represented by 8-noded quadratic isoparametric plane elements. For the numerical integration four Gaussian integration points are used to evaluate the stiffness integral figure (3.13). The global stiffness matrix of the concrete is assembled in the standard manner, leading to

$$[K_c] \cdot [D_c] = [P_c] \qquad (3\text{-}20)$$

where

$[K_c]$ is the global stiffness matrix of the concrete structure which contains the contribution of all concrete element stiffness matrices

$[D_c]$ is the vector containing the global deformations of all degrees of freedom of the concrete.

$[P_c]$ is the vector containing all external loads applied to concrete.

3.4 Reinforcement Modelling

In this research reinforcing steel is modelled by strings of two noded bar elements joined together to represent each reinforcement bar. Only one degree of displacement is considered at each node being the displacement of the reinforcement along the axis of the bar. Thus, linear variation of longitudinal displacement is assumed along the bar axis. The numbering of steel nodes is done independent of the concrete nodes numbering. One dimensional, linear, elastic stress-strain relationship is assumed.

If the nodes at a bar element ends are marked 1 and 2 figure (3.14) then the element stiffness matrix is given by:

$$\begin{bmatrix} p_1 \\ \\ p_2 \end{bmatrix} = (E_s.a_s) / s \begin{bmatrix} 1 & -1 \\ \\ -1 & 1 \end{bmatrix} \begin{bmatrix} u_1 \\ \\ u_2 \end{bmatrix}$$

where

p_1 , p_2 are axial forces at nodes 1 and 2 respectively

u_1 , u_2 are axial deformations at nodes 1 and 2 respectively

a_s is cross-sectional area of the bar

s is bar element length

The global load displacement relationship is presented here for the purpose of the derivation of the method.

$$[K_s] . [D_s] = [P_s] \qquad (3\text{-}21)$$

where

$[K_s]$ is the global stiffness matrix of all the steel reinforcements involved in the structure so that it contains the contribution of all the steel elements.

$[K_s]$ has a special form as used in this method and it is always a banded matrix of band width equals 3 , i.e. a tri-diagonal matrix

$[D_s]$ is the vector containing the displacements of all the steel nodes of all the bars .

$[P_s]$ is the vector containing the applied load to steel .

Note that, although the shape functions describing the concrete displacement variation over the element and the element boundaries are quadratic and the steel displacement variation is linear, the error in compatibility is reduced by dividing the steel into small segments and further reduced by the integration of distributed bond stresses into lumped bond forces. Many steel nodes are usually used per concrete element (typically 7 to 10) to represent the distribution of bond stress within an element and thus there is only a little improvement in compatibility to be gained by using 3 noded bar element for steel.

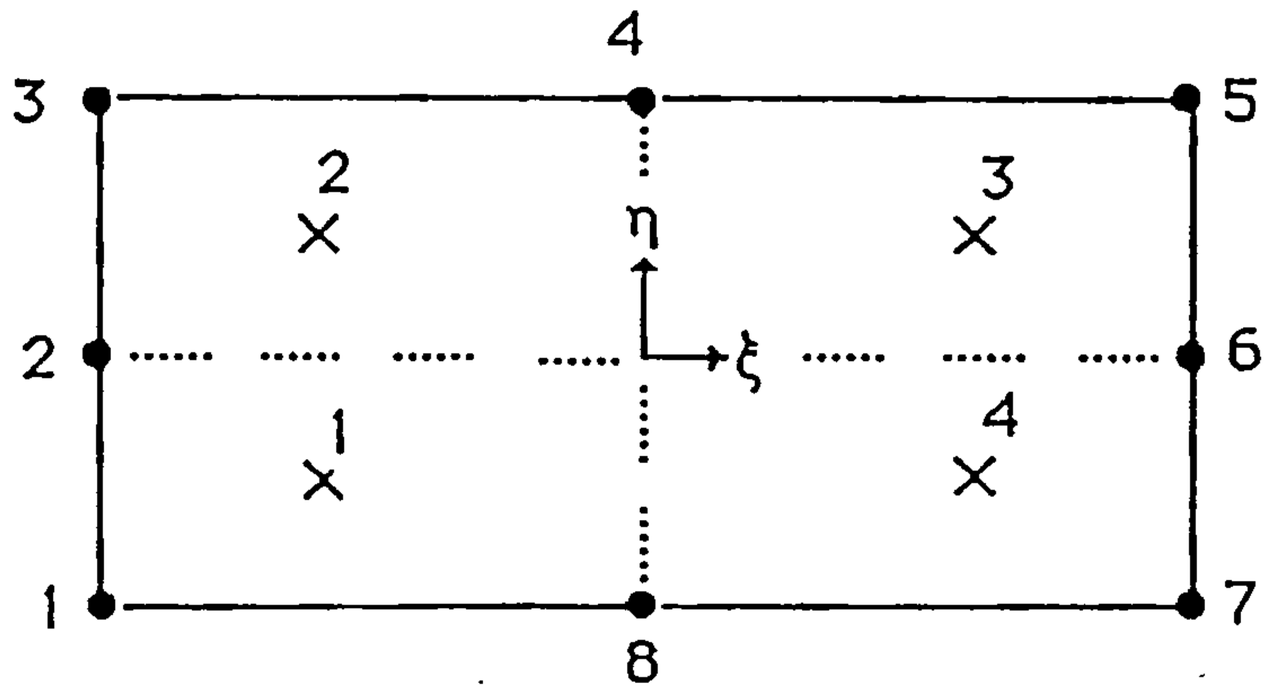

Figure (3.13) - Quadrilateral element with four Gaussian integration points.

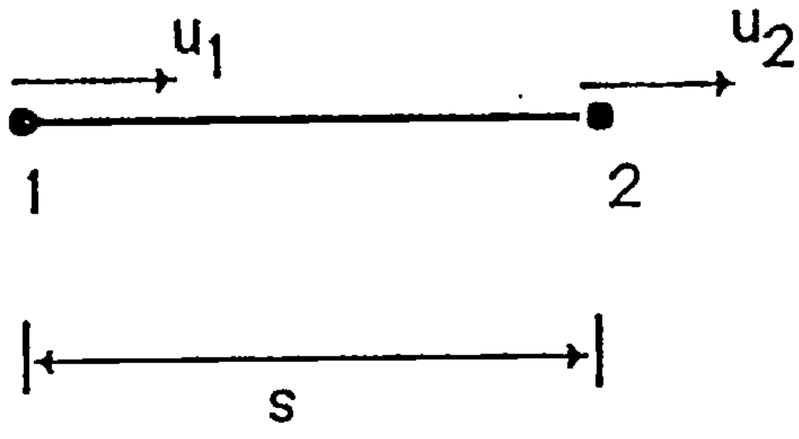

Figure (3-14) - Axial displacements at the nodes of a two noded bar element

3.5 The overall system of equations

In section (3.3) the concrete has been modelled separately which lead to the load-displacement relation given by equation (3-20). Also in section (3.4) the steel has been modelled separately and that leads to the load-displacement relation given by equation (3-21) . In this section the two materials will be interconnected by the system bond matrix developed in section (3.2.6) and which was expressed in equation (3-19) to represent a mass of reinforced concrete.

The displacement vector in equation (3-20) contains concrete displacements alone. In order to keep concrete and steel displacements separated equation (3-20) is written in the following form

$$\begin{bmatrix} [K_c] & 0 \\ 0 & 0 \end{bmatrix} \cdot \begin{bmatrix} [D_c] \\ [D_s] \end{bmatrix} = \begin{bmatrix} [P_c] \\ 0 \end{bmatrix}$$

The above form is advantageous in the solution of the resulting equations as will be shown in chapter 4.

The same thing is repeated for the steel in equation (3-21) which for the same reasons as mentioned above is represented in the following form

$$\begin{bmatrix} 0 & 0 \\ 0 & [K_S] \end{bmatrix} \cdot \begin{bmatrix} [D_C] \\ [D_S] \end{bmatrix} = \begin{bmatrix} 0 \\ [P_S] \end{bmatrix}$$

The equilibrium equation of the complete structure in terms of the concrete degrees of freedom, D_c and the steel degrees of freedom, $[D_S]$ is shown by equation (3-22) below.

$$\left[\begin{bmatrix} [K_c] & 0 \\ 0 & 0 \end{bmatrix} + \begin{bmatrix} 0 & 0 \\ 0 & [K_S] \end{bmatrix} + \begin{bmatrix} [K_B] & -[C]^t.[K_b] \\ -[K_b].[C] & [K_b] \end{bmatrix} \right] \cdot \begin{bmatrix} [D_c] \\ [D_S] \end{bmatrix} = \begin{bmatrix} [P_c] \\ [P_S] \end{bmatrix} \quad (3\text{-}22)$$

Equation (3-22) describes the behaviour of the complete system. The stiffness matrix given relates the displacement at all degrees of freedom of concrete and at all steel degrees of freedom to the applied loads to concrete and/or steel. The solution of this relation will be explained in chapter 4.

3.6 Modelling of reinforcement anchorage

3.6.1 General

One of the design criterion of reinforced concrete structures is to prevent the reinforcing bars from pulling out at the ends upon loading of the concrete member. Such conditions can be accomplished by end anchorage of the reinforcement .

In the method adopted the anchorage can be achieved in two ways:

i) Anchorage by high bond.

ii) Anchorage by applying a force.

3.6.2 Anchorage by high bond

The bond has been modelled by springs holding the steel and the concrete together, and thus the amount of slippage between the concrete and the steel depends on the stiffness of these springs. Reinforcement anchorage at a certain point can be treated as the point having perfect bond with the concrete surrounding it, i.e. equation (3-1) holds for such a node. Thus the reinforcement anchorage at the point can be modelled by a spring with very high stiffness value. This can be seen from Equation (3-4b) repeated here

$$(U_{cj} - U_{sj}) \cdot b = P_{cj}$$

it can be re-arranged as

$$(U_{cj} - U_{sj}) = \frac{P_{cj}}{b} \qquad (3\text{-}23)$$

The slip between concrete point c_j and the steel node s_j $(U_{cj}- U_{sj})$ in equation (3-23) approaches zero when the spring stiffness (b) approaches infinity. Leading to an infinite value for R_0

In this method the anchored steel node will refer to a node with infinite bond so that R_0 value at that node will be set to a very high value typically a thousand times higher than R_0 at other steel nodes.

3.6.3 Anchorage by applying an external force

In this section the development length concept for anchorage of reinforcement will be used in deriving another way of representing anchorage .

Anchorage can be achieved by applying an external force to the steel acting at the node which is to be anchored so as to prevent the steel node from moving with respect to the surrounding concrete. This external force is calculated from the average bond stress over the development length of the reinforcement. The method is presented now

Consider a steel node s_j of the steel bar shown in figure (3-15a). This node is to be anchored to the surrounding concrete

represented by node c_j. If the slip at that node is *delta* Δ, the necessary force to bring the two nodes together is calculated from the average bond stress over the development length (l_d) of the steel bar assuming linear variation of bond stress over l_d, figure (3-15 b).

Hence

$$f_{bs} = (\Delta / 2) . \ l_d \ . \ R_0 \ . \ \Omega \qquad (3\text{-}24a)$$

where

f_{bs} is the average bond force acting on l_d and which is necessary to push back the node sj to the point of anchorage.

l_d is the development length of the reinforcement needed for the transfer of force between the reinforcement and the concrete. Its initial value may be selected according to the Building Codes requirements .

The applied force on the concrete which is necessary to establish equilibrium with the steel can be obtained from equation (3-24a) by calculating the equivalent nodal forces of the concrete using equation (3-12) leading to

$$f_{bc} = [C_{ej}]^t . \ f_{bs} \qquad (3\text{-}24b)$$

where

f_{bc} is the average bond force applied at the nodes of the concrete element accommodating the steel node.

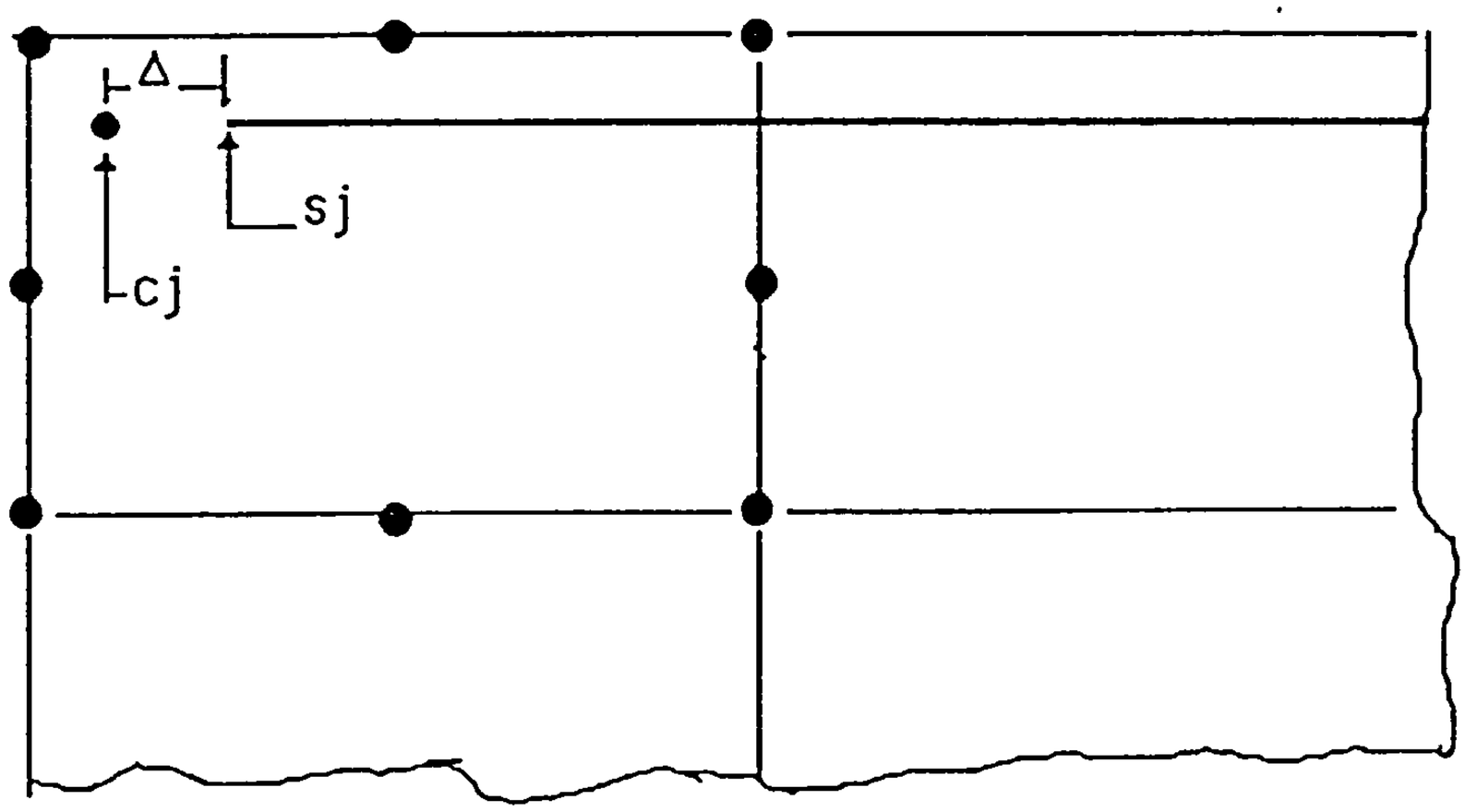

(a) - Anchorage of a reinforcement bar to the surrounding concrete.

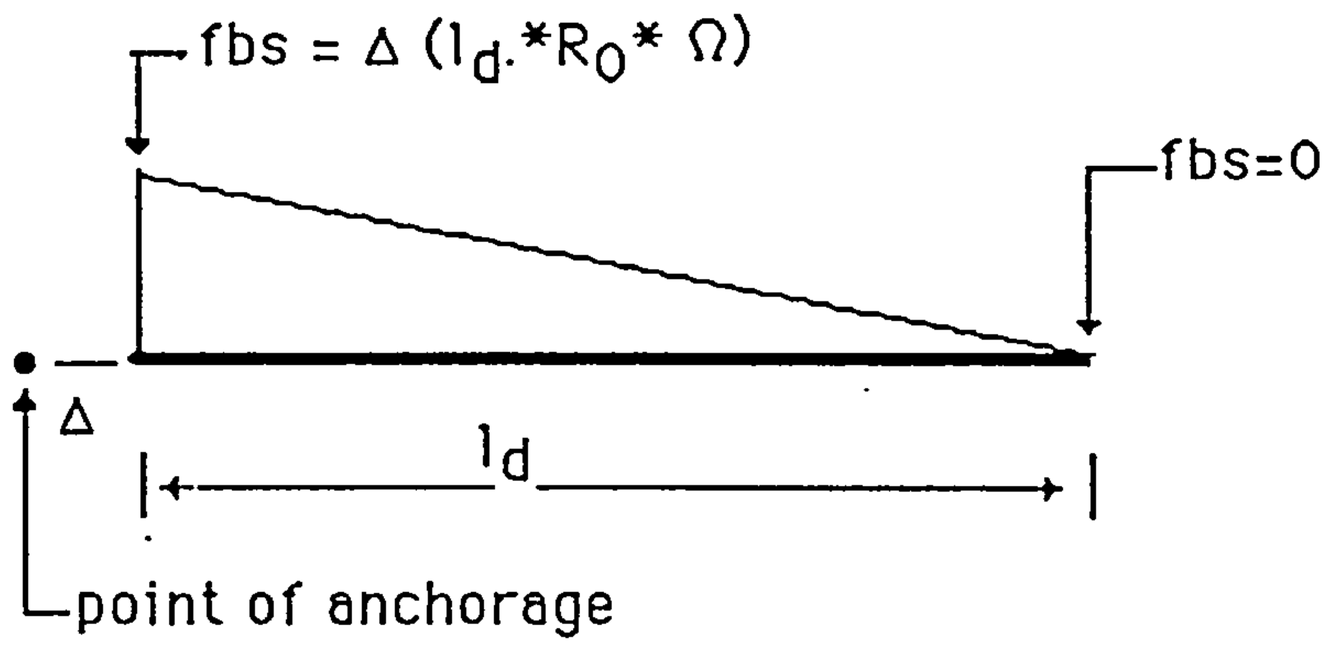

(b) - Bond force variation over the bar length due to Δ

Figure (3-15) -Reinforcement anchorage by applying external force

The solution of both equations (3-24a) and (3-24b) depends on knowing the value of Δ in advance. So their application can be done in an iterative fashion.

From the solution of equation (3-22) the value of Δ can be calculated. As the value of Δ is made known, then the forces of equations (3-24) is calculated.These forces can now be assembled in the load vector of equation (3-22). Another solution has to be obtained for the system again and a new value of Δ is calculated. The process is repeated until the value of Δ becomes sufficiently small.

The application of this method is demonstrated in chapter 4. This can be achieved in an efficient way.

3.7 Summary

A new method for the analysis of reinforced concrete by finite element method has been developed. The method uses bond between reinforcement and the surrounding concrete as the basis for the development of the theory. Bond is modelled by springs joining the steel and the concrete. Bond inter-forces were derived from the springs stiffness and the relative movement between the steel and the surrounding concrete. The stiffness bond matrix for one steel node was first established from the bond interforces. Then the element bond matrix was established for all steel nodes within a concrete element. The global bond matrix was assembled from the bond matrix of the concrete elements which have steel bars passing through them. The concrete and the steel have each been modelled and analysed separately. The process of combining them into a mass of reinforced concrete was achieved by interconnecting the two materials through the global bond matrix. Thus the system load-displacement equations for the complete structure were established. Modelling of reinforcement anchorage by two methods was discussed.

Chapter 4

4. SOLUTION OF EQUATIONS

4.1 Introduction

In solving problems by finite element method usually large number of simultaneous, linear algebraic equations have to be solved. In this chapter appropriate methods which can be applied for the solution of the system equilibrium equations presented in section (3.4) are discussed.

The solution of the resulting set of simultaneous equations can be accomplished by direct technique methods such as Choleski reduction or the direct Gaussian elimination procedure. But, since the global stiffness matrix i.e. equation (3-22) is assembled from all degrees of freedom of concrete and of total degrees of freedom of all the reinforcement bars present then this will lead to a very large matrix with large band width. Conventional methods of solving such a large number of system equations (i.e. by direct solution) is expensive from computer point of view. Therefore, new approaches will be examined for the solution of the resulting system of equations. Advantage of the separate representation of matrices in equation (3-22) will be taken in establishing an approach based on iterative technique.

In general by using direct technique methods the answer will be given in a fixed number of steps and a unique solution will be produced. The indirect method technique will involve an iterative procedure which will start by an initial approximation to the

solution and generates a sequence of approximate solutions which converges to the true solution if the iteration process was successful or diverges for unsuccessful process.

The possibility of a direct solution is discussed. Two out of several other possible iterative schemes for the solution of equation (3-22) are studied and presented.

While studying the different methods that can be applied for the solution of the system equations presented in section (3-5) the methods will be compared for efficiency in terms of computer time required to perform the number of arithmetic operations needed in the solution of the resulting equations

The method of applying external force to model steel anchorage will be demonstrated.

4.2 Illustrative problems

In the discussion of the methods that can be applied for the solution of the system equilibrium equations the following example will be used by the different methods for the purpose of testing and comparing these methods.

The single span beam shown in figure (6-1) will be analysed taking into account all the reinforcement involved in tension, compression steel and stirrups. The beam is simply supported and uniformly loaded. Further details of the beam are given in chpater 6.

The finite element mesh for concrete suitable for this method is shown in figure (6.2). There are 20 concrete 8-noded quadrilateral elements with a total of 85 nodes.

Another problem is given here which may be used in some cases to help in demonstrating some of the ideas when examining the different methods.

This problem is for a cantilever which is represented in the simple layout shown in figure (4-1) . It is loaded with uniformly distributed load. The reinforcement details and distribution are shown in the figure. There are a total of 13 bars groups with a total number of 130 nodes. The concrete mesh has 18 8-noded quadrilateral elements with a total number of 73 nodes figure(4-2).

The tension steel is fixed at the cantilever fixed end.

E_c=3640 k/in^2 (25.1 kN/mm^2)
E_s=29000 k/in^2 (200 kN/mm^2)
R_0=200 k/in^3 (54.3 N/mm^3)
Width = 12 inch (30.5 mm)

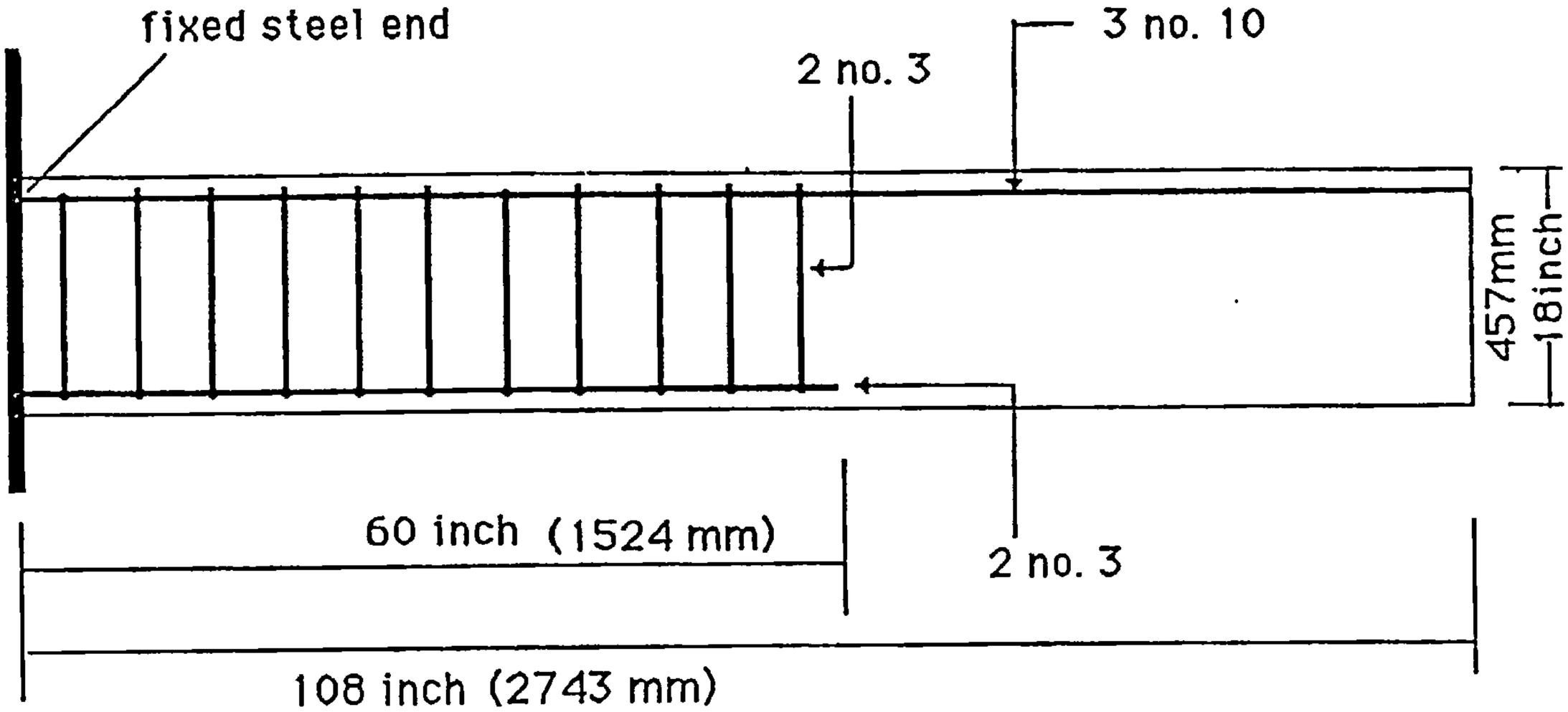

Figure (4.1) Details of Cantilever

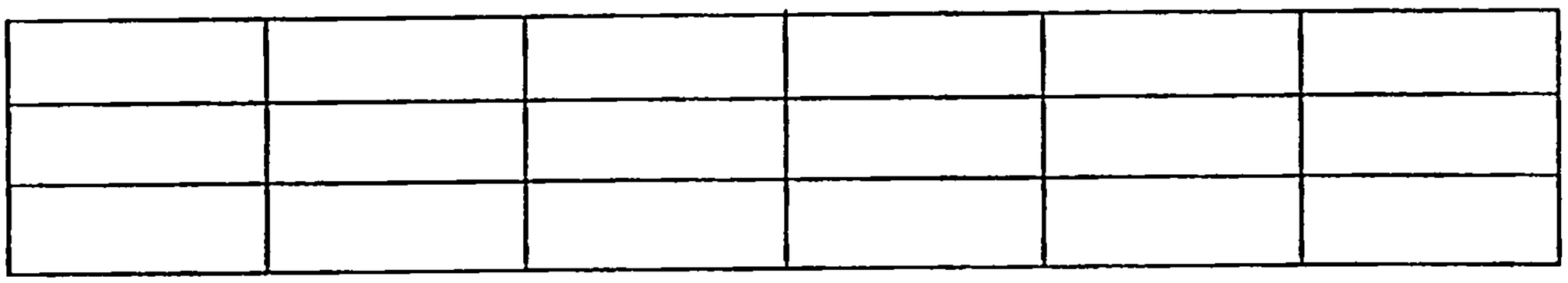

Figure (4.2) Finite Element Mesh For Concrete in the Above Cantilever

4.3 Direct solution

Direct solution of the set of simultaneous equations defined by equation (3.22) is straightforward and can be accomplished by any method such as Choleski reduction or the direct Gaussian elimination procedure.

To obtain a direct solution to equation (3.22) it will be rewritten in the following form :

$$\begin{bmatrix} [K_c]+[K_B] & -[C]^t . [K_b] \\ -[K_b].[C] & [K_s]+[K_b] \end{bmatrix} . \begin{bmatrix} [D_c] \\ [D_s] \end{bmatrix} = \begin{bmatrix} [P_c] \\ [P_s] \end{bmatrix} \quad (4\text{-}1)$$

The above matrix is a symmetrical banded matrix whose band width depends on the efficiency of the numbering scheme. In the above form of representation the concrete terms and the steel are given into separate quantities as they are derived in chapter 3. The actual elements of these matrices obtained for a direct solution is a mixture of terms corresponding to steel and to concrete assembled according to global degrees of freedom numbering. The associated mesh with this solution should have a continuous node numbering system for all the concrete and the steel degrees of freedom numbers.

Example of mesh assembly

The small mesh of figure (3-11) will be used to demonstrate the direct solution method. An efficient node numbering of the mesh which is suitable for direct solution is illustrated in figure (4-3) which corresponds to figure (3-11). The global matrix for a direct solution is assembled as shown in figure (4-4) which corresponds to the matrix shown in figure (3-12).

The beam solution :

Solution to the real beam given in section (4.2) will be used to demonstrate direct solution for the purpose of comparison with iterative solution. The tension reinforcement is divided into 40 elements or 41 steel nodes and the same thing is done to the compression reinforcement. Each of the strirrups is divided into 4 elements or 5 steel nodes. An efficient numbering scheme for all concrete and steel nodes was carried out. The maximum half band band width is found to be 66 . The number of simultaneous equations (N) to be solved is the same as the total degrees of freedom (TDOF) and equals to 474. Leading to a banded matrix of 474 X 66 elements which have to be stored and solved. The number of multiplications/divisions operations required for solving this system of equations using Choleski Algorithm is approximately equal to 1.1 millions operations.

The effect of increasing the number of steel nodes on the amount of calculations required is demonstrated here. The number of nodes for each stirrup is increased to 9 nodes instead of 5 nodes while keeping the number of steel nodes in the tension and the compression steel the same as before.

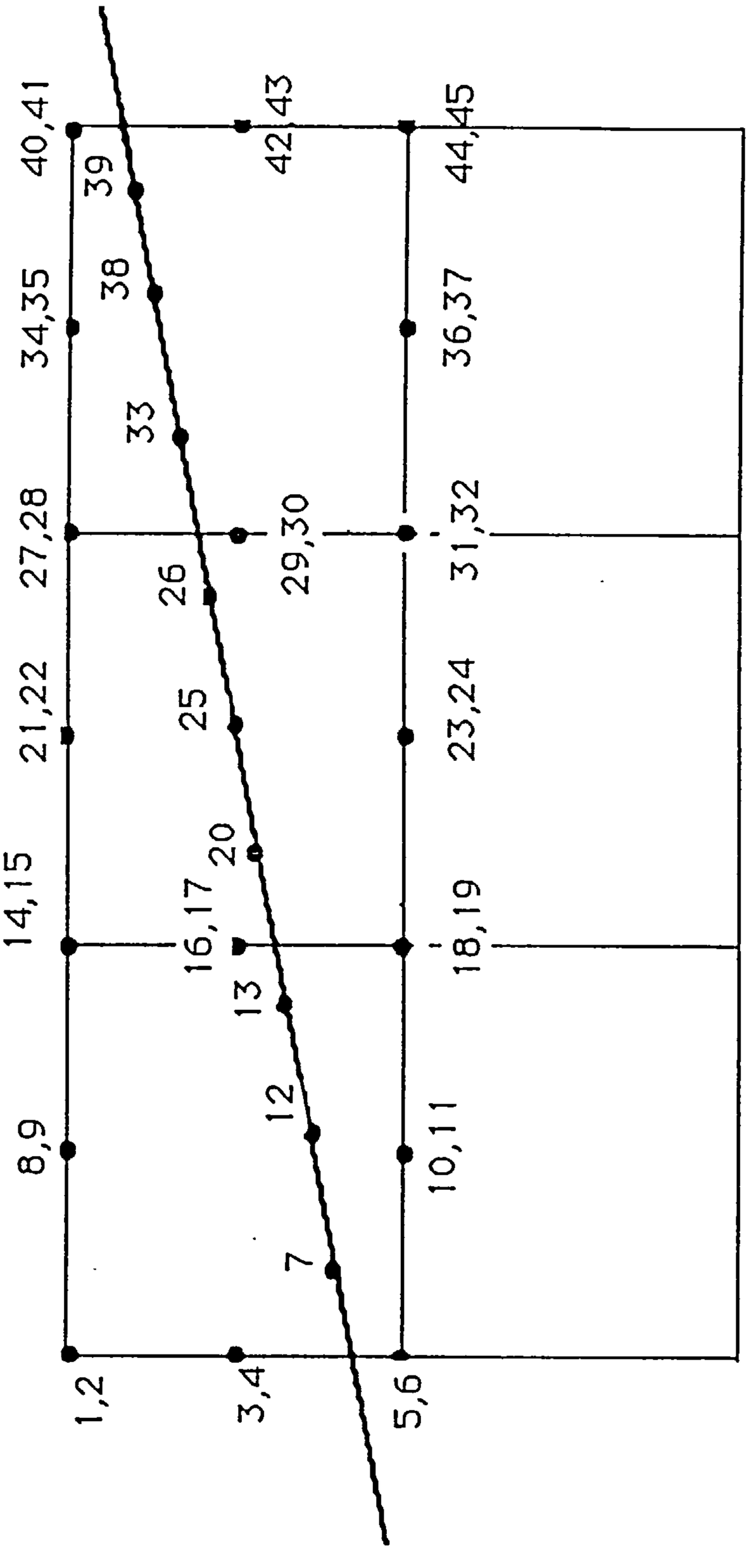

Figure (4.3) - Degrees of freedom numbering for a direct solution of the previous mesh shown in figure (3.11)

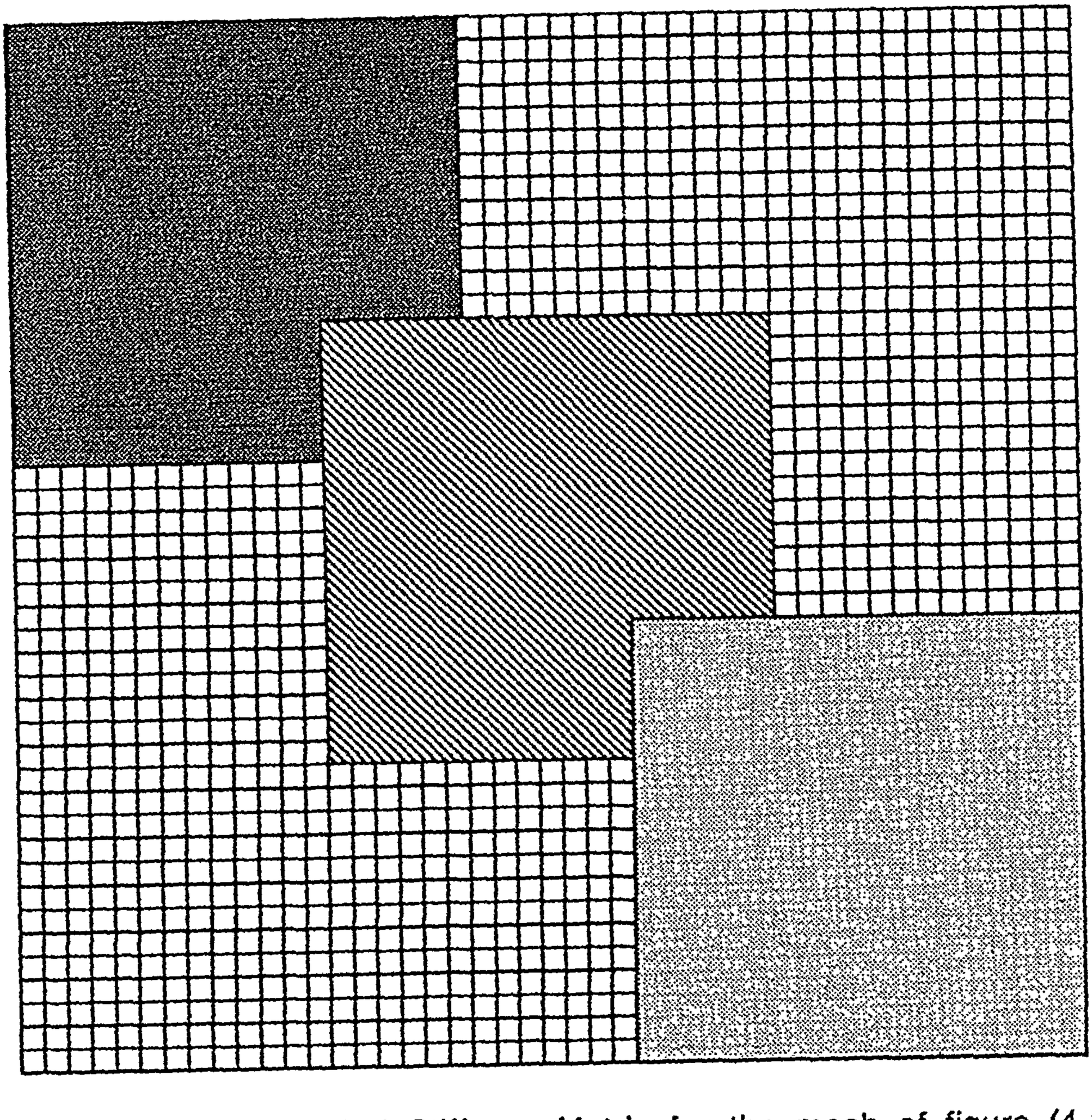

Figure (4-4) Global Stiffness Matrix for the mesh of figure (4-3).
(For Direct Solution)

In this case the total number of degrees of freedom becomes 654 and the half band width is 94. Leading to a number of arithmetic operations to over 3 million operations

The efficiency of this solution in terms of the number of arithmetic operations needed will be studied in comparison with the iterative methods of solution that will be discussed next. In this solution the concrete and the steel displacements are solved simultaneously and they are not separated.

4.4 Iterative methods of solution

4.4.1 General

Equation (3-22) is presented in a partitioned form of sub-matrices. This form of separate submatrices have been studied to find out the possibility of obtaining a new approach of solution for the resulting equations. Such solution may be made possible by indirect solution which involves an iterative procedure.

Solutions of simultaneous linear equations by iterative technique starts from an initial approximate solution and then a sequence of approximate solutions are generated. The process is repeated until a satisfactory solution is reached. Relaxation methods can be adopted to improve the convergence of the iterative methods. Thus slow converging iteration procedure can be accelerated by over-relaxation methods which is used to speed up the convergence, on the other hand, iteration methods that converge in an oscillatory manner can be improved using under-relaxation methods to obtain convergence in a faster manner. The decision to stop the iteration is based upon the convergence criteria set for the solution. Iteration may continue until satisfactory accuracy results. The number of iterations is usually restricted to some maximum so as to control over slow converging methods or diverging methods.

The iterative technique required for the solution of equation (3-22) is actually a combination of both direct and iterative methods. A direct solution to the set of finite elements related to

concrete done separately and another direct solution for the steel. The iterative solution of the complete structure is sought by determining the interforces and applying them in conjunction with the external loads to each set of finite elements.

i.e.

Forces on concrete = Loads applied to concrete + Interforces

Forces on steel = Loads applied to steel + Interforces

The purpose of the iteration process is to adjust the solutions obtained for the concrete and the steel during the iterations so that the final solution satisfies equation (3-22).

The system of matrices represented by equation (3-22) consist of the following

1) Concrete stiffness matrix $[K_c]$

2) Steel stiffness matrix $[K_s]$

3) Bond matrix containing bond stiffness terms related to concrete displacement and bond stiffness terms related to steel displacement.

Equation (3-22) can be re-written in a form suitable for the iterative method as follows :

$$[K_c][D_c] + [K_B][D_c] - [C]^t [K_b][D_s] = [P_c] \quad (4\text{-}2a)$$

$$[K_s][D_s] + [K_b][D_s] - [K_b][C][D_c] = [P_s] \quad (4\text{-}2b)$$

Different combinations of the above matrices can be formed which will lead to different forms of methods of solutions. Two of these

combinations have been studied thoroughly and are presented in the following two sections.

4.4.2 First method examined

4.4.2.1 The method

In this section an iterative scheme which was tried and found unsuccessful will be presented. In this method of solution the terms of the bond matrix related to the concrete will be added to the concrete stiffness matrix and the terms of the bond matrix related to the steel will be added to the steel stiffness matrix. This can be done by combining the appropriate matrices of equations (4-2) together and rearranging as :

$$[K_c+K_B] \cdot [D_c] = [P_c] + [C]^t \cdot [K_b] \cdot [D_s] \quad (4\text{-}3a)$$

$$[K_s+K_b] \cdot [D_s] = [P_s] + [K_b] \cdot [C] \cdot [D_c] \quad (4\text{-}3b)$$

In this form the term $[C]^t \cdot [K_b] \cdot [D_s]$ represents the interforces applied to concrete and the term $[K_b] \cdot [C] \cdot [D_c]$ represents the interforces applied to steel.

A solution to the above arrangements can be obtained by the following iterative scheme :

$$[K_c+K_B] \cdot [D_c^{1}] = [P_c] \quad (4\text{-}4)$$

$$[K_s+K_b] \cdot [D_s^{i}] = [P_s] + [K_b] \cdot [C] \cdot [D_c^{i}] \quad (4\text{-}5a)$$

$$[K_c+K_B] \cdot [D_c^{i+1}] = [P_c] + [C]^t \cdot [K_b] \cdot [D_s^{i}] \quad (4\text{-}5b)$$

where i refers to the iteration number. The iteration only involves equations (4-5).

Before the iteration solution starts [K_c+K_B] is assembled and reduced to banded lower triangle matrices once only. The same thing is also done to [K_s+K_b].

The iterative solution of the above arrangements is summarised in the following steps :

1) Total load is applied to the structure so that

$$[\,P_c\,] = \text{full load} \qquad \text{or} \qquad [\,P_s\,] = \text{full load}$$

2) Calculate [$D_c^{\,1}$] using equation (4-4). This will be the initial approximate solution.

3) Total forces on steel are calculated from equation (4-5a) according to $[\,P_s\,] + [\,K_b\,] \,.\, [\,C\,] \,.\, [\,D_c\,]$ using latest concrete displacements calculated.

4) Steel displacements are obtained due to the load calculated in step 3 and by solving equation (4-5a) using the reduced form of [K_s+K_b].

Thus, this is not an full solution but a back-substitution in the reduced form of [K_s + K_b].

5) Total forces on concrete is calculated and applied according to

$$[P_c] + [C]^t \,.\, [K_b] \,.\, [D_s]$$

using the latest steel displacements calculated.

6) The load found in step 5 is applied to the concrete and the concrete displacements are calculated by solving equation

(4-5b) using the reduced form of [K_c+K_B].

Steps 3 through 6 are repeated until the solution converges or until a maximum allowed number of iterations is reached.

The steel or the concrete solutions can be used for examining the convergence of the method. Since enormous numbers of data for displacements are available in every iteration corresponding to the total degrees of freedom of the concrete and the steel, the average of the absolute value of all displacements is used to examine convergence of the solution, that is

$$(\sum | D_{ci} |) / \text{TDOFC}$$

$$(\sum | D_{si} |) / \text{TDOFS}$$

where

TDOFC = Total degrees of freedom of concrete

TDOFS = Total degrees of freedom of steel

These average values are found to be a good indication of the convergence of the method. Any of the two quantities can be used as can be seen while discussing the method.

The convergence of the solution was found to be extremely slow. Hundreds of iterations are allowed without much hope for convergence of the solution. This can be seen from figure (4-5) which shows the convergence behaviour of the solution of the beam problem using the steel displacements to examine the convergence. After 200 iterations the solution is far from convergence.

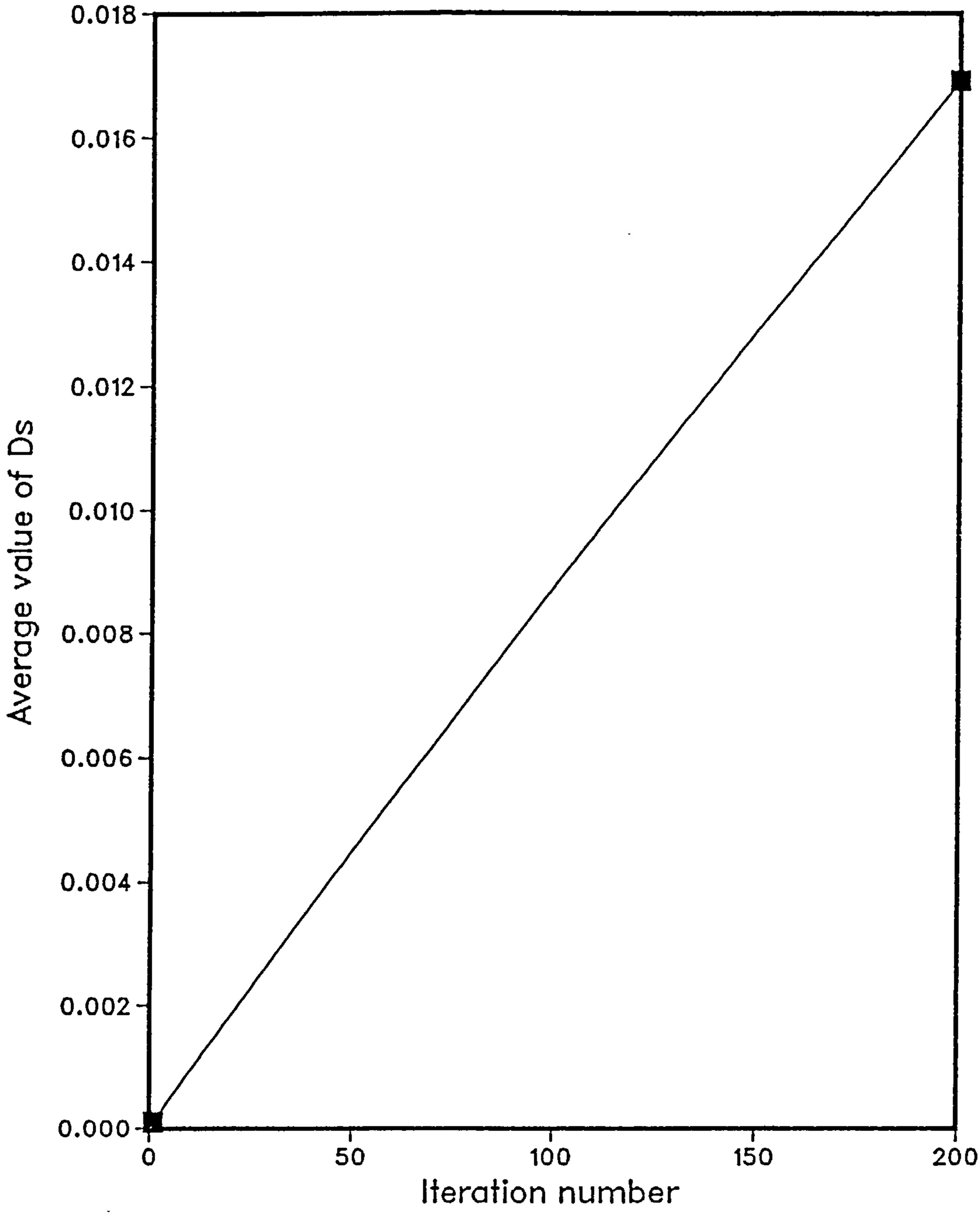

Figure (4-5) - Convergence of the first method examined.

4.4.2.2 Application of accelerator

It was necessary to use a relaxation method to speed up the slow convergence of the solution . An overrelaxation (accelerating) factor *beta* (β) is applied to the solution. A constant accelerator factor β_s is applied to the steel displacements in every iteration to correct for the current iteration solution and another constant accelerator β_c is applied to the current concrete displacements. The application of these factors is done according to

$$[D_s^i] = [D_s^{i-1}] + \beta_s . ([D_s^i] - [D_s^{i-1}]) \quad (4\text{-}6a)$$

$$[D_c^i] = [D_c^{i-1}] + \beta_c . ([D_c^i] - [D_c^{i-1}]) \quad (4\text{-}6b)$$

Equation (4-6a) is applied after solving for the steel displacements in step 4, while equation (4-6b) is applied after solving for the concrete displacements in step 6. The application of the two factors within the iterative solution is given here in equation form :

$$[K_c + K_B] . [D_c^1] = [P_c]$$

$$[K_s + K_b] . [D_s^i] = [P_s] + [K_b][C] . [D_c^i]$$

$$[D_s^i] = [D_s^{i-1}] + \beta_s . ([D_s^i] - [D_s^{i-1}])$$

$$[K_c + K_B] . [D_c^{i+1}] = [P_c] + [C]^t . [K_b] . [D_s^i]$$

$$[D_c^{i+1}] = [D_c^i] + \beta_c . ([D_c^{i+1}] - [D_c^i])$$

There are a number of other methods for applying equations (4-6)

to the solution other than the one shown in the above equations and which depends on where to apply equation (4-6) within the iterative loop. These have been studied but the form shown above is adopted.

The major difficulty was in finding the values of $ß_s$ and $ß_c$ that will speed up the rate of convergence without upsetting the solution. The choice for the value of any of the two *betas* was completely arbitrary. Only through experimentation the values of $ß_s$ and $ß_c$ were chosen. It was necessary to limit their sizes as large values will disturb the convergence of the solution . The maximum value allowed were limited to be less than 2.0

i.e.

$$1.0 \leq ß_s < 2.0$$

$$1.0 \leq ß_c < 2.0$$

The values of the two factors are independent.

As convergence was extremely slow the effective value for either of the two constants as obtained from experimentation were very close to 2.0

The same beam problem is solved again after introducing the two overrelaxation factors. Figure (4-6) shows the convergence of the method using different values for the accelerating factors. Several points can be seen from this graph i) the great effect of the accelerating factors on the convergence of the solution ii) The need for high values of *betas* . iii) The convergence of the method is best described when using $\beta_c = \beta_s = 1.98$

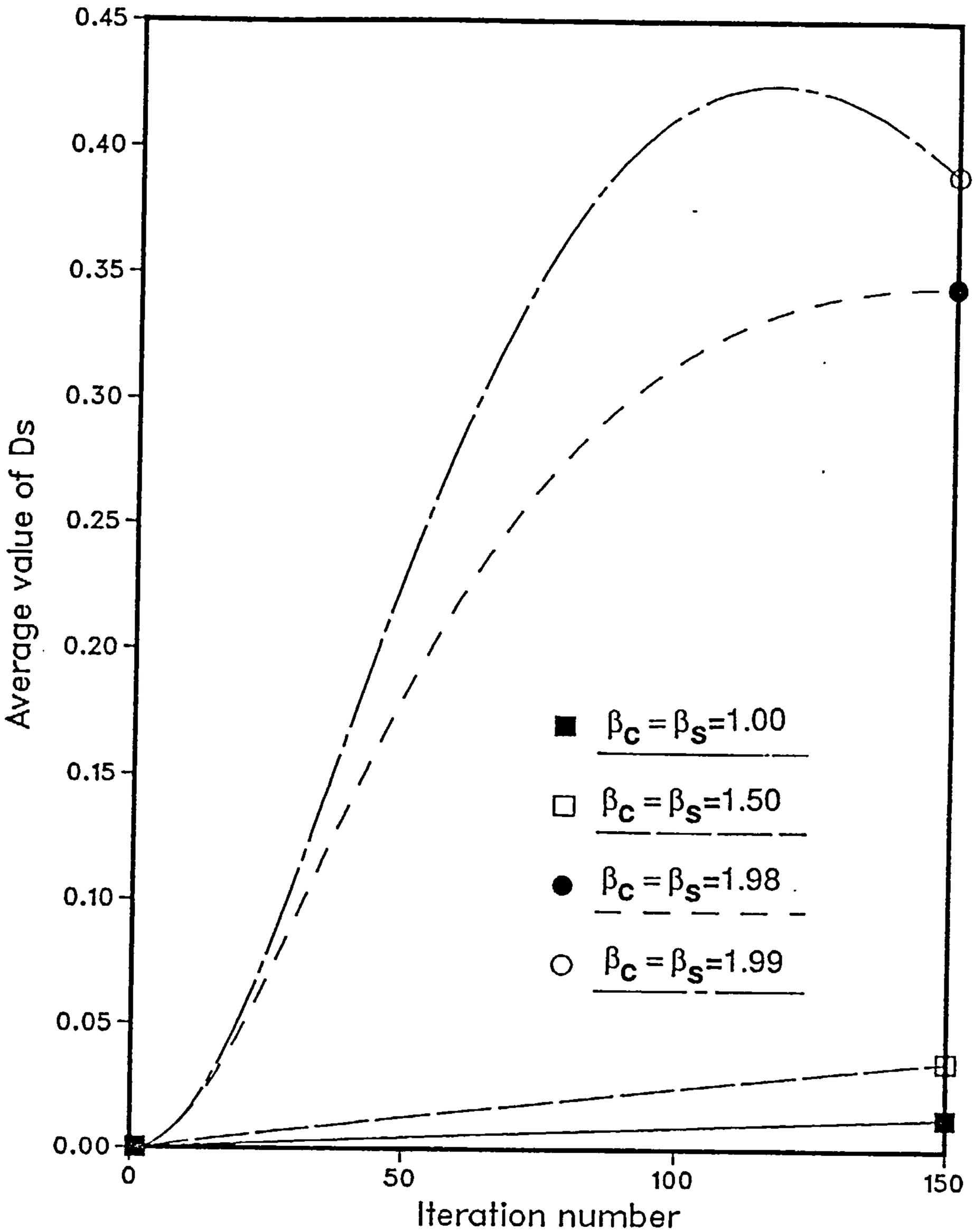

Figure (4.6) - Effect of applying accelerators on the convergence of the first method examined.

Therefore the solution using a constant accelerator of 1.98 for both concrete and steel solutions was studied thoroughly for the steel and the concrete solutions. The results were encouraging but still need to be improved. Allowing for larger number of iterations upsets the solution again.

4.4.2.3 Solution starting with a better value

The solution in the previous section started with initial concrete displacements obtained from equation (4-4) . The extra stiffness added to the concrete matrix $[K_c]$ have obviously caused a rough start of the solution . Another starting value can be obtained by simply calculating the deflection of the concrete nodes by solving the problem for plane concrete alone ignoring the presence of the steel. The purpose of which is to provide a better approximation of the starting value for the iterative process. This will lead to replacing equation (4-4) with

$$[K_c] . [D_c] = [P_c] \qquad (4\text{-}7)$$

Obviously the concrete deformations obtained using the above equation are too high since the stiffening effect of the reinforcement is absent.

It would be legitimate therefore to scale these values down by some factor κ. Thus a constant κ whose value is less than one is applied for all concrete displacements once only before starting

the iteration process as illustrated in flowchart (4.1). In equation form this is given by

$$[D_c^0] = \kappa . \ [D_c]$$

$$0 < \kappa < 1.0$$

The value of κ can be found from two different approaches :

i) As already noted that the high values of the concrete displacements are due to the absence of the stiffening effect of the reinforcement from the solution of equation (4-7). Therefore it is straightforward to calculate a value of κ from the different stiffnesses of the problem . Thus κ can be estimated from the relative stiffness of the structure with and without reinforcement as follows

$$\kappa = \frac{\text{stiffness of the structure without reinforcement}}{\text{stiffness of the structure with reinforcement}}$$

The value of κ, of course, depends on each individual problem . It has to be estimated manually from the bending stiffness for the two cases allowing for the ratio of Young's modulus to steel and concrete. For the beam problem the value of κ is estimated to be 0.75 . Figure(4-7) shows the effect of applying different values of κ to the beam problem. The solution without the effect of applying κ (i.e. κ=1.0) starts from a very high initial approximate value for concrete and the values are reduced as iteration proceeds. The effect of using the value of κ of 0.75 is shown.

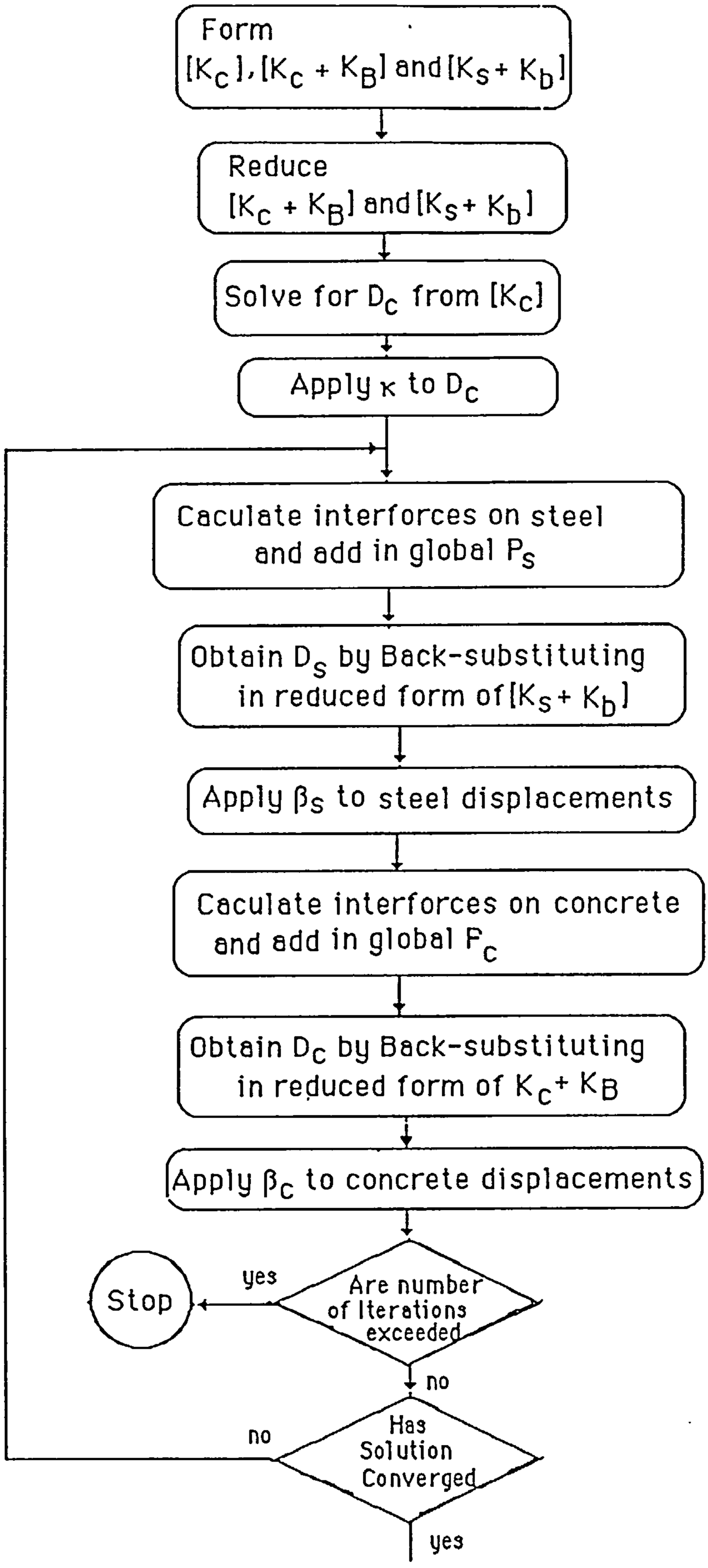

Flowchart (4-1) - Final form of solution for the first method attempted.

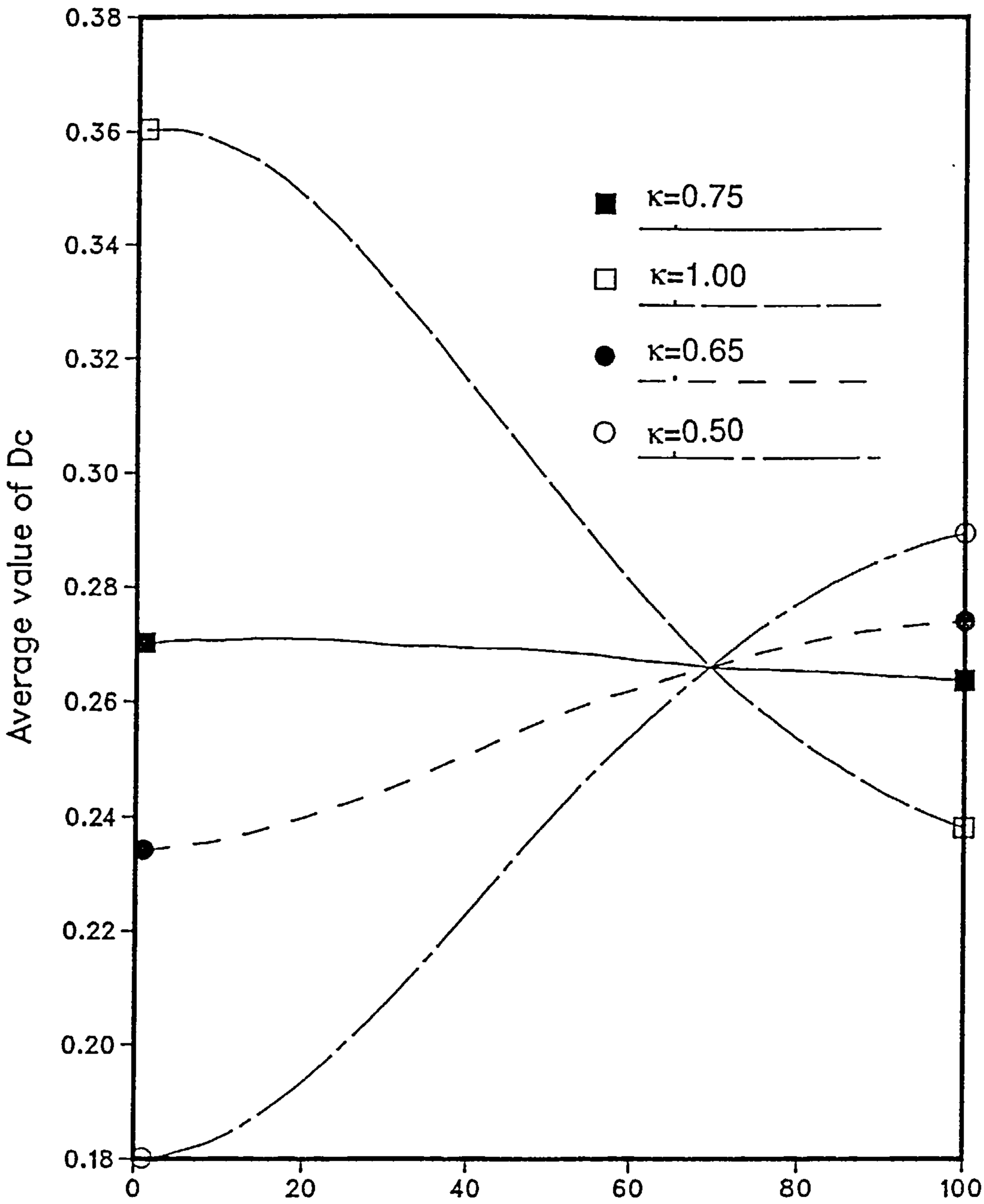

Figure (4-7) - Effect of applying different values of κ on the convergence of the beam problem while $\beta_c=\beta_s=1.99$

ii) The value of κ can be derived mathematically from first few iterations. This is made possible by identifying the upper and lower limits of κ . An upper limit for κ of 1.0 and a lower limit of 0 have already been given. However, it can be safely assumed that the exact concrete deformations of the complete structure is greater than one half the value obtained from equation (4-5) . Leading to the following

$$0.5 < \kappa_e < 1.0$$

The exact value of κ or "κ_e" can be obtained in terms of κ=1.0 and κ=0.5 as follows. The slopes for the two convergence curves of κ=0.5 and κ=1.0 can be calculated from the concrete displacements obtained from the first two iterations. The following slopes can be calculated for the two values of κ as

$$\text{when } \kappa=1.0 \quad \text{slope} = (D_c^2 - D_c^1) / (1.0 - \kappa_e) \qquad (4\text{-}8a)$$

$$\text{when } \kappa=0.5 \quad \text{slope} = (D_c^2 - D_c^1) / (0.5 - \kappa_e) \qquad (4\text{-}8b)$$

where

D_c^1 = concrete displacement at first iteration

D_c^2 = concrete displacement at second iteration

By assuming the two slopes to be equal the equations (4-8) yield the following

$$\frac{(D_c^2 - D_c^1)_{\kappa=1.0}}{(D_c^2 - D_c^1)_{\kappa=0.5}} = \frac{(1.0 - \kappa_e)}{(0.5 - \kappa_e)}$$

where

$(D_c^2 - D_c^1)_{\kappa=1.0}$ is the value at κ =1.0

$(D_c^2 - D_c^1)_{\kappa=0.5}$ is the value at κ=0.5

By substituting numerical values in the above formula from the first two iterations an approximate value of κ_e can be found. For the general case κ can be obtained after the i^{th} iteration when comparing concrete displacements to the ones obtained in any preceding iteration.

The effect of the values assigned to the relaxation parameters is also illustrated when solving the cantilever problem in figure (4.1). Figure (4-8) shows the convergence of the cantilever when using different values of β_c , β_s and using different values of κ . Convergence of the problem is obtained for the two cases of β_s=1.99, β_c=1.8 and κ=1.0 or 0.5 after about 40 iterations. The values of β_s=1.99, β_c=1.99 and κ=1.0 or 0.5 causes violent behaviour of the iterative solution but it looks that the two curves are approaching convergence if the iteration was allowed to continue.

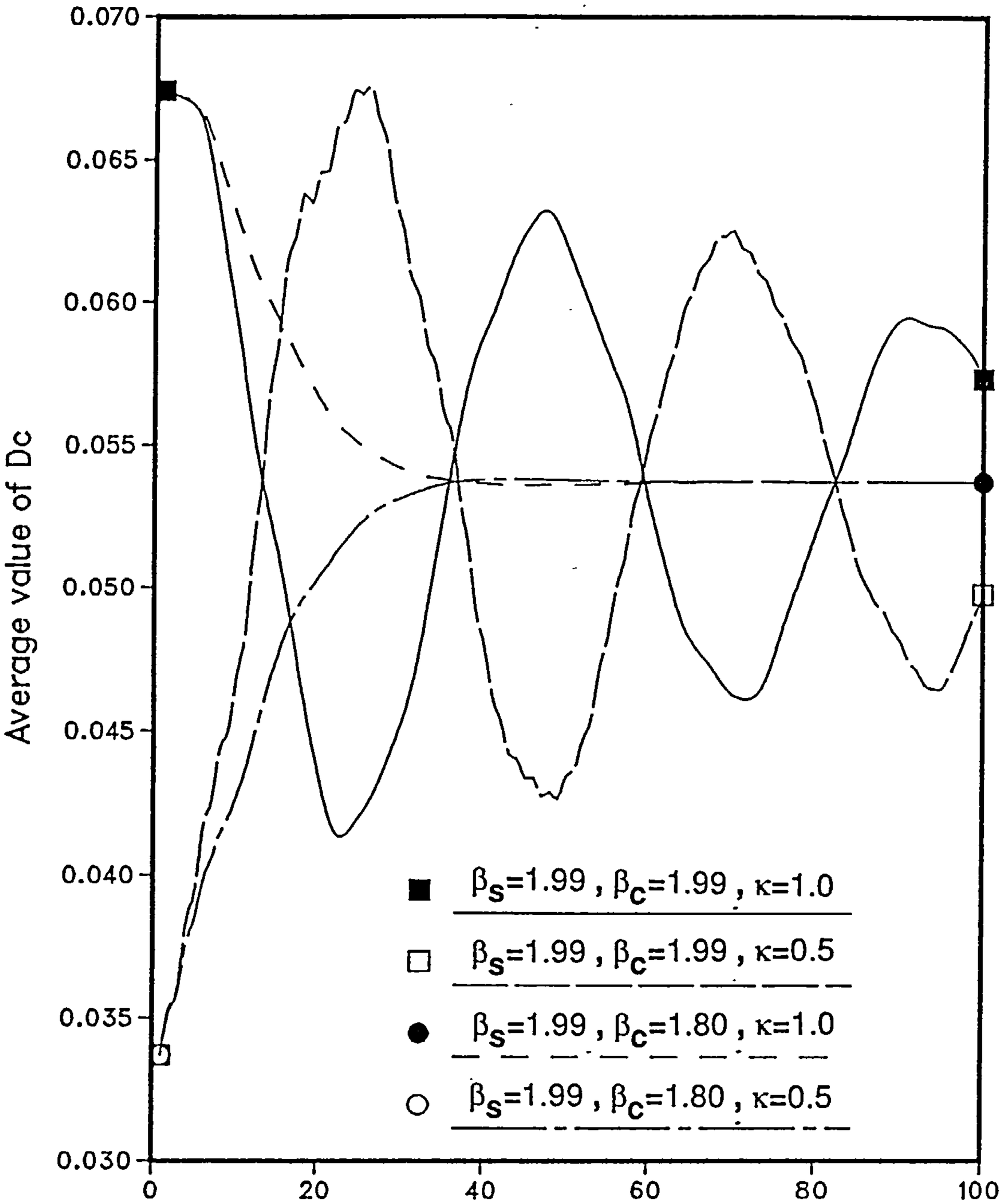

Figure (4.8) - Convergence of the solution for the cantilever in figure (4.1) using different values of β_c, β_s and κ.

4.4.2.4 Conclusion

This method has been examined thoroughly. Very great effort was put into the method. Different approaches to improve the solution have been implemented. The results were always studied thoroughly which included calculating the first and the second differences of the concrete and the steel solutions, studying bond forces convergence, the different methods of applying β_s and β_c, effect of different κ values and physical interpretations of the results.

The number of iteration required for the convergence of the beam solution is always 50 or more which is very high. The amount of arithmetic operations for the 50 iterations is not any better than the direct solution . Different accelerating factors have to be used . It was always a difficult problem to find a method for determining the accelerator parameters. The displacements changed very little at each iteration suggesting that the left hand side of equation (4-3) included excessive stiffness. This suggested an alternative described next

4.4.3 Adopted method of solution

4.4.3.1 The method

It was shown in the previous section that when the stiffness terms of the bond matrix was added to both the steel and the concrete matrices the extra stiffness have caused the convergence of the method to be extremely slow. Also it was shown that by starting the iteration solution with a concrete displacement obtained from the solution of $[K_c] . [D_c] = [P_c]$, the convergence of the solution is improved .

These observations led to rearranging the equations of solution presented in the form given by equations (4-2) such that the extra stiffness coming from bond terms can be removed from the concrete stiffness matrix. This can be achieved using the following iteration scheme which is yet another way of representing a solution to equations (3-22) :

$$[K_c] . [D_c^{i+1}] = [P_c] - ([K_B] . [D_c^{i}] - [C]^t [K_b] . [D_s^{i}]) \quad (4\text{-}9a)$$

$$[K_s + K_b] . [D_s^{i+1}] = [P_s] + [K_b] . [C] . [D_c^{i+1}] \quad (4\text{-}9b)$$

Before the iteration solution starts $[K_c]$ is assembled and reduced to banded lower triangle matrices once only . The same thing is also done to $[K_s+K_b]$.

The iterative solution of the above arrangements is summarised in the following steps :

1) Total load is applied to the structure so

$[P_c]$ = full load applied to concrete

or $[P_s]$ = full load applied to steel

2) Solution starts with an initial value of zero deformations for all the concrete and the steel starting solutions or

$$[D_c^0] = 0$$

and $[D_s^0] = 0$

3) Total forces on concrete are calculated and applied according to

$$[P_c] - ([K_B] . [D_c] - [C^t] . [K_b] . [D_s])$$

by substituting the previous obtained values of D_c and D_s

for the first iteration this will reduce to $[P_c]$.

4) Concrete solution is obtained due to the load calculated in step 3 and using the reduced form of $[K_c]$

It is noted here that in the first iteration the solution of $[D_c]$ is identical to that obtained by equation (4-7).

5) Total forces on steel are calculated according to

$$[P_s] + [K_b] . [C] . [D_c]$$

using the concrete deformations obtained in step 4.

6) Steel solution is obtained due to the load as calculated in step 3 and using the reduced form of $[K_s + K_b]$.

Steps 3 through 6 are repeated until the change in the solution becomes sufficiently small .

4.4.3.2 Convergence Criterion

The convergence of the solution can be examined from the behavior of the concrete displacements, the steel displacements or the bond forces calculated in every iteration. The three quantities depend on each other. Experimentation have shown that the the concrete displacements are the most sensitive indicator of convergence.

The measure used for judgement of convergence is the sum of the absolute values of the concrete displacement for all degrees of freedom

i.e.

$$((\Sigma \mid D_c \mid) / TDOFC)$$

The iteration is stopped when the maximum change in any value of the concrete displacement is less than a specified tolerance (λ)

$$\frac{(\mid D_c^{i} \mid - \mid D_c^{i-1} \mid)_{max}}{\mid D_c^{i} \mid} < \lambda$$

Where the value of the tolerance (λ) is set to

$$\lambda = 1 / 1000$$

This means that iteration cycle is stopped when the change in every element of [D_c] is less than one thousandth of its current value.

4.4.3.3 Convergence of the method

The solution obtained this way converges extremely rapidly . The convergence for the beam problem defined in section (4-2) and solved by the previous method converges now in 13 iterations where it needed several hundreds of iterations by the previous method.

The way the solution converges is in an oscillatory manner as shown in figure (4-9). The reason for this can be seen from the physical interpretation of equations (4-9). In equation (4- 9a) the applied loads and the bond interforces act on the concrete alone without any stiffening by the steel or the bond, leading naturally to displacements which are too large . This leads in turn to too large an estimate of the bond interforces in equation (4-9b) and to steel displacements which are too large. By comparing figures (4.5) and figure (4.9) the great improvement obtained using this method over the previous method is quite clear. In the earlier method the concrete matrix was over stiffened by including the bond component.

4.4.3.4 Damping factor (α)

In the previous method an over-relaxation factor was needed to speed up the convergence of the method. In this method although the convergence was quite rapid it may still be improved by the relaxation method using an under-relaxation, or damping, factor. It is quite simple to calculate automatically a damping factor

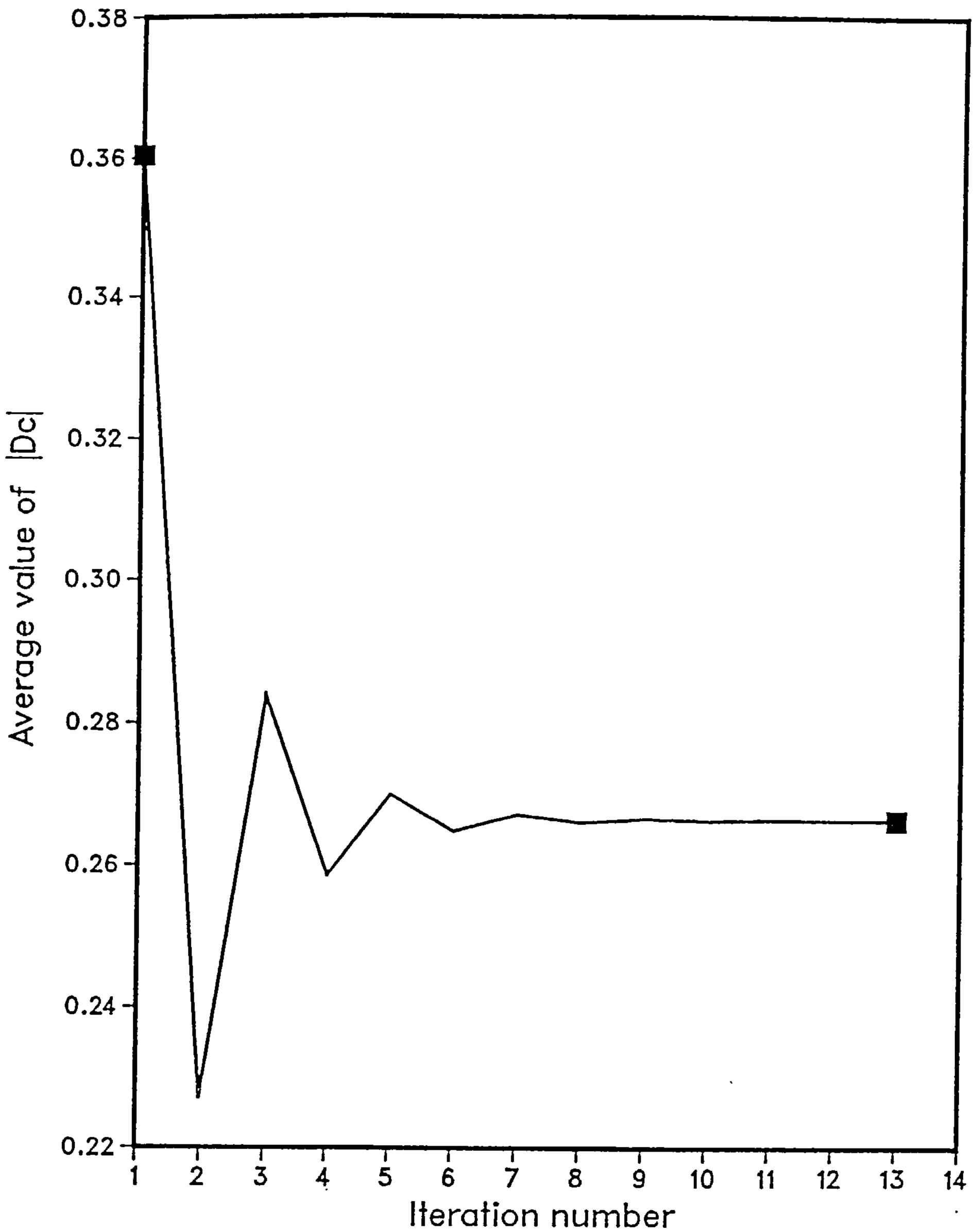

Figure (4-9) - Convergence of the adopted method of solution.

alpha (α) which allows for the extra stiffening due to steel. The value of *alpha* is to relate the calculated value of the concrete displacement to the " exact " value " $D_{c,exact}$ " . Thus the concrete displacements caused by each increment of force are reduced by multiplying by a constant damping factor *alpha* of less than one ($1.0 < \alpha$) in order to correct concrete displacements .

The value of *Alpha* can be derived from the first two undamped iterations alone , by considering what value is needed to yield the exact solution . The following derivation of *alpha* is presented :

If [D_c^1] is the concrete deformation after one undamped iteration then the exact deformation is obtained by multiplying by α or

$$[D_{c,exact}] = \alpha \cdot [D_c^1] \qquad (4\text{-}10a)$$

After two undamped iterations the concrete displacement is [D_c^2] and thus the exact deformation is

$$[D_{c,exact}] = [D_c^1] + \alpha \cdot ([D_c^2] - [D_c^1]) \qquad (4\text{-}10b)$$

By solving equations (4-10a) and (4-10b) simultaneously for the value of *alpha* that will yield

$$\alpha = \frac{\Sigma | D_c^1 |}{2 \cdot \Sigma | D_c^2 | - \Sigma | D_c^1 |} \qquad (4\text{-}11)$$

The superscripts 1 and 2 refers to the iteration number

Note that the sum of all degrees of freedom of the concrete displacement have been used instead of using individual concrete displacements. This is because a constant factor alpha will be applied to all concrete displacements which was found to be very effective otherwise a number of alphas corresponding to TDOFC have to be used.

The *alpha* factor will be used for all iterations starting by the values obtained in the second iteration [D_c^2] . The application of this factor is illustrated here

$$[D_c^i] = [D_c^{i-1}] + \alpha . ([D_c^i] - [D_c^{i-1}]) \qquad (4\text{-}12)$$

The complete iterative process is summarised in flowchart (4-2). The convergence of the solution of the beam problem is now obtained in 6 iterations using this process . Figure (4-10) shows the effect of applying the damping factor on the convergence of the beam problem.

4.4.3.5 Another form for applying the *Alpha* factor

Another method for applying the *alpha* factor defined by equation (4-11) can still be implemented using the same idea when deriving α factor the purpose of which is to seek a faster convergence method . In this new method also the concrete displacements caused by each increment of force are reduced and that by applying

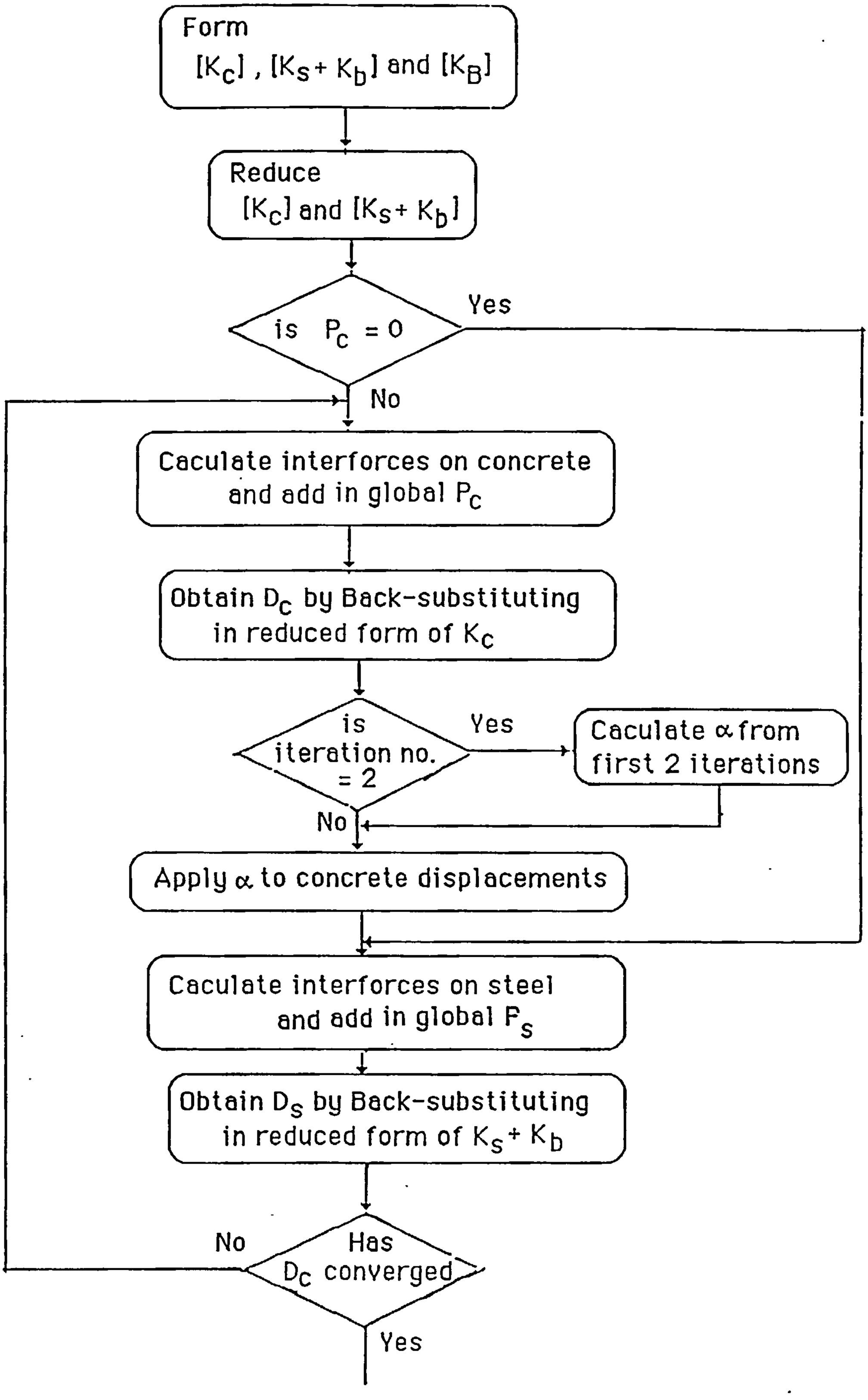

Flowchart (4.2) - Adopted Method of Iteration

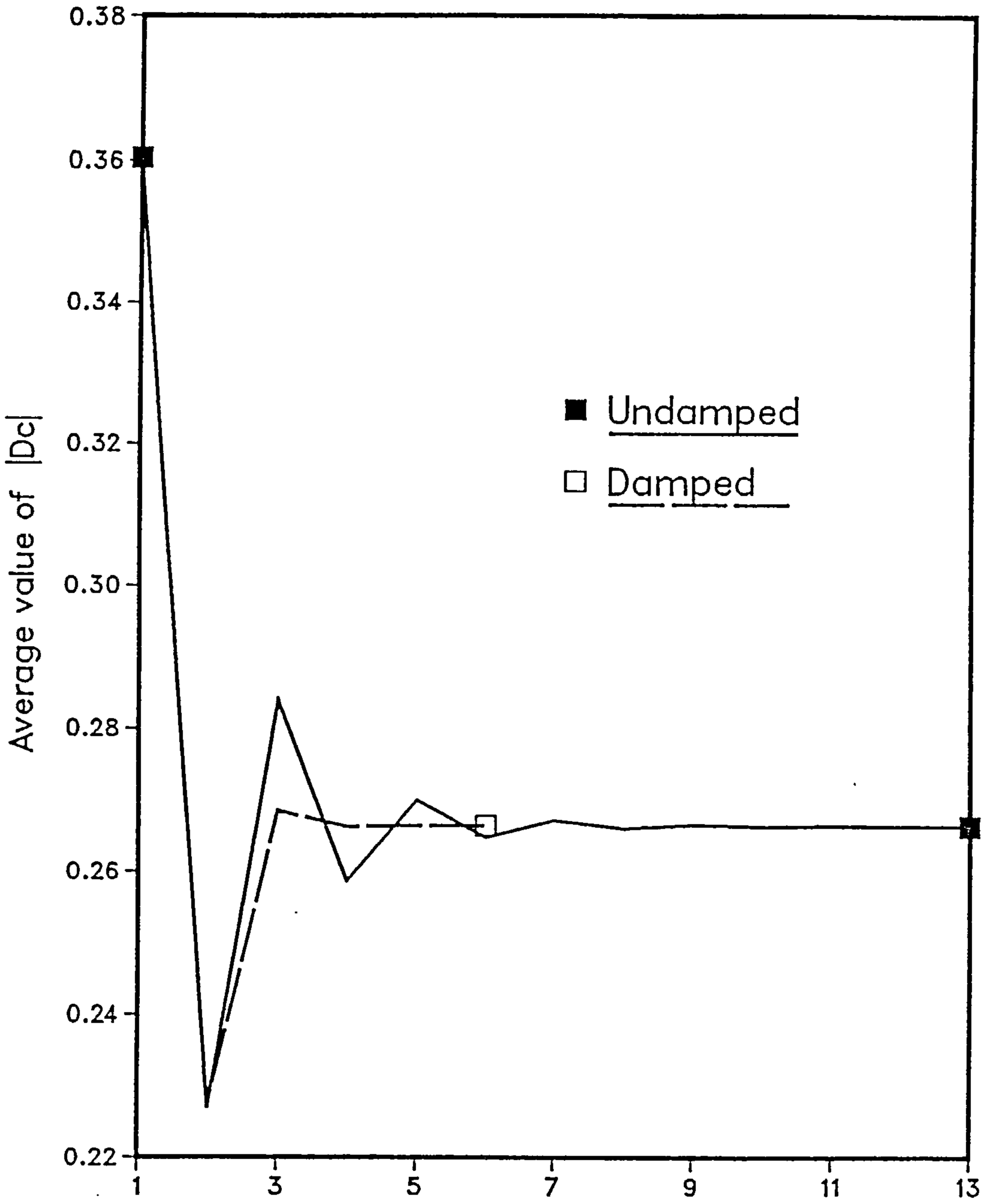

Figure (4-10) - Effect of applying the damping factor (α) on the convergence of the adopted method.

alpha in a different form. Alpha is assumed to be effective starting from the first iteration cycle. The argument for this application is illustrated here

In the second iteration D_c^2 is calculated from

$$[D_c^2] = [D_c^1] + \alpha . ([D_c^2] - [D_c^1]) \qquad (4\text{-}13a)$$

But this is also adjusted by α giving

$$[D_c^2] = \alpha [D_c^1] + \alpha ([D_c^1] + \alpha \{[D_c^2] - [D_c^1]\} - \alpha [D_c^1]) \qquad (4\text{-}13b)$$

leading to

$$[D_c^2] = \alpha [D_c^1] + \alpha [D_c^1] + \alpha.\alpha [D_c^2] - \alpha.\alpha [D_c^1] - \alpha.\alpha [D_c^1]$$

or

$$[D_c^2] = 2\alpha [D_c^1] - 2\alpha . \alpha [D_c^1] + \alpha . \alpha [D_c^2]$$

$$[D_c^2] = 2 \alpha (1- \alpha) [D_c^1] + \alpha . \alpha [D_c^2] \qquad (4\text{-}14)$$

By presenting it in general terms the following form is obtained

$$[D_c^i] = 2 (\alpha - \alpha^2) . [D_c^{i-1}] + \alpha^2 . [D_c^i] \qquad (4\text{-}15)$$

Application of *alpha* in this form to the beam and the cantilever problems of section 4.2 are illustrated in table (4.1) which shows the concrete average deformations as obtained by applying the damping factor in the two forms. The convergence of the solution

Problem Solved	Iteration Number	$D_c^i = D_c^{i-1} + \alpha (D_c^i - D_c^{i-1})$		$D_c^i = 2\alpha (1 - \alpha) D_c^{i-1} + \alpha^2 D_c^i$	
		$(D_c^i - D_c^{i-1})_{max} / D_c^i$ occurs at		$(D_c^i - D_c^{i-1})_{max} / D_c^i$ occurs at	
		d.o.f #	Value	d.o.f #	Value
Beam Problem Figure (6.1)	1	84	1.0	84	1.0
	2	84	0.56	84	0.56
	3	84	0.018	84	0.016
	4	84	0.00297	84	0.00229
	5	84	0.00015	84	0.000512
	6	84	0.000048	84	0.0001
	7	84	0.000007	84	0.000023
Catilever Problem figure (4.1)	1	120	1.0	120	1.0
	2	120	0.41	120	0.407
	3	120	0.035	120	0.0261
	4	120	0.0041	120	0.00259
	5	120	0.00032	120	0.00082
	6	120	0.000054	120	0.00014
	7	120	0.0000013	120	0.000032

Table (4-1) - Effect of the method of application of (α) on the convergence of the solution

did not improve. The first form of applying α requires less number of iterations to obtain a solution for the beam problem. The same thing is noted in the convergence for the cantilever problem. Since no improvement has been obtained then it is recommended to use the first form which does not include α square term.

4.4.3.6 Comments on the method

The method discussed in this section has shown considerable improvement over the method discussed in section (4.3) i.e. figures (4.5) and (4.9).

It is appropriate here to make some comments on the computations involved in the iterative method.

First, it should be noted that the matrix $[K_s + K_b]$ is a tri-diagonal matrix with a half-band width of only two and also that it can be created directly from the reinforcement and bond data without the overheads of the conventional assembly process. This is made possible because the steel nodes are numbered independently of the concrete degrees of freedom. $[K_s + K_b]$ is assembled for all steel bars. It is, of course , symmetrical and so its reduction by Choleski is very simple.

Secondly, it is also not necessary to assemble the bond matrix $[K_B]$. It can be more efficiently left as element related matrices.

Thus, the term $[C_e]^t.b.\ [C_e]$ is calculated for every steel node within the element and assembled in the element $[K_{Be}]$. Also it is not necessary to assemble the bond matrix $[K_b].[C]$. It can be more efficiently left as terms related to steel nodes i.e. $b.C_{ej}$. All the operations in equations (4-9) can then be performed on those matrices by selecting the relevant displacements from $[D_c]$ and $[D_s]$ according to element node numbers .

Third, another obvious point to be discussed is that the left hand side matrices $[K_c]$ and $[K_s + K_b]$ of equations (4-9) need be reduced to banded lower triangular matrices once only at the start of the iterative cycles. Because of the form of $[K_s + K_b]$ this is a trivial operation and the computational effort is principally that of assembling and reducing $[K_c]$.

Finally, the back-substitutions through the reduced $[K_c]$ needed in equations (4-9) makes little contribution to the solution time .
The amount of computation involved in the solution of this method can be summarised in the following steps :

1) reduction of $[K_c]$

2) reduction of $[K_s + K_b]$

3) performing the multiplication $[C_e]^t.\ [K_{be}]\ .\ [C_e]\ .\ [D_e]$ repeated NCE times. The element bond matrix $[C_e]^t.\ [K_{be}].\ [C_e]$ is performed once before the iteration process. For 2 dimensional

8-noded concrete element this matrix dimension is 16 by 16.

4) Back-substitutions through the reduced $[K_c]$ to obtain $[D_c]$

5) Performing the multiplication $[C]^t$. $[K_b]$. $[D_s]$. The multiplication $[C]^t$. $[K_b]$ is performed once before the iteration process. $[D_s]$ size is the same as TDOFS.

6) back substitutions through the reduced (K_s+k_b) to solve for $[D_s]$

Steps 3 through 5 are repeated for the number of iterations needed.

Comparison with the Direct Solution

The amount of calculations needed for the solution of the beam problem based on a direct method of solution have been done in section 4.3. The amount of multiplications/divisions operations required for this same problem based on the iterative method as in the above steps is estimated to be 180,000 operations for the six iterations when having 41 nodes for each of the tension and compression reinforcement and 5 steel nodes for each stirrup. Comparing this figure with the one needed for the direct solution which is approximately 1.1 million operations shows that the iteration method is more efficient.

Further, when the number of steel nodes in every stirrup is increased to 9 instead of 5 the amount of calculations for the iterative method is approximately 220,000 while in the direct solution the number of operations was approximately 3 million

operations.

Therefore, the increase in the number of steel nodes which is expected to improve the solution for the steel have very little influence on the amount of calculations and thus computer time when using the iterative method.

Example of computer time

The computer time needed for the solution of this problem starting from reading the input data stage up to obtaining the complete solution is 55 seconds of computer CPU time using Multics system.

4.5 Anchorage by applying an external force

4.5.1 General

The idea of steel anchorage has already been discussed in section (3-5) and it was found that anchorage can be modelled either by

i) Using a high value for the bond stiffness parameter, or

ii) by applying an external force to the concrete at the point which is to be anchored. The first method is straightforward since it only requires setting the spring stiffness at the point to be anchored to a very high value which may be a thousand times or more higher than the regular value. However the second method of steel anchorage involves an iterative process as discussed in section (3-6) and it's implementation is demonstrated here.

The iteration for anchorage can be easily adopted within the overall iteration process for the solution of the system equations. In this way the iteration process will serve two purposes.

The implementation of the method within the iterative solution is summarised in the following steps :

1) Solving for concrete displacements.

2) Obtaining concrete displacements at the position of the anchored nodes using current concrete values and equation (3-11)

3) Solving for steel displacements.

4) Getting current steel displacements of the anchored nodes.

5) Calculating Δ from steps 2 and 5 for each anchored node.

6) Knowing Δ, f_{bs} and f_{bc} can be calculated according to equations (3-24) and then applied to the structure.

All above steps are repeated until Δ becomes sufficiently small. Thus the iterative process adjusts the values of the concrete and the steel displacements at the point of anchorage to satisfy equation (3-1).

4.5.2 Calculation of development length

The calculation of f_{bs} is obtained from an assumed value given for the development length (l_d) to start with.

The value of l_d is entered in the input data. Length of l_d entered may be larger or smaller than the required length for anchorage. The exact length can be calculated in the second iteration by noting the following :

1) In the first iteration Δ is obtained before applying any external load i.e. Δ_1 is obtained when $f_{bs0} = 0$ is applied.

where f_{bs0} is the initial external force on steel.

2) In the second iteration Δ_2 is obtained after applying f_{bs1}.

where f_{bs1} is the external force on the steel applied at the end of the first iteration of the solution.

Figures (4-11) shows the two possible cases

i) when f_{bs1} is larger than the required value causing the anchored steel node to be pulled in the opposite direction figure (4-11a)

ii) when f_{bs1} is smaller than the required force for anchorage so Δ is reduced a little but not small enough figure (4-11b).

$F_{bs,exact}$ (f_{bse}) which will cause Δ to be zero can be calculated from figures (4-11). The two figures will lead to the following relationship

$$F_{bs,exact} = f_{bs0} + \frac{\Delta_1}{\Delta_1 - \Delta_2} (f_{bs1} - f_{bs0})$$

but $f_{bs0}=0$

let $$\omega = \frac{\Delta_1}{\Delta_1 - \Delta_2}$$

leading to

$$f_{bse} = \omega \; f_{bs1}$$

The value of ω can be applied from the second iteration. Flowchart (4-3) shows the application of this anchorage method within the iterative method of solution.

Anchorage is achieved when the maximum value of Δ for all steel nodes is less than some tolerance. The tolerance value is chosen arbitrarily to be 10^{-6} mm. Therefore if the relative displacement between the anchored steel node and the surrounding concrete is less than the above tolerance then anchorage is successful. Actually, as will be see in chapter 6, a much smaller value for Δ than the above specified tolerance is reached by the end of the iterative solution of the system equations and no need for further iterations to achieve anchorage.

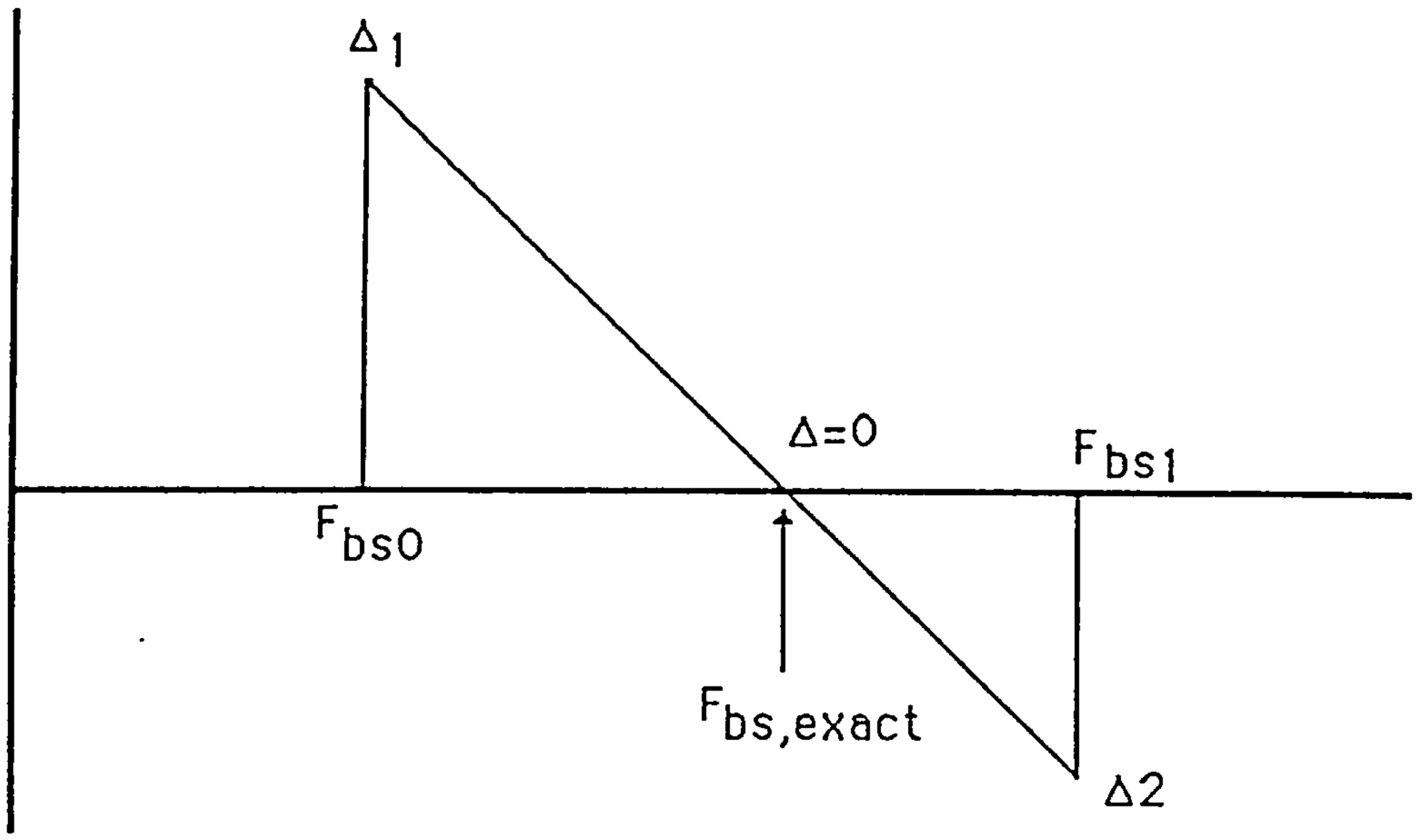

(a) - Effect of large external applied force

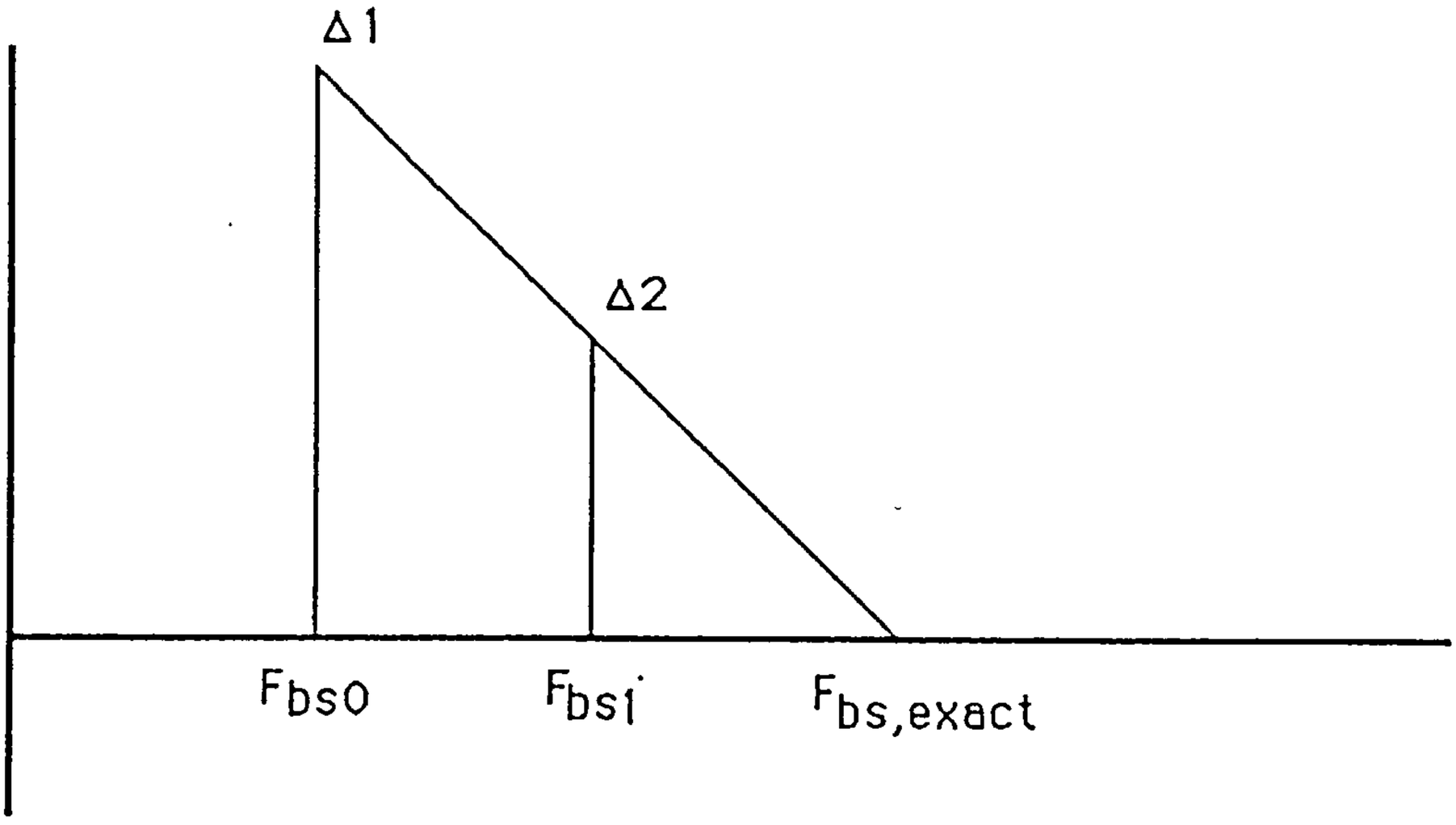

(b) - Effect of small external applied force

Figure (4-11) - Calculation of External Force Nedded For Reinforcement Anchorage

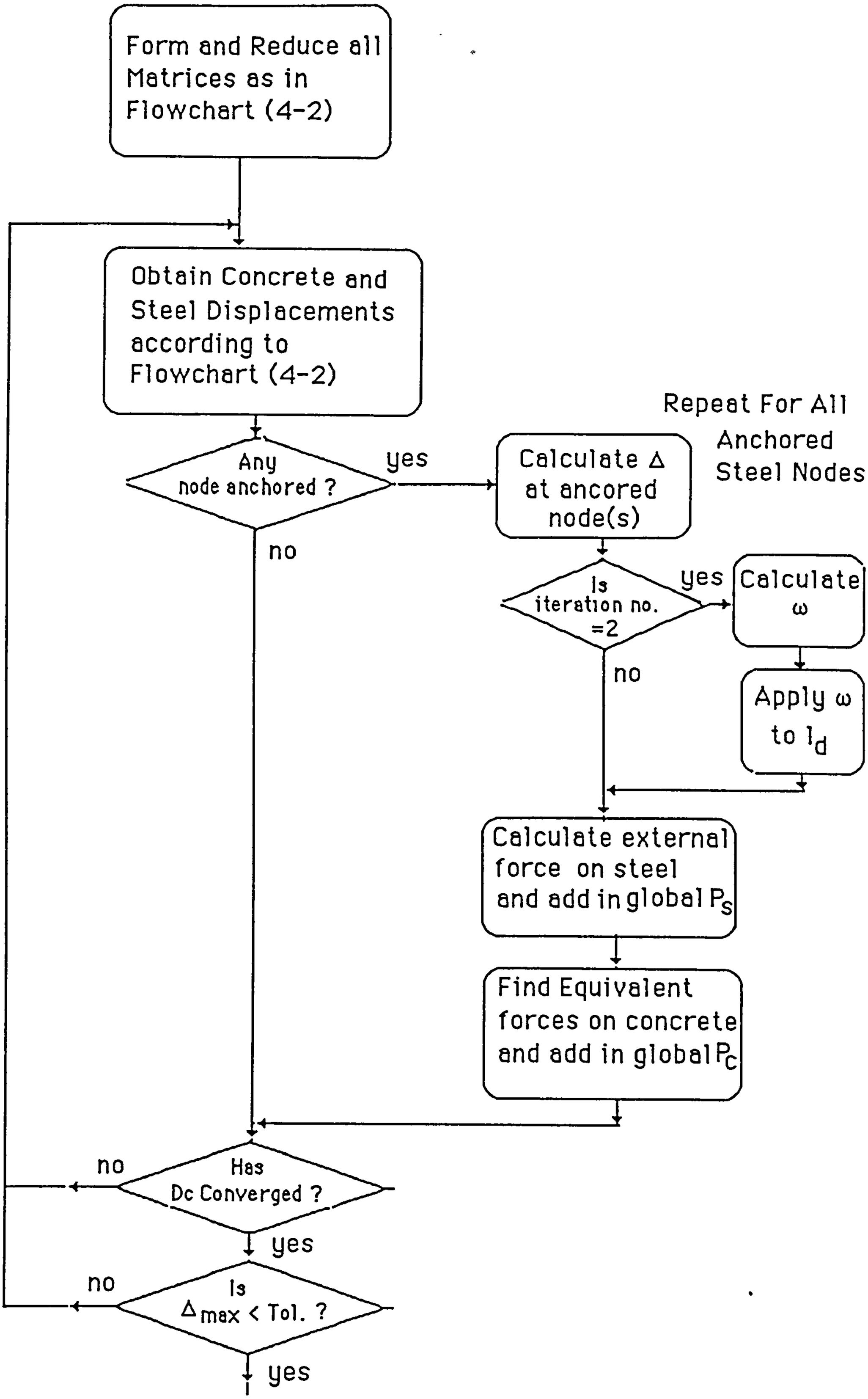

Flowchart (4-3) - Inclusion of the iterative method for anchorage within the iterative method of solution

4.6 Summary

Methods for solution of the system equations derived in chapter 3 is presented in this chapter. Direct method of solution was discussed. Two iterative methods were studied thoroughly. The first iterative method examined was not successful although great effort was put into improving the method, it is very slow and needs several accelerating parameters to improve the convergence rate. Another iterative method was examined and it was found to converge extremely rapidly. It showed several advantages over the other methods and therefore is adopted. The advantages of the method adopted is :

i) The method convergences quite rapidly

ii) It is quite efficient as compared to the direct solution

iii) The damping parameter needed for accelerating convergence can be calculated automatically within the method.

The method of anchoring steel by applying an external force was demonstrated.

Some results will be given in chapter 6.

Chapter 5

5. NON-LINEAR BEHAVIOUR OF CONCRETE, STEEL AND BOND

5.1 Introduction

A new method for modelling of reinforcement and bond between concrete and reinforcement in finite element analysis of reinforced concrete was derived in chapter 3. As already pointed out the approach taken in the development of the theory is through the simplest possible constitutive laws for the concrete and reinforcing steel which may be used to describe the behaviour of each material. Thus simple linear elastic stress-strain relationship for the two materials and for bond have been used. Analysis of reinforced concrete using an assumed linear behaviour of its constituents may be true at low level of loading. However the actual behaviour of the two materials and of bond between the two materials at general loading levels is more complex especially for concrete. In fact an accurate analysis of reinforced concrete is made complicated by a number of factors among which are the following factors :

1. The non-linear stress-strain relationship of concrete.
2. The nonlinear bond stress-slip relationship.
3. Yielding of steel.
4. Cracking of concrete under increasing load.
5. Crushing of concrete.
6. Local failure of bond.
7. Effect of dowel action in the steel reinforcement.

Including nonlinear material behaviour in the method of solution is discussed in chapter 7 and is demonstrated for nonlinear bond behaviour.

In this chapter the constitutive laws of concrete and steel presented in literature will be reviewed briefly. Also, the constitutive laws used for the two materials in this thesis will be explained. Experimental work on bond is reviewed. Nonlinear bond stress-slip relationship is discussed.

5.2 Concrete

5.2.1 Brief review of concrete behaviour

Concrete is an inhomogenous anisotropic material whose characteristics change with load level and the length of load application. Stress strain relationship for concrete is strictly nonlinear. Much effort is continually directed towards investigations of different constitutive relationships for concrete. Investigations into the stress-strain relationship of concrete have been directed to the three known formulations namely uniaxial, biaxial and triaxial formulations.

Figure (5.1) shows a typical stress-strain curve for the case of uniaxial loading of concrete. A brief survey of the formulation of the stress strain relationships of concrete under uniaxial loading is given by Popvics (1970). The literature of Chen, C. T. and Chen W. F. (1975) gives a summary of the results for biaxial and triaxial stress states. Figure (5.2) illustrates the strength failure envelope for the case of biaxial loading. The figure shows relationships obtained by several authors. The shape of the failure surface in triaxial stress state is approximately as shown by figure (5.3) which is reported in the literature of Chen, C. T. and Chen W. F. (1975).

Representation of nonlinear stress-strain relation of concrete in finite element analysis of reinforced concrete can be based on any of the above presented formulations. Constitutive relationships are normally stated in matrix form to be suitable for finite element analysis. A constitutive relationship for the uniaxial

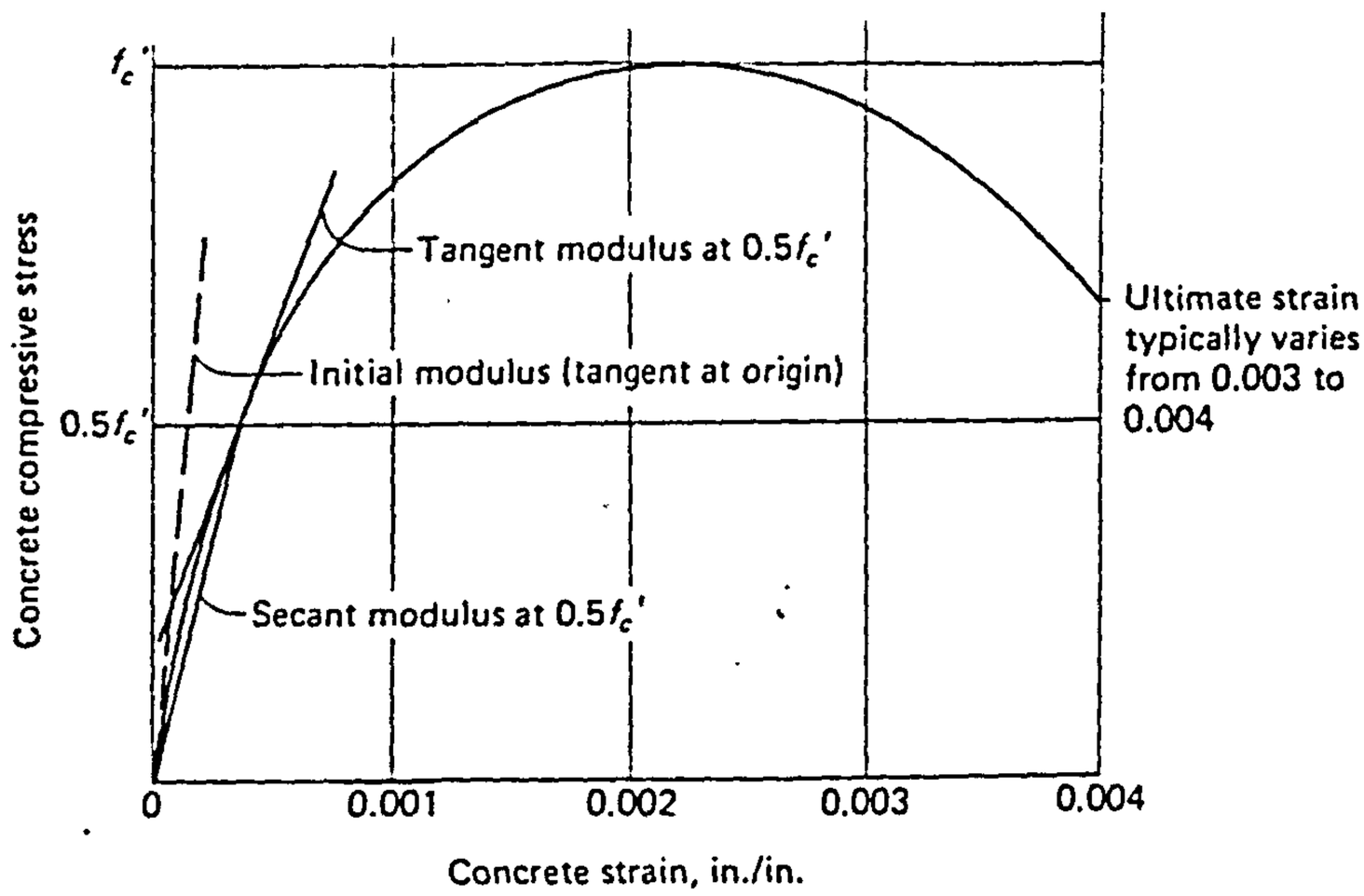

Figure (5.1) - Typical Stress-Strain Curve for Concrete in compression, after Wang and Salmon (1985).

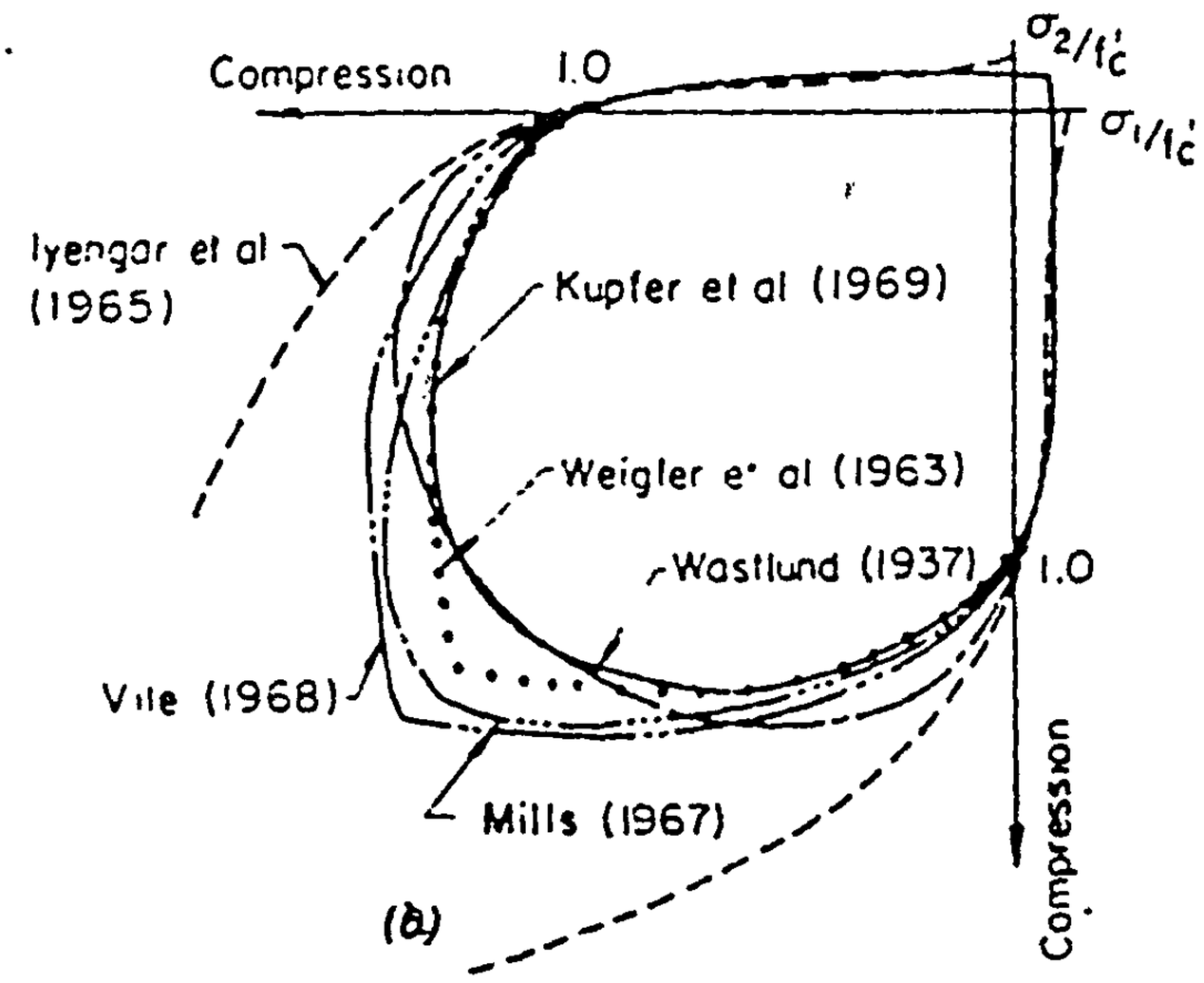

Figure (5.2) Failure Envelope in Biaxial Stress State, after Chen C. T. and Chen W. T. (1975).

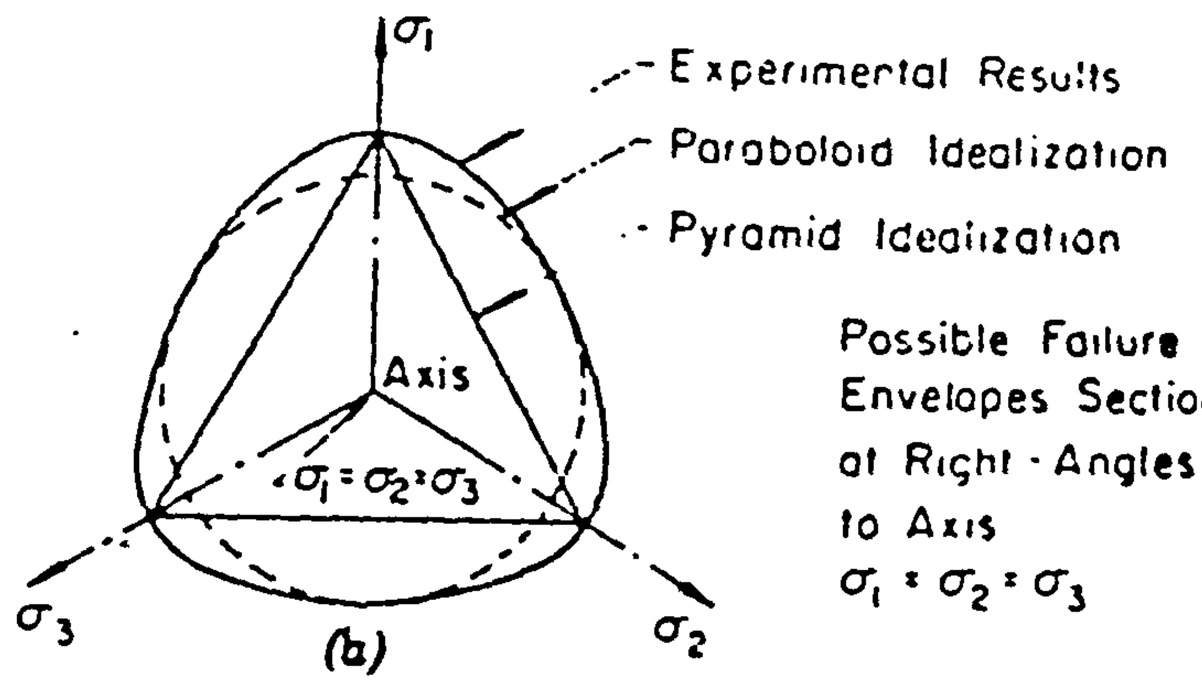

Figure (5.3) Failure Envelope in Triaxial Stress state, after Chen C. T. and Chen W. T. (1975).

stress-strain relationship is found for example in the work of Saenz (1964). A constitutive relation for an elastic orthotropic material in biaxial stress for example can be found in the work of Liu et al.(1972). Other forms of concrete stress strain relations for biaxial state is given by Kupfer and Gerstle (1973) and Darwin and Pecknold (1977). An analytical form of the stress strain strain relation for concrete in triaxial state is proposed by Ahmad and Shah (1982) and by Chen, C. T. and Chen W. F. (1975).

It is appropriate to comment here on the difference between using a linear elastic model for concrete versus using a concrete model based on biaxial formulation. Using the linear elastic relationship places no limit on compressive or tensile stresses which may be carried by the concrete, while the failure strength envelope will allow only realistic compressive and tensile stresses to be carried by the concrete. Also, higher stresses are predicted by linear analysis as compared to non-linear analysis. However the linear elastic relationship holds for stresses up to 30% of the ultimate strength of concrete. Also in tension concrete behaves in a linear elastic manner.

Cracking of Concrete:

Cracking is an essential effect of the inelastic behaviour of concrete. Including cracks of concrete in the analysis of reinforced concrete is very important to accurate modelling of concrete. Effect of cracks in finite element analysis of concrete can be included at locations when tensile failure condition of concrete is met.

5.2.2 Concrete constitutive laws

In the previous section the constitutive laws governing the behaviour of concrete available in literature were explained. However in the model developed in this work concrete behaviour is simplified by assuming linear elastic stress strain relationship. Also, cracks which develops in concrete are not handled. The three dimensional state of stress of a reinforced concrete structure is approximated by two dimensional analysis.

Concrete stresses are defined by:

$$\sigma = \begin{bmatrix} \sigma_x \\ \sigma_y \\ \tau_{xy} \end{bmatrix}$$

where

σ_x , σ_y are the normal stresses in the x and y directions

τ_{xy} is the shearing stress

The corresponding strains are defined by

$$\varepsilon = \begin{bmatrix} \varepsilon_x \\ \varepsilon_y \\ \gamma_{xy} \end{bmatrix} = \begin{bmatrix} \partial/\partial x & 0 \\ 0 & \partial/\partial y \\ \partial/\partial y & \partial/\partial x \end{bmatrix} \cdot \begin{bmatrix} u \\ \\ v \end{bmatrix}$$

where

ε_x ε_y are the normal strains in the x and y direction

γ_{xy} is the shearing strain

u, v are the displacements in the x and y directions.

For uncracked, isotropic material the stress-strain relationship is given by

$$\sigma = D \varepsilon \qquad (5.1)$$

where D is the elasticity matrix

i) For plane stress D is defined by

$$D = \frac{E}{1-\nu^2} \begin{bmatrix} 1 & \nu & 0 \\ \nu & 1 & 0 \\ 0 & 0 & (1-\nu)/2 \end{bmatrix} \qquad (5.2)$$

ii) For plane strain D is defined by

$$D = \frac{E}{(1+\nu)(1-2\nu)} \begin{bmatrix} 1-\nu & \nu & 0 \\ \nu & 1-\nu & 0 \\ 0 & 0 & (1-2\nu)/2 \end{bmatrix} \qquad (5.3)$$

Where

E is the uniaxial elastic modulus

ν is Poisson's ratio

5.3 Steel constitutive law

Steel in reinforced concrete structures may be assumed to be loaded in direct tension or compression. Its behaviour can be adequately described by uniaxial stress strain curve. A typical stress-strain relationship of steel is shown in figure (5.4). Steel shows linear elastic relation for the first part of the curve. For any additional stresses beyond the yield stress steel shows plastic deformation. In the application of the method to reinforced concrete problems in chapters 6 and 8 steel is assumed to have yield stress of 400 MPa or 60,000 psi.

In this thesis steel behaviour is taken to be linear elastic and yielding of steel is not considered. This assumption is adequate for the solution of the reinforced concrete problems selected in this research.

The stress-strain relationship is given by :

$$\sigma = E_s \varepsilon \qquad (5.2)$$

where

ε is the axial strain in steel.

E_s is the elasticity modulus for steel.

Modulus of elasticity of steel is taken to be 200,000 MPa or 29,000,000 psi.

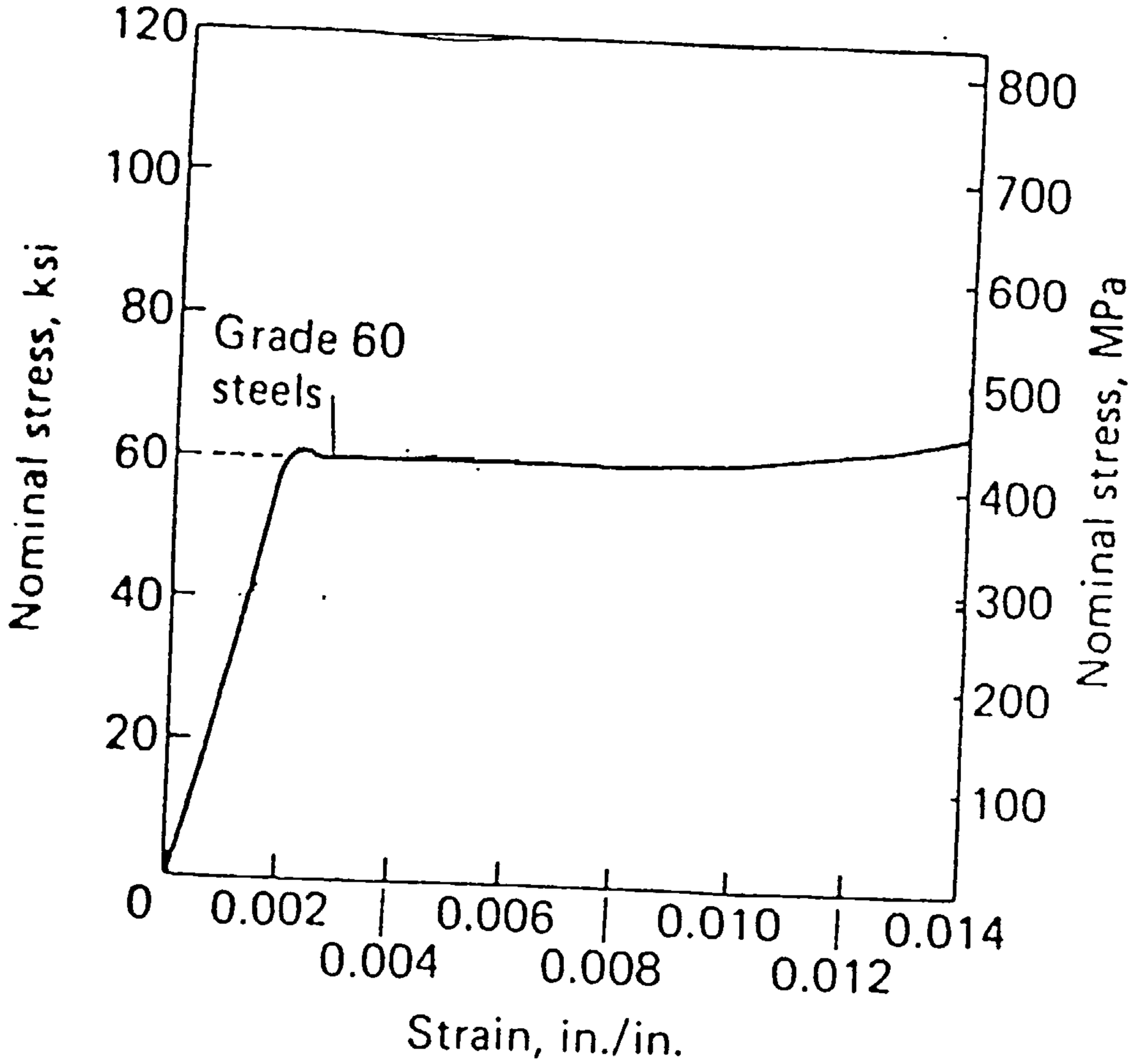

Figure (5.4) Typical Stress-Strain Curve for reinforcing steel in tension, after Wang and Salmon (1985)

5.4 Bond

5.4.1 A brief review of experimental work on bond

In chapter 2 a review of research on finite element analysis of reinforced concrete which include bond was presented. It was shown that bond stress-slip curve and the associated bond stiffness value are very often included in modelling of bond in finite element analysis. Further, bond stress-slip curves are obtained from experimental measurements of steel and concrete strain distribution along the steel concrete interface. Slip of an embedded bar over a given length is the total relative movements between the bar and the surrounding concrete over the given length. Experimental measurements of the slip along the concrete steel interface is a very difficult problem. In this section a brief review of experimental work done on the study of bond is presented.

Parsons (1984) literature on bond gives a comprehensive review on the experimental research on bond. Work on bond was started by Abrams (1913) who studied bond using plain and deformed bars in pull-out and beam tests. He found that bond resistance in deformed bars was greater than in plain bars. Glanville (1930) measured load distribution in the bar and published his theoretical and experimental results on bond. Clark (1946) and (1949) worked on different designs of deformed bars. Studying bond is normally done by attaching electrical strain gauges to bars embedded in concrete. This method of studying bond is found in the work of Wilkins (1951), Mains (1951), Peattie and Pope (1956), Perry and Thompson (1966) and Nilson (1972). Test results on pullout

specimens showed the great importance of the tubs in the outside surfaces of the bar on bond.

Mains (1951) used a steel bar with a built-in electrical strain gauges. This was done by cutting the bar longitudinally into two halves. In one half of the bar a groove was made to place the strain gauges then the bar was welded back into place. Specimens were used using plain and deformed bars. The results of tests indicated that stress magnitude and distribution in the reinforcement and bond stress affected by the cracks. Very high stress occurs near a crack. The bond stress distribution in the longitudinal direction was not uniform in pull-out test.

Peatte and Pope (1956) have studied the longitudinal steel stress in plain bars for pull-out and torsion tests. Strain gauges were mounted in longitudinal slots on the bar. A theoretical analysis of the pull-out test was developed and was based on adhesion, friction and bearing. In the adhesion stage the steel stress is in proportion to the applied load and the distribution of load is exponential until a critical strain in the concrete develop then rupture of adhesion occurs at the loaded end and moves toward the unloaded end as applied load is increased. Parland (1957) performed experimental tests to determine the distribution of stress in steel. Perry and Thompson (1966) used a similar technique to Mains method to study the stress distribution at a crack in constant moment region of a reinforced concrete beam.

Tanner (1971) and Nilson (1972) have used a similar method to Mains for measuring internal strains in steel and strains in

concrete at the interface with steel by placing strain gauges on the steel surface. Thè internal displacement in the concrete and steel can be obtained from the strains. Slip at any point along the bar is obtained from the difference between the concrete and steel displacements. Thus the bond stress-slip relationship is obtained for any point along the bar. Experiments showed that the bond stress-slip relationship is not unique. and it depends upon the strength of concrete and the distance from the loaded end of the beam.

Tassios and Yannopoulos (1981) have observed that there is no unique relationship between bond stress and slip and that it changes with position. Dorr (1978) used bars with grooves milled on the outer surface of the specimen. The bond stress-slip was investigated and also the influence of hydrostatic pressure.

Allwood (1980) investigated the stress distribution in the reinforcement in a beam column connection by attaching the strain gauges to the polished outer surface of the steel. Allwood found that the steel stress distribution is different than that which is usually assumed in design. Spencer et al. (1982) studied the bond of deformed bars under cyclic loading using fibre reinforced concrete. They mounted the strain gauges in grooves on both sides of the bar.

Mechanism of bond

Experimental research work on bond studied the essential aspects of mechanism of bond. The bond action between reinforcing steel bars and concrete is made up of three components e.g. Lutz and Gergery (1967) :

1) Chemical adhesion.
2) Friction.
3) Mechanical interlock between concrete and steel.

Bond in plain bars depends mainly on adhesion and friction with some mechanical interlock due to roughness of bar surface while for deformed bars depends mainly on mechanical interlock which gives deformed bars superior bond strength.

5.4.2 Bond stress-slip relationship

Bond stress can be thought of as the shearing stress between reinforcing bar and the surrounding concrete. Bond stress-slip relationship is strictly non-linear and it varies with the position along the bar. Experimental results of bond stress-slip relationship are presented based on average or local values. To include such a relation in analysis by finite element method normally an average bond stress-slip relationship is used. Different relations are obtained by different investigators. The degree by which these results differs is illustrated in figure (5.5)

which shows the average bond stress-slip relationship obtained by a number of investigators. Figure (5.6) compares bond stress-slip relationship obtained by Allwood (1980) with results obtained by other investigators. Local bond stress-slip relationship is shown in figure (5.7) given by Nilson (1972). Figure (5.7) shows separate curves which are established at different distances from the end face of the specimen. Further, bond stress-slip relationship is affected by the lateral pressure between concrete and steel as shown in figure (5.8). The figure illustrates the effect of lateral pressure on bond strength from the results of two investigators.

The above bond stress-slip relationship shows clearly that the relationship is nonlinear. To incorporate such a relationship in finite element analysis Nilson (1968) used a third order polynomial to express the nonlinear bond stress-slip relationship based on experimental results. However very little work has been done in establishing a more detailed model that can describe the behaviour of different aspects of bond. One of such investigations is the model described by Allwood, Parsons and Robins (1984) which incorporates past relevant research on the behaviour of bond and which allows for the effect of lateral pressure between concrete and steel. The model is based on extending the concept of local ultimate bond strength to create a local bond stress-slip relationship depending on the radial interface pressure in concrete and steel as load is applied. The model is explained next in detail because it will be used for nonlinear behaviour of bond in chapter 7.

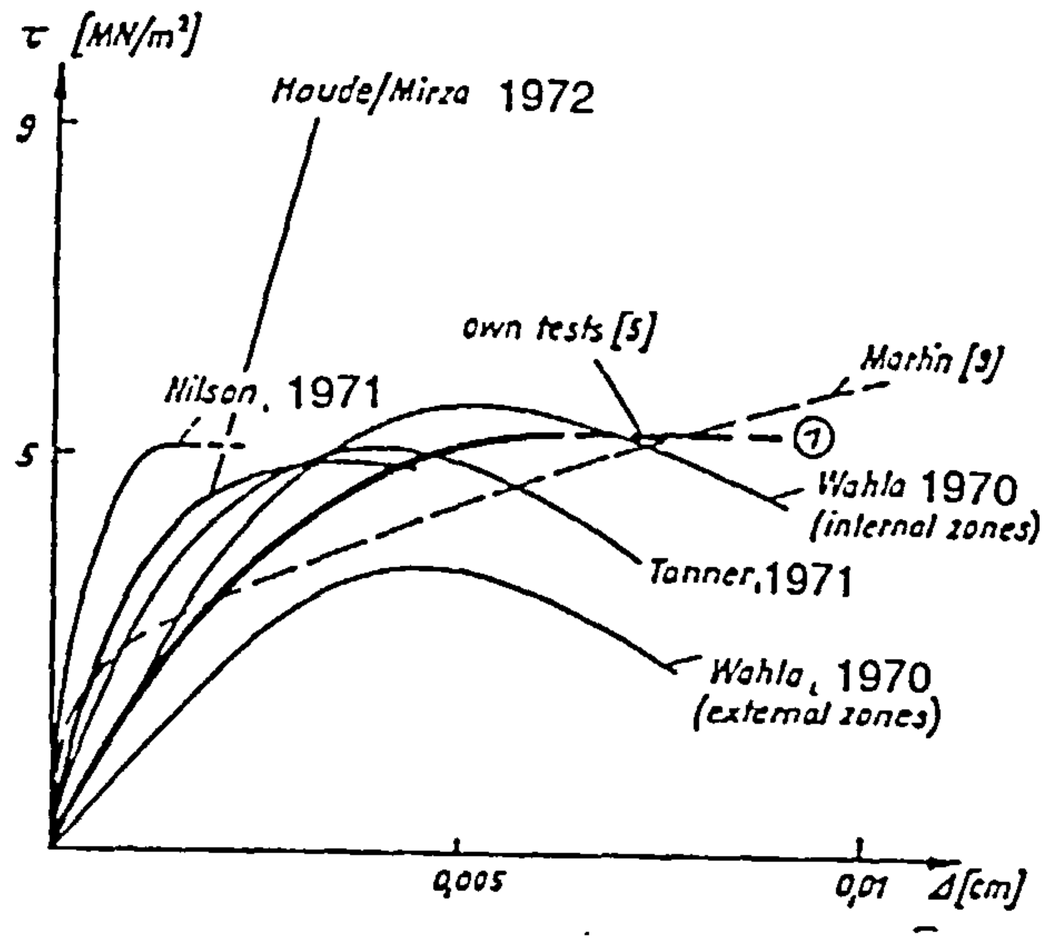

Figure (5.5) - Average bond stress slip relationships of different researchers, after Dorr(1978).

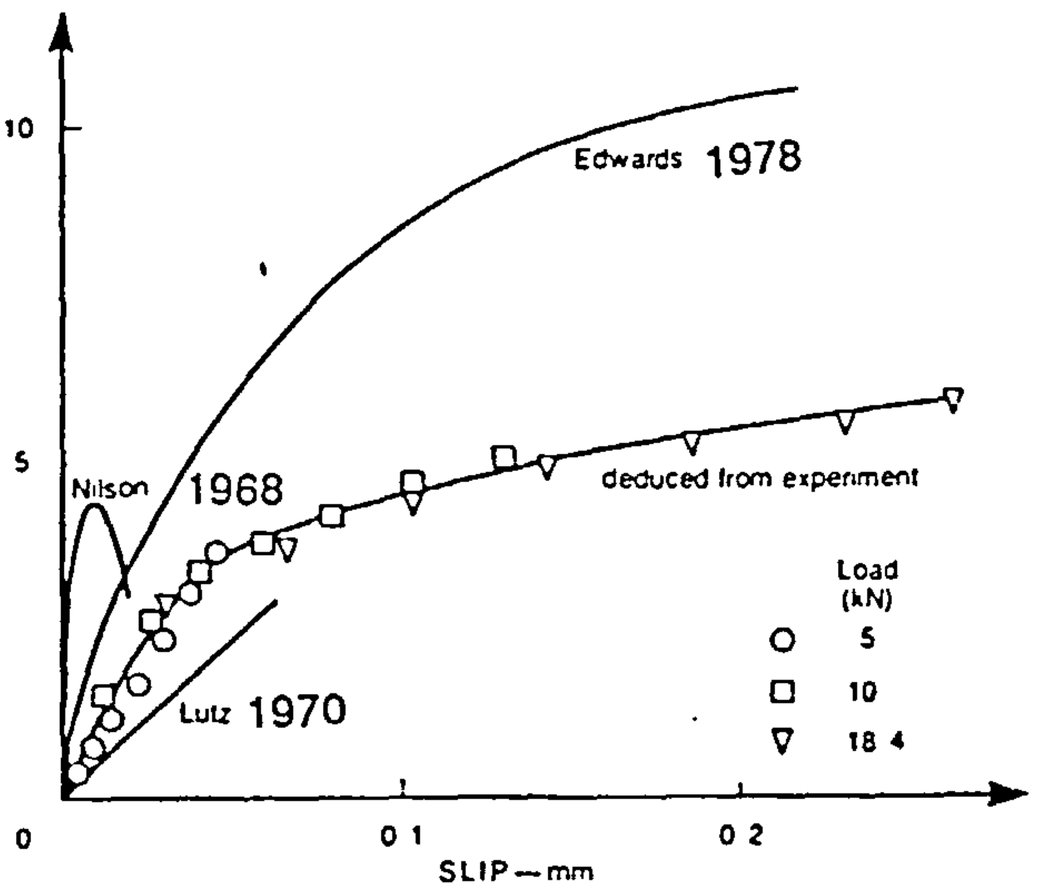

Figure (5.6) - Bond stress slip relationship, after Allwood (1980)

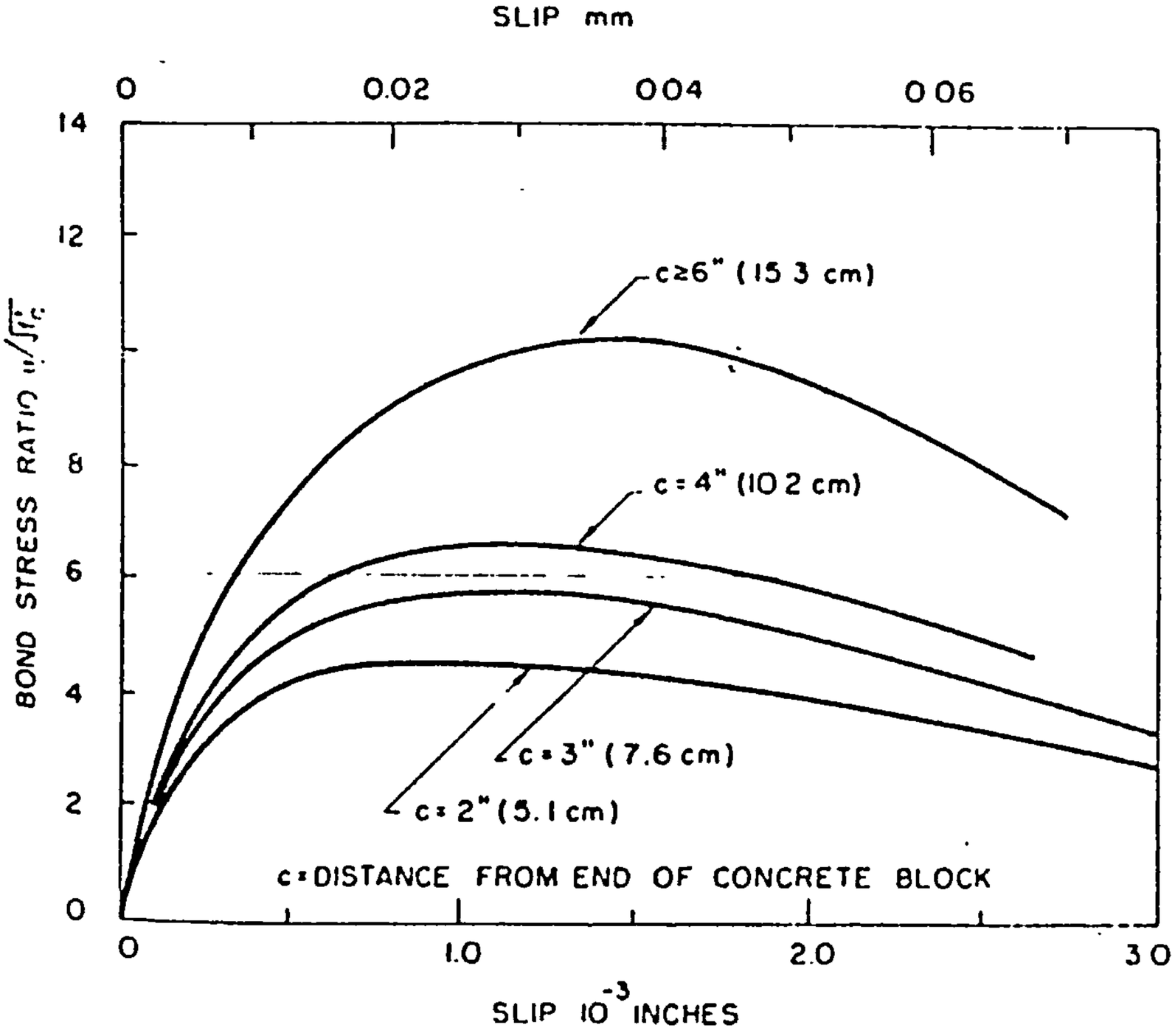

Figure (5.7) - Local bond stress slip curves at different distances from the end face of the specimen, after Nilson (1972).

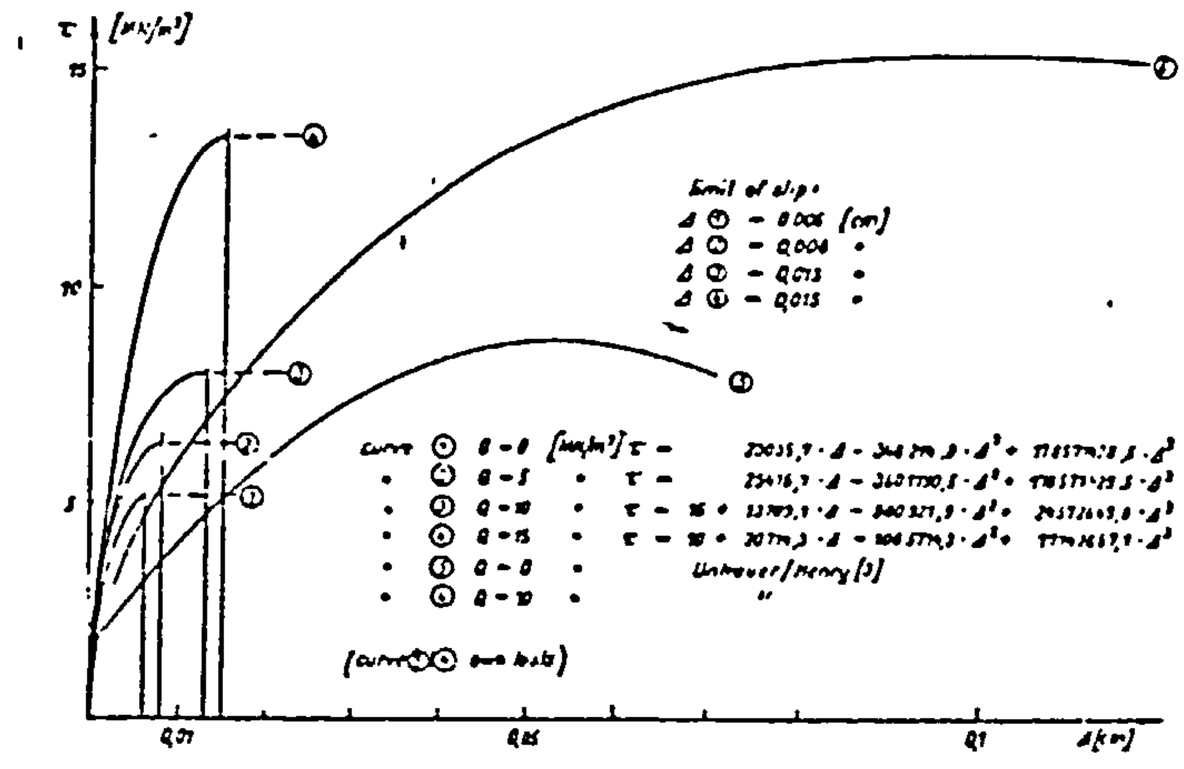

Figure (5.8) - Effect of lateral pressure on bond stress slip relationship for results of Dorr and Untrauer and Henery (1965), after Dorr (1978).

5.4.3 Nonlinear bond model by Allwood et. al.(1984)

The model described by Allwood et al. (1984) incorporates a nonlinear bond stress-slip relationship within a detailed modelling of bond. The model predicts the bond stress-slip relationship up to and beyond local failure of bond. Although the model is developed primarily for plain bars it has been developed further to cover deformed bars. Since the ultimate bond stress has been studied extensively, the model had extended the concept of ultimate bond strength and the radial interface pressure to create a local bond stress slip relationship. The model allows for the effect of lateral pressure between concrete and steel which is found to modify the bond strength. It consists of the following stages:

1) A nonlinear relationship for bond stress versus slip is assumed for the bond below ultimate value, which is a function of the ultimate bond stress

2) The ultimate local stress is assumed to be a function of adhesion and radial pressure between reinforcing bar and the surrounding concrete.

3) Once local ultimate bond stress is reached then excessive slip will take place and a reduction of bond will occur.

Ultimate bond stress:

As the concrete shrinks it generates radial pressure at the bar concrete interface and so bond strength develops between concrete and steel. Further, the radial interface pressure is modified by stresses carried by concrete and steel due to applied load. A linear relationship is assumed between ultimate bond stress and

radial pressure expressed as :

$$q_u = q_0 + \mu . P_r \qquad (5.5)$$

where

P_r radial pressure existing at the concrete steel interface.

q_u local ultimate bond stress

q_0 ultimate bond stress associated with initial shrinkage

μ coefficient of friction

The relation is shown in figure (5.9). Contraction of the bar as it carries axial load relieves some radial pressure while concrete lateral pressure exerted against the bar increases radial pressure. Including these effects in equation (5.5) gives the following relation for the ultimate bond stress :

$$q_u = q_0 + \mu (\sigma_{rconc} - \sigma_{rbar}) \qquad (5.6)$$

where

σ_{rcon} = compressive radial pressure

σ_{rbar} = Tensile interface radial pressure due to bar contraction

<u>μ and q_0 explicit values</u>

The values assigned to coefficient of friction μ and q_0 affect the way bond failure occurs and are estimated based on experimental evidence. Also, μ and q_0 values depend on bar type. For plain bars μ and q_0 values are 0.4 and 2 N/mm^2 respectively while for deformed bars the values are 1.05 and 9.5 N/mm^2 respectively.

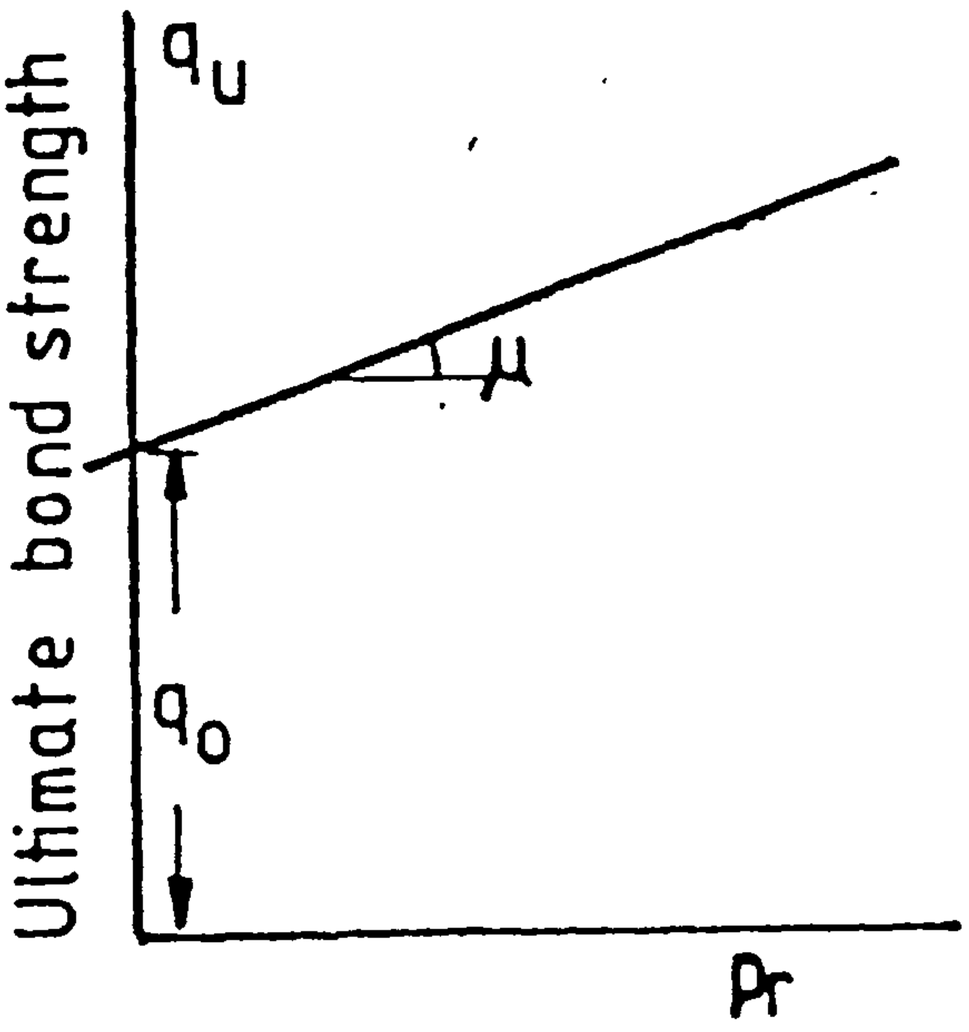

Figure (5.9) - Ultimate Bond Strength vs. Radial pressure, after Allwood et al.(1984).

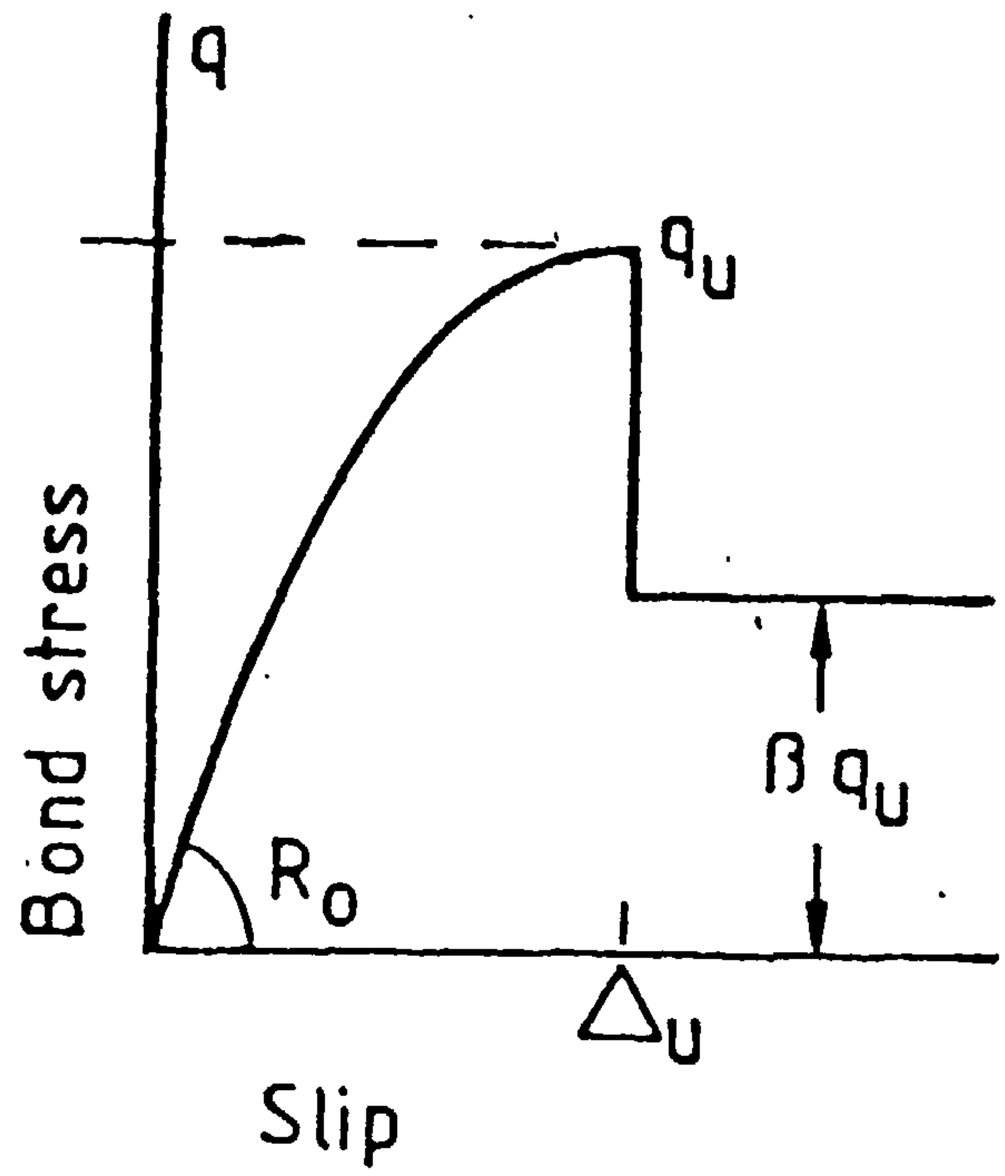

Figure (5.10) - Bond Stress Slip Relationship Used in the nonlinear Bond Model, after Allwood et al. (1984).

Concrete Lateral Pressure

The lateral concrete stresses exerted on the bar were calculated by considering the problem of an infinite plate with a circular hole into which an elastic circular disc has been inserted and the plate is subjected to uniaxial stress field. Extending the analysis to a circular steel elastic bar within an elastic concrete body is found in the work of Parsons (1984). Following the above analysis the average interfacial radial pressure is found to be 0.7704 times the uniaxial lateral pressure. Therefore, in the two dimensional analysis of the model the lateral stresses on the reinforcement is converted to an average interfacial radial pressure by the relation:

$$\sigma_{rconc} = 0.7704 \cdot \sigma_t \qquad (5.7)$$

Where

σ_t is the concrete stress acting at right angles to the bar.

σ_t is calculated from the concrete stresses components (σ_x, σ_y,τ_{xy}) at the level of steel bar nodes. Concrete stresses components at the level of the bar are calculated from the concrete stresses at the four quadrature points within the concrete element using least square technique. This is shown in greater detail in chapter 7 when discussing the method of solution.

Tensile interfacial radial pressure due to bar contraction :

Due to Poisson's ratio effect the radial contraction when the bar is axially loaded in tension will relieve the compressive interfacial radial pressure as calculated above. It is assumed in the model that the bar radial contraction and the associated interfacial

radial pressure could be estimated using Timoshenko's thick walled cylinder theory.

The following relation is thus obtained for the interfacial radial pressure due to bar contraction

$$\sigma_{rbar} = \frac{\sigma_s \cdot \nu_s}{\frac{E_s}{\left(\frac{1+\nu_c}{E_c}\right)+\left(\frac{1-\nu_s}{E_s}\right)}} \qquad (5.8)$$

where

ν_s, ν_c are Poissons ratios for steel and concrete respectively

E_s, E_c are Elasticity Modulii for steel and concrete respectively

Local bond stress-slip relationship :

The local bond stress slip relationship is assumed to be nonlinear according to Saenz' (1964) equation which was used to describe the uniaxial stress-strain curve for concrete. Using the form of Saenz equation here allows for the initial bond stress-slip modulus, the slip at maximum bond and maximum bond stress to be independent variables. Thus the nonlinear bond stress-slip relationship is assumed to be

$$q = \frac{R_0 \cdot \Delta}{1 + \left(\frac{R_0}{q_u/\Delta_u} - 2\right)\left(\frac{\Delta}{\Delta_u}\right) + \left(\frac{\Delta}{\Delta_u}\right)^2} \qquad (5.9)$$

where

Δ is bond slip

R_0 is initial bond stress-slip modulus

q is bond stress at given slip of Δ

q_u is local maximum bond stress

Δ_u is slip at ultimate bond stress

Figure (5.10) illustrates the bond stress slip relationship.

Initial bond stress slip modulus

Quite different values for the initial slope, R_0, have been used by different investigators. Nilson (1968) used a value of 1000 N/mm^2 per mm, while Allwood (1980) used a value of 75 N/mm^2 per mm which is calculated from his experimental results figure (5.6). In this thesis different values are used for R_0 depending on the reinforcement type i.e. plain or deformed steel bars. The value also depends on the problem type i.e. pull-out tests or flexural problems. For example in Pull-out test type of problems using plain bar the value of R_0 is given as 200 N/mm^2 per mm. Explicit values of R_0 are given for different problems in chapter 6 and 8.

Slip at ultimate bond stress :

The value for the slip at ultimate bond stress is assumed to be a constant value of 0.1mm.

Failure of bond

Failure of bond at any location is assumed to occur once the bond slip value has exceeded the maximum allowable slip "slip at ultimate bond stress". After bond failure has occured at a particular location the ultimate bond stress at the location can not be maintained because the adhesive component of bond will be distroyed which is an important component in bond for plain bars. Thus, the model assumes that the bond stress is reduced by a factor β when the slip exceeds the maximum allowable value of 0.1 mm. The value of β depends on the method of failure which is influenced by the bar type. Explicit value of β is taken to be 0.5 for plain bars and 1.0 for deformed bars.

Chapter 6

6. APPLICATION OF THE LINEAR BOND MODEL

6.1 Introduction

The purpose of this chapter is to demonstrate the application of the method described in chapter 3 by analysing different reinforced concrete problems. The solutions presented for all problems are obtained assuming linear elastic bond stress slip relationship for bond as well as linear elastic stress strain relationship for concrete and steel. Two dimensional plane stress analysis is used for the concrete.

Three different problems are selected for demonstrating the applicability of the method to reinforced concrete problems which are:

i) Simply supported beam

ii) Pull-out Test

iii) Cantilever Problem

The behaviour and design of these problems have been much investigated. Their solution here will show some of the details that can be included now in the analysis of reinforced concrete structures by finite element analysis using the present method. Thus solution of the above problems will demonstrate the following advantages of the method which includes:

Applicability of the method to real structures

Simplicity of the mesh needed by the method

Ability of the method to handle :

complex steel arrangements.

different orientation of the steel.

thin concrete covers.

steel anchorage

choice of applying load to either concrete or steel.

The importance of bond modelling in the solution of reinforced concrete problems will be examined by solving for different bond stiffness values. Further in the solution of the problems the effect of mesh size and also the effect of the choice of the number of steel nodes selected on the solution will be studied.

6.2 Bond initial stiffness modulus (R_0)

The initial bond stiffness modulus value is calculated from the slope of the bond stress-slip curve i.e. figure (5-6) for example. The value of R_0 when used in the present model reflects the bonding strength between concrete and steel. The greater the value of R_0 used in the solution the greater the gripping of the two materials together is assumed.

The value of the initial bond stiffness modulus ,R_0 , found by different investigators varies quite considerably i.e figures (5.5) and (5.6). However, The value of R_0 used in the solution of the above problems is given below.

For the pull-out test problem the value of R_0 to be used is 200 N/mm^3 or 737.67 $kips/in^3$. This value has been used by Allwood, Parsons and Robins (1984) in their non-linear bond model of plain bars and which is estimated from experimental results of pull-out tests. However very little is published about the value of R_0 for flexural cases. Allwood (1980) has used the value of 75 N/mm^3 in the analysis of a beam-column connection by finite element analysis. This value is calculated from the initial loading up to 5 kN in figure (5.6). In the analysis of the beam and the cantilever problems of this chapter the initial bond stiffness modulus value to be used is 54.3 N/mm^3, or 200 $kips/in^3$. This value has been found from experimentation to give the best results when solving the beam problem shown in figure (6.1) using different values of R_0.

It will be shown in chapter 8 when using the non-linear bond model that the value of R_0 will depend on the type of reinforcement. R_0 is given a higher value for modelling of bond in deformed bars than in the case of plain bars.

6.3 Single span beam

6.3.1 Details of the beam

In this section a real beam problem will be modelled and analysed by the method. It is a simply supported single span beam and is shown in figure (6.1). The beam is designed according to ACI 318-83 and is given by Wang and Salmon (1983). The details of the reinforcement which includes tension compression and shear reinforcement is shown in figure (6.1) and is summarised here:

Tension reinforcement	8 bars no. 9
Compression reinforcement	4 bars no. 7
45 stirrups	2 bars no. 3 / stirrup

The different parameters used for concrete, steel and bond are listed below:

$E_c = 3640 \ kips/in^2$

$E_s = 29000 \ kips/in^2$

$R_0 = 200 \ kips/in^3$

The beam is loaded with a uniform distributed load of 2.7 kips/ft . The width of the beam is 14 inch.

6.3.2 Finite element mesh

In constructing the finite element mesh for the concrete the elements are chosen to match the concrete stress distribution without worrying about the reinforcement. This leads to the simple finite element mesh for the concrete as shown in figure

(6.2). There are 20 8-noded rectangular isoparametric elements with a total of 85 concrete nodes. The load is applied at the concrete nodes located at top of the beam such that a uniform distribution of load is ensured.

The reinforcement is divided into 2-noded bar elements independent of the above concrete mesh. The number of steel nodes is chosen to match the steel stress distribution. Further, every bar has its own number of nodes. The choice of the number of bar elements is specified in the input data for every bar. All the steel shown in figure (6.1) is included in the analysis. The main reinforcement is divided into 40 2-noded bar elements. Thus each of the tension and the compression reinforcement has 41 steel nodes. Each stirrup is divided into 8 2-noded bar elements leading to 9 steel nodes in each stirrup. Thus, the total number of all steel nodes is 487.

Stirrups ends anchorage:

The stirrup ends are fixed to concrete because they are hooked around the tension and the compression reinforcement, and since the displacement of the main reinforcement in the vertical (y-axis) direction is ignored, therefore, the main reinforcement displaces laterally with the concrete and so does the stirrups ends.

To have more accurate modelling of the reinforcement the two ends of each stirrup (i.e. the top node and bottom node) are fixed to concrete by setting the value of the initial bond stiffness

E_c = 3640 kips/in^2 (25.1 kN/mm^2)
E_s = 29000 kips/in^2 (200 kN/mm^2)
R_0 = 200 kips/in^3 (54.3 N/mm^3)

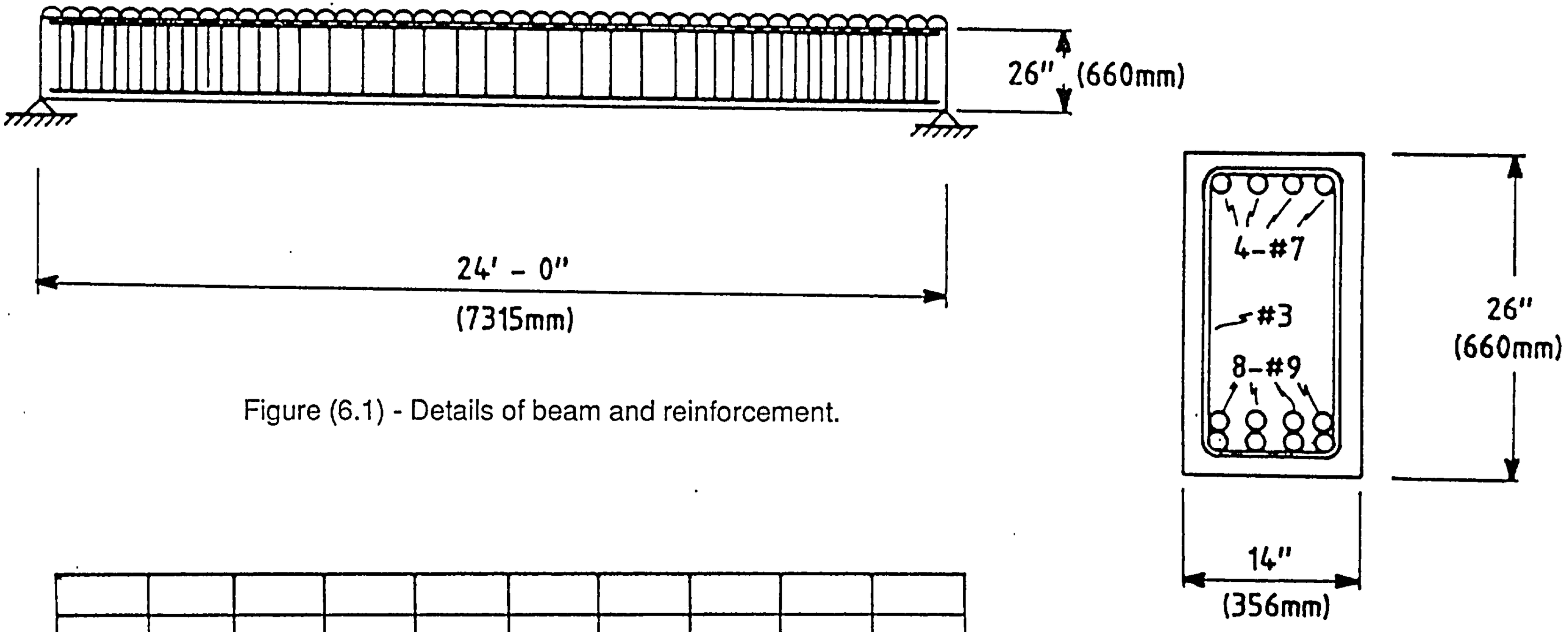

Figure (6.1) - Details of beam and reinforcement.

Figure (6.2) - Finite element mesh for concrete in the above beam.

modulus at these nodes to be a very high value. In this case R_0 is set to be a ten thousand times higher at the stirrups ends than at any other node. Thus

$$R_0 \text{ used at stirrup ends} = 200 \times 10000 \quad kips/in^3$$

6.3.3 Discussion of the results:

The problem has been solved with all the above details. The solution converges in 6 iterations. The central processing unit (CPU) time required for the formulation of the problem and obtaining the solution is 55 seconds using Honeywell Multics computer system. The effect of applying a damping factor on the convergence of this problem was shown in figure (4.10)

Stresses in reinforcement:

Figure (6.3) shows the stress distribution in the tension reinforcement as well as in the compression reinforcement. The stress curve shown reflects the expected pattern of the stress distribution in the main reinforcement of a simply supported beam. The dotted line shown in figure (6.3) represent the beam mid-span location.

Balance of forces:

Figure (6.4) shows the tensile forces carried by the tension and the compression steel along with the average longitudinal normal forces carried by the concrete.

At any cross-section of the beam the concrete force curve gives the average value of the tension and compression forces of all

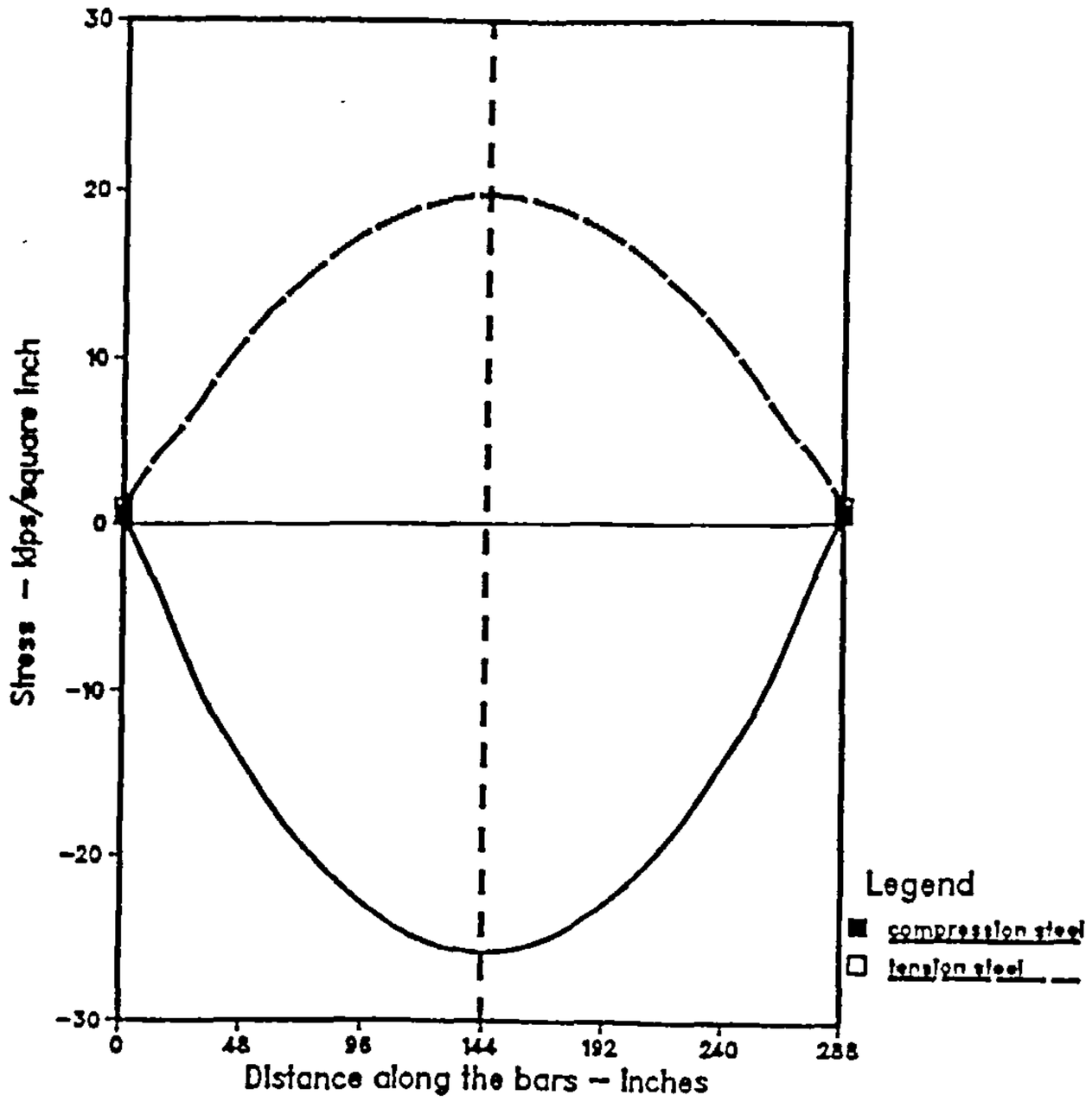

Figure (6.3) - Stress distribution in compression and tension Reinforcement.

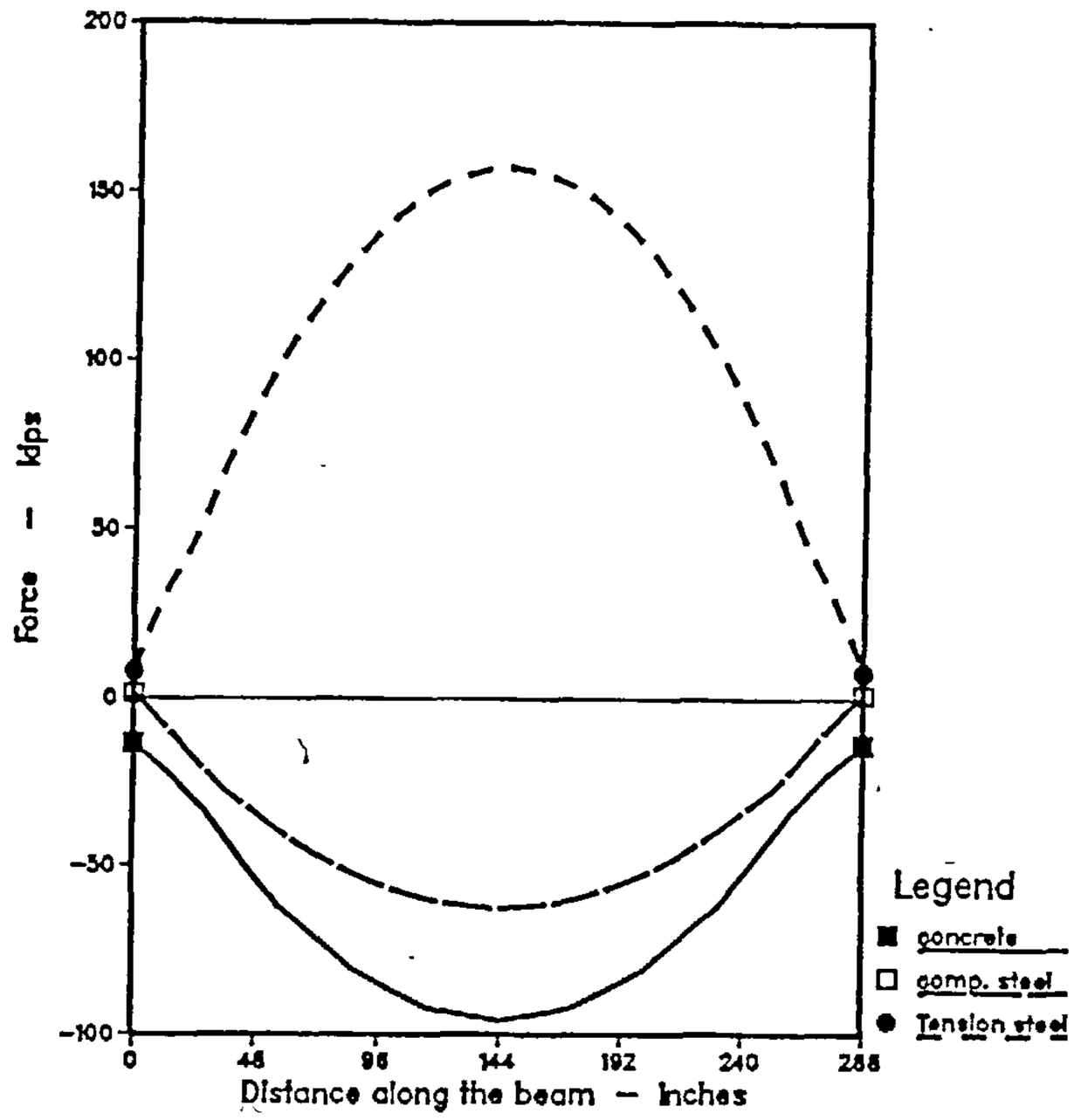

Figure (6.4) - Forces in main steel and average longitudinal forces in concrete.

concrete nodes acting on that cross section. The concrete forces curve in figure (6.4) shows some force to exist at the supports instead of showing zero force as it should be. This is due to the effect of the supporting forces in this region. Otherwise, the algebraic summation of the concrete and steel forces shown in figure (6.4) is always zero for any cross-section of the beam. So balance of forces is ensured.

Bond stresses:

Figure (6.5) shows the bond stress distribution along the tension and the compression reinforcement. The figure shows how the bond stresses near the ends of the beam are influenced by the distribution of the supporting forces of the beam. The bond on the tension steel is increased whilst that on the compression steel is reduced. Also the figure shows zero bond stress at mid-span of the beam which is expected because there is no relative movement between steel and concrete at this part of the beam.

It can be seen from figure (6.5) that there are some oscillatory variations in the bond stresses near the support. These variations coincide with the boundary of the concrete elements. This could be explained by examining the bond stresses. The bond stresses are calculated from the steel and the concrete displacements. By examining the steel and the concrete displacements, it is found that whereas the steel displacements varied quite smoothly, even down to their second differences, the concrete displacements did not. The concrete displacements are derived from equation (3.11) repeated here

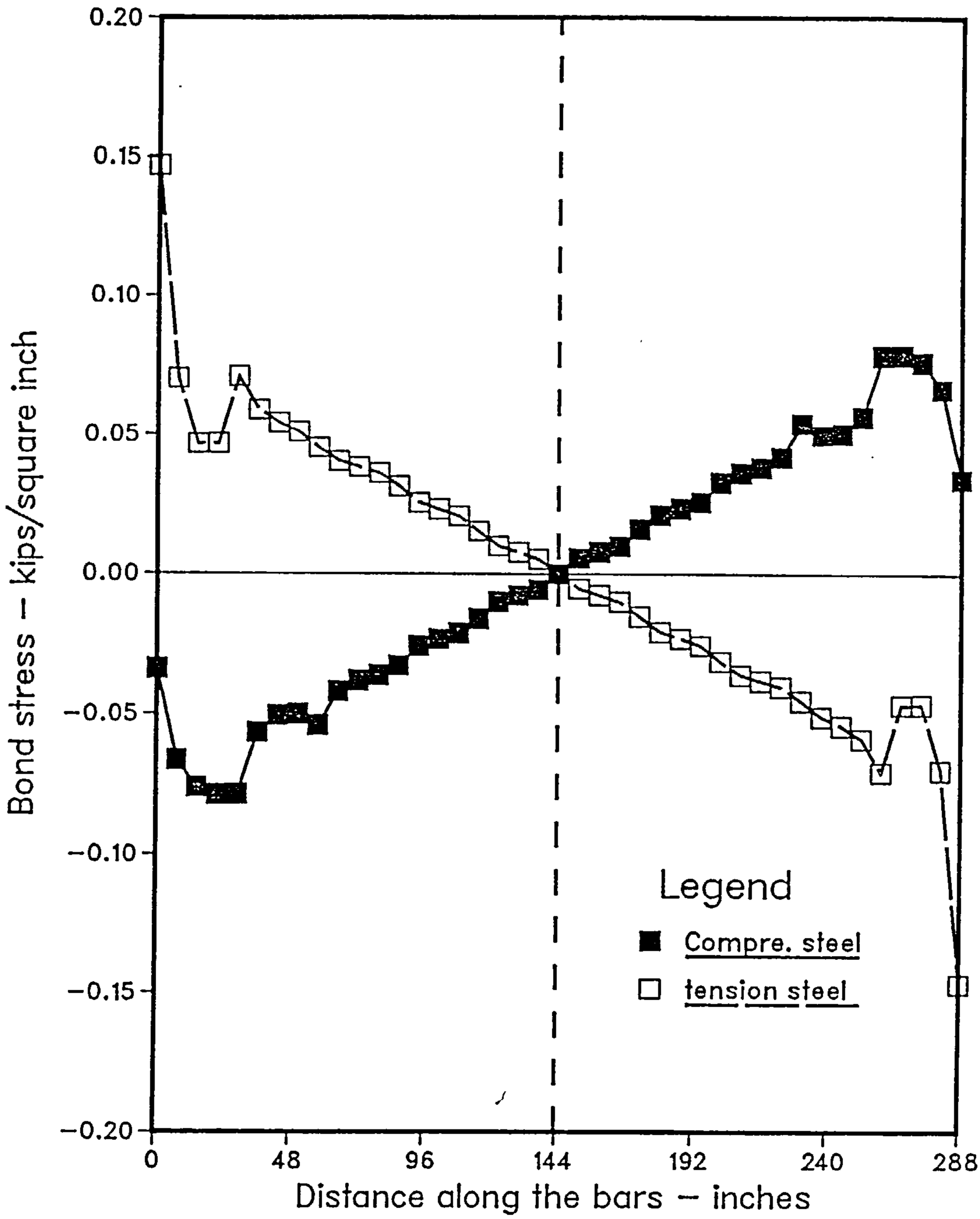

Figure (6.5) - Bond stress distribution along compression and tension reinforcement.

$$u_{cj} = C_e \cdot D_e$$

The second differences of these displacements showed large discrepancies at the boundaries of the concrete elements but smooth values away from the boundaries

This is very similar problem to that which occurs when calculating element stresses at points within an 8-noded elements, as first noted by Hinton and Campbell (1979). They showed that stresses derived from the shape functions were most accurate at the Gauss points and at their worst at the boundary edges. It is now common to derive such stresses by interpolating through the Gauss point values as recommended by Hinton and Campbell. It is possible that a similar smoothing process could be used to improve the bond stresses calculated by the method described in this research.

To see the effect of the number of steel nodes on the results, another solution has been obtained by selecting different number of bar elements for the steel. Each of the tension and compression reinforcement was divided into 36 steel nodes and the stirrups each 4 bar elements or 5 steel nodes. This is done to see the effect of the number of bar elements. There was not much difference in the two solutions.

Stress in stirrups:

Before discussing the stress in the stirrups it should be remembered that in this research only longitudinal deformation along the reinforcement axis are considered and that lateral displacement of the bars are not considered. Interforces normal to

the axis of the reinforcement are not included. Therefore the stirrups here do not contribute to the beam shearing strength. Analysis of the beam is done using the value of the bond initial stiffness modulus of 200 kips/in^3 for the main reinforcement as well as for the stirrups. However, it is not quite clear of what value of R_0 should be used for the stirrups. Steel used in stirrups have much smaller diameter than the main reinforcement which suggests a lower bond stiffness modulus to be used for the stirrups than for the main steel. The beam is analysed using three values of initial bond stiffness modulus for the stirrups which are R_0= 20, 50, and 200 kips/in^3. The value of R_0 for the main reinforcement is kept at 200 kips/in^3 all the time. Results for some of the stirrups selected at various location in the beam will be shown.

Figure (6.6) shows the stress in the first stirrup which is located next to the support. The figure shows the stress in this stirrup is in compression. The effect of the choice of R_0 on the stress distribution is noted. The stress in the stirrup reduces as the value of R_0 is reduced. Also, the stress curve becomes smoother as the value of R_0 is reduced. Figure (6.7) shows the stress in the stirrup at mid-span of the beam which is in compression for the upper part and in tension for the lower part. The same effect is noted here for the change in R_0 value as the first stirrup except that the stress curve is smooth at all the R_0 values. The stress in the middle stirrup is higher than that of the first stirrup. There are a number of published results for the study of stresses in

stirrups such as Kani (1969), Regan and Khan (1974), Ruhnau (1974). These studies of stirrups are related to cracks. However, Kani (1969) has stated that there are two zones of ineffective web reinforcement one near the loading part and the other near the support. The results obtained by Scordelis, Ngo and Franklin (1974) support this statement because their results indicate near zero forces in these zones. The results obtained using the present method as discussed above considering longitudinal deformation along the bar axis only shows that the stress in the stirrup near the support is lower than the stress in the other stirrup.

Bond stress in stirrups:

Figure (6.8) shows the bond stress in the first stirrup. The bond stress of the middle stirrup is shown by figure (6.9). Again the bond stress varies smoothly in the middle stirrup while the curve is irregular behaviour in the stirrup next to the support.

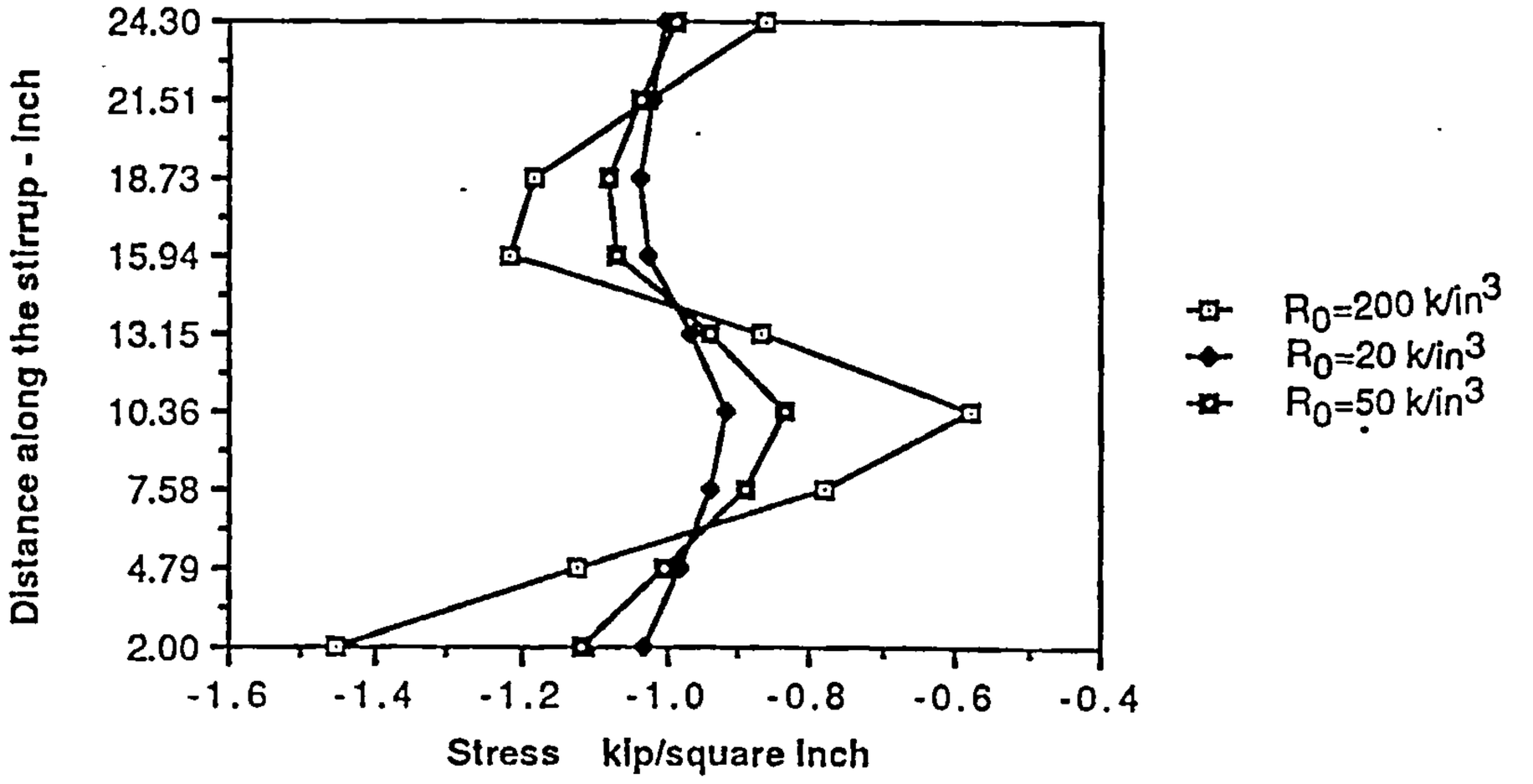

Figure (6.6) - Effect of R_0 on steel stress in stirrup next to the support.

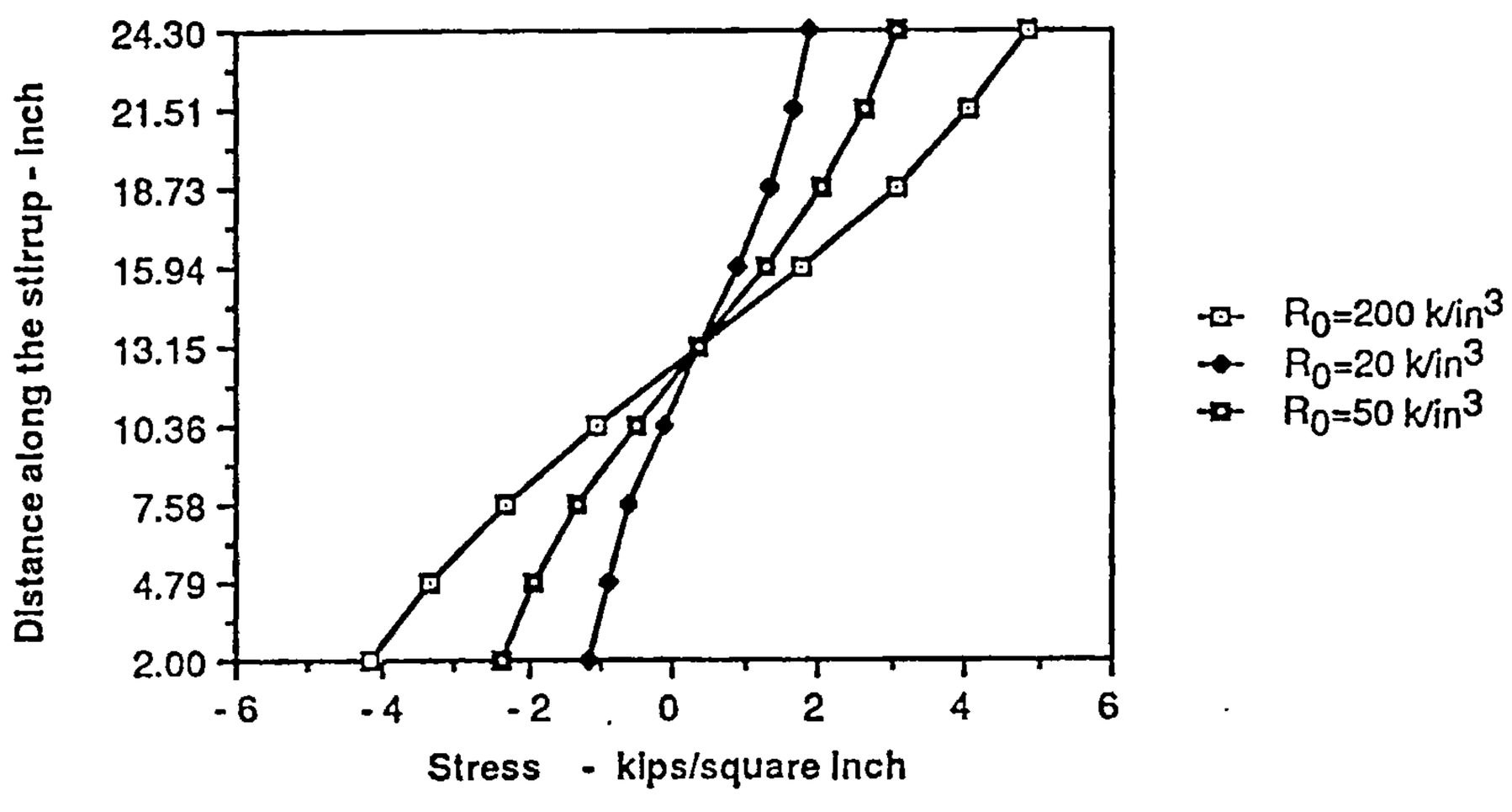

Figure (6.7) - Effect of R_0 on steel stress in stirrup at mid-span of the beam.

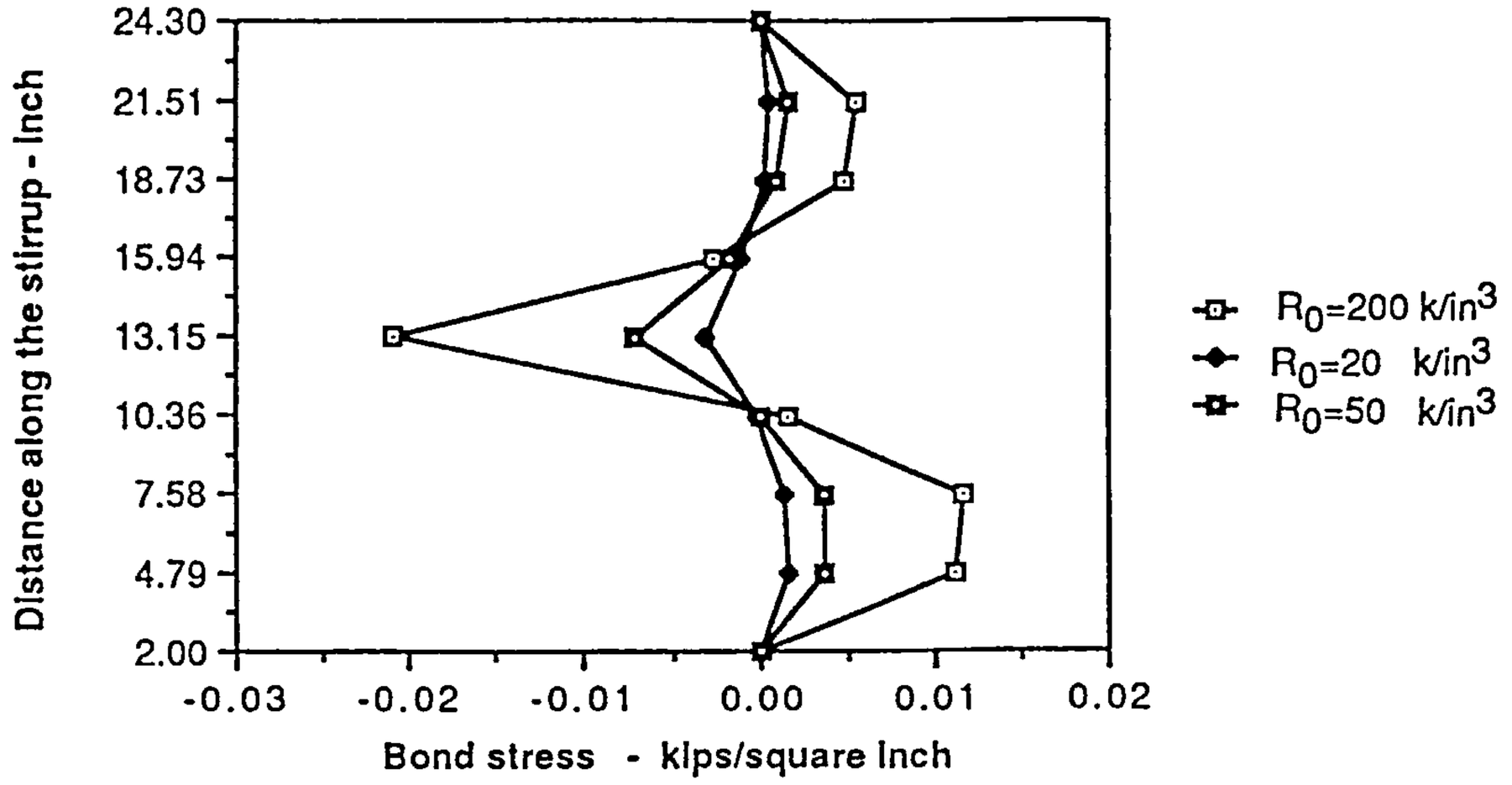

Figure (6.8) - Effect of R_0 on bond stress in stirrup next to the support.

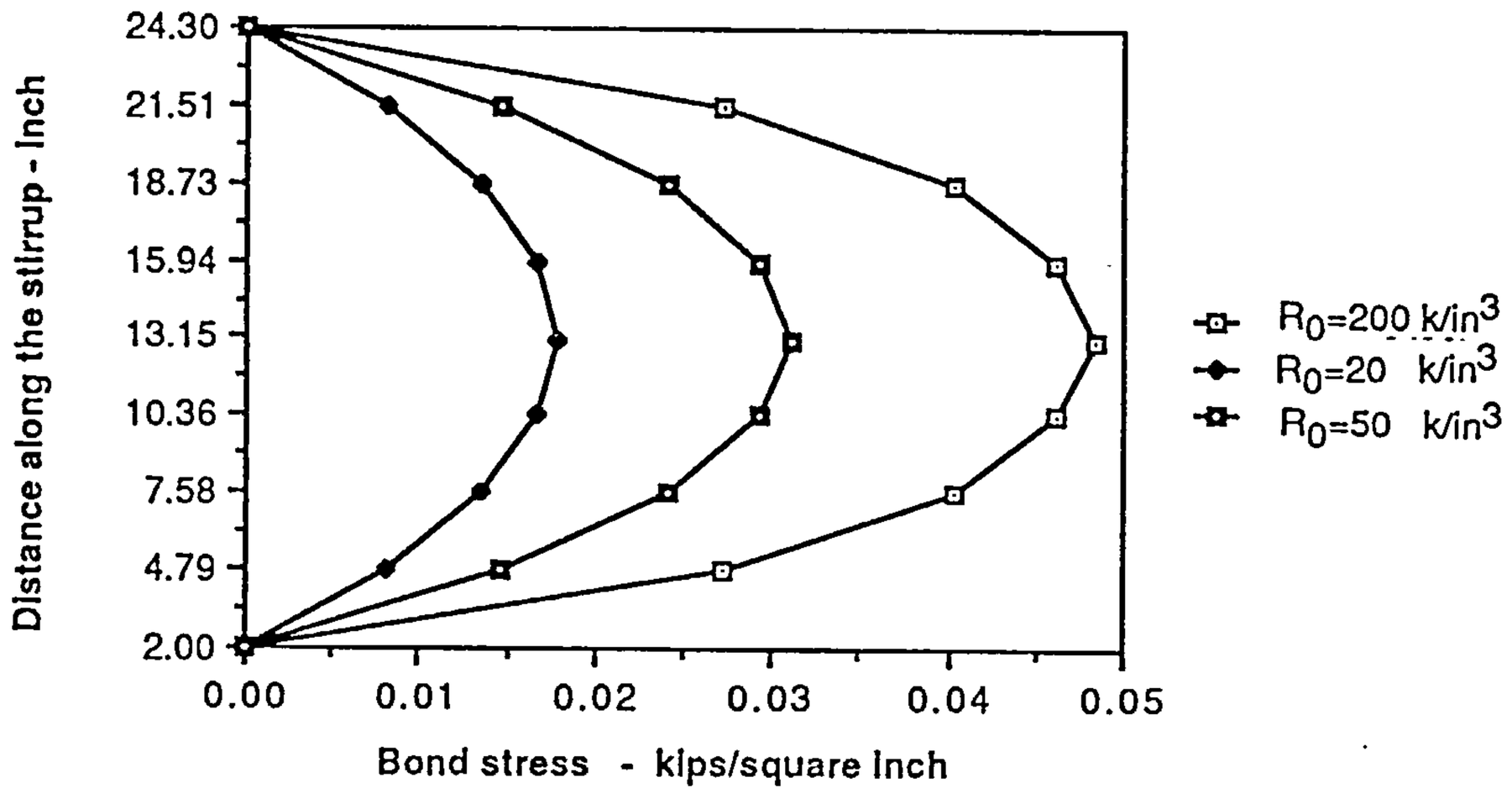

Figure (6.9) - Effect of R_0 on bond stress in stirrup at mid-span of the beam.

6.4 Pull-out test

6.4.1 Details of the problem

The pull-out test is a typical experimental test that is done to study the bond behaviour. In this test a steel bar is embedded in a block of concrete while a force is applied to pull the steel out of the concrete block.

The concrete cube dimensions used in this problem are 150mmx150mmx150mm. The reinforcement used is one steel bar embedded in the concrete cube as shown in figures (6.10). In this problem the load is applied to the reinforcement bar so that in equation (3.22)

$$[P_c] = 0$$

$$[P_s] = \text{full load}$$

The applied load is 2 kN and is acting away from the concrete figure (6.10). The diameter of the steel bar is 16 mm.
The different parameters used are listed here :

$$E_c = 33000 \text{ N/mm}^2$$

$$E_s = 200000 \text{ N/mm}^2$$

$$R_0 = 200 \text{ N/mm}^3$$

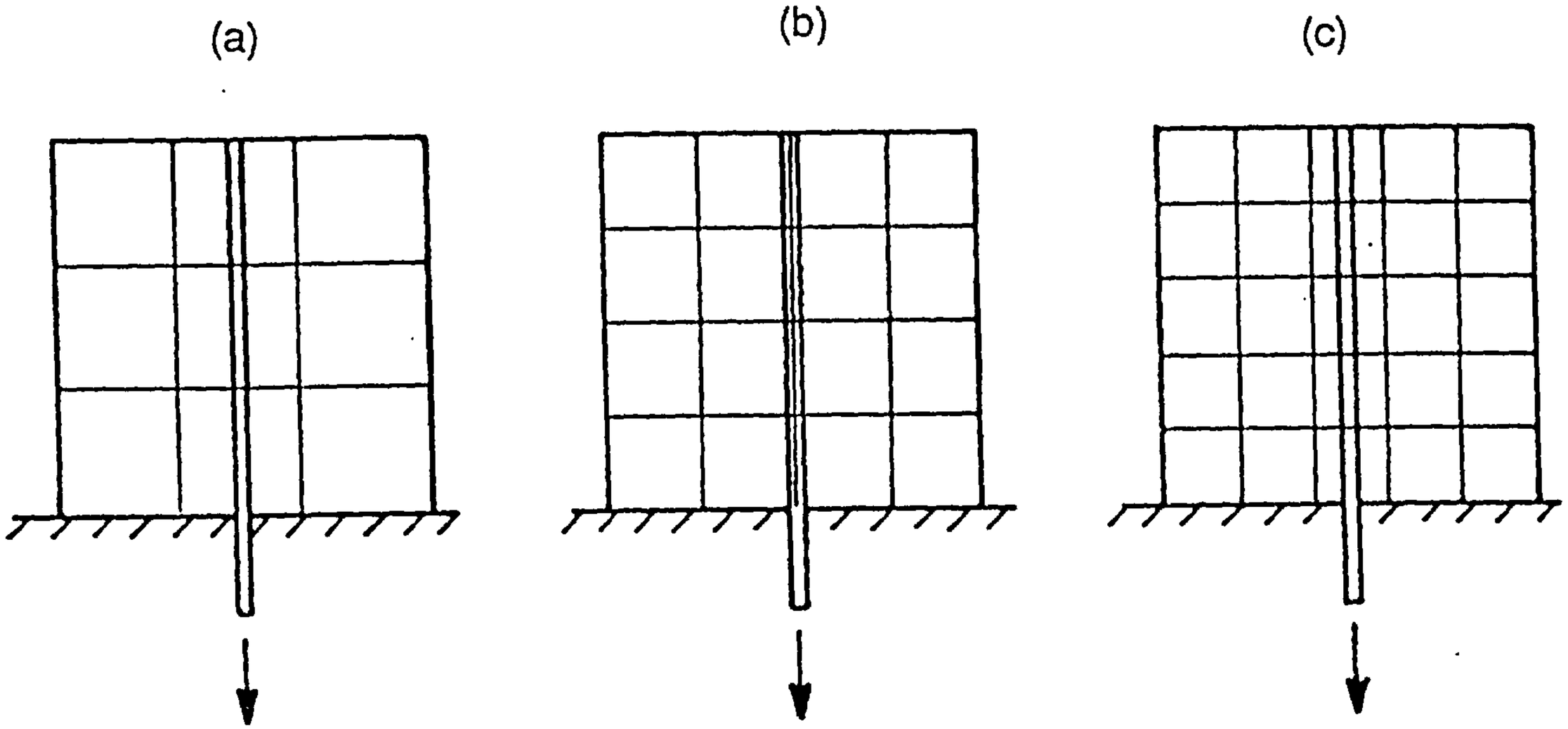

Figure (6.10) - Different meshes for pull-out test

6.4.2 Finite element mesh

The finite element mesh which is used in the analysis of this problem is shown in figures (6.10) . The concrete is represented by 8-noded rectangular, isoparametric elements. 3 different meshes are used :

i) 3x3 mesh with a total of 9 elements and 40 nodes figure (6.10a)

ii) 4x4 mesh with a total of 16 elements and 65 nodes figure (6.10b)

iii) 5x5 mesh with a total of 25 elements and 89 nodes figure (6.10c)

The problem will be solved for each of the above meshes to see the effect of mesh size. Also it is noted that the reinforcing bar location with respect to the concrete elements is different in each of the above meshes. In the case of the 4x4 mesh the steel bar lies along the boundary of the concrete elements while in the 3x3 and 5x5 meshes the steel bar lies across the concrete elements.

Two different sets of bar elements are used for the steel bar as follows:

i) 15 2-noded bar elements with a total of 16 nodes.

ii) 30 2-noded bar elements with a total of 31 nodes.

The results will show the effect of number of steel nodes on the solution.

6.4.3 Discussion of the results:

The problem have been solved for all the above cases. The solution converges in 4 iterations in all cases.

Effect of mesh size

There is no difference between the solutions obtained for the above 3 meshes on the reinforcing bar solution. Further, the bar location with respect to the concrete elements has no effect on the steel results in this problem. Figure (6.11) shows the bond stress distribution along the reinforcement bar for the 3x3 and 4x4 meshes using 31 steel nodes. The stress distribution in the bar is shown by figure (6.12) for the same selected concrete meshes and number of steel nodes. The solution obtained using the two meshes is the same.

The effect of the three meshes on the concrete stress distribution is studied. Figure (6.13) shows the stress in the concrete at the bar location and in the lateral direction of the bar axis. The stresses obtained using the 4x4 and 5x5 meshes are similar except at the bar loaded end where the concrete stress obtained using the 4x4 mesh is higher. The 3x3 mesh gives lower stress than the other two meshes. Figure (6.14) shows the concrete stresses at the bar location and in the longitudinal direction to the bar axis. The concrete stress given by the 3 meshes is the same at the free end of the bar, but, as at the loaded end of the bar the concrete stress varies showing the highest value for the 4x4 mesh then the 5x5 mesh then the 3x3 mesh.

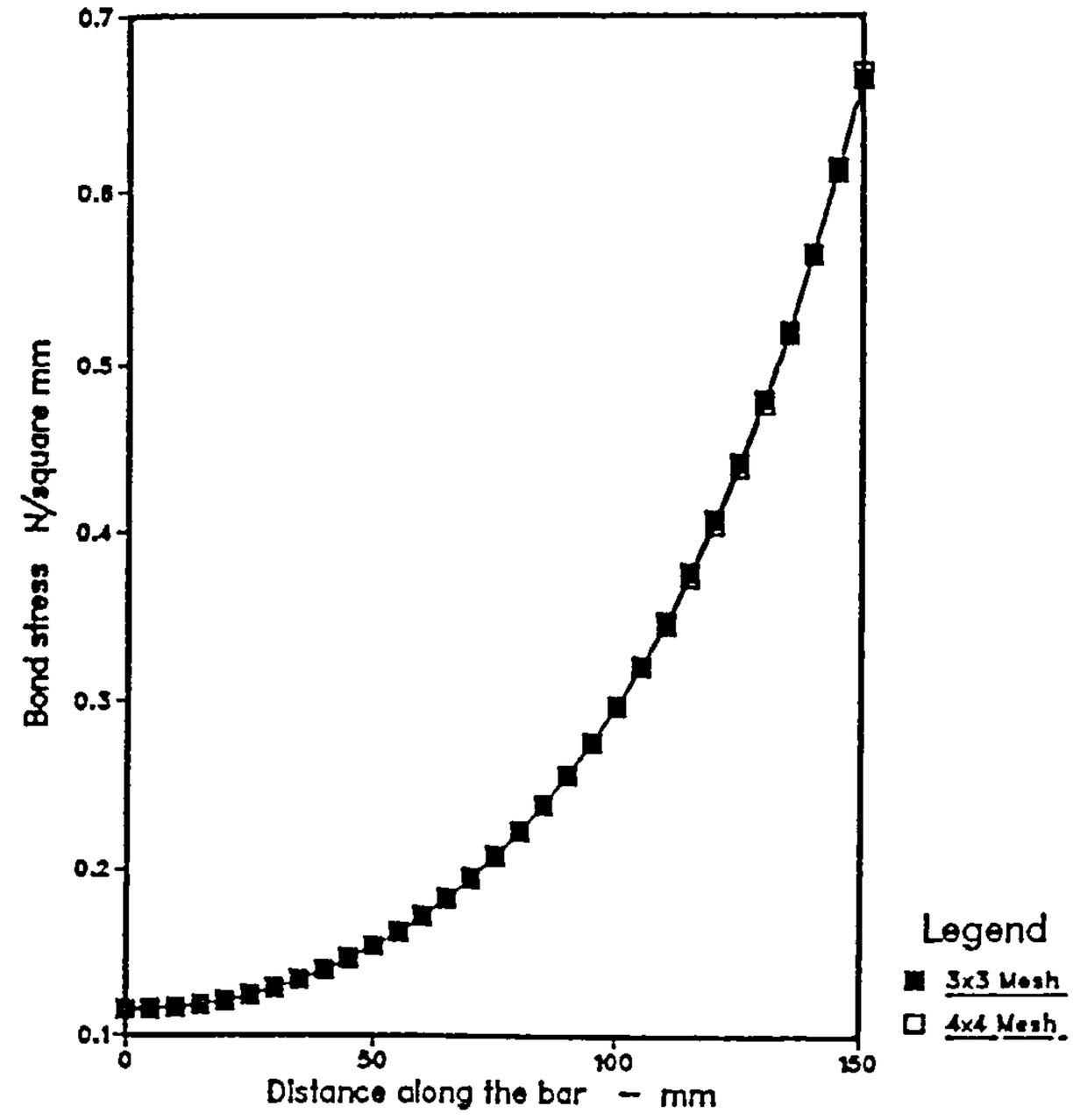

Figure (6.11) - Effect of mesh size on bond stress along the bar in pull-out test.

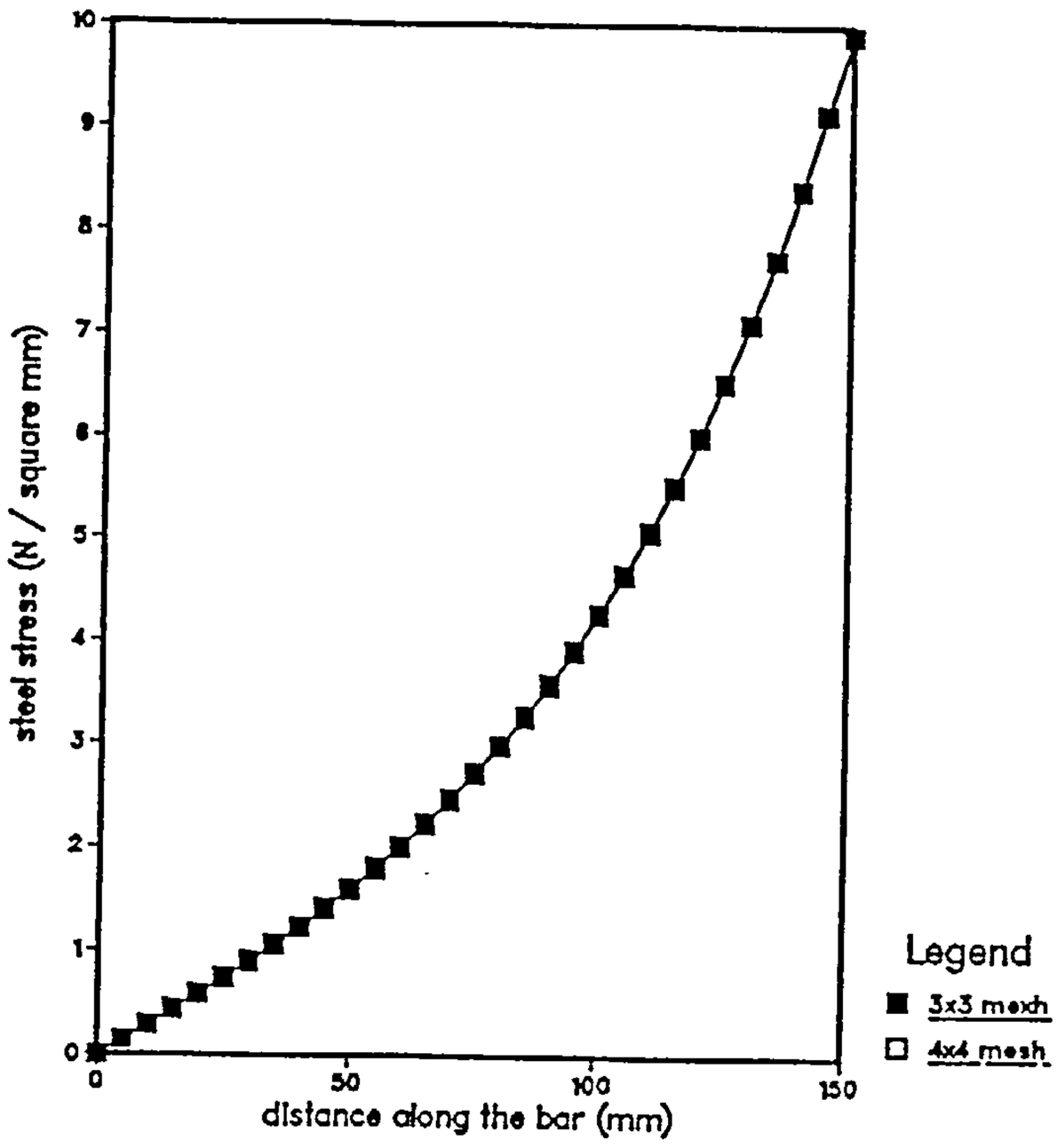

Figure (6.12) - Effect of mesh size on steel stress in pull-out test.

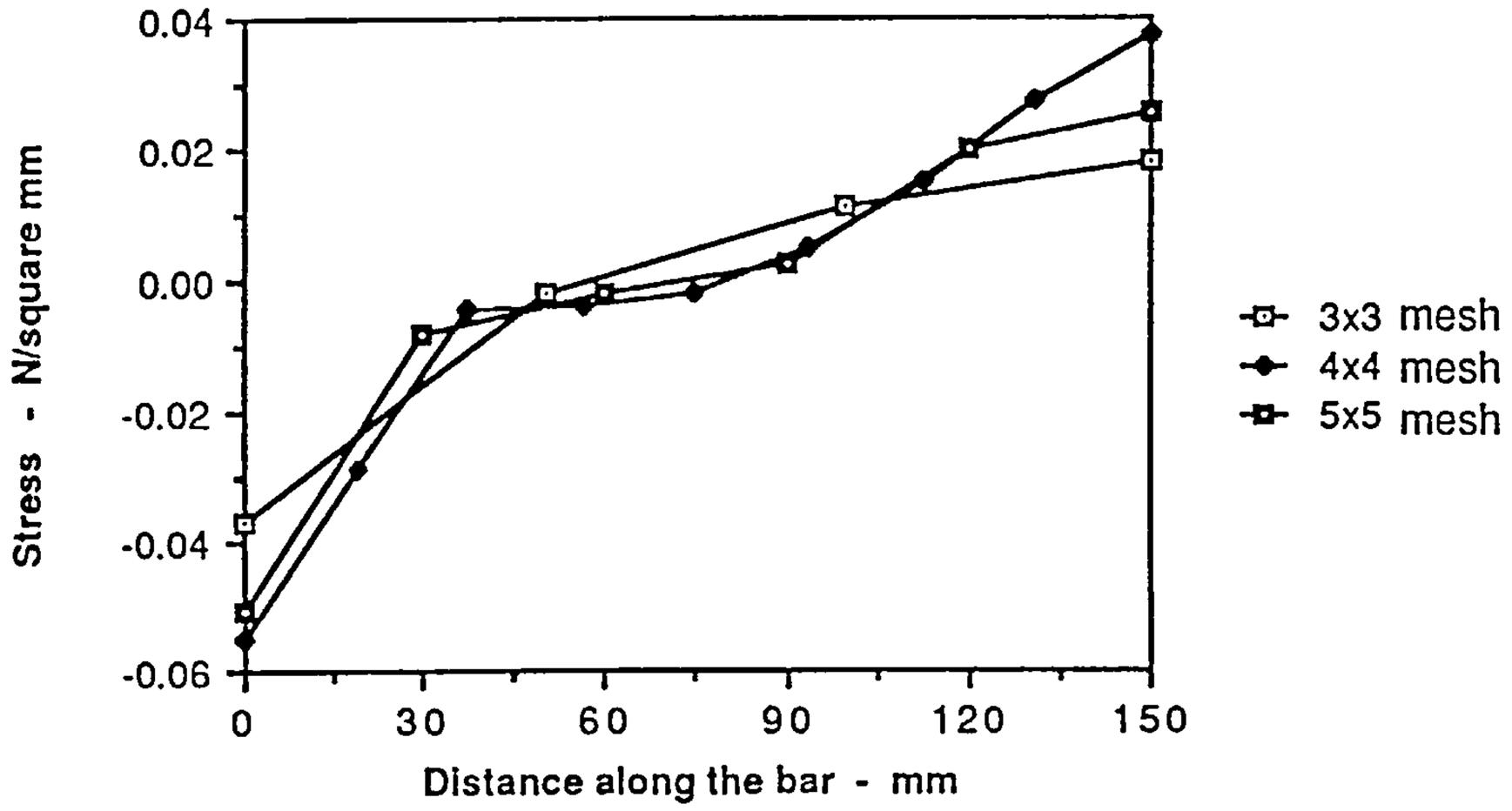

Figure (6.13) - Lateral concrete stress at the bar location in pull-out test.

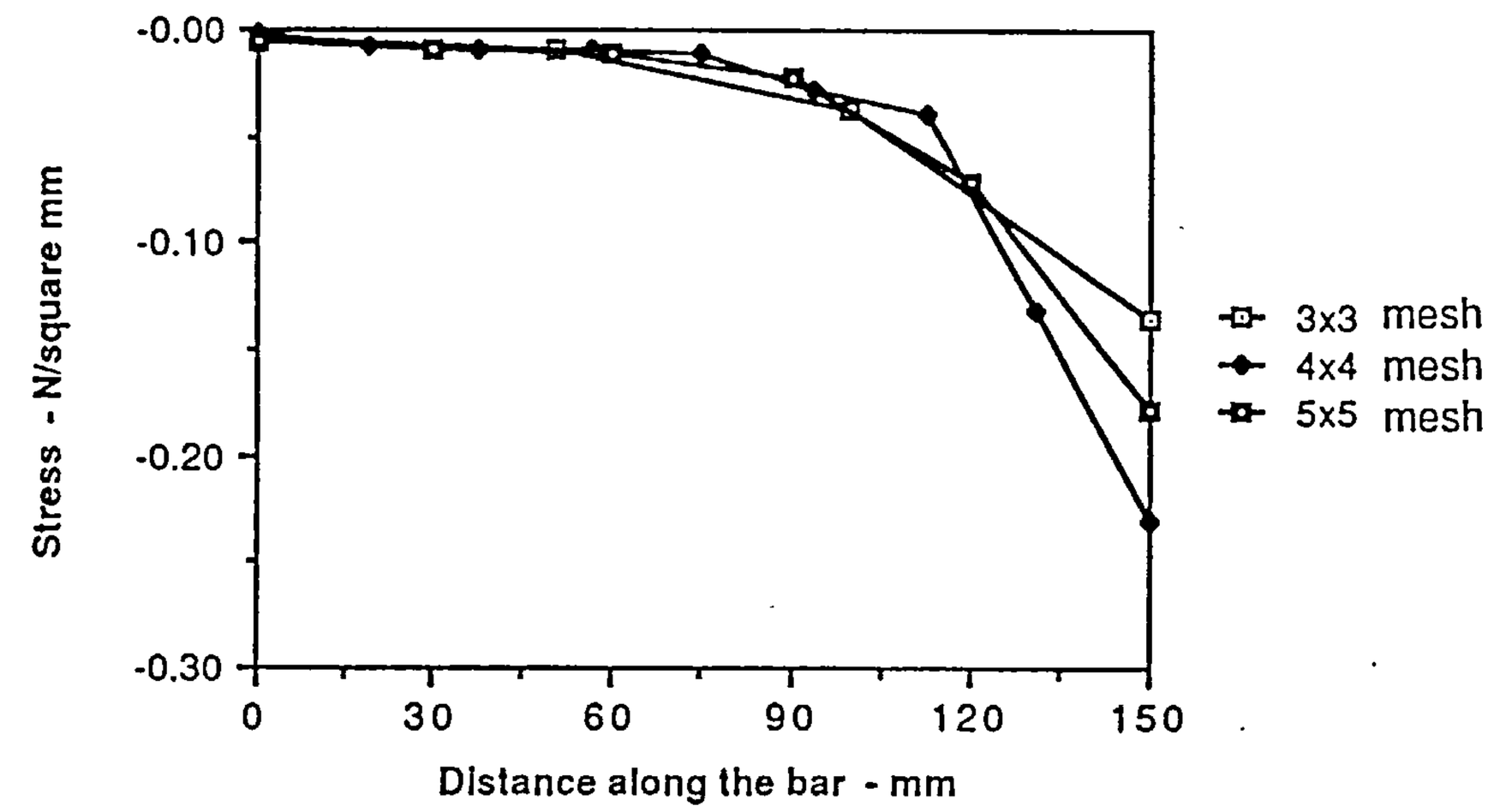

Figure(6.14) - Longitudinal concrete stress at the bar location in pull-out test.

The above led to studying the lateral concrete stress distribution in the supported face of the the concrete the results are shown in figure (6.15). The concrete stress distribution at the supported face in the case of the 3x3 and 5x5 meshes is smoother than the case of the 4x4 mesh. This is due to the way the concrete is loaded. Loading of the concrete in this case is accomplished according to equation (4.9a) repeated here:

$$[K_c] \cdot [D_c] = [P_c] - [K_B] \cdot [D_c] + [C^t] \cdot [K_b] \cdot [D_s]$$

In the 3x3 and 5x5 meshes the bar is passing across the concrete elements. In the above equation $P_c = 0$, thus, the load is transferred from the steel to the concrete through the bond interforces only using all the concrete element nodes which the bar is passing through them. While in the case of the 4x4 mesh the load is transferred only through the nodes located at the element edge. The situation is similar to a distributed load versus point load application. However this does not affect the balance of forces between the steel and the concrete at this surface but does show a higher stress in the concrete at the loaded end of the bar.

Effect of number of steel nodes

Figure (6.16) shows the bond stress distribution obtained using two different sets of numbers for steel nodes which are 16 and the 31 steel nodes. Figure (6.17) shows the stress distribution in the bar for the above selected numbers of steel nodes. Dividing the bar into 15 2-noded bar elements will give 4 steel nodes per concrete element while dividing the bar into 30 bar elements will produce 8 steel nodes per concrete elements. As it can be seen from the above two figures the number of steel nodes has no effect on the solution in this case.

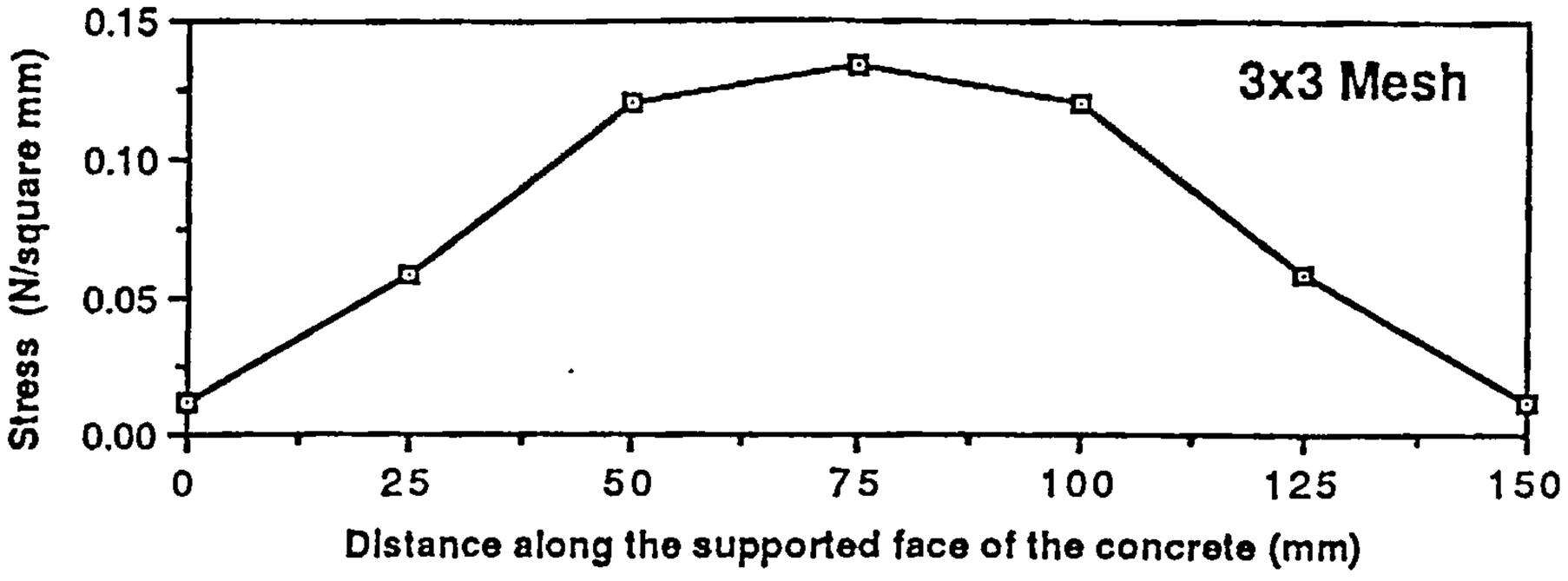

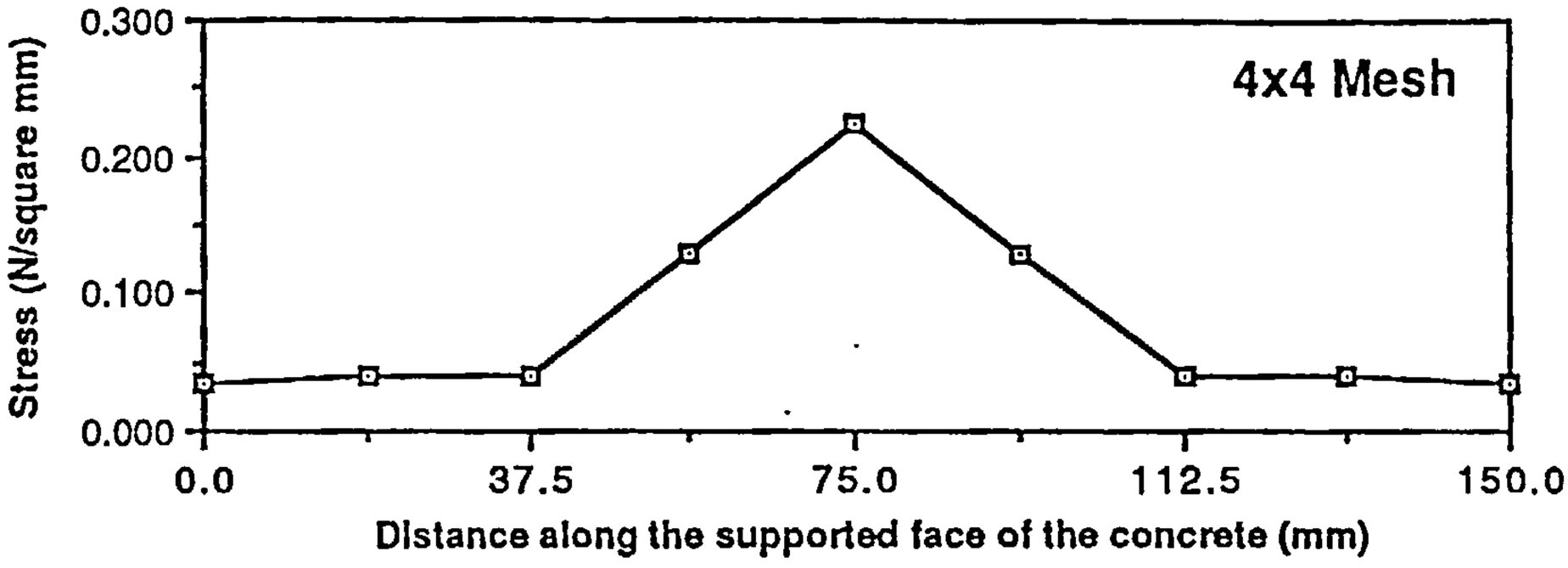

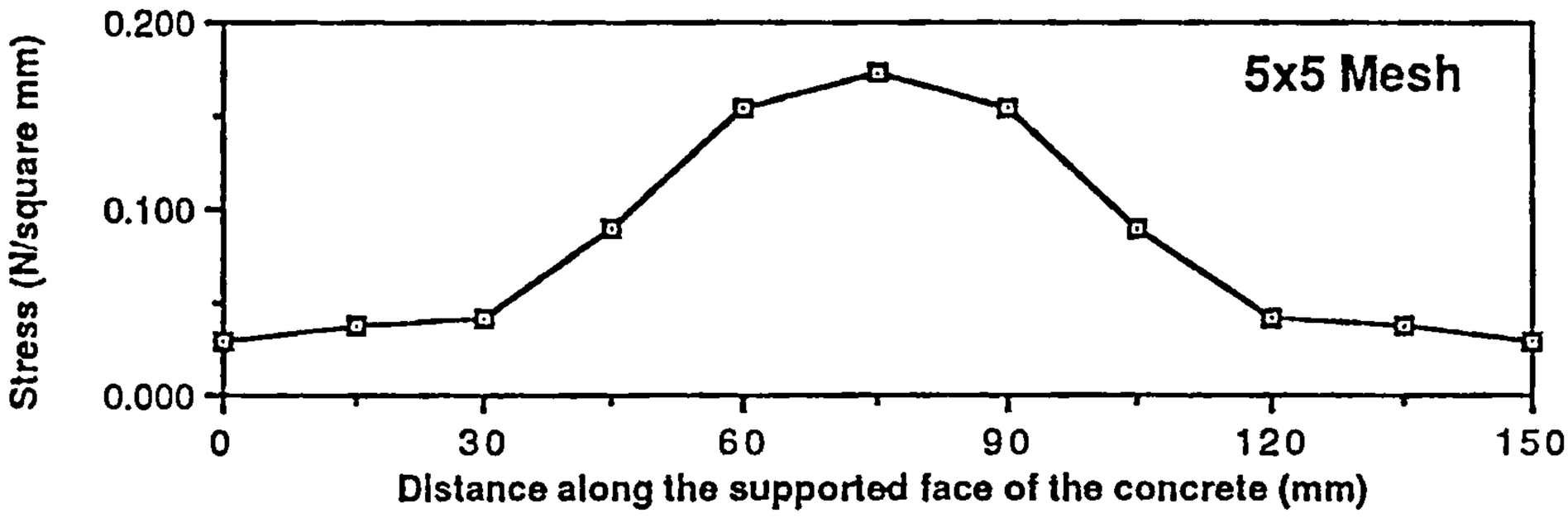

Figure (6.15) - Stress between concrete and support for the different meshes used in pull out test.

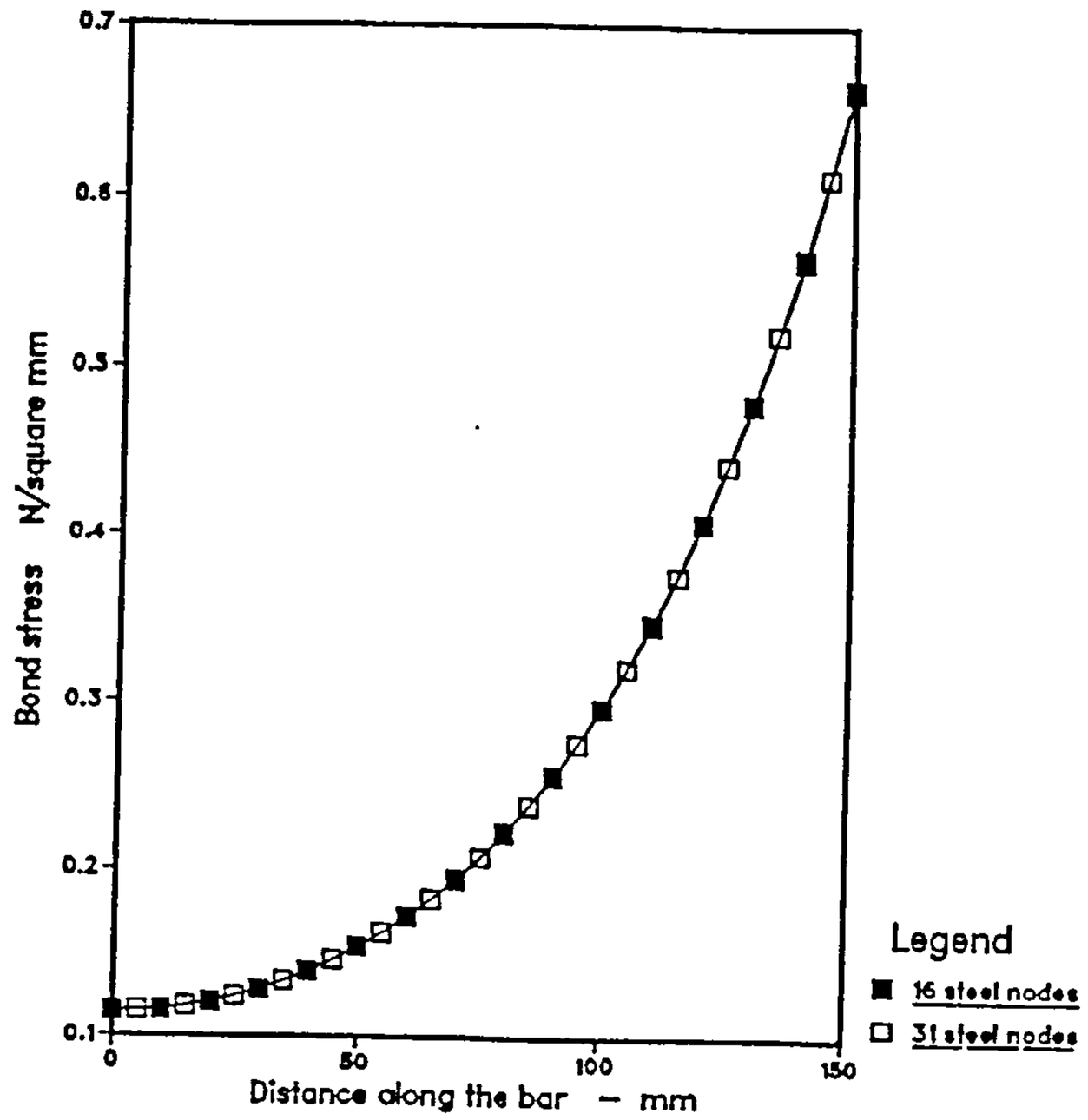

Figure (6.16) - Effect of number of steel nodes used on bond stress in pull-out test

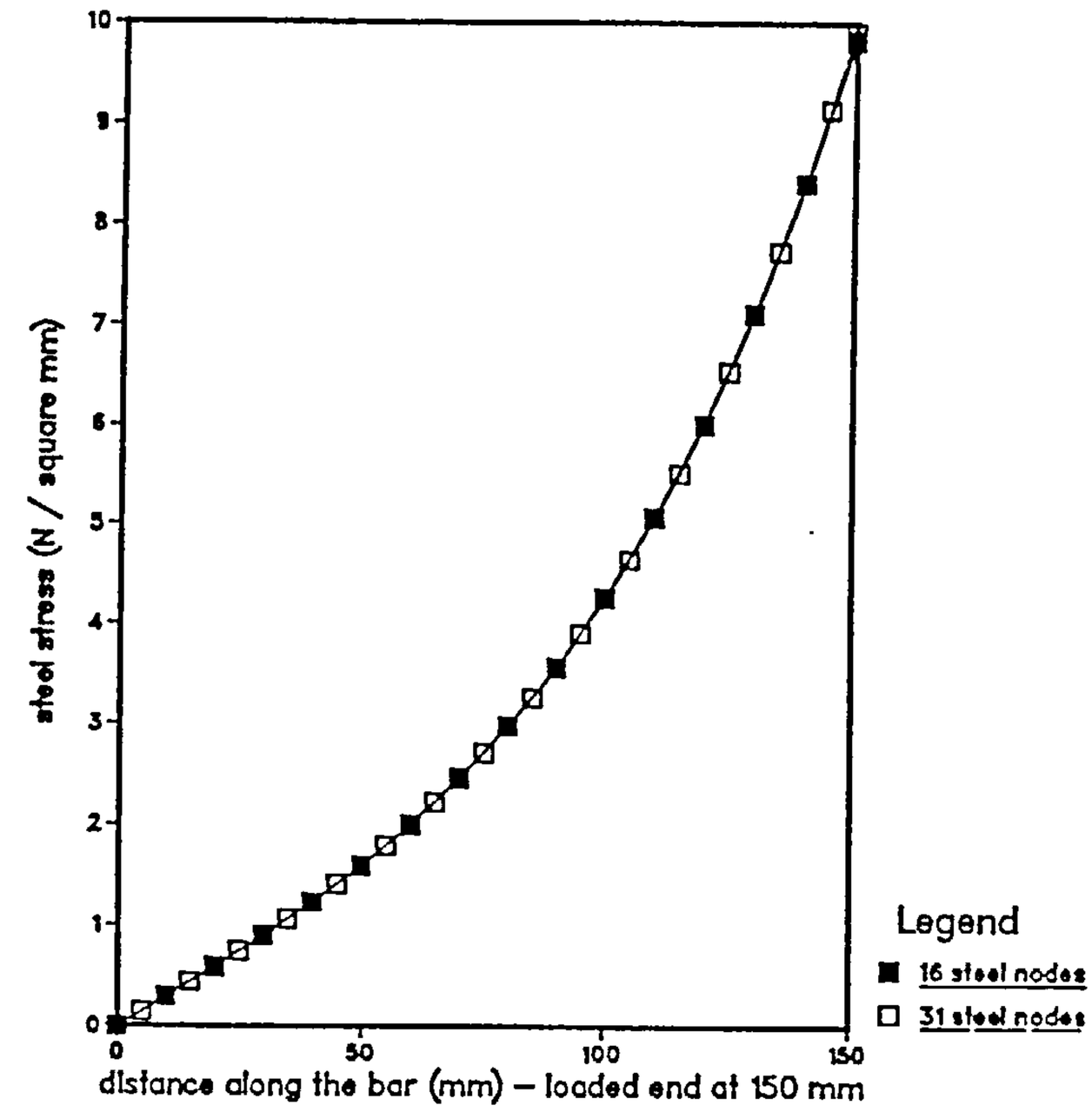

Figure (6.17) - Effect of number of steel nodes used on steel stress in pull-out test

6.5 Cantilever

6.5.1 Details of the problem

Figure (6.18) illustrates a real reinforced concrete cantilever and column layout. The cantilever length is 144 inch (3658 mm) and which is designed according to ACI Code 318-83. All the reinforcements shown in the figure which includes details such as curtailed bars, stirrups and ties are included in the analysis. The reinforcement consist of :

Cantilever: 2 bars no. 8 full length tension reinforcement
1 bar no. 8 curtailed bar for tension reinforcement.
2 bars no. 3 to hold stirrups
14 stirrups 2 bars no. 3 / stirrup

Column : 4 bars no. 8 longitudinal reinforcement
10 ties 2 bars no.3 / tie

Including such reinforcements will demonstrate the ability of the method to handle various reinforcement arrangements and orientations.

The parameters used for concrete,steel and bond are the same as used in the beam of section (6.3.1).

6.5.2 Finite element mesh

The difficulties faced in constructing a finite element mesh for this problem by the conventional finite element analysis is

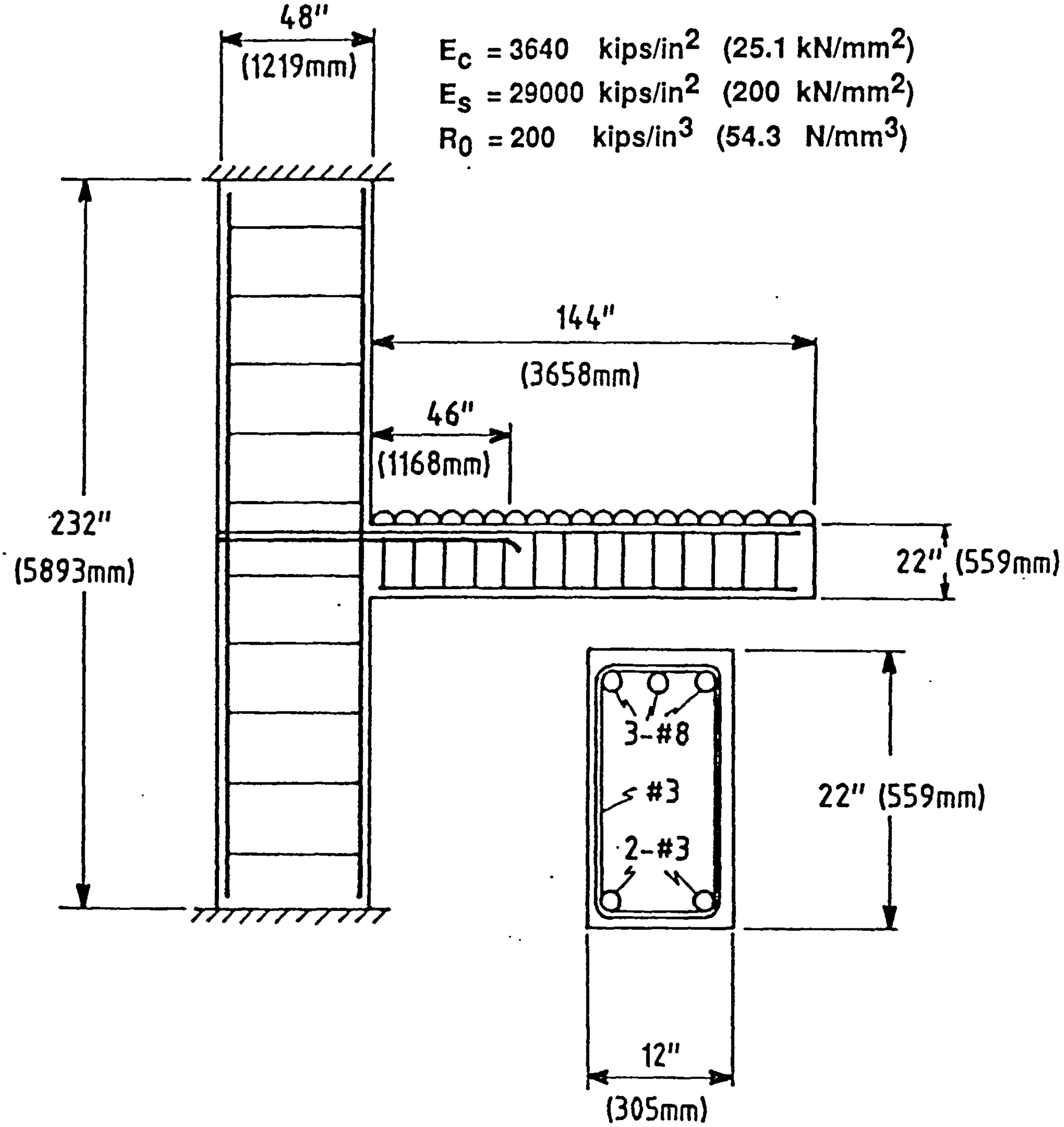

Figure (6.18) - Details of cantilever and reinforcement.

discussed in section (3.1). Using the method developed in chapter 3 leads to selecting a suitable finite element mesh for the concrete alone. Thus, the concrete mesh shown in figure (3.5) is used for this problem. There are 42 8-noded rectangular concrete elements with a total of 165 nodes.

Each of the reinforcing bars was divided into a different number of 2-noded bar elements on its own. Full length reinforcement is divided into 96 bar elements and curtailed bar into 47 bar elements. Rest of reinforcement are divided into different numbers of bar elements. There are 29 reinforcement bar groups with a total of 350 steel nodes.

The stirrup ends are also fixed to the concrete by high bond for the same reason given in section 6.3.2 . The same thing is done to the tie ends.

Anchorage of tension reinforcement

From the design of the cantilever it is found that the straight embedment of the tension reinforcement is enough to anchor the bars both in the column and in the beam. To demonstrate the applicability of the method to reinforcement anchorage the tension steel ends will be anchored in the column using the two methods explained previously which is anchorage by high bond and by applying a force.

6.5.3 Results and discussion

The solution of this problem is obtained in 5 iterations using two dimensional plane stress analysis.

Stress in tension reinforcement:

Figure (6.19) shows the stresses in both the full length and the curtailed tension steel of the cantilever. Of interest in the figure the occurrence of the peak stress in the cantilever tension steel which is lying outside the column and not at the column face. This reflects the increasing contribution made by the curtailed bars to resisting the bending moment in this zone.

Bond stress along the tension bars:

Figure (6.20) shows the bond stress distribution along the full length tension bars. The dotted straight line in the figure represents the location of the column face. The peak bond stress occurs virtually at the column face. Again as in the beam problem there are irregularities in the bond stress curves which coincide with the concrete element edges. These irregularities is an affect of the same phenomenon noted in the bond stresses of the beam problem section (6.3.3). The same explanation given for the beam problem holds here.

Figure (6.21) shows the bond stress distribution in the curtailed tension bar along with the full length bar. The bond stress at the free end of the full length bar is zero while the bond stress at the curtailed bar free end is not zero as may be expected although no anchorage is applied at either of the two ends. The reason for this is as follows. The last few inches of the curtailed bar is much less

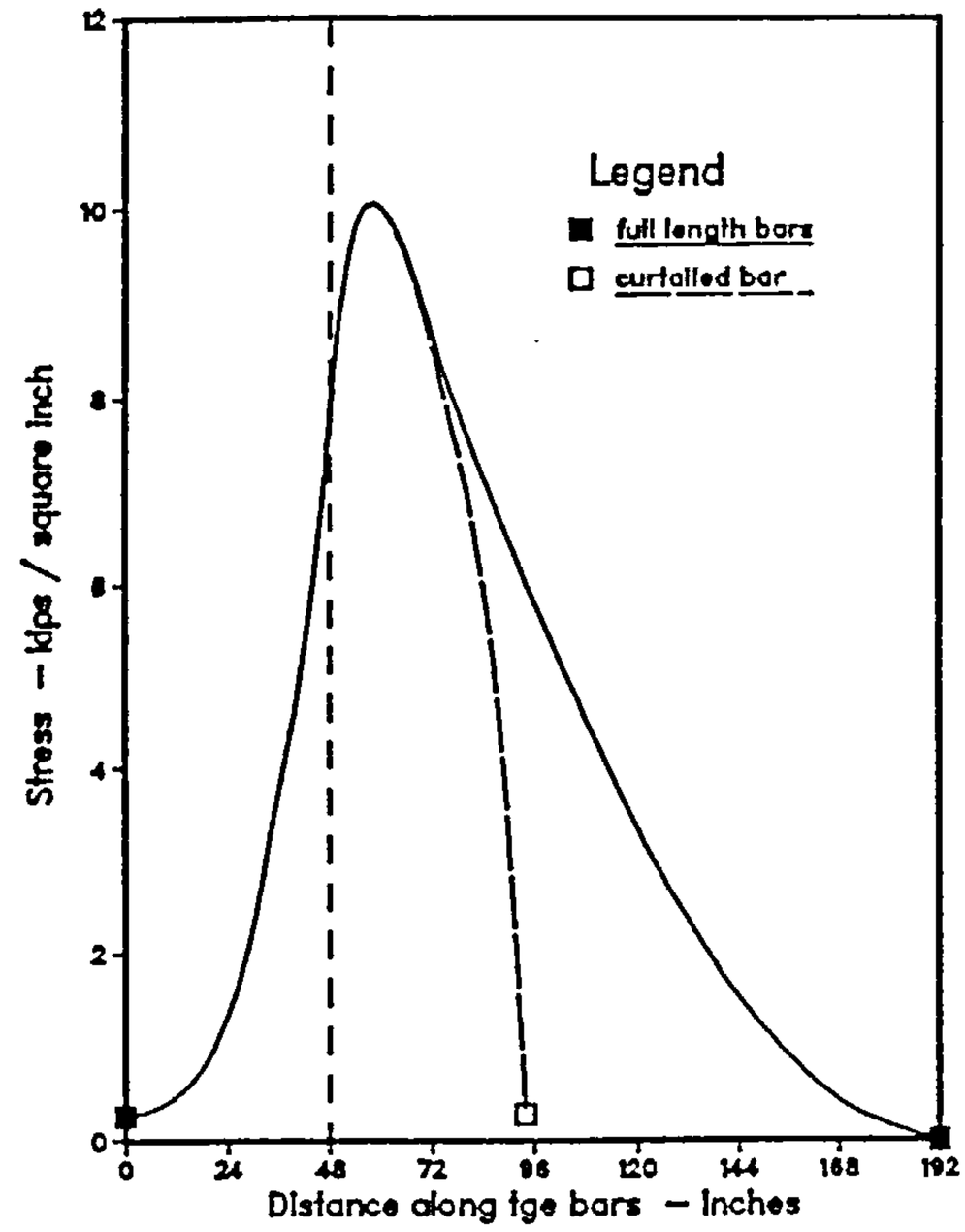

Figure (6.19) - Stress in tension steel for the cantilever.

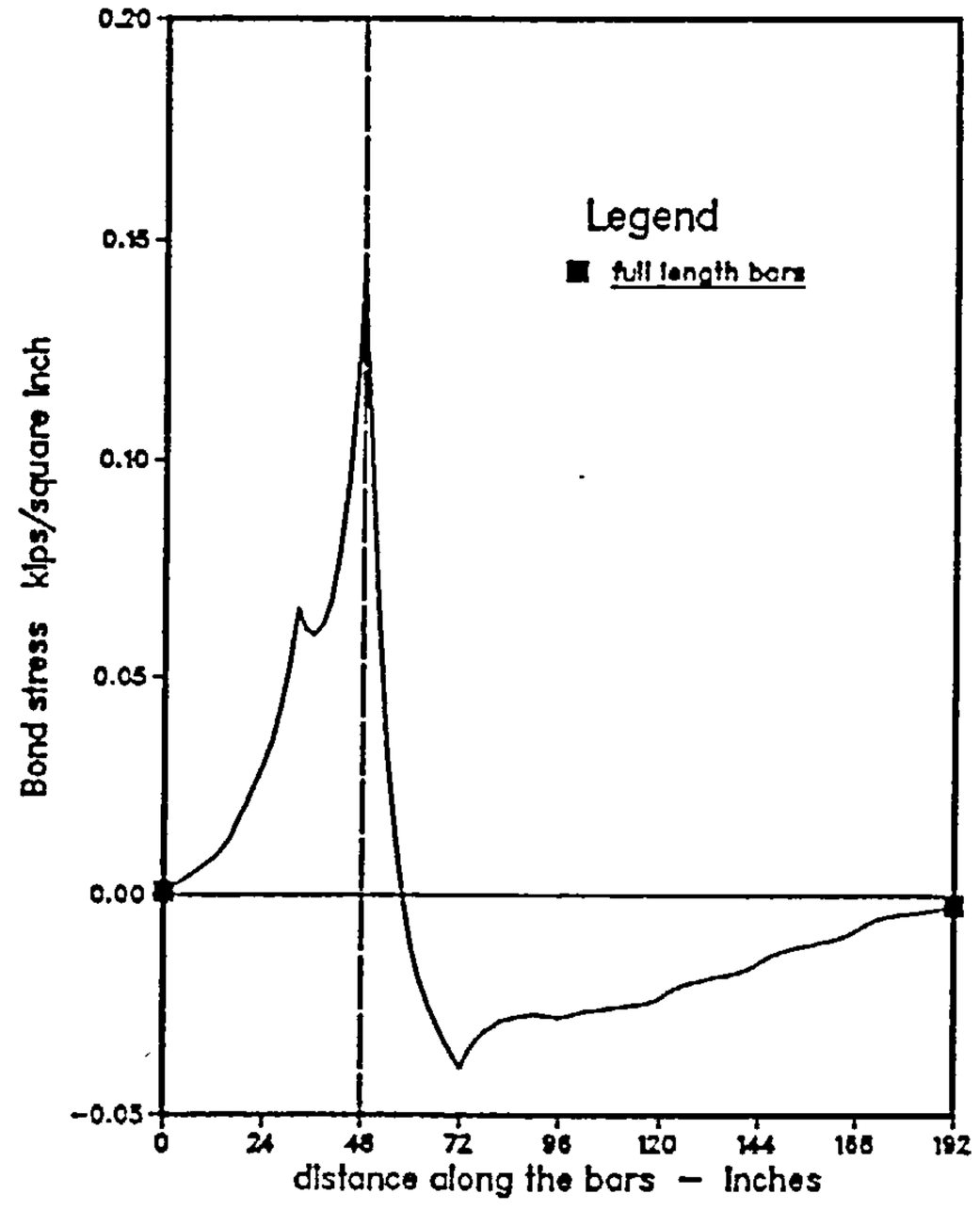

Figure (6.20) - Bond stress along the full length bar in the cantilever.

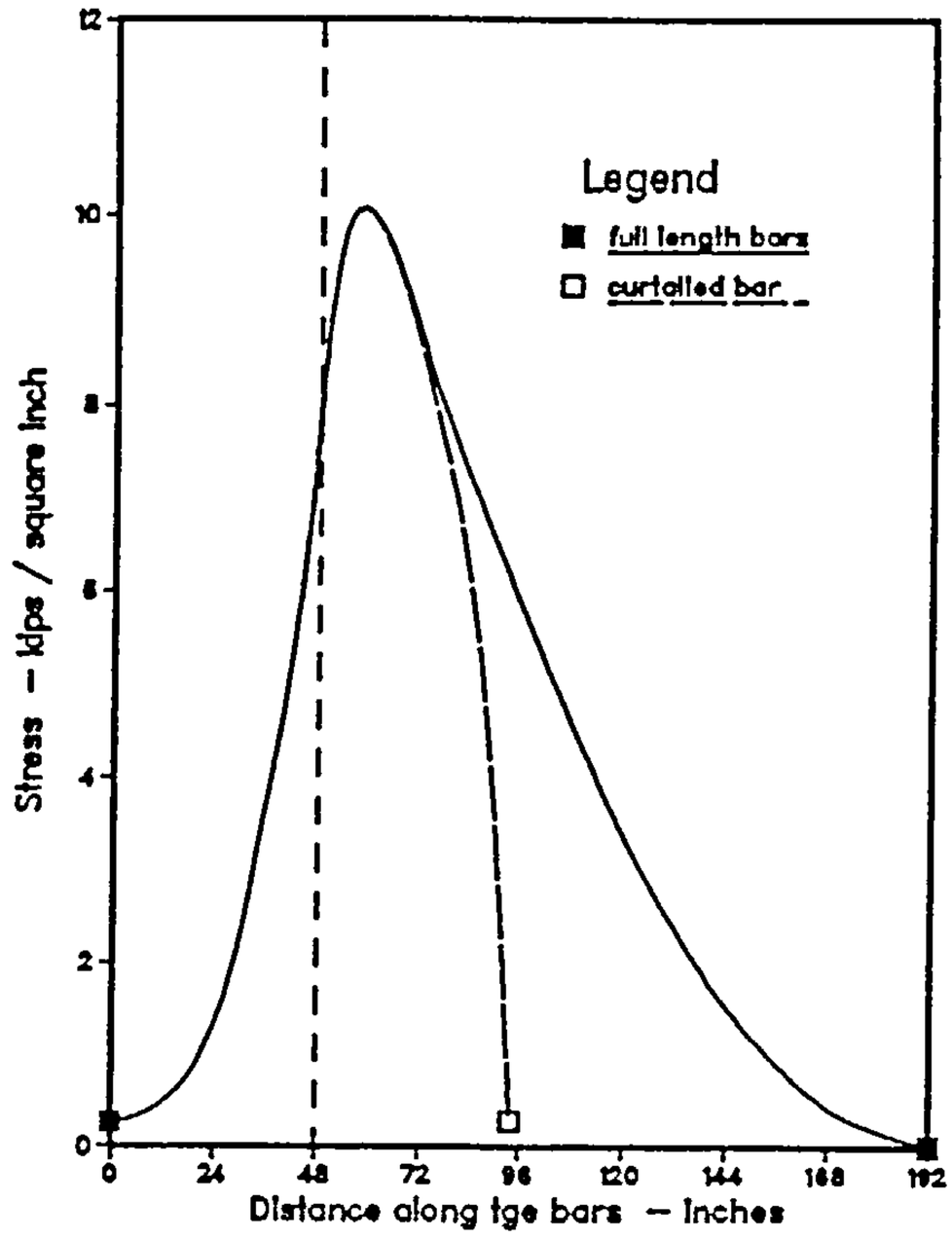

Figure (6.19) repeated

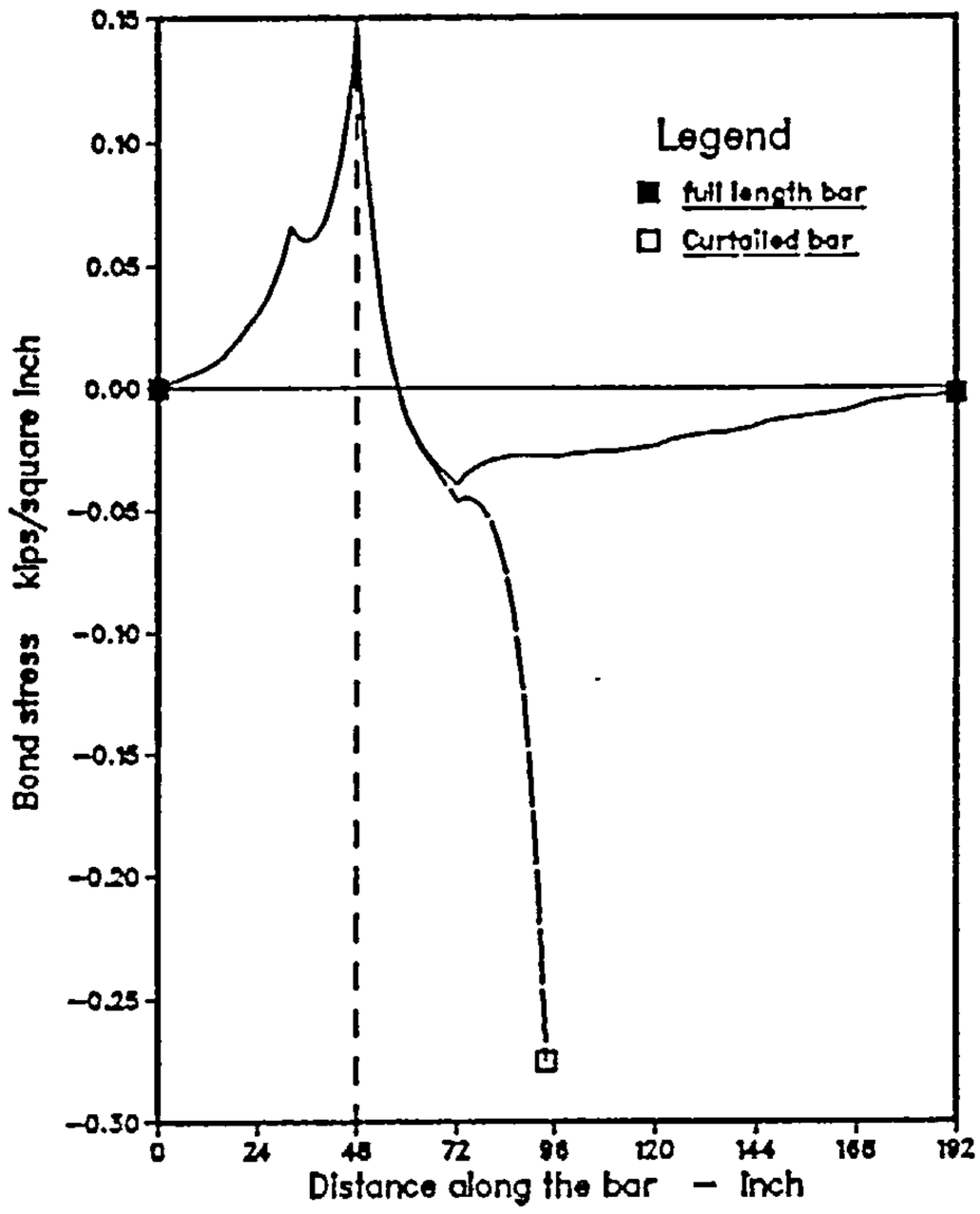

Figure (6.21) - Bond stress along both tension reinforcement bars.

effective in carrying load when compared to the corresponding part of the full length bar as shown in figure (6.19). Thus the steel nodes in this area gains very little or zero extra deformation due to loading of this part of the bar. Therefore, steel nodes in this area can not deform as much as do the corresponding nodes in the full length bars although they occupy the same position as far as the model is concerned. The effect of this is greatest at the free end. Thus, the difference between displacements of these nodes specially the free end of the curtailed bar and the surrounding concrete is greater than the corresponding nodes in the full length bars. Since the bond stress is calculated from the relative displacement between the concrete and the steel, therefore, this will show a bond stress to exist at the free end of the curtailed bar and which is greater than the corresponding bond stress of the full length bar in that area.

Anchorage of tension reinforcement

i) Anchorage by high bond

The solution obtained above is obtained with the tension reinforcement being anchored to the concrete at the column face. Anchorage is done here by setting the value of R_0 at nodes numbers 1 and 98 which corresponds to the first nodes in the full length and curtailed tension bars respectively to be 10000x200 kips/in^3 . Figure (6.22) shows the steel stress in the tension bars for the two cases with and without anchorage. The stress is zero when no anchorage is used and there will be stress in the bar ends if the ends are anchored. The effect will be more clear if a shorter

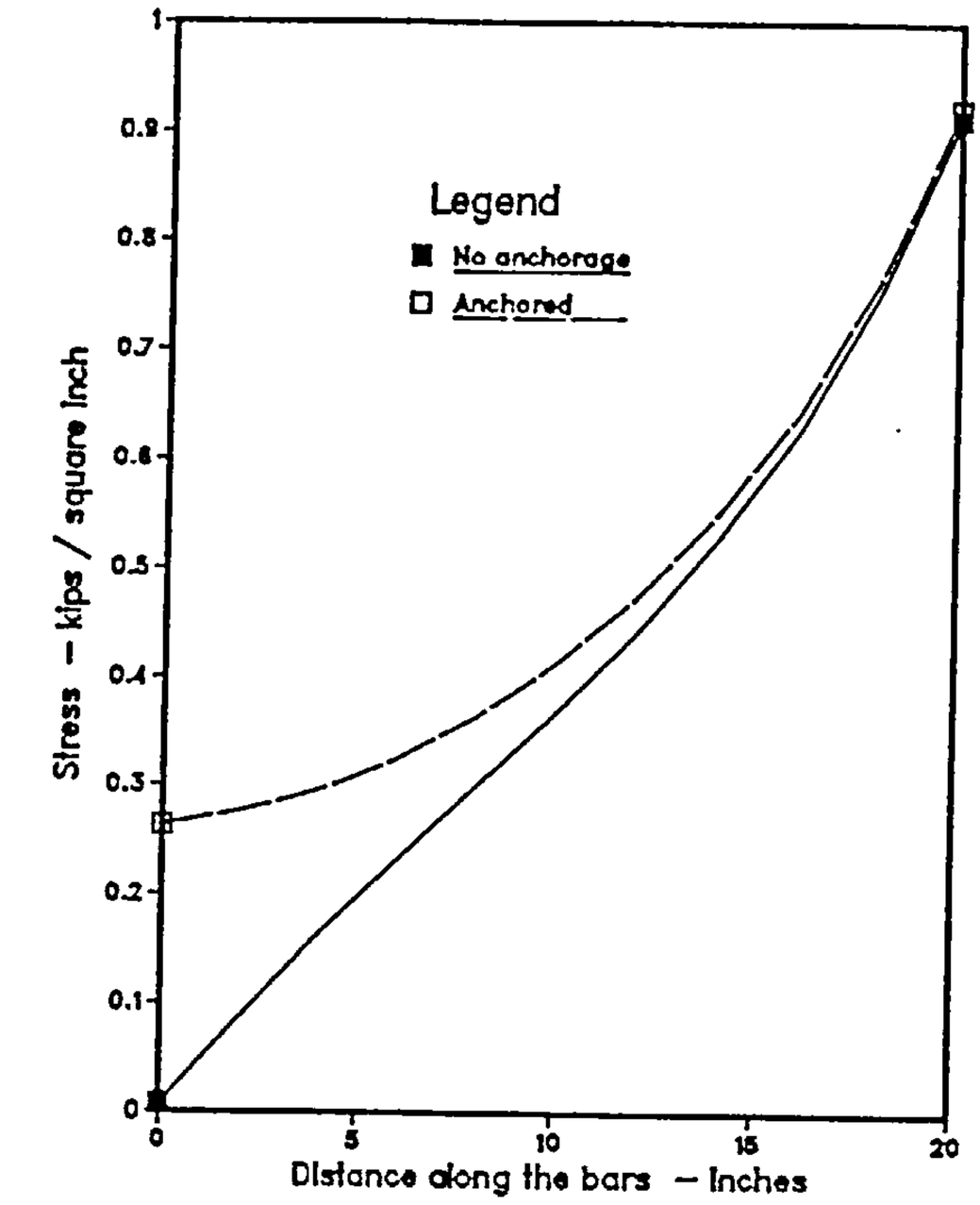

Figure (6.22) - Effect of anchorage on stress in tension steel near the anchored end.

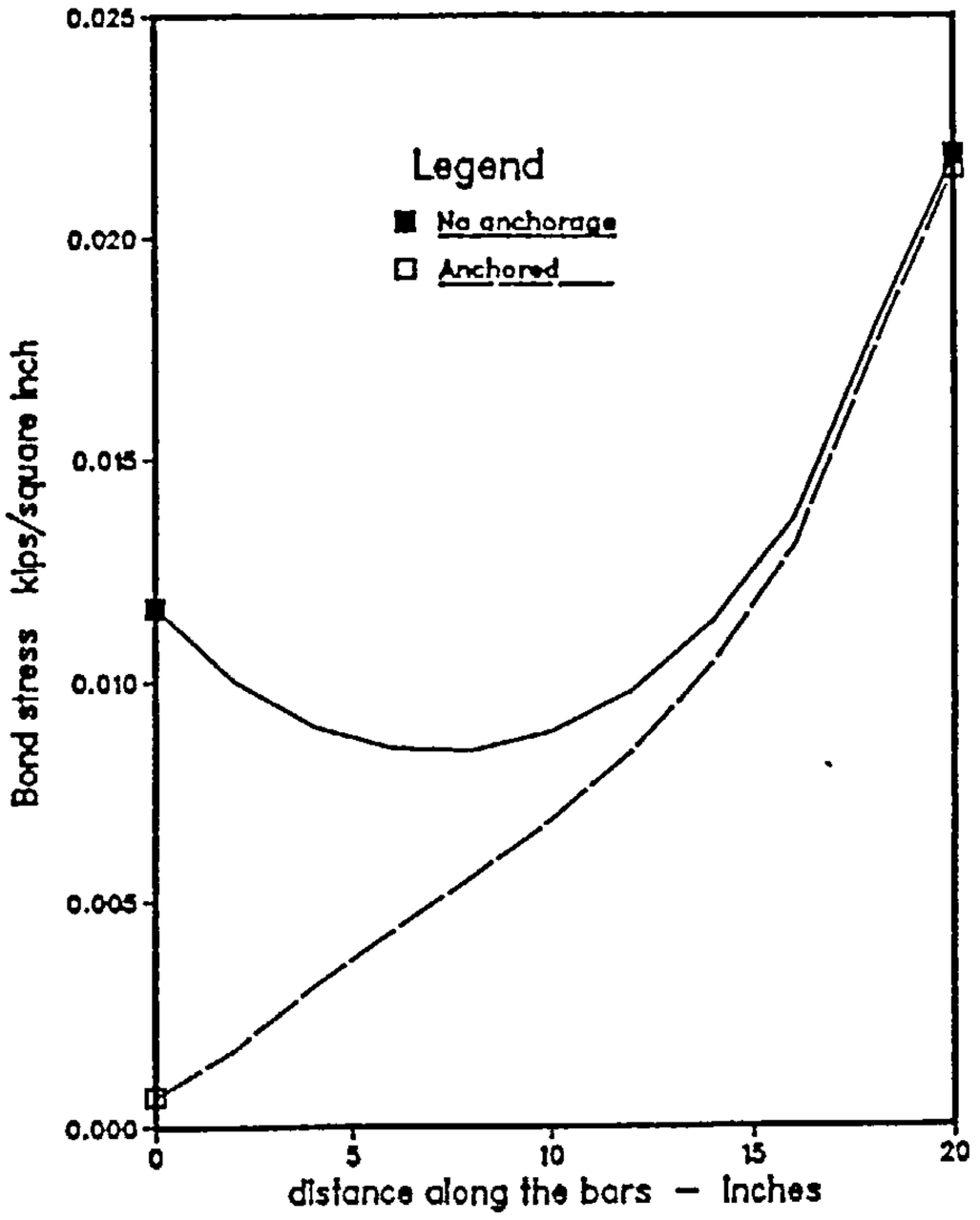

Figure (6.23) - Effect of anchorage on bond stress near the anchored end.

embedment length of the bars is used within the column. Figure (6.23) shows the effect of anchorage on bond stress. The anchored end shows zero bond stress when the bar ends are anchored. The solution obtained reflects the expected behaviour.

ii) Anchorage by applying a force

The purpose of this solution is to apply an external force to the tension bars at the bars ends which are to be anchored as explained in chapter 4. This is done by specifying an approximate development length, d_l, which is entered in the input data of the program along with the nodes numbers which are to be anchored. In this case a development length of 12 inches is the approximate value entered for both full length and curtailed bars. The program calculates a development length of 10.87 inches which is needed to hold the tension bars end to the concrete so that the relative movement results between the bar end and the surrounding concrete is less than a specified tolerance. i.e 10^{-6} mm (section 4.6). The number of iterations needed for the solution is the same as in the case of anchorage by high bond i.e. no extra number of iteration is required to achieve this method of anchorage.

The solution obtained is the same as the one obtained using high bond for both the stress produced in steel and the bond stress as shown in figures (6.24) and (6.25) respectively.

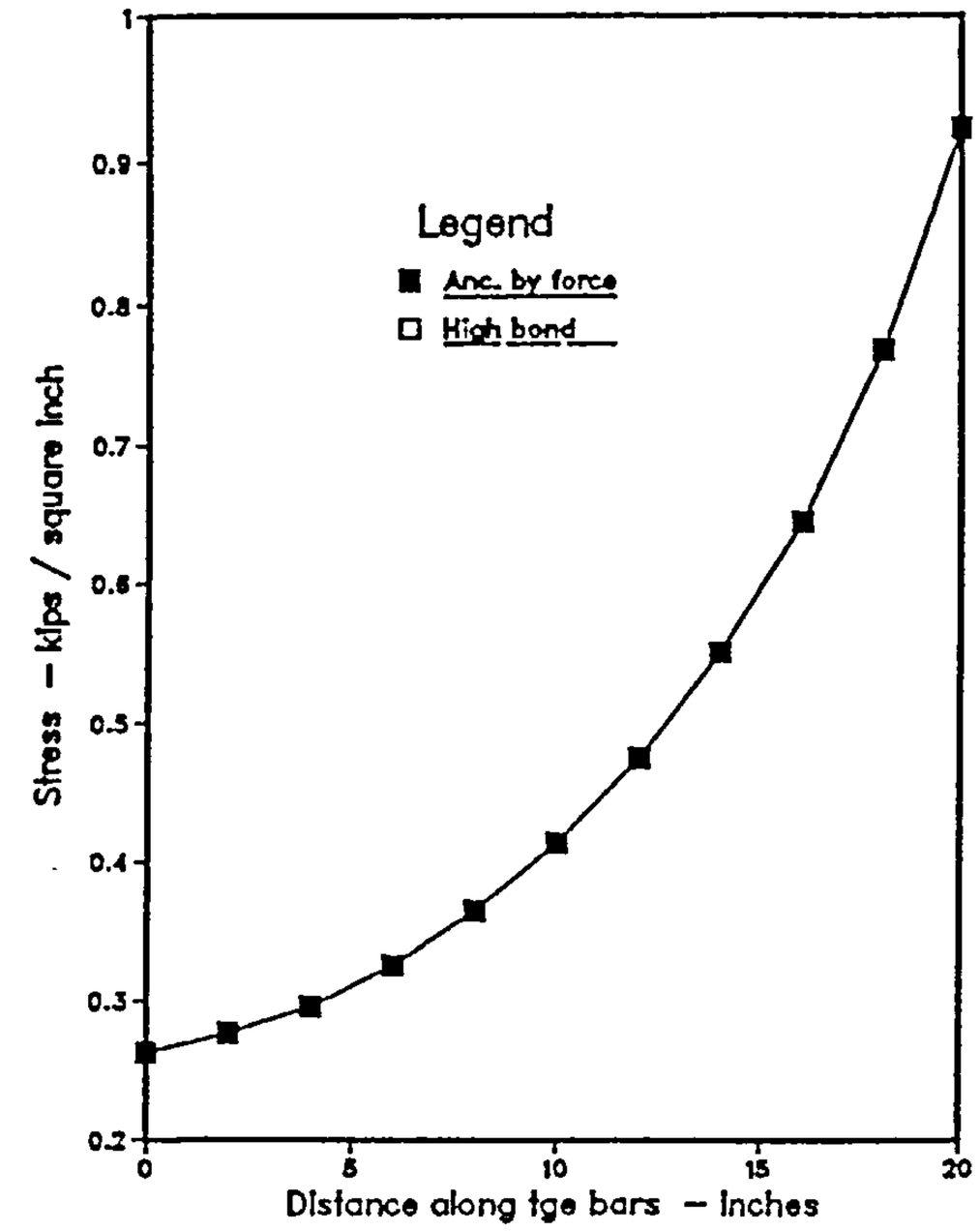

Figure (6.24) - Effect of method of anchorage on steel stress.

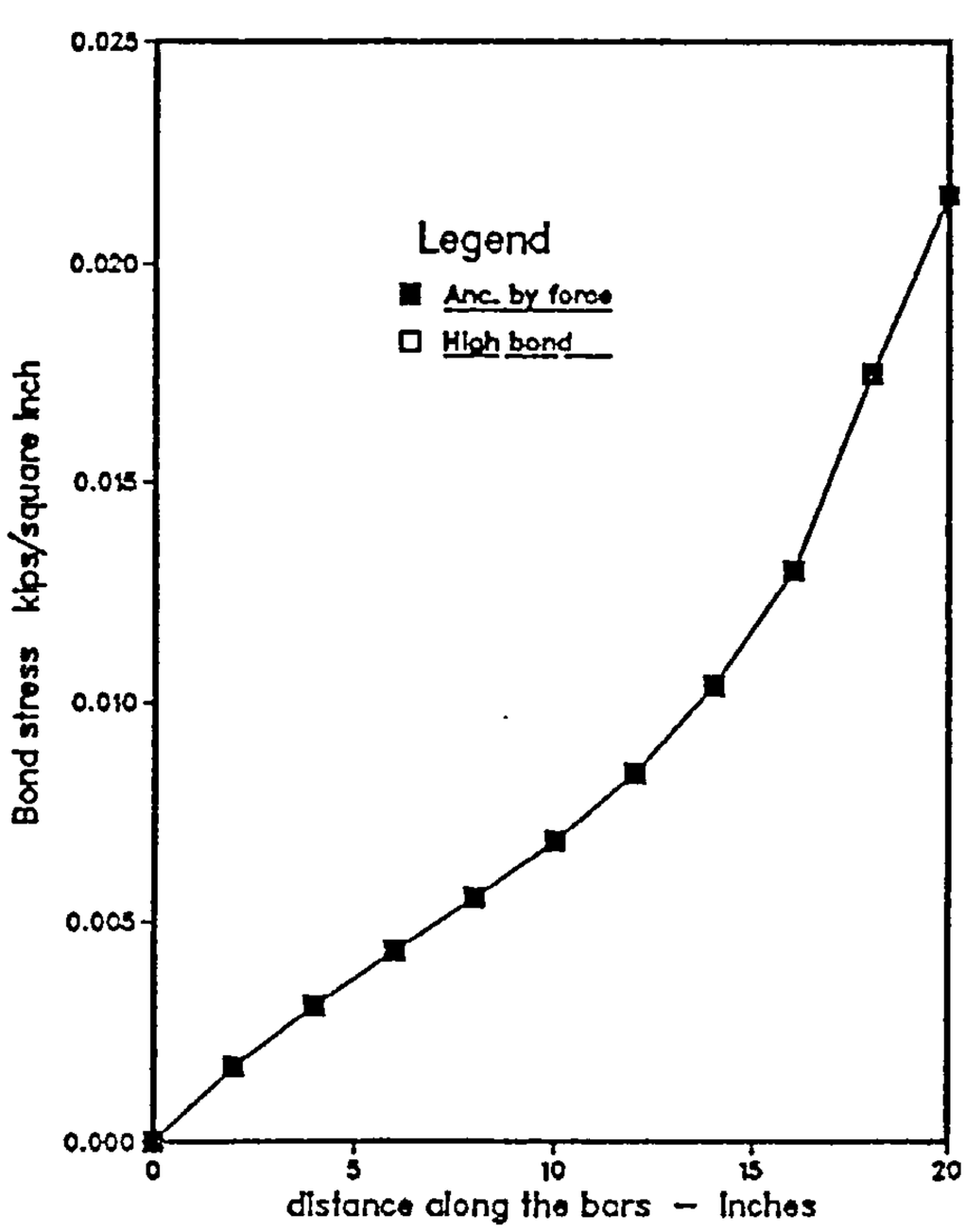

Figure (6.25) - Effect of method of anchorage on bond stress.

Effect of bond stiffness modulus: Figure (6.27) shows how the bond stiffness R_0 affects the stress distribution in the full length tension bars. It will be noted how sensitive the peak stress is to the choice of value for R_0. It is also noted that large R_0 values reflect greater bond strength between the steel and the concrete and so the stress in the steel increases as R_0 increases. Figure (6.28) shows the bond stress distribution for the different R_0 values used.

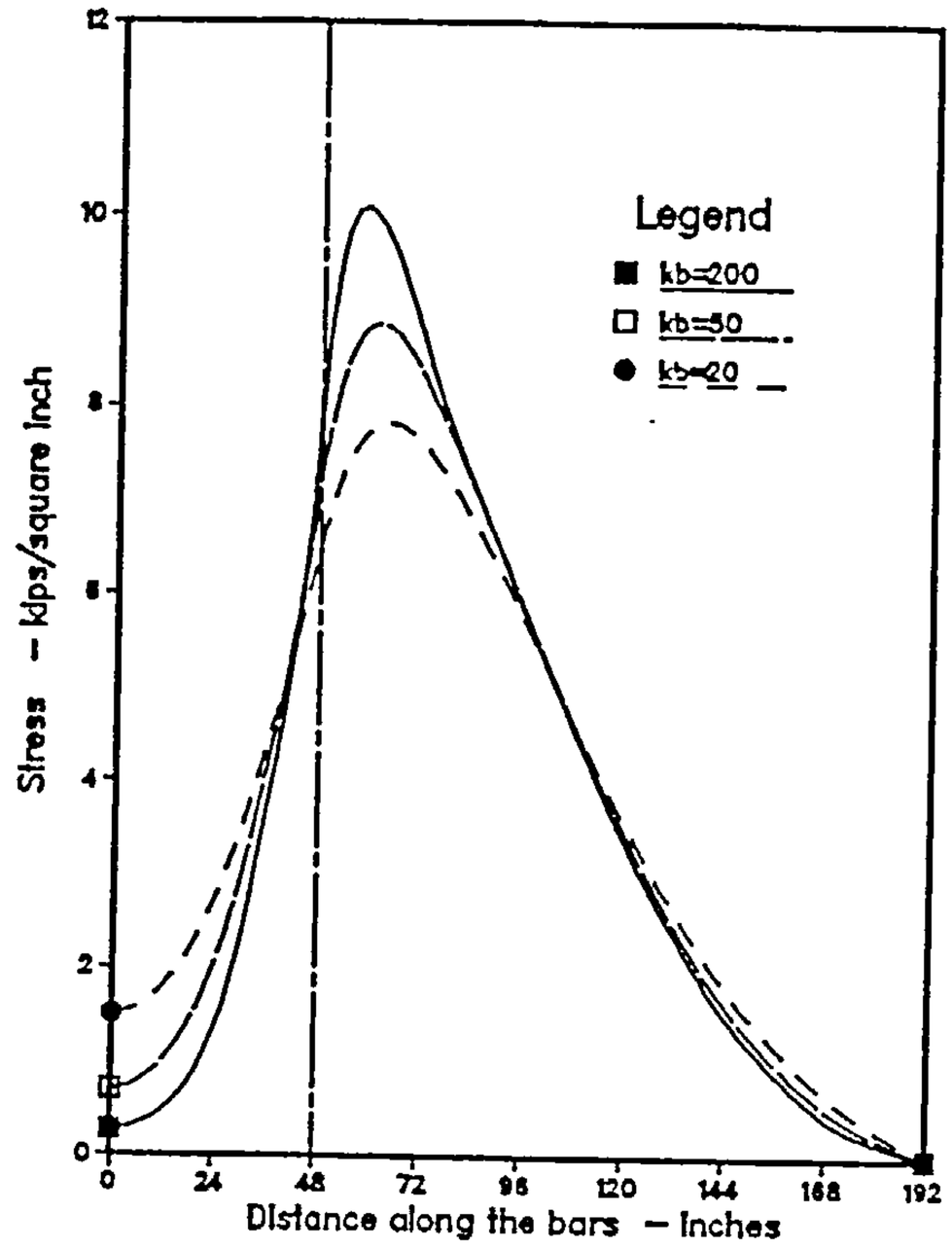

Figure (6.26) - Effect of R_0 on the steel stress in the full length bar.

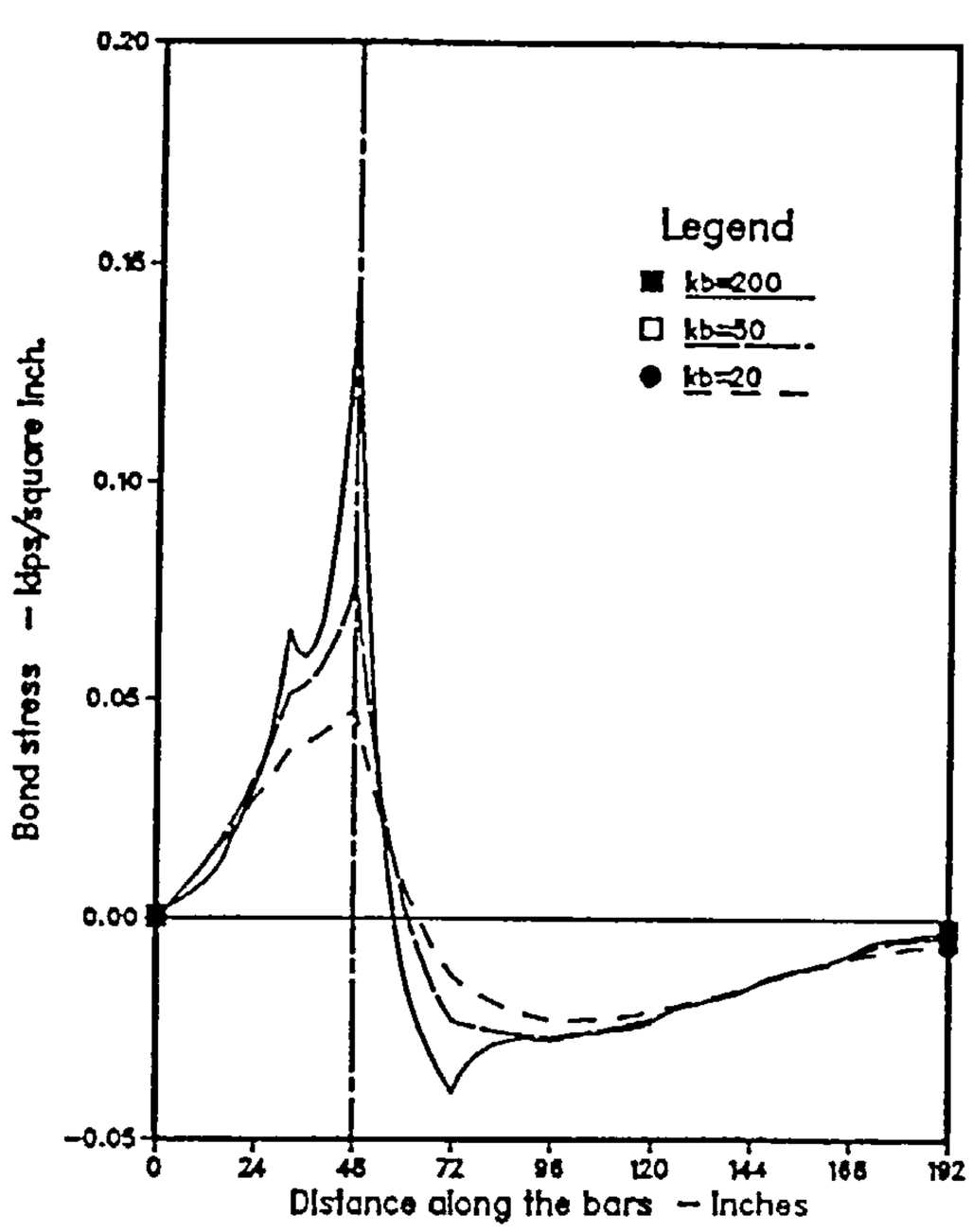

Figure (6.27) - Effect of R_0 on the bond stress in the full length bar.

Chapter 7

7. SOLUTION OF NONLINEAR BOND BEHAVIOUR

7.1 Introduction

The purpose of this chapter is to demonstrate the way in which nonlinear material behaviour can be included along with the method of solution presented in chapter 4.

The bond model developed in chapter 3 was based on linear elastic stress-strain relationship for concrete and steel. Also linear elastic bond stress-slip relation was used for bond between steel and the surrounding concrete. A more appropriate analysis is to consider nonlinear behaviour of all above elements of reinforced concrete. However, since in this thesis, material modelling is not of primary importance but how to include a nonlinear method of solution of nonlinear material behaviour with this new method of modelling is more important, further, this research is more concerned about modelling of bond between concrete and steel using the new method presented in chapter 3, therefore, a nonlinear stress-slip relationship for bond is adopted. The linear bond model developed in chapter 3 will form the basis for the nonlinear bond model.

The method of solution can be used with any nonlinear bond model. As pointed out in chapter 5 a nonlinear bond model described by Allwood et al. (1984) which incorporates many details about bond behaviour was selected.

In this chapter techniques for solution of nonlinear material behaviour are reviewed briefly. An incremental iterative method is adopted and thus is explained in detail as applied to the nonlinear bond model of Allwood et al. Convergence of the incremental iterative method is discussed.

7.2 Nonlinear methods of solution

In general techniques used in the solution of nonlinear material behaviour can be broadly classified into three types :

i) Incremental loading method.

ii) Iterative methods

iii) A combination of the two approaches

i) Incremental loading method :

In this method the load is subdivided into small load increments such that a linear approximation can be assumed for each of the load increments. Further, as the solution of a load increment is obtained a new stiffness matrix is calculated using the current slope of the stress-strain relationship. Then the next load increment is applied and a solution is obtained using the stiffness matrix obtained from the updated slope. The method is illustrated in figure (7.1). A better approximation can be obtained by reducing the size of the load increments but on the other hand this increases the number of times for recalculating the stiffness matrix which is an expensive operation from computer point of view.

ii) Iterative method:

Iterative methods require resolution of the problem until a solution which satisfies the nonlinear relationship is obtained. This can be done by direct iteration as shown in figure (7.2). In this method the full load is applied to the structure and the solution is repeated until a satisfactory solution is reached.

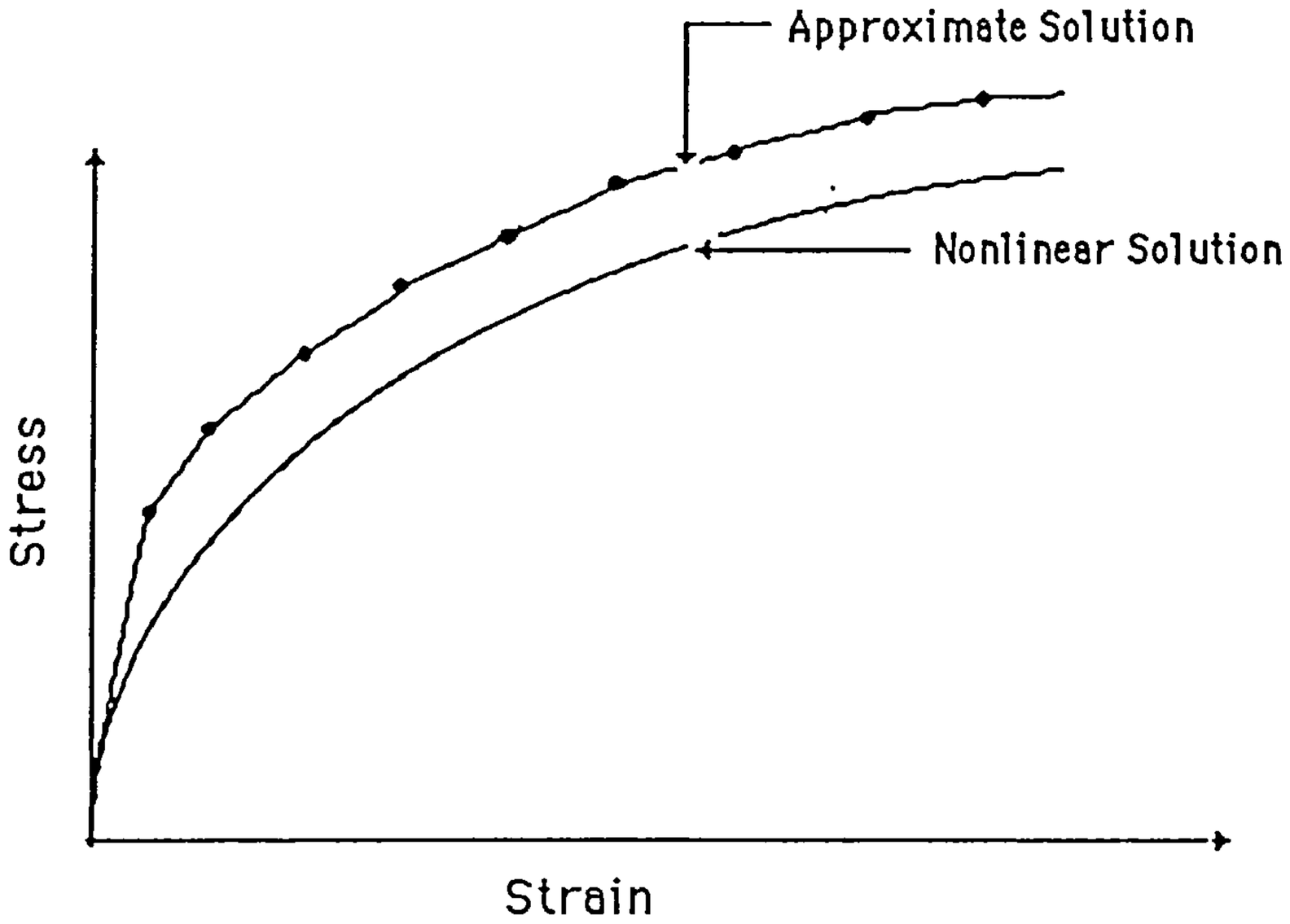

Figure (7.1) - Incremental loading method.

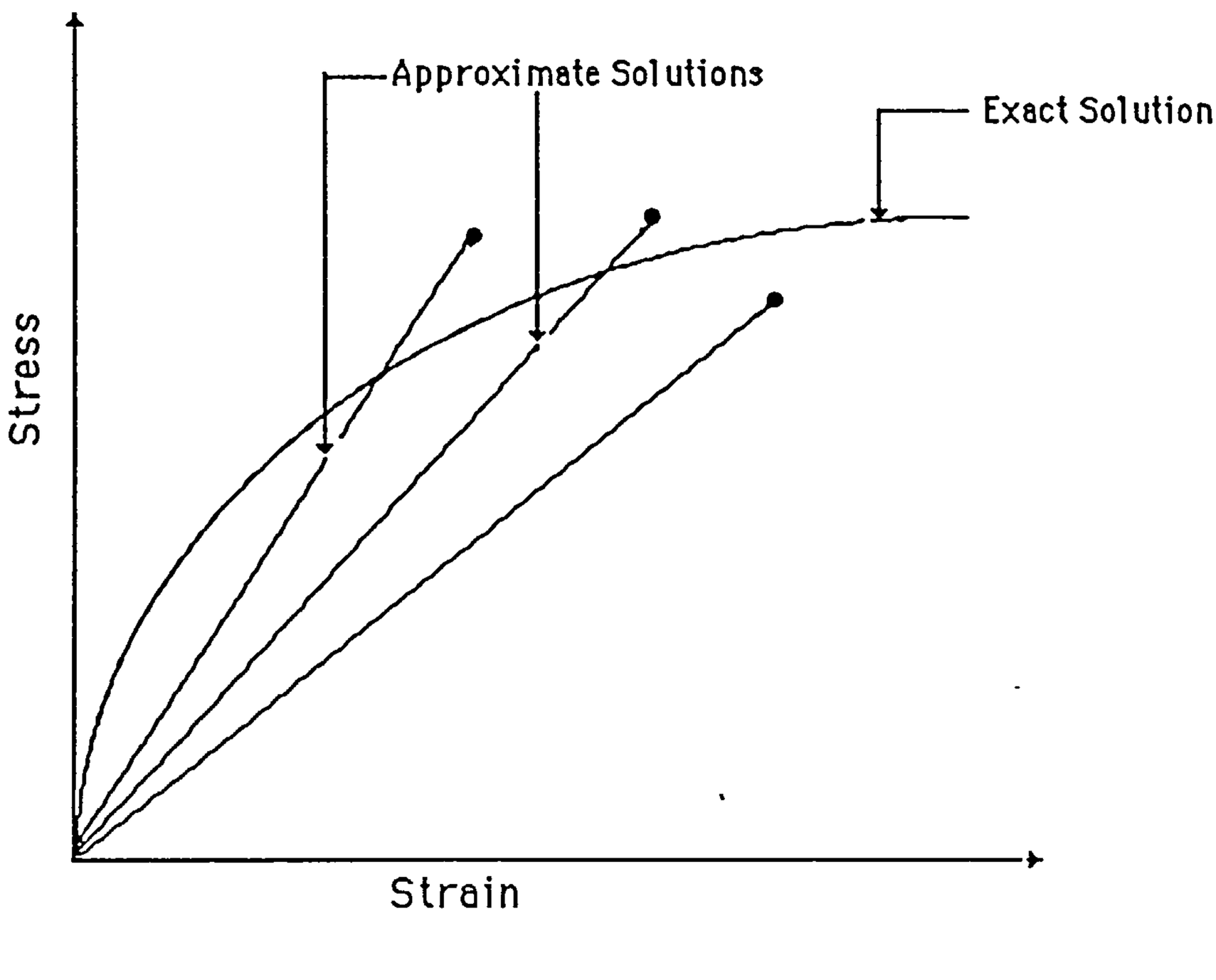

Figure (7.2) - Direct iteration method.

Another iterative method is the method of residual forces. In this method a solution is obtained using linear relationship then the linear solution is compared to the nonlinear "exact" solution. The difference between the two solutions is the out of balance residuals which are a measure of lack of equilibrium. These residuals are then applied to the structure to restore equilibrium. The process is repeated until the residuals become sufficiently small. There are two methods to achieve this which are the initial stress method and the initial strain method.

The initial stress method is shown in figure (7.3). A solution is obtained using linear elastic analysis which is represented by point 1 in figure (7.3). The solution is then compared to the exact solution represented by point 2. The difference between the two solutions represents the out of balance stresses or residual stresses. The residual stresses are then applied to the structures at nodal points in the form of forces. If needed, these forces can be transferred at element nodal points using the virtual work principle as in the case of concrete. A new solution is thus obtained which is indicated by point 3 in the same figure. The process is repeated until every residual stress becomes smaller than a specified tolerance. In this process the stiffness matrix needs to be calculated only once.

The method may still be improved to obtain faster convergence by using either the tangent or the secant stiffness approaches figures (7.4). This is accomplished by recalculating the stiffness matrix during the solution, based on the accumulated level of strain or displacement, using the current secant or tangent values of

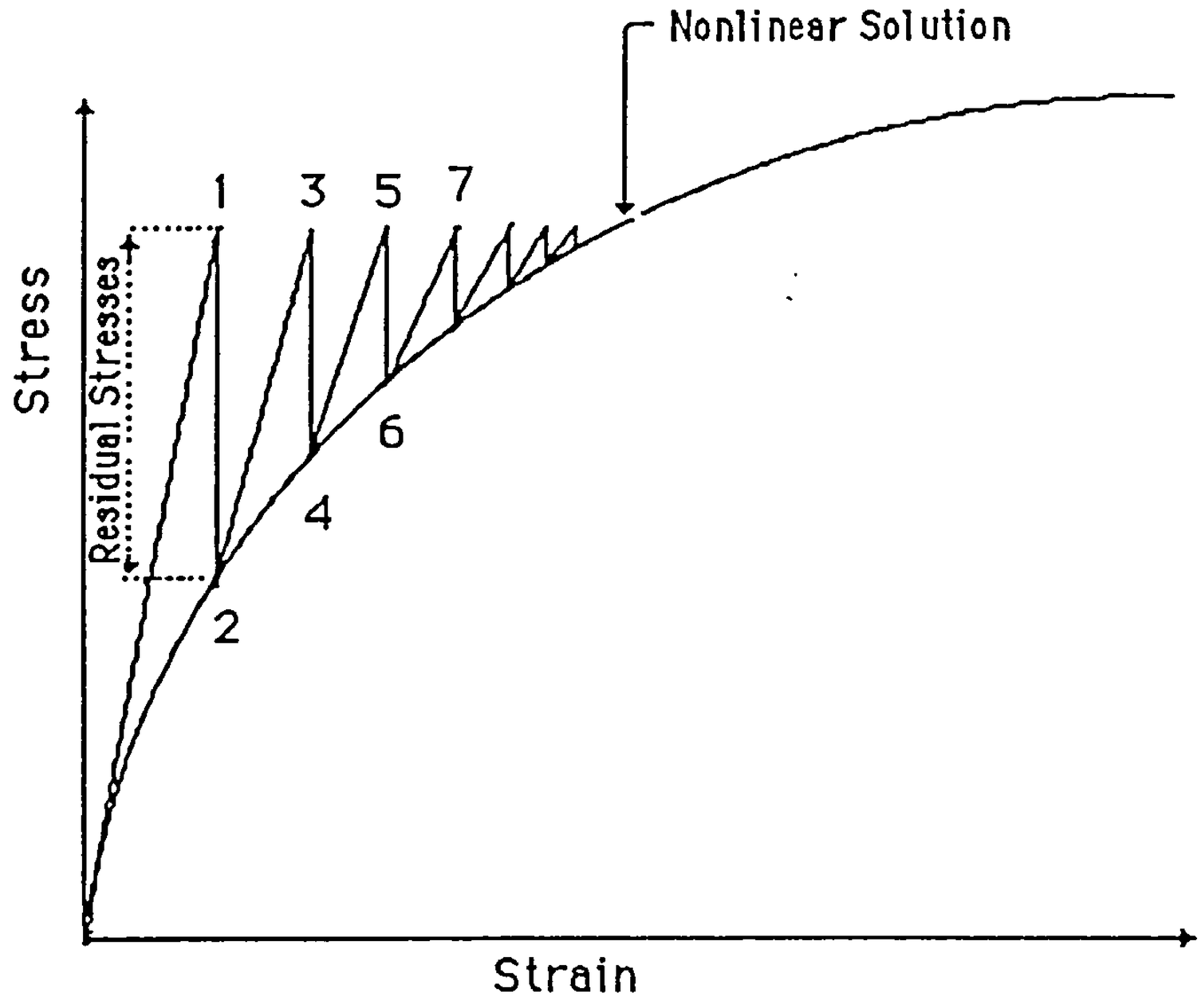

Figure (7.3) - Initial stress method.

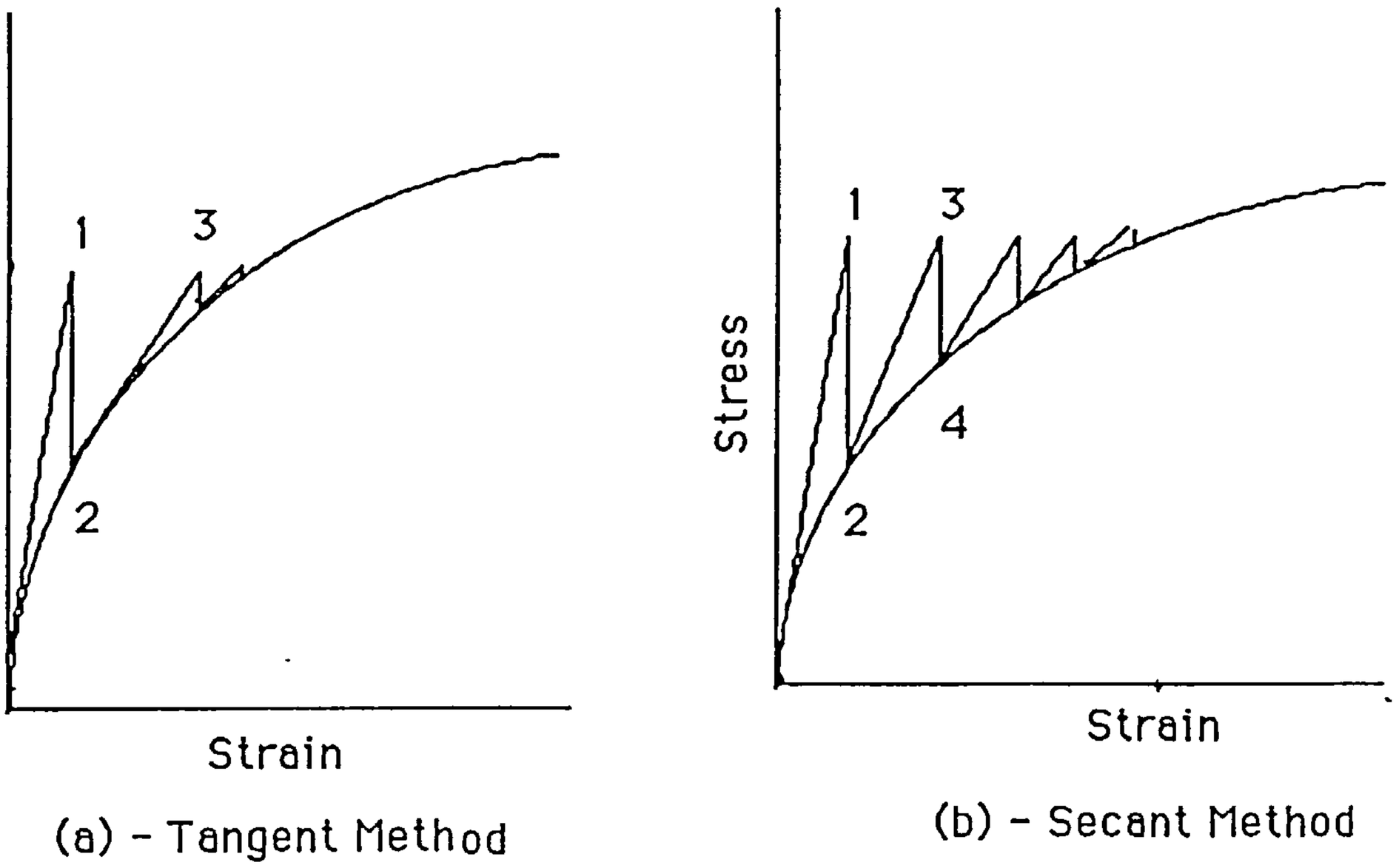

(a) - Tangent Method

(b) - Secant Method

Figure (7.4) - Tangent and Secant methods.

modulii. The solution converges faster than the initial method but involves extra calculations of the stiffness matrix.

iii) Combined solution

A solution can be obtained using the incremental and the iterative methods of solution presented above which is expected to be superior to both methods. In this method the load is divided into small increments and an iteration method is adopted for each increment of load. A new stiffness matrix is calculated at the beginning of each load increment based on the updated tangent of the stress strain curve. This method has been adopted and is explained in detail as used with the nonlinear bond model.

7.3 Nonlinear bond solution

7.3.1 Procedure outline

The nonlinear method of solution used in this research is a combination of the incremental and the iterative techniques introduced in the previous section. The linear solution presented in chapter 4 forms the basis for the nonlinear solution. Thus, both linear and nonlinear solutions involve iterative schemes. The iterative solution of the linear case will be in the middle of the iterative nonlinear solution. See flowchart (7.1).

The method is explained now in details for nonlinear bond behaviour. Flowchart (7.1) shows the basic steps for the nonlinear solution. The nonlinear bond behaviour is according to the Allwood et al. bond model presented earlier in chapter 5. The steps are outlined below :

1) The total load is divided into small increments.

2) Stiffness matrices namely K_s+K_b and K_B are calculated using the initial stiffness modulus, R_0.

3) A load increment is applied and the problem is solved using the linear method presented in chapter 4. It should be remembered that at this stage the solution will give the following among other things

i) Concrete displacements at concrete nodal points.

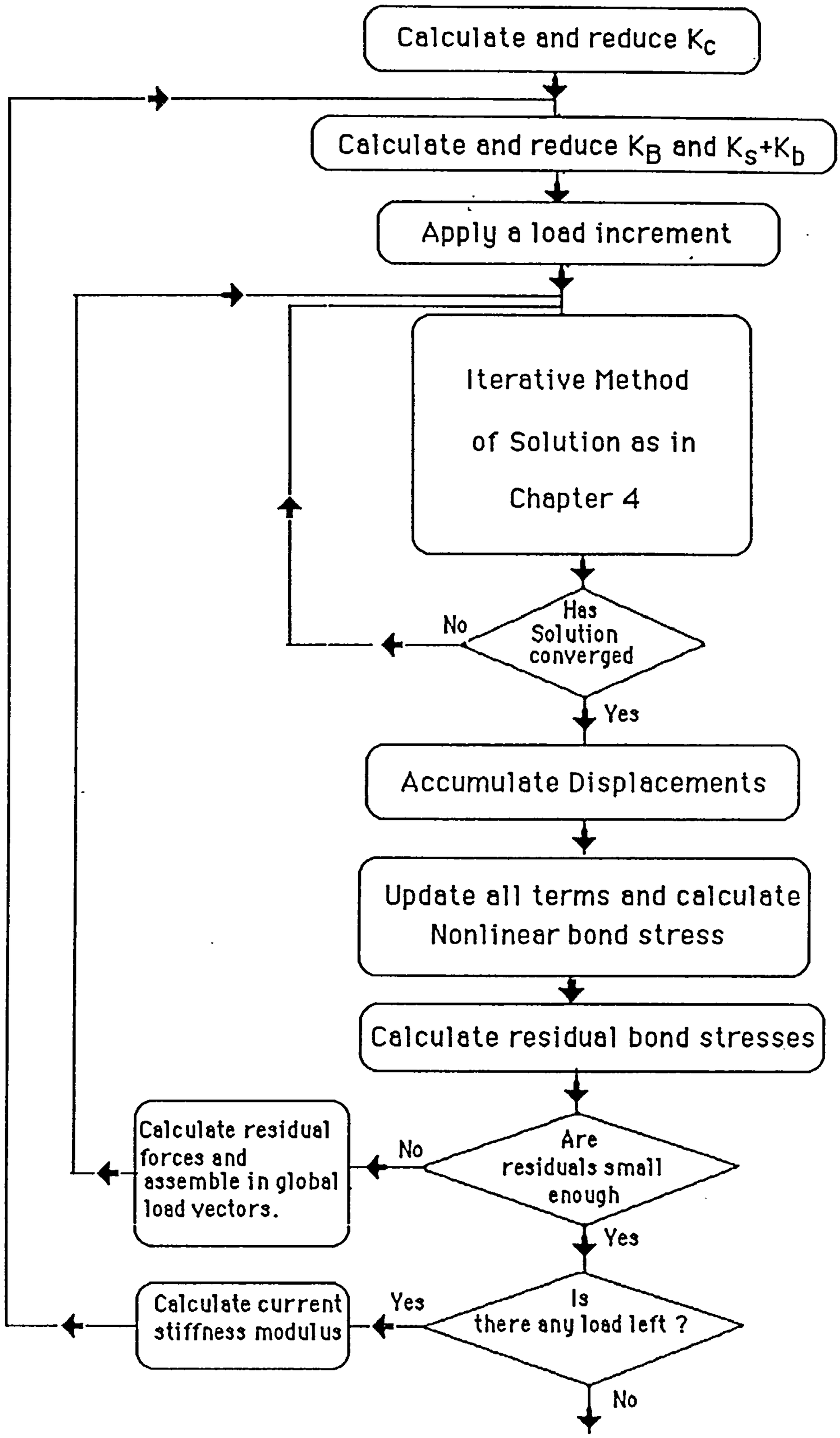

Flowchart (7.1) - Nonlinear method of solution for bond.

ii) Three components of concrete stresses at quadrature points.

iii) Axial steel stresses and displacements at steel nodes.

4) Concrete and steel displacements are accumulated at their respective nodes and in the proper direction.

5) Interfacial radial pressure on steel caused by concrete is calculated from equation (5.7) as follows. Concrete stresses at the steel nodes location lying within the boundary of a certain concrete element are calculated from the concrete stresses at the quadrature points of the concrete element. This is done by using the local least square stress smoothing technique for 2 dimensional parabolic isoparametric elements as presented by Hinton, Scott and Ricketts (1975) . The smoothed stresses are assumed to have bilinear variation over the element. The following relation is derived from the above paper :

$$\sigma(\xi,\eta) = [\ 1 \quad \xi \quad \eta \quad \xi.\eta\ ].\ (1/4)\begin{bmatrix} 1 & 1 & 1 & 1 \\ -\sqrt{3} & -\sqrt{3} & \sqrt{3} & \sqrt{3} \\ -\sqrt{3} & \sqrt{3} & \sqrt{3} & -\sqrt{3} \\ 3 & -3 & 3 & -3 \end{bmatrix}\begin{bmatrix} \sigma_i \\ \sigma_{ii} \\ \sigma_{iii} \\ \sigma_{iv} \end{bmatrix} \quad (7.1)$$

where

σ_i ,σ_{ii}, σ_{iii}, σ_{iv} are stresses at the four quadrature points.

ξ,η are local coordinates.

Equation (7.1) is repeated for all three stress components (σ_x ,σ_y, τ_{xy}) at every quadrature point for every steel node in the same concrete element. Thus, concrete stresses are now available at the steel bar nodes. The normal forces on the bar at the steel nodes are calculated from the stress components and from the degree of inclination of the bar with respect to the concrete element through which it passes to obtain σ_t. Then σ_{rconc} is calculated from equation (5.7).

7) Steel interfacial radial pressure is calculated using equation (5.8).

9) Ultimate bond strength is calculated using equation (5.6).

10) If Δ at a steel node is greater than the maximum allowable slip (Δ_u), then this means that local bond failure has occurred. Therefore, bond stress is reduced to $\beta.q_u$ at that node. If Δ is less than Δu then bond stress is calculated according to equation (5.9).

11) Residual bond stresses at all steel nodes are found from the difference between bond stresses from linear analysis and from nonlinear analysis (Δq).

12) If Δq is greater than some specified tolerance then Δq is converted into equivalent forces by multiplying Δq by the corresponding bar priemeter and the appropriate length of the bar element at the steel node. This is repeated for all steel nodes. An

equivalent force can be found at the concrete element nodes using the principle of virtual work according to equation (3.12). Residual forces are assembled in the corresponding global load vectors P_c and P_s respectively and another solution starts using the same stiffness matrices which are already in the reduced form. Thus, this adds up to the efficiency of the method.

13) If residuals are less than the specified tolerance then a new slope is calculated, new stiffness matrices are calculated and a new load increment is applied.

Stiffness matrices are only recalculated at the end of each load increment and are not recalculated within the load increment to obtain a faster solution as in the initial tangent method. Thus, the method used in the solution of each load increment is the initial stress method.

7.3.2 Convergence of the method

In order to examine the convergence of the method the pull-out test shown in figure (6.10) is used selecting the 4x4 concrete mesh. The concrete cube sides each measure 100 mm. The parameters of a deformed bar are used according to table (8.5). The above problem was solved three times using a different set of load increments each time. Table (7.1) compares the number of iterations needed for the convergence of the solution. In general, small load increments give smaller residuals and thus reduce the number of iterations needed for the nonlinear solution to converge for that load increment, but, at the same time this increases the total number of iterations needed to obtain the complete solution of the problem table (7.1(c)). further, the number of times needed to recalculate the stiffness matrices also increases. On the other hand, large load increments give large residual bond stresses and thus increase the number of iterations needed for the residuals to vanish in the nonlinear solution of that load increment, i.e. load increment number 1 in table (7.1(a)).

However, It is found that a faster solution can be obtained by dividing the total applied load into load increments of different sizes. Larger sizes of the load increments are applied first then the smaller ones table (7.1). The 5 load increments in table (7.1(a)) are faster than the 22 small load increments in table (7.1(c)) when comparing the total number of iterations needed for the complete solution. Also, stiffness matrices have to be recalculated only 5 times for solution of table (7.1(a)) while it was necessary to repeat the procedure 22 times for the solution in

table (7.1(c)).

Convergence of the solution near ultimate load is sensitive and requires small load increments. Small load increments are important for following up failure of bond more closely if it should occur. The same problem is solved again using smaller load increments for the last 2 kN of the load table (7.2). Table (7.2(a)) is the same as table (7.1(b)). Load increments for the last 2 kN are reduced by 1/2 in table (7.2(b)) as compared to table (7.2(a)) and further by another factor of 1/2 in table (7.2(c)). As a result the predicted load at which failure of bond occurs are 22 kN, 22.5 kN and 22.75 kN for the three solutions as in tables (7.2(a),(b),(c)) respectively.

No difficulties were faced during the solution of the problems. In all cases the solution continues until failure of bond has occurred. The computer program then stops due to failure of bond and not to failure of solution.

(a)

Increment		No. of Iterations	
No.	Size	Resid.	Displ.
1	10	9	44
2	5	6	29
3	5	12	59
4	1	5	19
5	1	8	24
Total	5	22	40	175

(b)

Increment		No. of Iterations	
No.	Size	Resid.	Displ.
1	5	5	24
2	5	5	24
3	2.5	3	14
4	2.5	4	19
5	2.5	4	19
6	2.5	7	28
7	1	5	20
8	1	7	21
Total	8	22	40	169

(c)

Increment		No. of Iterations	
No.	Size	Resid.	Displ.
1	1	2	9
2	1	2	9
3	1	2	9
4	1	2	9
5	1	2	9
6	1	2	9
7	1	2	9
8	1	2	9
9	1	2	9
10	1	2	9
11	1	2	9
12	1	2	9
13	1	2	9
14	1	2	9
15	1	2	9
16	1	2	8
17	1	3	13
18	1	3	12
19	1	3	12
20	1	4	16
21	1	4	16
22	1	6	21
Total	22	22	55	233

Table (7.1) - Effect of load increments size on the convergence of the solution.

(a) - (Table(7.1(b))				(b)				(c)			
Increment		No. of Iterations		Increment		No. of Iterations		Increment		No. of Iteration	
No.	Size	Resid.	Displ.	No.	Size	Resid.	Displ.	No.	Size	Resid.	Displ.
1	5	5	24	1	5	5	24	1	5	5	24
2	5	5	24	2	5	5	24	2	5	5	24
3	2.5	3	14	3	2.5	3	14	3	2.5	3	14
4	2.5	4	19	4	2.5	3	19	4	2.5	3	19
5	2.5	4	19	5	2.5	4	19	5	2.5	4	19
6	2.5	7	28	6	2.5	7	28	6	2.5	7	28
7	1	5	20	7	0.5	2	8	7	0.25	2	8
8	1	7	21	8	0.5	3	11	8	0.25	2	8
				9	0.5	3	9	9	0.25	2	7
				10	0.5	4	12	10	0.25	2	7
				11	0.5	8	24	11	0.25	2	6
								12	0.25	2	6
								13	0.25	2	6
								14	0.25	2	6
								15	0.25	2	6
								16	0.25	2	6
								17	0.25	3	9
Total	8	22	40	169	11	22.5	48	192	17	22.75	51	203

Table (7.2) - Effect of increment size in the last few loads.

7.3.3 Nonlinear part of the program

A few steps are illustrated about the nonlinear part of the program

Failure of bond.

As load increments are added to the structure then local failure of bond starts to progress throughout steel nodes. The program keeps a record of all steel nodes which failed. At the end of the solution of each load increment the program gives the number of the steel nodes that have failed. Once failure of all steel nodes has occurred then the program stops giving the appropriate message.

Tolerance on residuals

The tolerance used to examine the convergence of the nonlinear solution is the size of the residual bond stresses. The solution is assumed to converge when the difference between the linear and the nonlinear bond stresses is less than 1% of the nonlinear bond stress.

Input data.

The input data for the nonlinear part includes more information to be added to the linear part. One thing is explained here about load increments. The program divides the total applied load into increments based on the number of load increments desired as entered in the input data and, then, it subdivides each load increment into further smaller loads based on the information in the input data.

Output Solution

The output of the computer solution contains many details. This is given in Appendix "B".

Anchored steel nodes

Anchorage of steel nodes is not part of the nonlinear bond analysis. Thus, the program avoids anchored nodes during the nonlinear part of the solution.

Example of CPU time

The CPU time required for the solution of the pullout problem explained above as for the solution in table (7.1(b)) is four minutes and zero seconds using Honeywell Multics System.

Chapter 8

8. APPLICATION OF THE NONLINEAR BOND MODEL

8.1 Introduction

The application of the bond model described in chapter 3 for the case of linear elastic bond stress slip relationship was illustrated in chapter 6. The method was then extended to accommodate a nonlinear bond behaviour. The objective of this chapter is to show the application of the bond model after introducing the nonlinear bond stress slip relationship as described by Allwood et al. (1984) and which is done according to the nonlinear method of solution introduced in chapter 7.

The iterative method of the nonlinear bond solution discussed in chapter 7 requires that the total applied load be divided into a number of increments. The load increments are then added gradually. This will allow examining and following the solution obtained in each load increment. This advantage of the method will be taken in examining the bond stress behaviour as well as the stress distribution in the reinforcement and in the concrete as the load is gradually increased. To study the deterioration in bond due to loading the gradual increase of load will continue until failure of bond occurs.

The nonlinear bond model was described by Allwood et al. (1984) and was developed basically to model bond for plain bars embedded in concrete. The method was then extended for modelling of bond in concrete structures reinforced with deformed bars. This is

accomplished by changing some of the parameters within the model so that an adequate behaviour of bond between each type of reinforcement and the surrouding concrete can be described. Thus, problems which are selected are classified into two classes according to the reinforcement type:

i) Concrete structures reinforced with plain bars

ii) Concrete structures reinforced with deformed bars

For each type of reinforcement a separate set of problems will be solved.

The analysis of the different problems is carried out using nonlinear bond stress slip relationship but still a linear elastic stress strain relationship is assumed for concrete and steel. The solution obtained will be checked against experimental results or other analytical solutions whenever possible.

8.2 Application of the bond model to plain bars

8.2.1 General

In this section application of the model to concrete structures reinforced with plain bars will be demonstrated. The bond model for plain bars is based on an assumed frictional mechanism of bond.

Since one of the objectives of the solution is to predict the deterioration in bond due to loading using the present model the selected problems are typical of those of bond tests. In order to evaluate the solution obtained using the present model, solution to some of the problems selected have been already obtained either analytically or experimentally by other investigators.

Two reinforced concrete problems will be solved which are:

i) Pull-out test by Parsons (1984).

ii) Pull-out test by Standish (1982).

Numerical and experimental solutions of the above tests are available and they will be checked for available results.

8.2.2 Bond, concrete and steel parameters

The nonlinear bond model requires several bond parameters to be present in order to establish the nonlinear bond stress slip

relationship based on Saenz curve (1969). Further, these parameters are used in predicting the deterioration of bond. Table (8.1) summarises the values of the different bond parameters needed in the nonlinear bond model for analysis of concrete structures reinforced with plain bars. These values have been given by Allwood et al. (1984) and which were used in their nonlinear analysis of bond. Some of these values are estimated from the experimental results of Robins and Standish (1982). Table (8.2) lists the parameters used for concrete and steel in the solution of the different problems.

8.2.3 Failure criterion

It is essential for the nonlinear modelling of bond to include bond failure criterion. The controlling factor which will be used to test for local bond failure is the amount of the gross relative deformation (slip) developed between the steel and the surrounding concrete. An estimated value for tolerance slip at which the maximum bond stress occurs is chosen to be a constant value of 0.1 mm. This value based on experimental evidence.

In the present model once the gross relative slip of steel with respect to concrete at any steel node has exceeded 0.10 mm then the bond at that node is assumed to fail. When local bond failure occurs the maximum bond stress will not be maintained because the adhesive component of bond will be destroyed and so a reduction of bond strength is expected. Therefore the failure of

Parameter	Symbol	Value
Initial bond stress/slip modulus	R_0	200 N/mm^3
Slope of local ultimate bond stress radial pressure.	μ	0.40
slip at ultimate bond stress	Δ_u	0.10 mm
Reduction factor of ultimate bond stress for slip greater than Δ_u	β	0.50
Bond stress due to shrinkage	q_0	3 N/mm^2,or 2 N/mm^2

Table (8.1) - Parameters used for modelling of bond between concrete and plain bars, after Allwood et al. (1984)

Parameter	Symbol	Value
Modulus of elasticity for concrete	E_c	33 kN/mm^2
Poisson's ratio for concrete.	ν_c	0.20
Modulus of elasticity for steel	E_s	200 kN/mm^2
Poisson's ratio for steel	ν_s	0.30

Table (8.2) - Concrete and steel parameters.

bond is modelled by a drop of the bond stress to be one half the ultimate bond stress at that node i.e. the value of β is equal 0.5. Local failure of bond at steel nodes will continue gradually from one node to the other as the load is increased until bond at all steel nodes have failed.

8.2.4 Pull-out test by Parsons (1984).

The test selected here is intended to simulate a block of concrete such as exists in a pull out test. The concrete block and the reinforcing steel as well as the parameters used are detailed according to the test run by Parsons (1984) for his experimental and analytical investigations of bond.

The reason for selecting this test is to compare the results obtained analytically and experimentally by Parsons with the results obtained using the present model. This is possible because of the following points :

1) Parsons (1984) has used the same nonlinear bond model with the same bond parameters as shown in table (8.1) for his analytical solution by conventional finite element analysis using the following :

a) Bond element used in his study is the 6 noded shearing element section (2.2.1) and shown in figure (2.5).

b) Nonlinear stress-strain relationship for concrete is used in his analysis considering cracking of concrete.

2) Parameters used in the analytical solution is selected to represent his experimental tests.

The concrete cube used in this test has the dimensions 150mmx150mmx150mm. One reinforcing plain steel bar is used. The diameter of the bar is 16 mm. The parameters for bond are as shown by table (8.1) with q_0 (the initial stress due to shrinkage)= 2.0 N/mm^2. Parameters for concrete and steel are shown by table (8.2). Finite element mesh of the concrete block is the 4x4 mesh shown in figure (6.10b). The steel bar is divided into 30 2-noded bar elements leading to a total of 31 steel nodes. Node number 1 represents the free end of the bar while node number 31 represents the loaded end of the bar.

Load Application:

The load is applied at the bar end having node number 31 and in the direction outward of the concrete cube. The purpose of the test is to apply the load gradually to the steel bar until bond between the reinforcing bar and the concrete fails. Loading starts by applying a pulling load of 2 kN and then increasing the load by adding increments of 2 kN for the next 4 increments. Then the load increments are reduced to 1 kN until deterioration of bond occurs at all steel nodes table (8.3).

Results and Discussion :

Failure load:

The maximum pulling load reached just before failure of bond at

all steel nodes occurs is at a load of 12 kN. As the next increment of load is added the bond fails at all steel nodes. This happens at a load of 13 kN. Parsons (1984) ran two experimental pull out tests on this cube and he found that the failure loads in the two tests were 12 kN and 14 kN. Failure load predicted by the present model lies within the experimental values.

Stress in the bar:

Figure (8.1) shows the stress distribution in the reinforcing bar as the load is gradually increased. It is noted from figure (8.1) that the shape of the stress curve changes from a concave shape at the very low loads level to a convex shape at the high load level near to bond failure. Figure (8.2) shows the experimental and the analytical results obtained by Parsons for the load distribution in the bar of this test along with the results obtained from the present model. The stress distribution obtained using the present model is very close to Parsons analytical solution using 6 noded shearing element section (2.2.1). The maximum load predicted by the present model is the same as the maximum load shown for the experimental results.

Bond stress :

Figure (8.3) shows the bond stress distribution along the reinforcing steel bar as the pulling load is gradually increased. At low levels of load figure (8.3) shows the bond stress is maximum at the loaded end and is decreasing as the free end of the bar is approached. The same phenomena is noticed until the pulling load of 8 kN is reached. At a pulling load of 10 kN the bond stress reaches maximum at the loaded end and stays almost constant

load inc. number	increment size	Total load applied
1	2 kN	2 kN
2	2	4
3	2	6
4	2	8
5	2	10
6	1	11
7	1	12
8	1	13 kN

Table (8.3) - Loading of pull-out test using 16 mm plain bar.

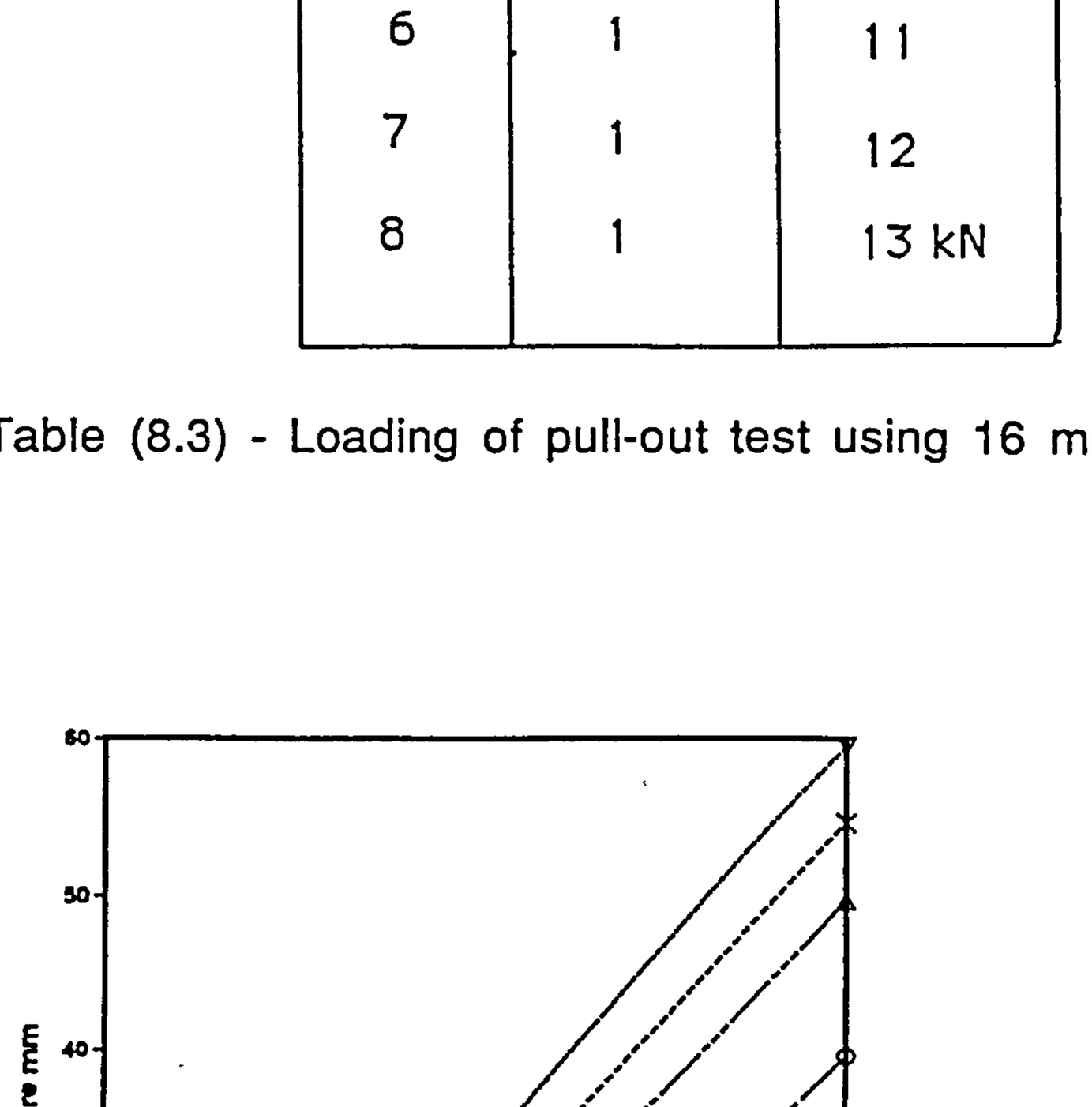

Figure (8.1) - Reinforcement stress in pull-out of 16 mm plain bar.

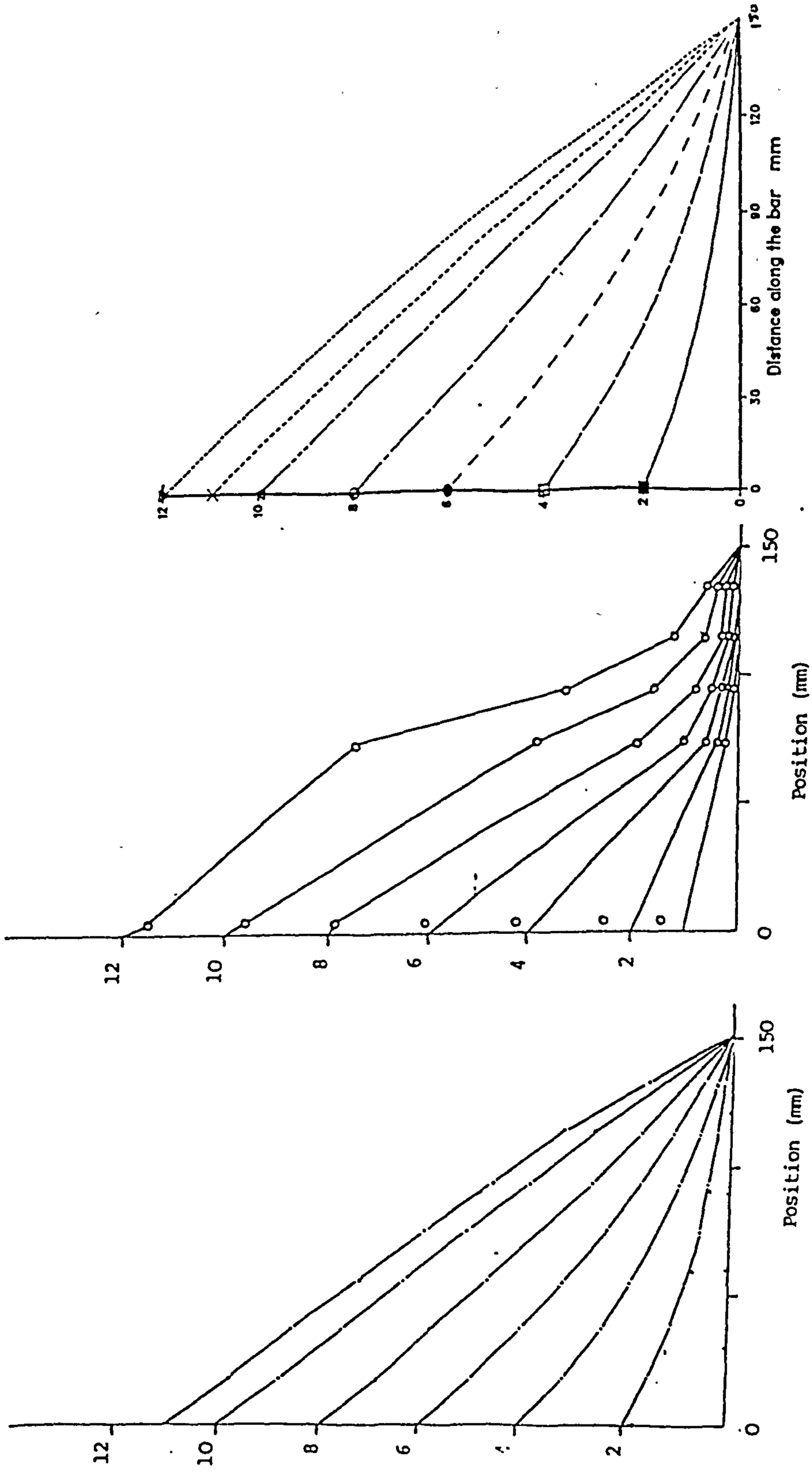

Experimental results by Parsons Present method.

Analytical results by Parsons (1984).

Figure (8.2) - Load distribution in the 16 mm plain bar in pull out test.

throughout the rest of the bar. When the pulling load is increased after this stage failure of bond is approached and it is shown that at the last two loads before bond failure the bond stress is maximum at the free end and is minimum at the loaded end. This shows that the failure of bond occurs at the loaded end first and spreads towards the free end. By studying the actual values obtained in the computer output none of the steel nodes slip exceeds the maximum allowable slip, that is 0.1 mm, up to the maximum pulling load of 12 kN. But at 13 kN all the nodes exceed the maximum allowable slip and so failure of bond at all steel nodes occurs.

Figure (8.4) shows the bond stress distribution for this problem as obtained by Parsons analytical solution. The figure shown is reproduced from Parsons actual results so that the loading end corresponds to the solution obtained in figure (8.3). The similarities between the two solutions can be seen.

Concrete stress:

Figure (8.5) shows the concrete stress distribution at the bar level in the perpendicular direction of the bar axis while figure (8.6) shows the concrete stress distribution in longitudinal direction of the bar axis. It is noted that the maximum tensile concrete stress reached is less than the tensile fracture stress of the concrete. Figure (8.7) shows the concrete stresses obtained by Parsons analytical solution for this test. Again the load in the case of Parsons is applied in the left end of the bar as compared to the loading for the present work.

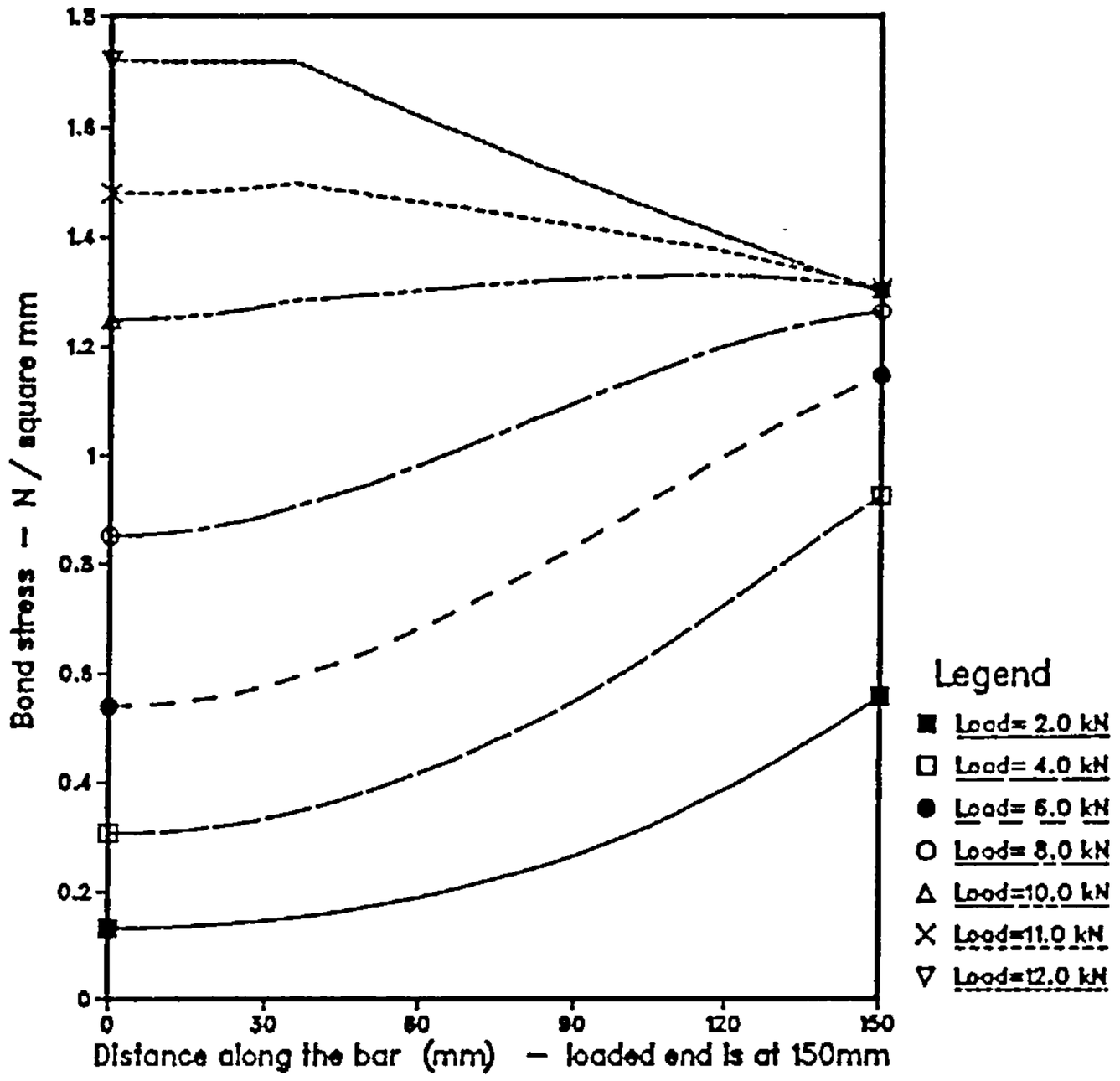

Figure (8.3) - Bond stress distribution along reinforcement.

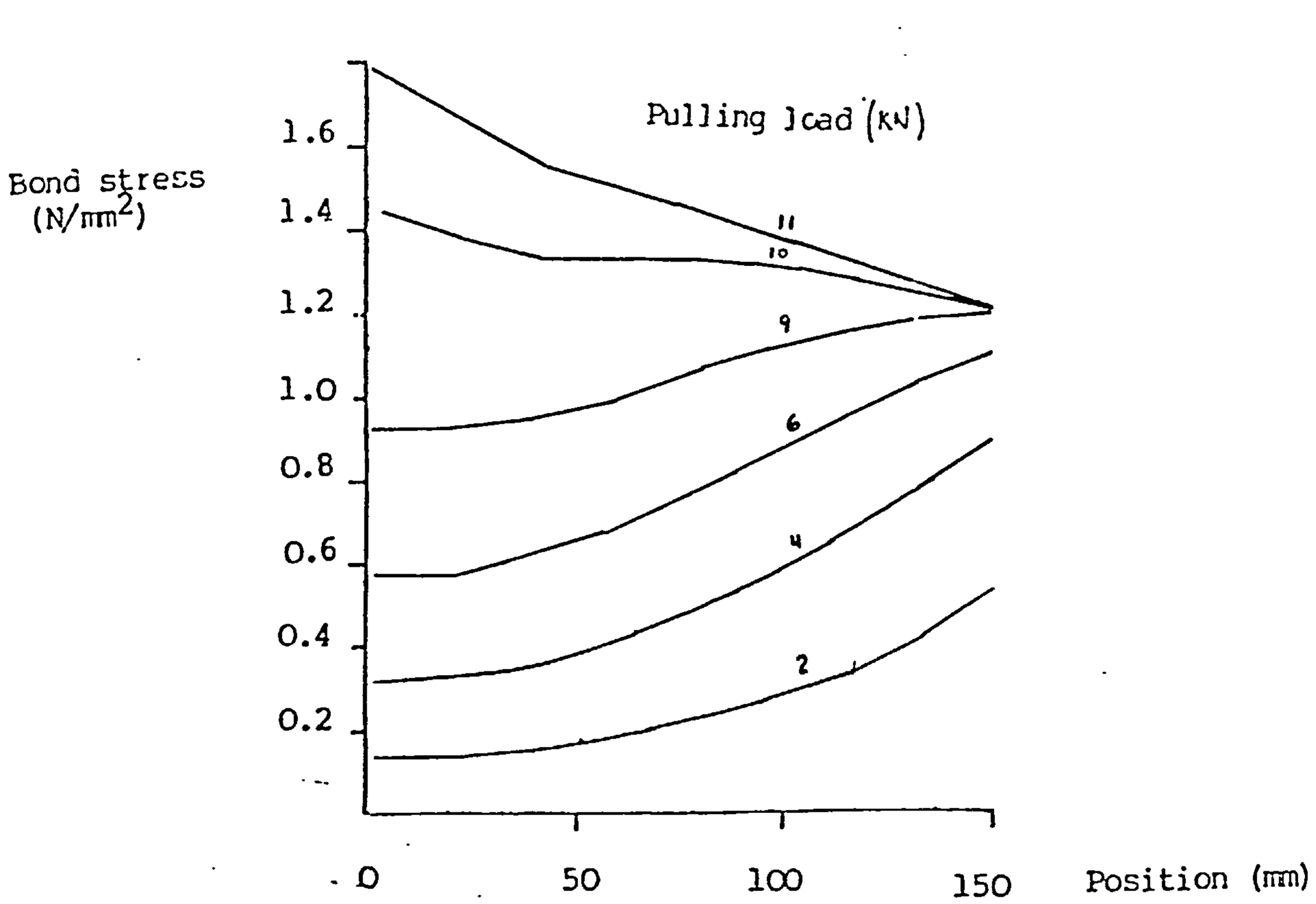

Figure (8.4) - Analytical bond stress distribution, after Parsons.

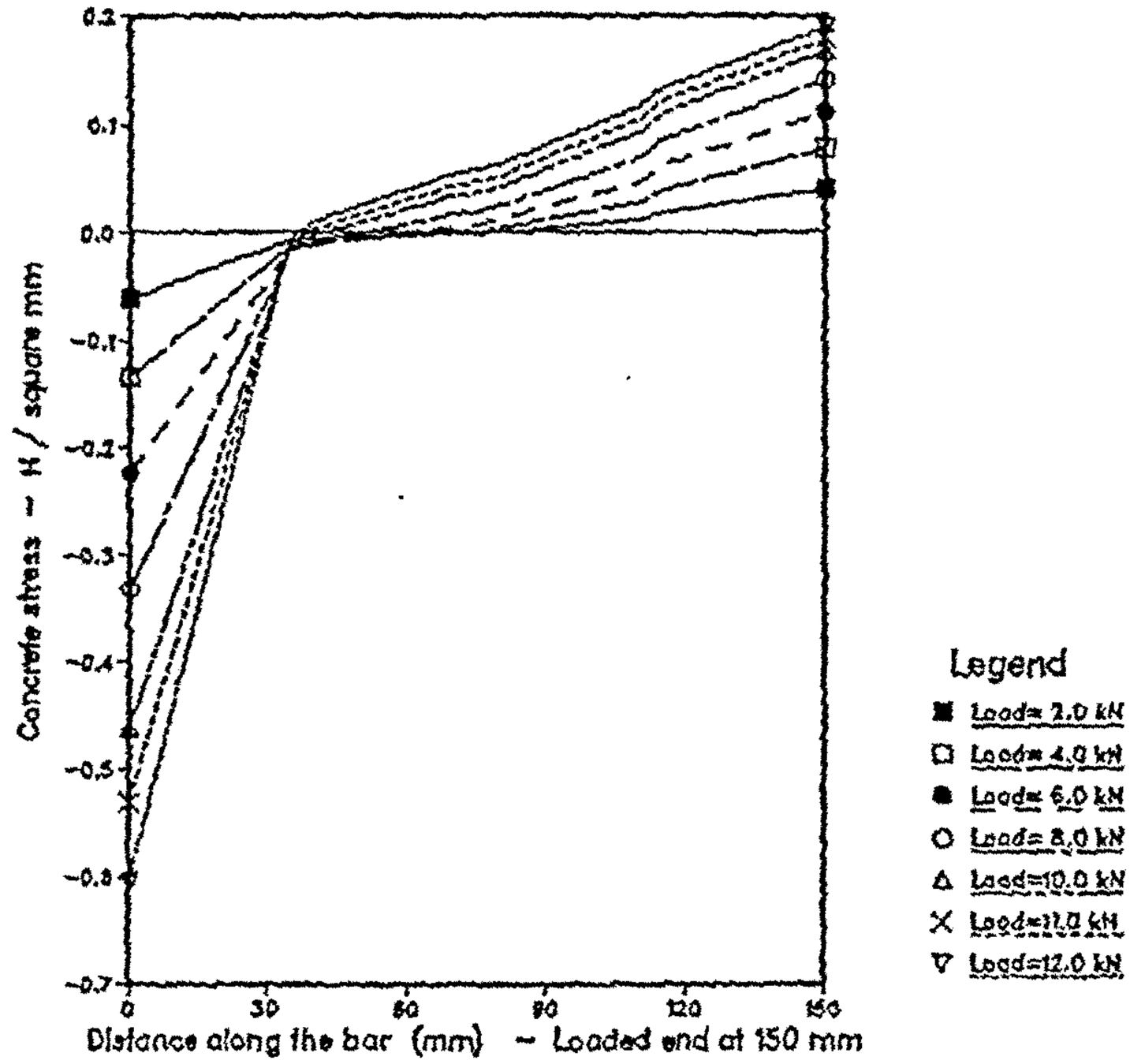

Figure (8.5) - Lateral concrete stress at bar level in pull out test of plain bar.

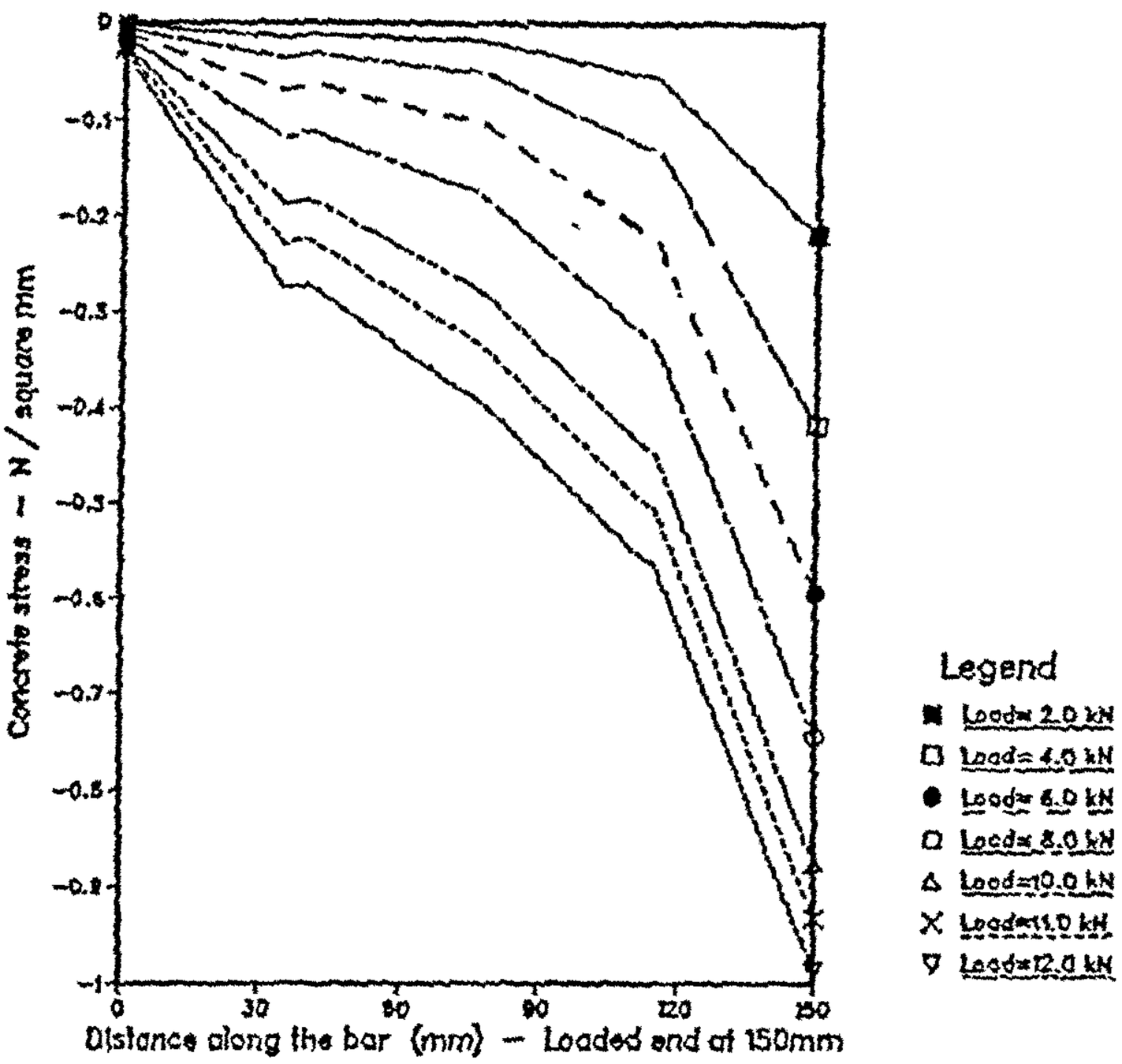

Figure (8.6) - Longitudinal concrete stress at bar level in pull out test of plain bar.

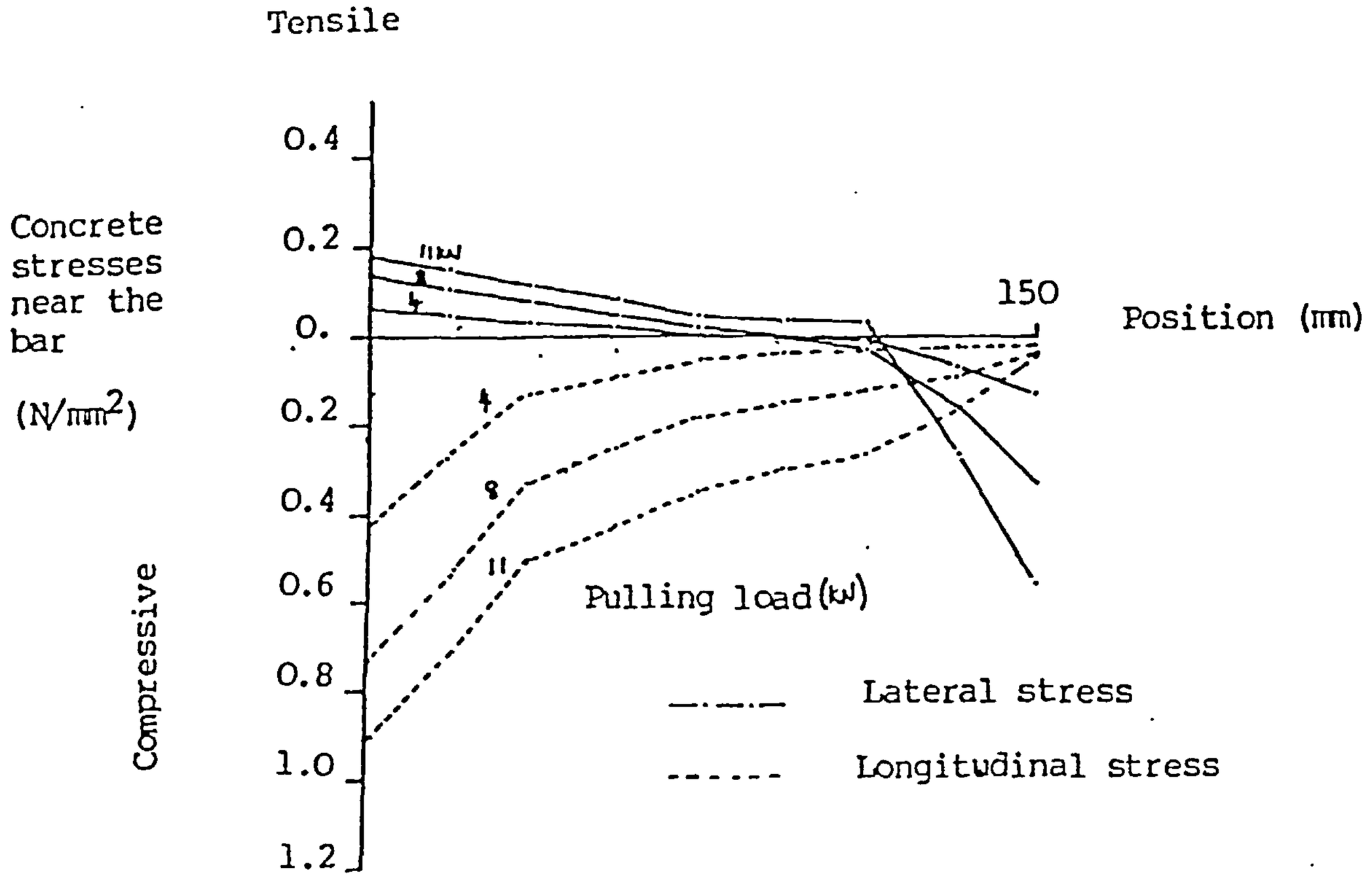

Figure (8.7) - Analytical concrete stress near the bar, after Parsons (1984).

load inc. number	increment size	Total load applied
1	2 kN	2 kN
2	2	4
3	1	5
4	1	6
5	1	7
6	1	8
7	0.5	8.5
8	0.5	9.0
9	0.5	9.5
10	0.5	10.0

Table (8.4) - Loading in pull-out test(12 mm plain bar)

8.2.5 Pull-out test by Standish (1982).

In the pull-out test presented in this section the concrete block and the reinforcing steel as well as the parameters used are detailed according to the test run by Standish (1982) in his experimental work. The difference of this test and the test presented in the previous section is in the following a) The dimensions of the concrete cube of this test are 100mmx100mmx100mm. b) The reinforcement bar is a plain round steel bar with 12 mm diameter. c) q_0 (initial bond stress) equals to 3 N/mm^2 with the rest of the bond parameters are as shown in table (8.1). The same concrete mesh as the previous problem is used and also the same number of elements is used in the reinforcing bar.

The purpose of this test is to compare the results obtained from the finite element solution obtained using this method as compared to some of the available experimental results obtained by Standish (1982) and also to the analytical results obtained by Parsons (1984) for this test.

Load Application:

The load is applied to the steel bar in increments of 2 kN for the first 4 kN of pulling load and then by increments of 1 kN for the next 4 kN of load. It is then reduced to load increments of 0.5 kN until failure of bond occurs table (8.4) (on previous page).

Results and Discussion:

Failure load:

All the steel nodes have failed at a pulling load of10 kN. The maximum applied load prior to bond failure is 9.5 kN. The experimental results of Standish for this test gives a failure load of 10 kN while the analytical solution of Parsons predicts a failure load of 9 kN.

Figure (8.8) shows the free end slip obtained by this method as compared to the experimental results obtained by Standish (1982) and by the analytical solution of Parsons (1984). The free end slip obtained by this method shows a better match with the experimental results obtained by Standish.

Stress in steel:

The stress distribution in the steel bar for all load increments is shown by figure (8.9). The stress distribution is very similar the pull-out test of section 8.2.2.

Bond stress:

Figure (8.10) shows the bond stress distribution along the bar for all load increments.

Concrete stress:

Figure (8.11) shows the concrete stresses at the bar level and in the perpendicular direction to the bar axis for all load increments. Also it shows the concrete stress at the bar level and in the direction of the bar axis. Figure (8.12) shows the concrete stresses near the bar as obtained by Parsons analytical solution using the same nonlinear bond model. The two figures are very similar, but, again the load in the case of Parsons solution is applied at the opposite end.

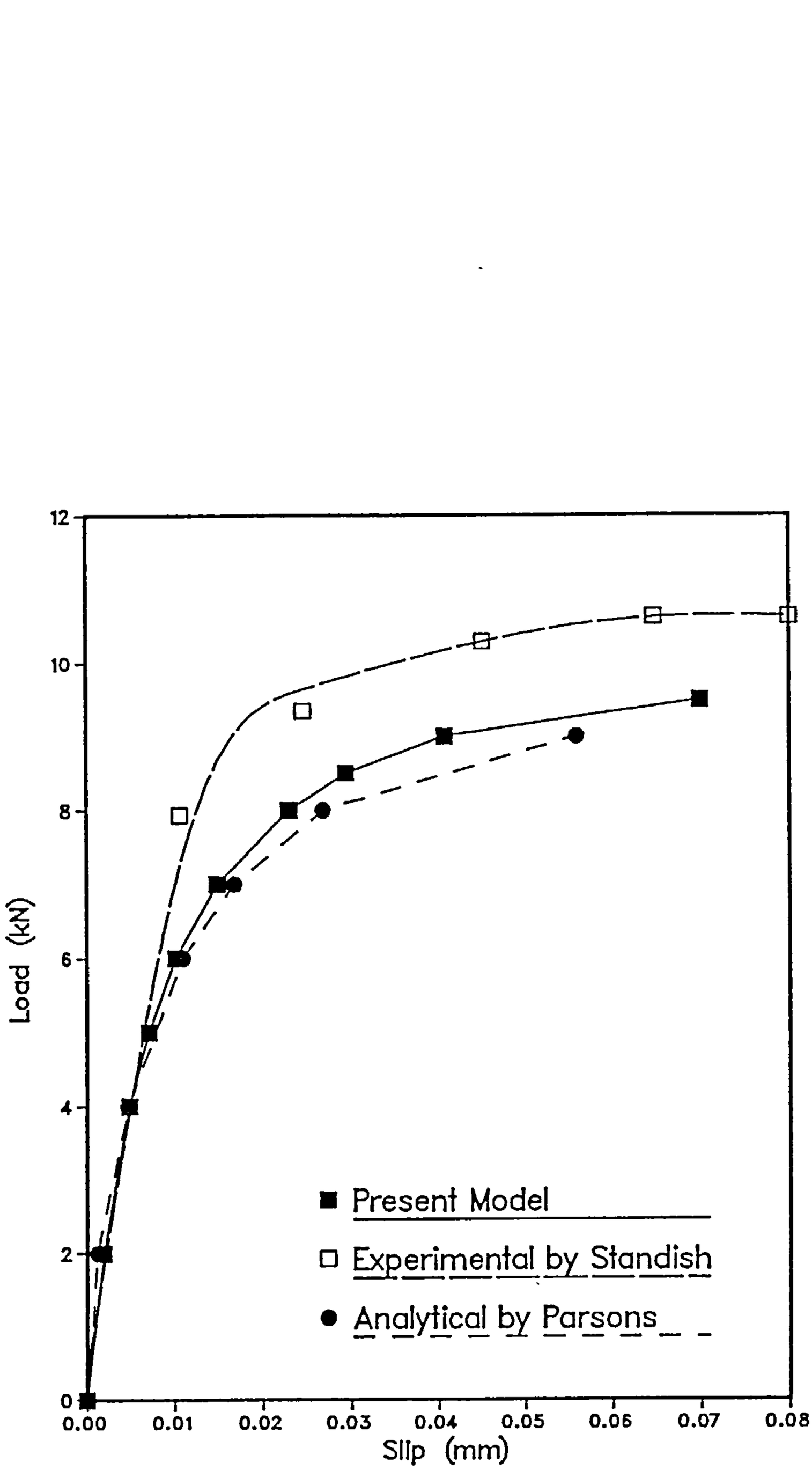

Figure (8.8) - Free-end slip of the 12 mm plain bar.

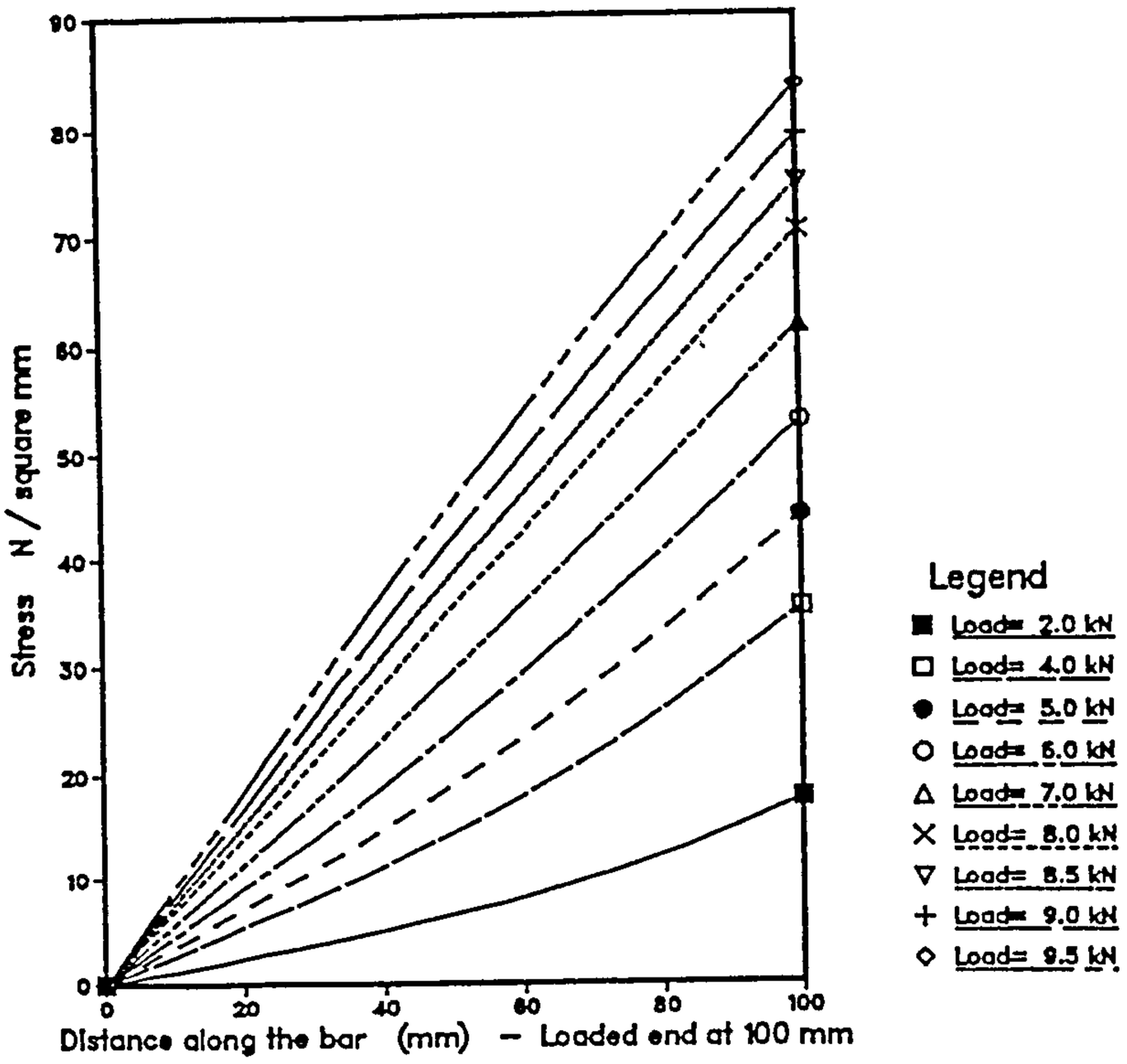

Figure (8.9) - Stress distribution in the 12 mm plain bar.

Bond Stress along the bar for Pullout Test using 12mm plain bar

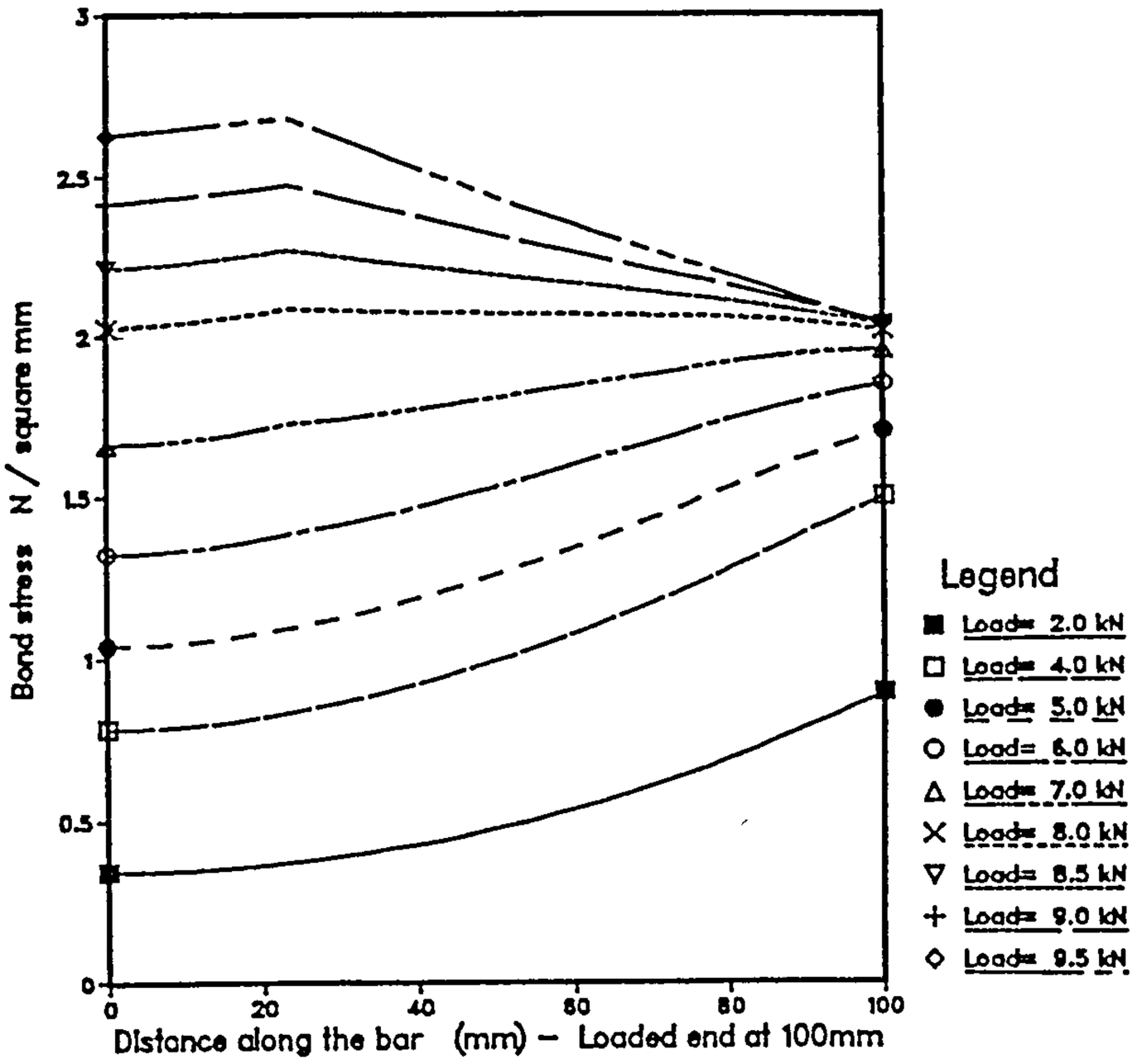

Figure (8.10) - Bond stress distribution in the 12 mm plain bar.

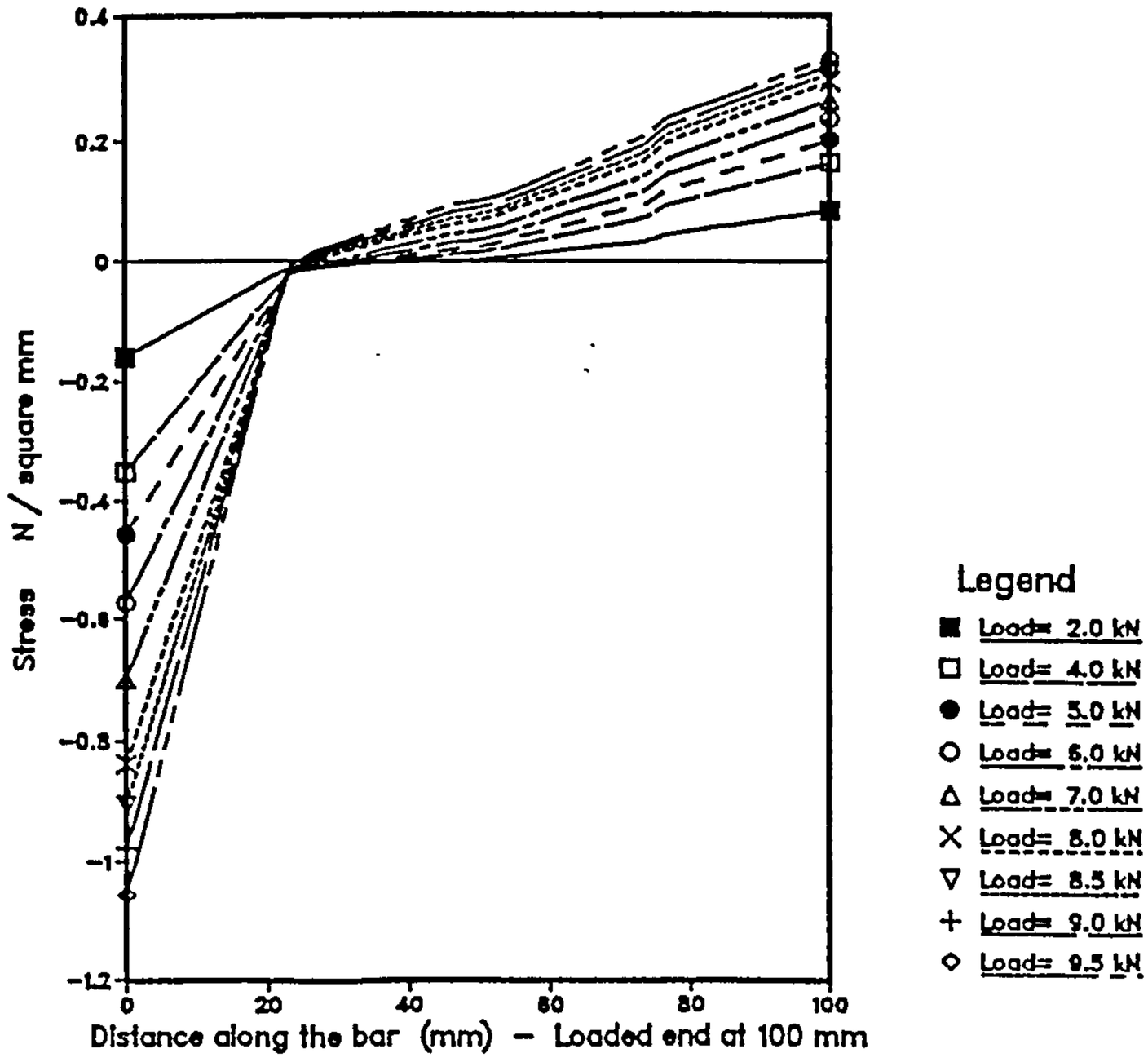

(a) - Lateral concrete stress.

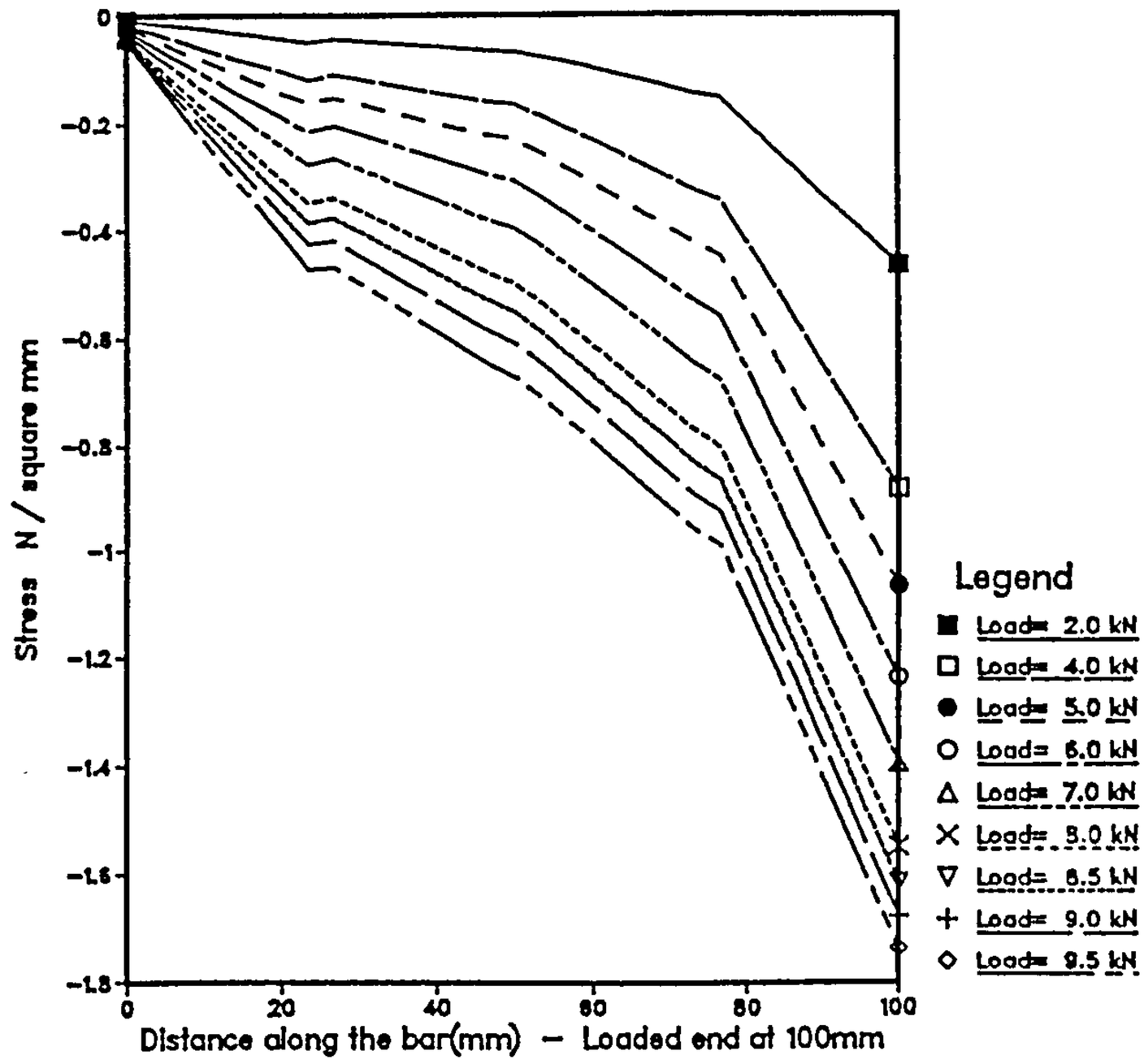

(b) - Longitudinal concrete stress.

Figure (8.11) - Concrete stress at the 12 mm plain bar level.

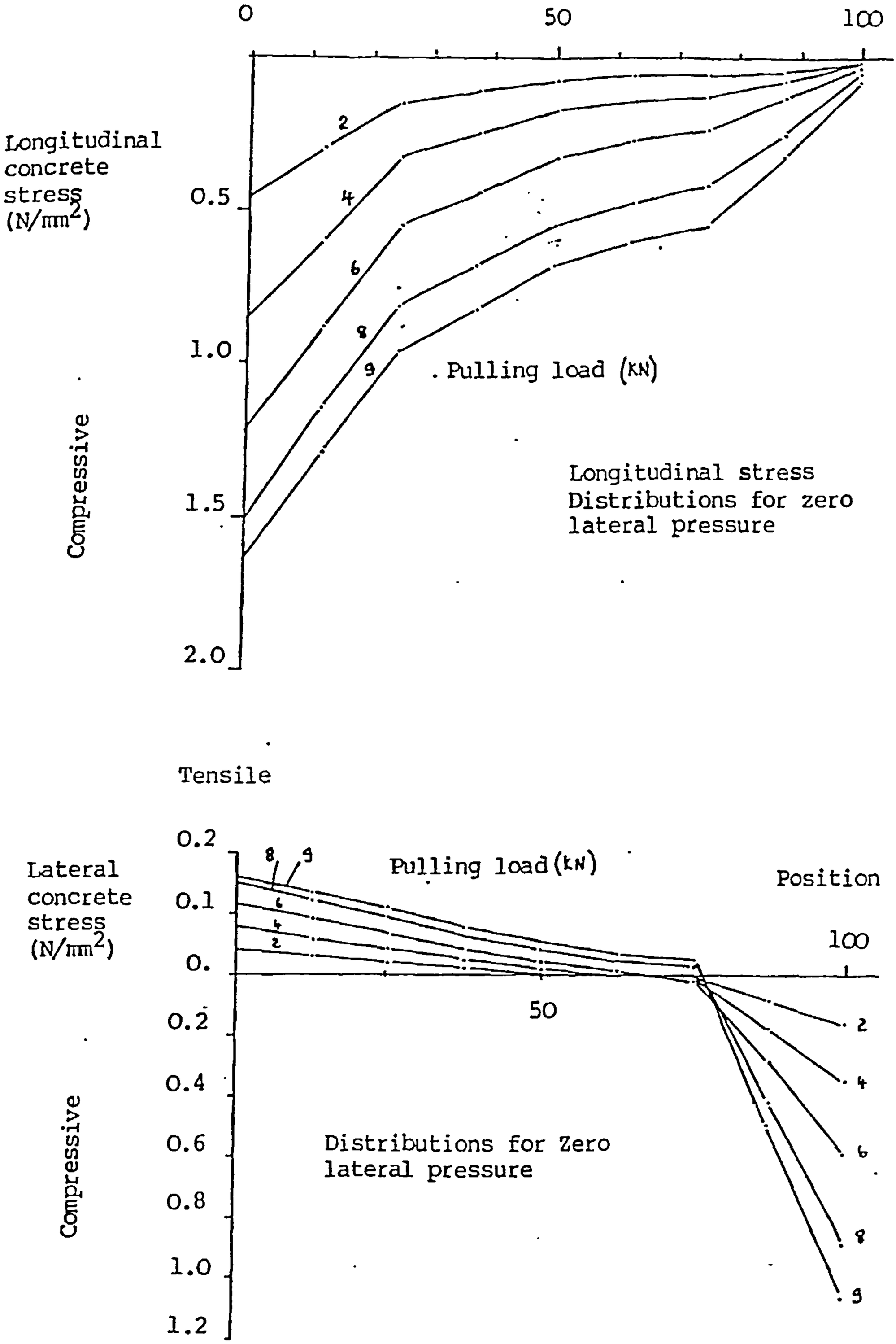

Figure (8.12) - Analytical concrete stresses near the 12 mm plain bar, after Parsons (1984).

8.3 Application of the bond model to deformed bars

8.3.1 General

In this section the bond model will be applied to analyse concrete structures reinforced with deformed bars. Although the bond model was developed for plain bars based on an assumed frictional mechanism of bond, it will be used for modelling of bond for deformed bars where the bond relies mainly on the mechanical interlock of the ribs bearing against the surrounding concrete. This will be done by adjusting the value of the parameters used in plain bars to be adequate for modelling of bond between deformed bars and the surrounding concrete based on experimental observations.

The problems selected here are a pull-out test as in the case of plain bars in addition to a flexural problem. Analysis of the following problems is carried out :

1) Pullout test by Standish (1982).

2) Cantilever problem.

8.3.2 Bond Parameters

From the experimental results of Robins and Standish (1982) in studying the effect of lateral pressure on bond of reinforcing bars in concrete they found that at zero external lateral pressure applied on the concrete the mode of failure of the deformed bars, the primary cause of failure was splitting of the concrete surrounding the bar. When lateral stress is applied to the cube and

for stress beyond 10 kN/mm^2 failure is caused by shearing. Based on these observations there are two sets of bond parameters derived one for each type of failure. However, since this work is not intended to study the effect of lateral pressure on bond, no external pressure will be applied on the concrete cube and the data for splitting type of failure is selected. Table (8.5) shows all bond parameters used in modelling of bond between concrete and deformed bars and which represent the splitting case.

As shown in Table (8.5) the value for R_0 given for deformed bars is very high as compared to the value for R_0 used in modelling of plain bars table (8.1) and this is to reflect the better bonding of deformed bars. The value of bond stress due to shrinkage of concrete is increased to 9.5 kN/mm^2 as found from the results of Robins and Standish (1982). The coefficient of friction value are increased from 0.4 to 1.05. This is also to reflect the greater friction obtained between the deformed bar and the concrete as the concrete pressure increases on the bar as a result of loading.

8.3.3 Failure Criterion

Failure of bond in the case of deformed bars at any steel node occurs when the local gross relative slip between concrete and the reinforcement exceeds 0.1 mm which is the same as in plain bars except that for slips greater than 0.1 mm the bond stress will be maintained at its maximum value and so the value of β is increased from 0.5 to 1.0. Complete deterioration of bond in the structure occurs when bond at all steel nodes have failed.

Parameter	Symbol	Value in SI Units	Equivalent in Imperial units
Initial bond stress/slip modulus	R_0	1000 N/mm^3	3684 k/in^3
Slope of local ultimate bond stress radial pressure.	μ	1.05	1.05
slip at ultimate bond stress	Δ_u	0.10 mm	0.00394 in
Reduction factor of ultimate bond stress for slip greater than Δ_u	β	1.0	1.0
Bond stress due to shrinkage	q_0	9.5 N/mm^2	1.378 k/in^2

Table (8.5) - Bond Parameters for modelling of bond between concrete and deformed bars as used in Allwood et. al model (1984).

8.3.4 Pull-out test by Standish (1982).

The pullout test to be modelled by the method for the case of deformed bars will be according to the pull-out test details of Standish (1982) as described in section (8.2.7) except for the reinforcement which is replaced by one deformed bar with nominal diameter of 12 mm. The value of the parameters used for modelling of bond are shown in table (8.5) and the parameters used for concrete and steel are shown in table (8.2).

The analytical solution obtained for this test using the present bond model will be compared with the experimental results of Standish and the analytical solution of Parsons. Such a comparison is possible because the bond parameters used correspond to the work of both authors and for the same reasons given in section (8.2.5)

Finite element mesh for the concrete block is still the same as in section (8.2.5) and also the reinforcement is represented in the same way.

Load application:

The load is applied to the bar at the bar end node number 31. Load is applied incrementally, first at pulling load increments of 5 kN for the first three increments then at increments of 2.5 kN for the next two increments. Finally load increments is reduced to 0.5 kN for the rest of load until failure of bond at all steel nodes occurs as shown in table (8.6) (page 223).

Results and Discussion :

Failure of bond at all steel nodes occurs at a load of 23.0 kN. Unlike the plain bar case this does not happen at once. At the load of 22.0 kN it is found that bond at the nodes in the next 60 mm of the bar length starting from the loaded end have already failed. By adding the next increment of load (0.5 kN) the bond at the remaining nodes in the bar fails. From the experimental results of Standish the failure load for this test is found to be 22 kN while the analytical results of Parsons predicts a failure load of 20.5 kN.

Free-end slip

Figure (8.13) shows a comparison for the slip of the free end of the bar as obtained from the present model solution and the free end slip as obtained from the experimental results of Standish and the analytical model of Parsons.

The very good prediction of the free end slip obtained using the present model when compared to the experimental results of Standish as shown by figure (8.13) is obvious.

The better solution obtained by the present model as compared to Parsons model for the failure load as well as for the free end slip is obvious for the case of deformed bars while in the case of plain bars the difference between the two solutions is not so obvious. It is appropriate to comment here on modelling of bond as developed in this research and modelling of bond using 6 noded bond interface element shown by figure (2.6) as in the case of Parsons work.

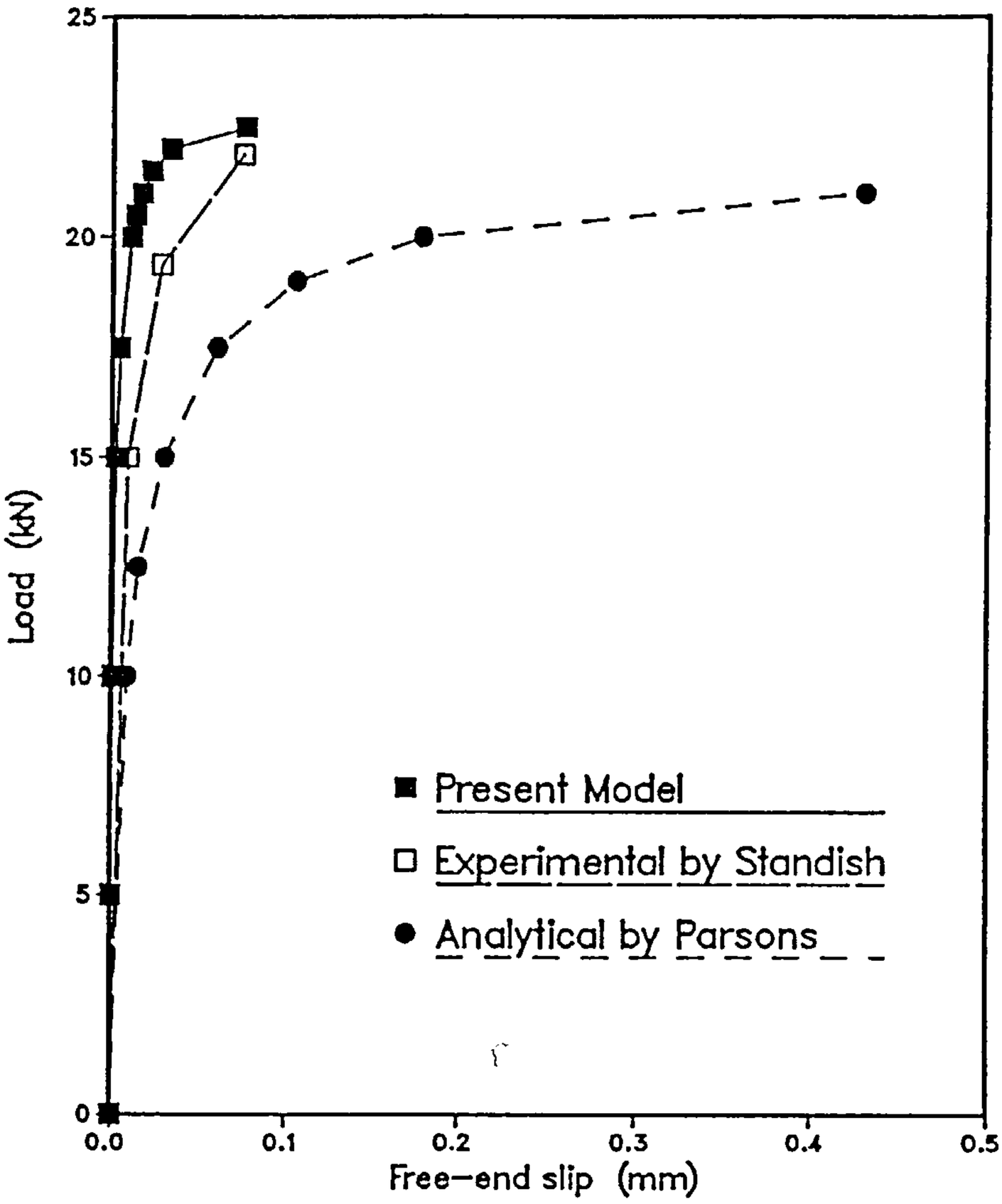

Figure (8.13) - Free end slip of the 12 mm deformed bar in pull out test.

In the solution of this problem Parsons used 4 bond elements which results in only 9 points along the length of the steel bar for evaluating bond stresses, while using the present model the bond stresses are evaluated at 31 nodes. This difference of the number in nodes for evaluating bond stresses affects the results especially in the case of deformed bars. In deformed bars the change of bond stresses is rapid due to the value of μ=1.05. So, using 31 nodes for evaluating bond stresses the model can follow the change of bond stresses closely which results in more accurate prediction of the free end slips and the higher failure loads obtained than when using 9 points for evaluating stresses.

In the case of plain bars the value of μ used is 0.4 which leads to slow change of bond stresses and in this case the number of points for evaluating bond being 9 is good enough to follow the failure of bond. Therefore the results obtained by the present model for the case of plain bars shows slight improvement over the solution obtained by Parsons.

Although the present method treats concrete as linear elastic material, this has not much effect on the results of the pull-out tests since some of the results obtained are superior to the ones obtained by Parsons using nonlinear stress-strain relationship for concrete.

Compressive stresses carried by concrete is less than 13 % of the ultimate compressive strength of concrete. Also tensile stress carried by concrete is less than 8% of the tensile strength of concrete.

Stress in the bar:

Figure (8.14) shows the stress in the bar for all load increments. The stress curve shape obtained at low level of loading is the same as in the case of plain bars except that the curvature here is more obvious. As the applied load increases the shape of the curve changes gradually and becomes convex at the maximum load applied. Figure (8.15) shows a comparison between the stresses obtained at the maximum applied load for deformed and plain bars.

Bond stress:

The bond stress obtained for this test for all load increments is shown in figure (8.16). The deterioration of bond can be followed from the bond stress curves at high loads which is more obvious than in the case of plain bars.

Concrete stress:

Again concrete stresses at the bar level are calculated at all steel nodes locations in the perpendicular direction to the bar axis and are presented in figure (8.17) . Concrete stresses at the bar location and in the direction of the bar axis are shown by figure (8.18).

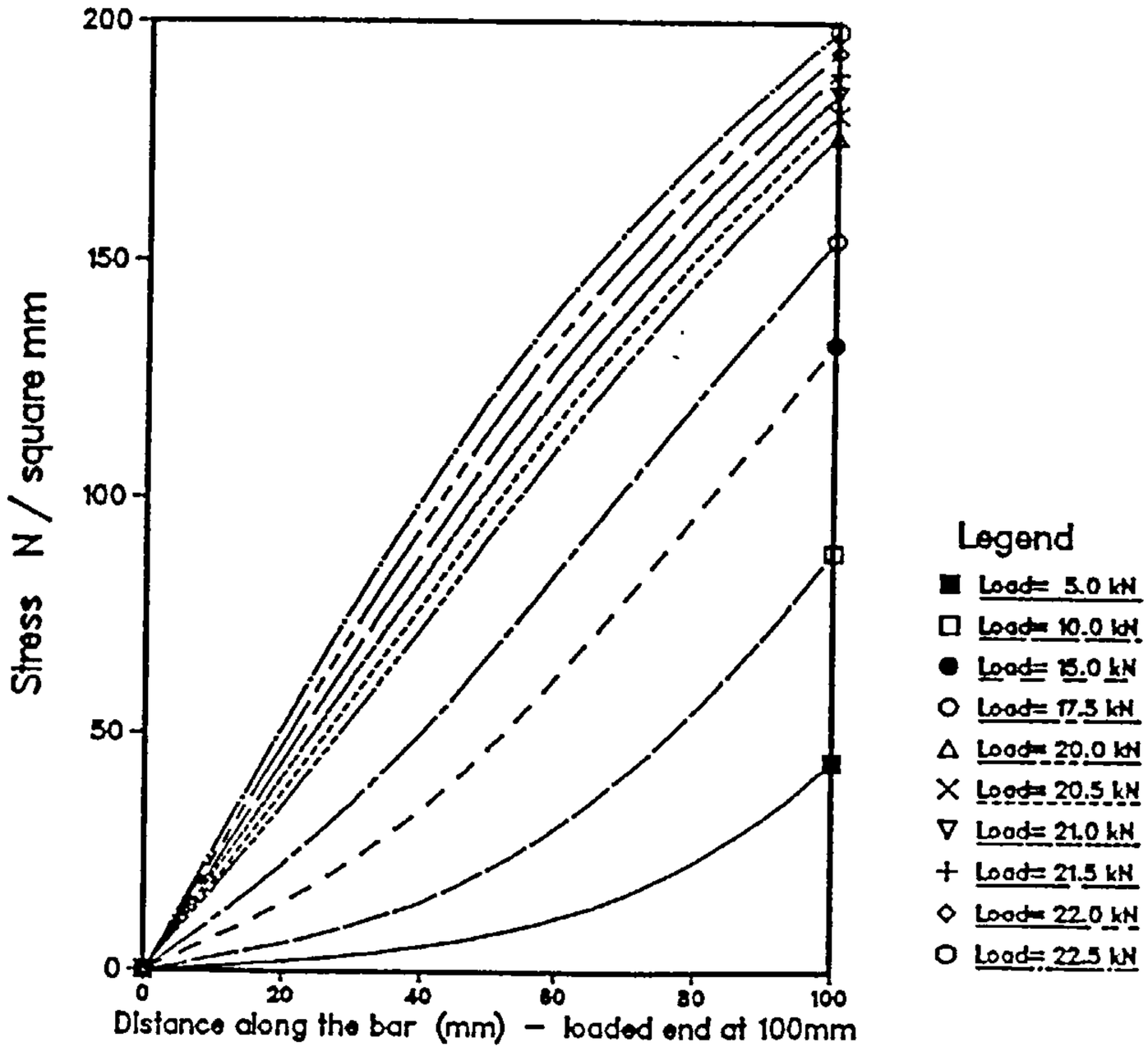

Figure (8.14) - Stress distribution in the 12 mm deformed bar.

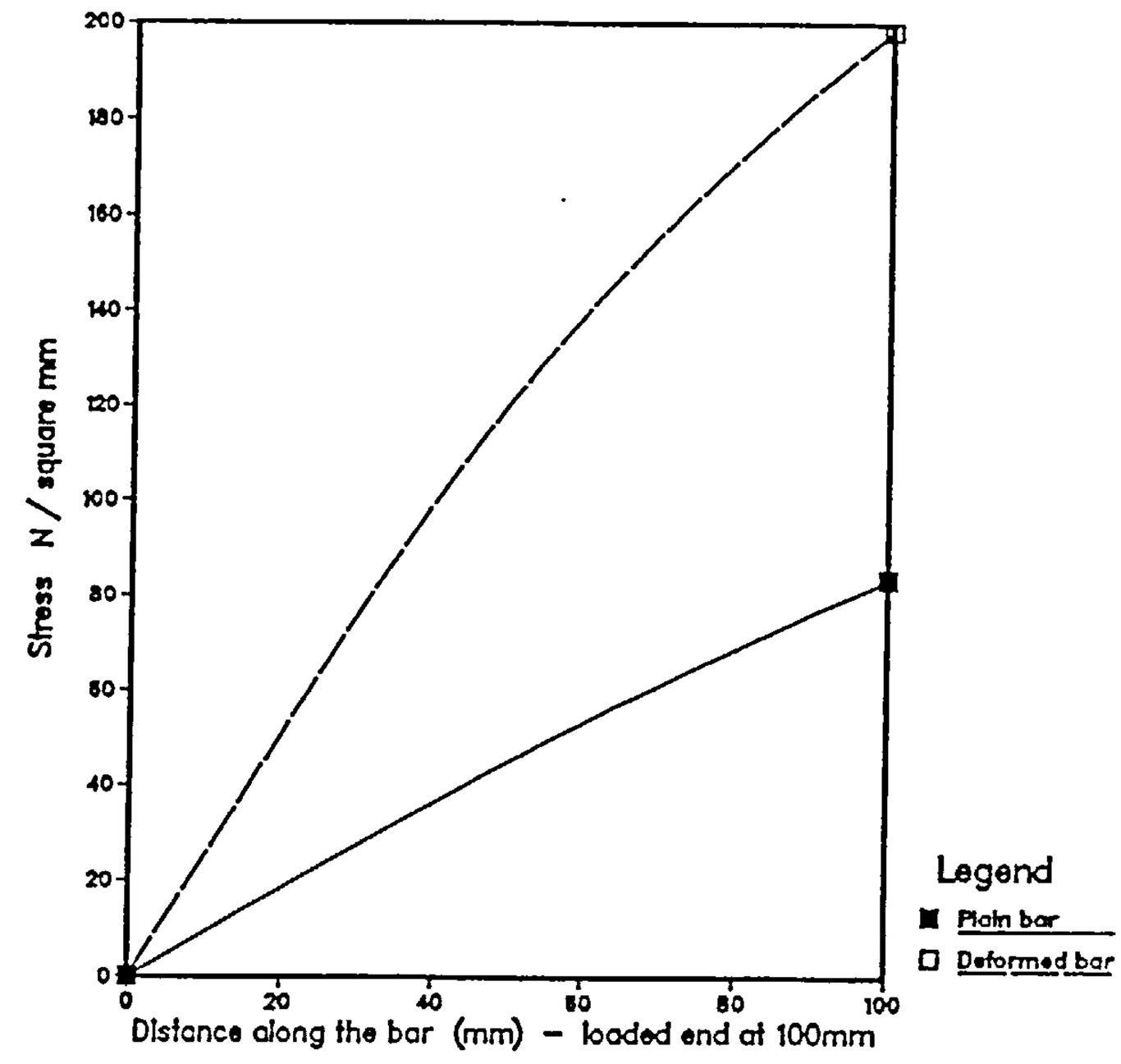

Figure (8.15) - Steel stress at maximum applied loads.

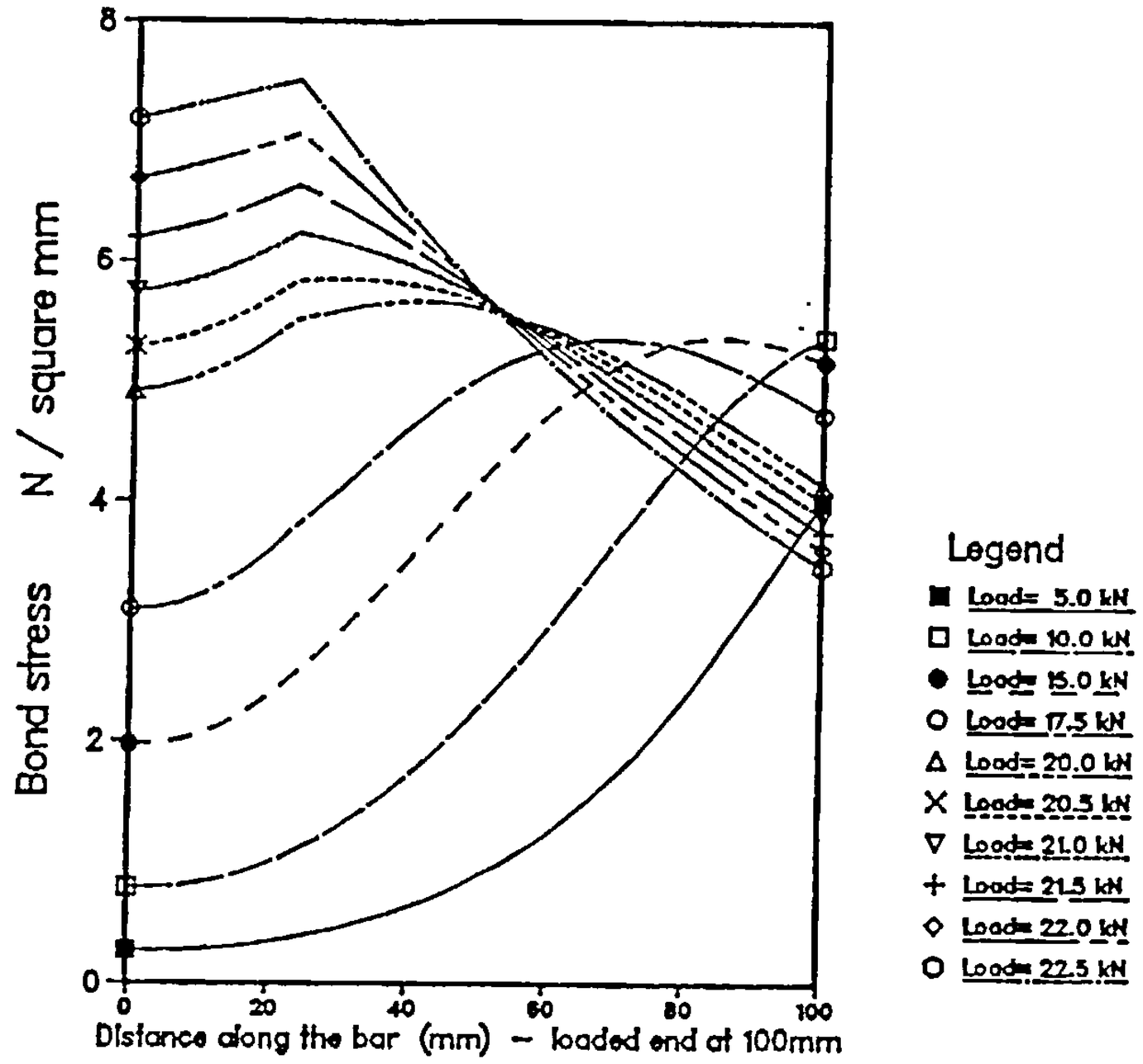

Figure (8.16) - Bond stress along the 12 mm deformed bar.

load inc. number	increment size	Total load applied
1	5	5
2	5	10
3	5	15
4	2.5	17.5
5	2.5	20.0
6	0.5	20.5
7	0.5	21.0
8	0.5	21.5
9	0.5	22.0
10	0.5	22.5
11	0.5	23.0

Table (8.6) - Loading of the 12 mm deformed bar in pull out test.

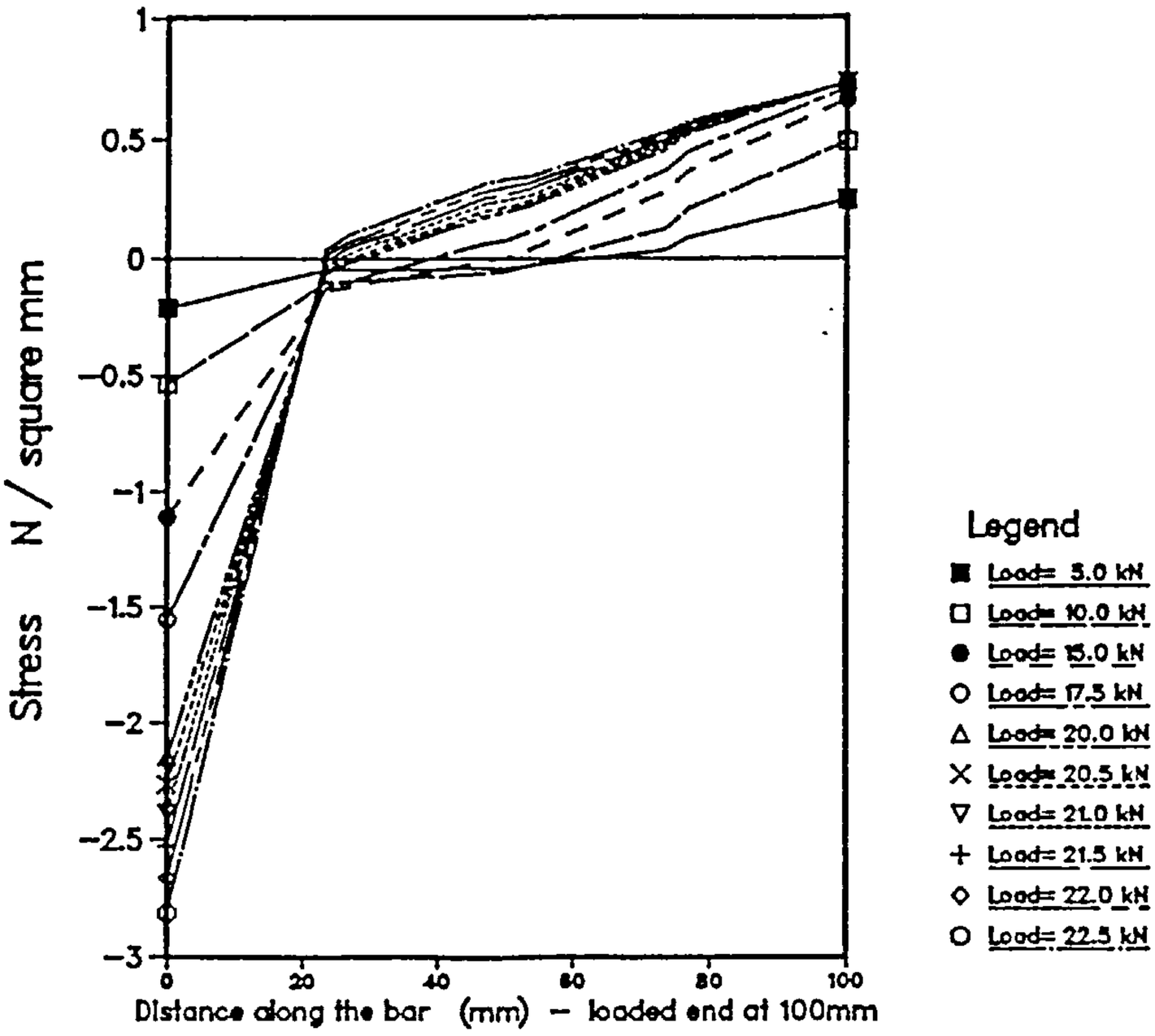

Figure (8.17) - Lateral concrete stress at the deformed bar level.

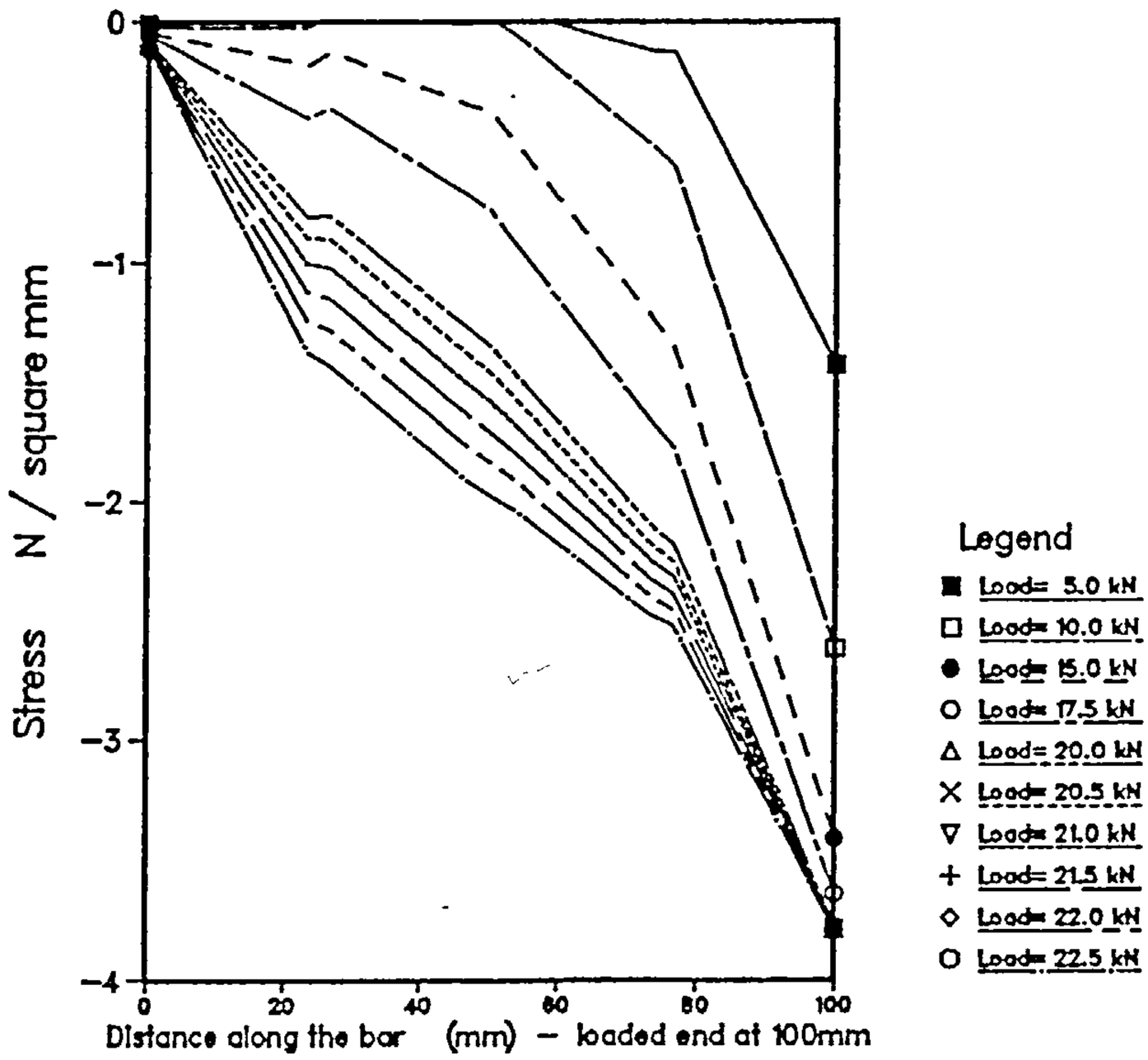

Figure (8.18) - Longitudinal concrete stress at the deformed bar level

8.3.5 Cantilever

The cantilever details to be analysed in this section are shown by figure (6.18). Analysis of the cantilever has been demonstrated in section (6.4) for the linear case. The purpose of the solution using the nonlinear bond model is to study the effect of the nonlinear bond stress slip relationship on the behaviour of the solution as the load is increased.

The solution will be carried out using the bond parameters shown by table (8.5) when selecting the equivalent parameters values in imperial units.

Full length and curtailed tension reinforcement will be anchored at the bar end in the column by high bond stiffness values. Also stirrup and ties ends will be anchored to the concrete in the same manner for the same reasons given in section (6.3.2). The value of the bond stiffness modulus used for anchorage is 1000 times greater than the initial bond stiffness or

$$R_0 = 1000 \times 3684 \quad \text{kips/inch}^3$$

This value will stay constant all the time for all loads increments and it will not be affected by the change in slope of the nonlinear bond stress slip curve as are the rest of the nodes.

The finite element mesh is the same as in section 6.4. The same number of nodes is selected for the reinforcement.

Loading:

The first load applied is a uniformly distributed load of 2.7 kips/ft

which is the full loading of the cantilever as designed in section 6.4. The load is then increased by increments of 0.9 kips/ft for four increments.

Results and Discussion:

The solution of this problem for all load increments takes 81 minutes and 31 seconds from the computer central processing unit (CPU) time using Multics system whereas as for the pull-out problems the solution takes about 4 minutes. The output gives details of stress and bond at all the 350 steel nodes in every load increment.

Stresses:

Figure (8.19) shows stresses in the full length tension reinforcement for four load increments. It is noted from this figure that the stresses show some irregularities in the reinforcement stresses which coincide with the concrete element boundaries. Further it is noted that these irregularities become smoother as the applied load is increased. These also appear in figure (8.21) but exaggerated since bond stress are obtained from the derivative of bar stresses. The explanation for this behaviour is very similar to the problem discussed in the linear case when examining the irregularities in the bond stress curve. In this problem the steel is not loaded directly but it is loaded through the bond interforces which are calculated from the concrete displacements at the steel nodes. Loading of steel is achieved according to equation (4-9b) repeated here :

$$[K_s+K_b] \cdot [D_s] = [P_s] + [K_b] \cdot [C] \cdot [D_c]$$

The iteration superscript on $[D_c]$ is removed

Since no load is applied directly to the steel in this problem then $[P_s] = 0$ and so the steel loading comes from the term $[K_b] \cdot [C] \cdot [D_c]$. The term $[C].[D_c]$ will evaluate the concrete displacements at the steel nodes location within the 8-noded concrete element using shape functions. As pointed out in chapter 6, this method of evaluating concrete displacements will create a problem at the boundaries of the element which is very similar to the problem that occurs when calculating element stresses at points within 8-noded element as first noted by Hinton and Campell (1974), where they showed that stresses derived from the shape functions were most accurate at Gauss points and at their worst at the boundary edges.

This problem affects the solution when k_b value is very high such as in the first load increment where k_b equals 3684 kips/in^3 compared to k_b equals to 200 kips/inch^3 in the linear case solution presented in chapter 6. The size of the forces applied to steel is a function of the k_b value, thus for high k_b value, the effect of such irregularities is very clear on the solution of the reinforcement. The irregularity of the forces applied to steel is maximum at the element boundaries and thus its effect can be seen there. In the linear case where k_b is constant ($k_b=R_0=200$ kips/in^3), the loading of the steel produces a smooth stress pattern. In the nonlinear solution as the load is added the "slip"

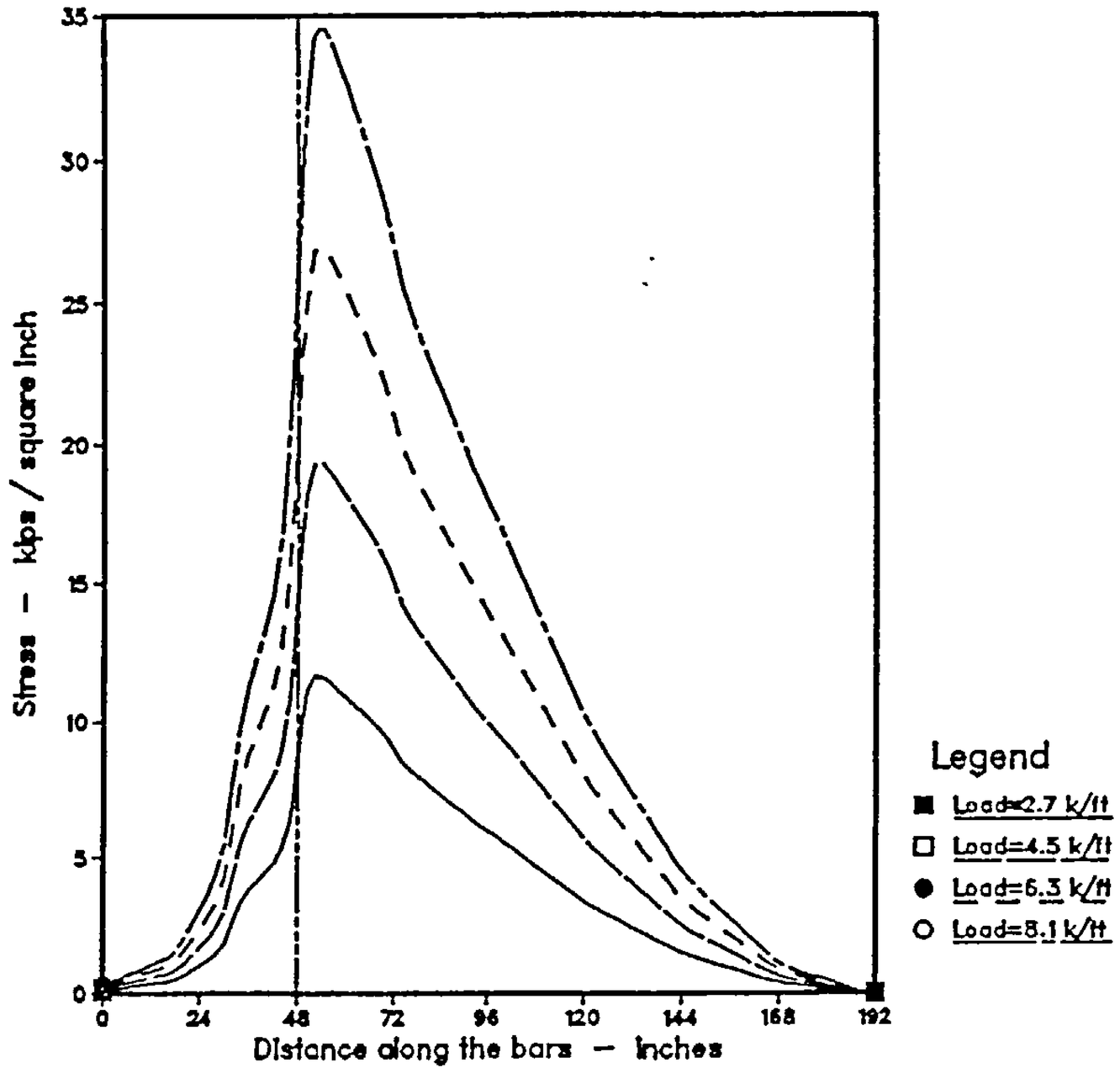

Figure (8.19) - Steel stress in full length bar.

Stress in curtailed bar of the cantilever

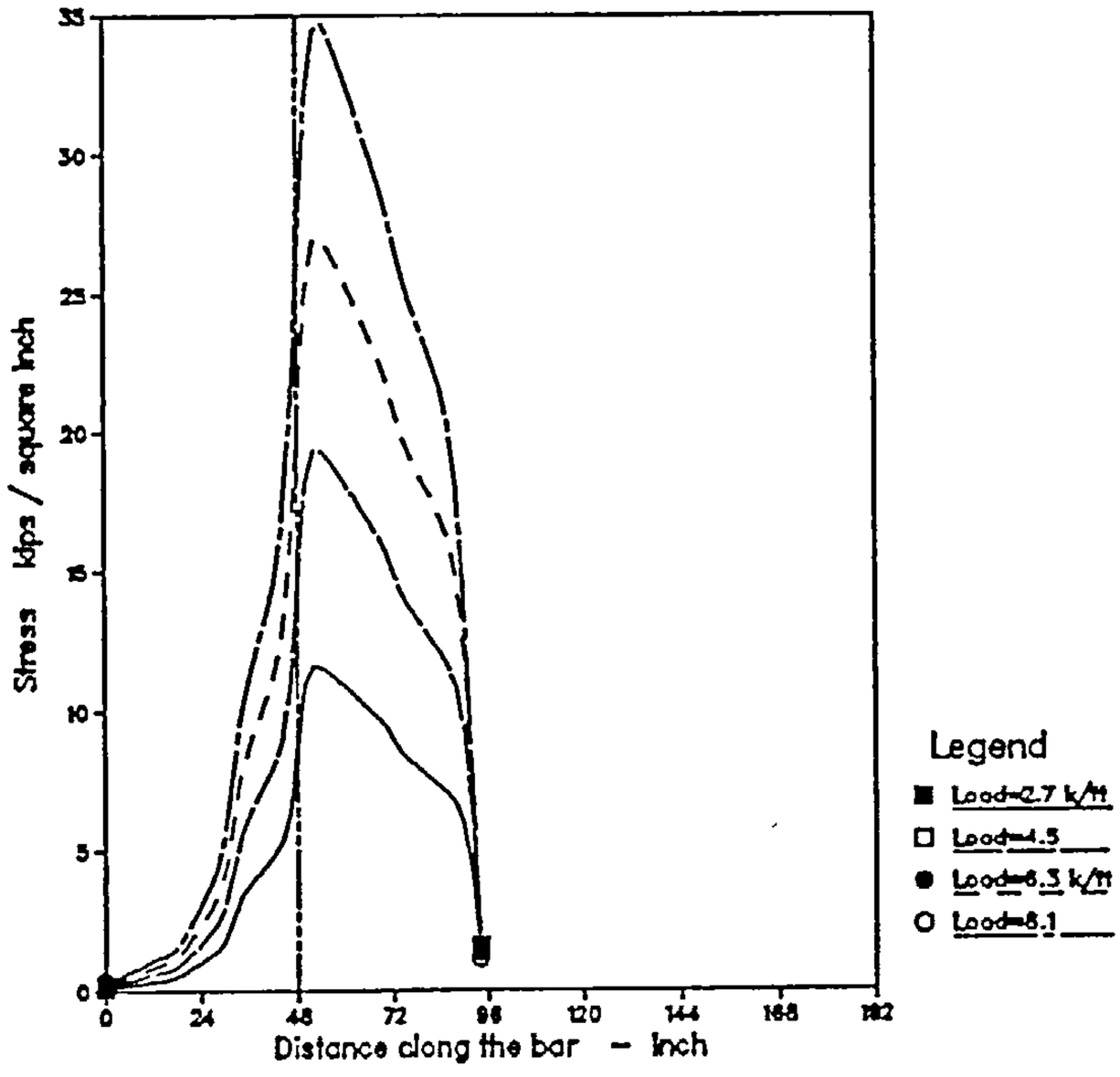

Figure (8.20) - Steel stress in the curtailed bar.

increases and so the value of the slope of the nonlinear bond stress slip curve becomes smaller and so does the value of k_b. Therefore, the irregularities in the reinforcement solution is removed as load increases and so the shape of the stress curve for the steel becomes smoother at high loads.

Figure (8.20) shows the stress in the curtailed bar for the same load increments as in figure (8.19).

Bond Stresses:

Figure (8.21) shows the bond stress for the full length bar. The results show that the bond starts to deteriorate as the last load increment is applied and occurs near the maximum stress in the tension reinforcement. A drop in the bond stress is observed at that area. This can be seen more clearly from the numerical values of the solution.

It was the purpose of the solution to obtain deterioration in bond at all steel nodes location as in the case of pull-out tests. But with the limitation imposed by the present modelling of concrete this was not possible.

Modelling of bond in the present work depends on the relative movement, or deformations, between reinforcement and the surrounding concrete. If a nonlinear stress strain relationship of concrete is considered as it should, then the concrete deformations especially at those locations where high stresses are carried by the concrete, will be different than in the case of linear analysis of concrete. Therefore the bond stresses are expected to be quite affected by nonlinear concrete analysis in

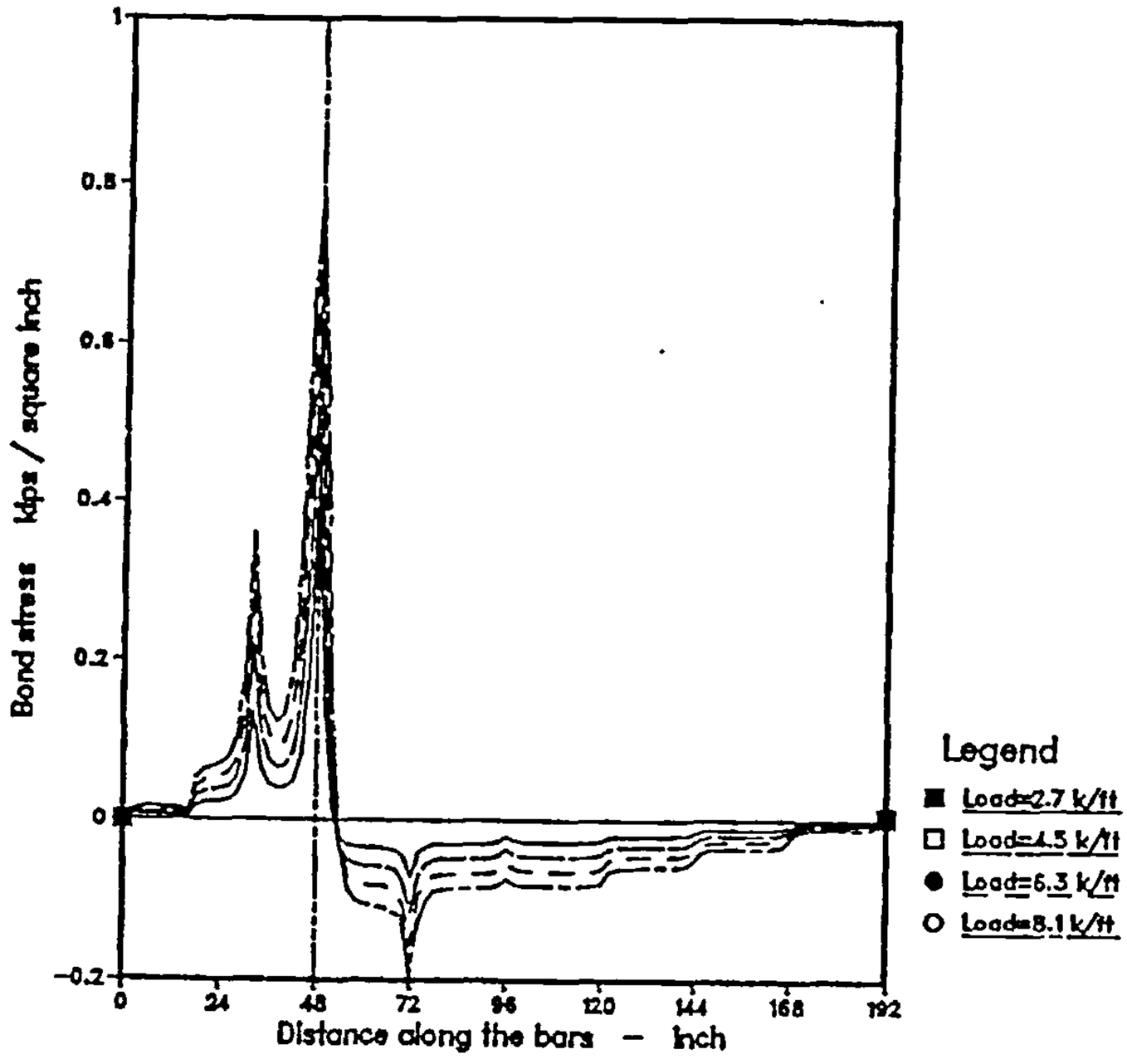

Figure (8.21) - Bond stress distribution along the full length bar.

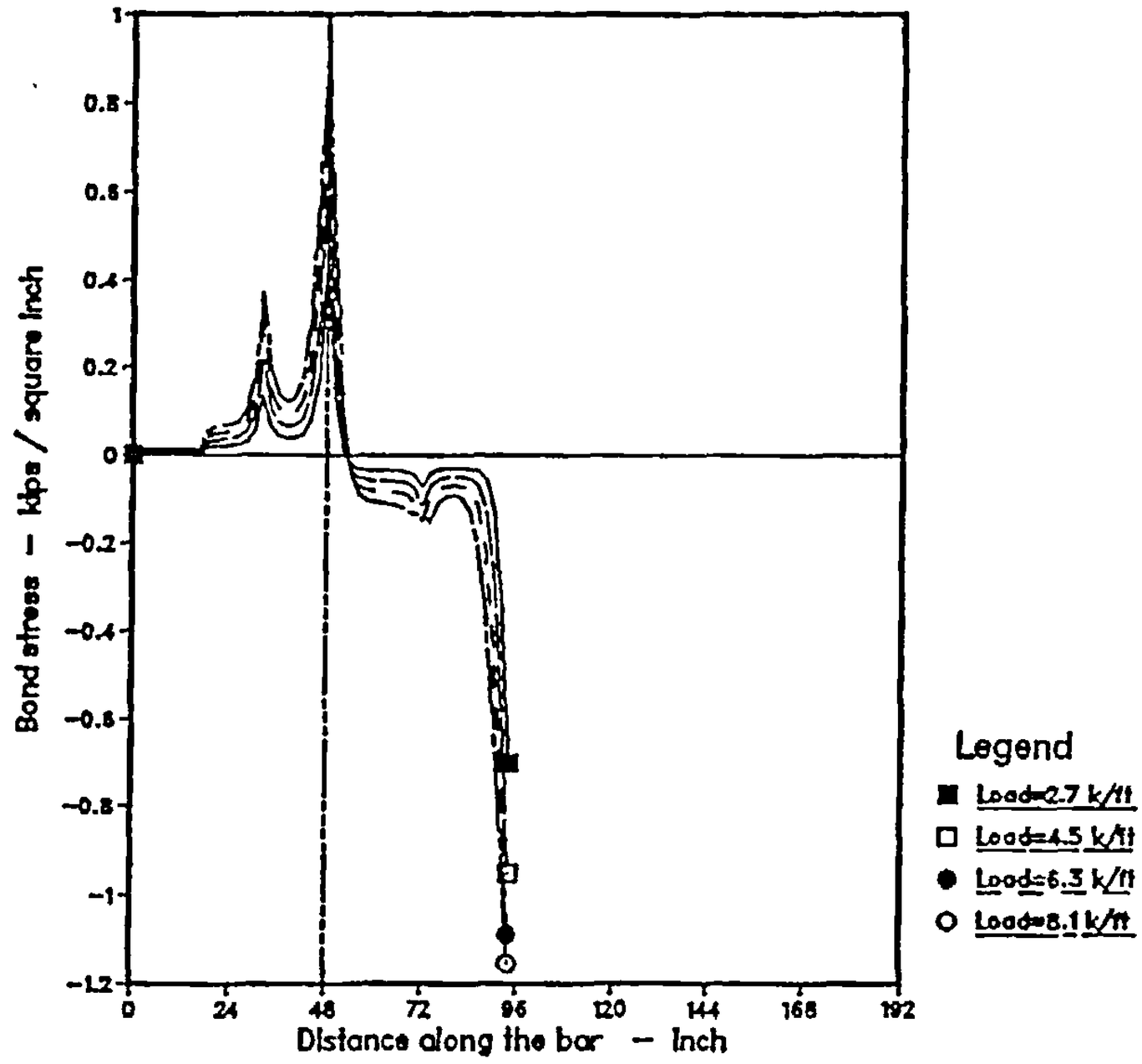

Figure (8.22) - Bond stress distribution along the curtailed bar.

this problem. The second thing to notice is that the nonlinear bond stress slip relationship depends on the ultimate bond stress calculated which in turn depends on the radial interface pressure developed between the concrete and the steel as expressed by equation (5.6) repeated here:

$$q_{ult} = q_0 + \mu \cdot (\sigma_{rconc} - \sigma_{rsteel})$$

Since there is no restriction imposed on the maximum stresses carried by the concrete or the steel, this will lead in some circumstances to the quantity $[\mu \cdot (\sigma_{rconc} - \sigma_{rsteel})]$ being negative and its absolute value greater than q_0 which will lead to incorrect calculation of the bond stresses. For the above reasons complete deterioration of bond could not be demonstrated.

This problem did not happen in pull-out test problems because the concrete stresses developed were not very high and the linear analysis of concrete seems to be quite adequate.
The irregularities in the bond stress curve are for the same reasons mentioned in the linear case analysis of the beam and the cantilever (chapter 6).

The bond stresses for the tension curtailed bar is shown in figure (8.22) and the same thing is noted about the curtailed bar as in the case of the full length bars except her deterioration of bond starts to take place at the free end of the bar.

Chapter 9

9. CONCLUSIONS

9.1 Objectives:

The objective of the work done in this research was as follows:

i) To develop a new method for modelling of bond and reinforcement in finite element analysis of reinforced concrete.

ii) To find an efficient method of solution for the resulting equations.

iii) To show the application of the method to some reinforced concrete structures.

iv) To extend the method so that it covers nonlinear bond behaviour.

v) To show application of the nonlinear bond model.

9.2 Achievements

A new method of representing the steel in finite element analyses of reinforced concrete structures was described in chapter 3 in which the concrete and the steel are analysed separately. Bond forces, calculated from bond stiffness and the relative displacement between reinforcement and the surrounding concrete, are used to transfer load between concrete and steel.

Two iterative methods of solution were studied thoroughly. An iterative method which converges extremely rapidly and which is much more efficient than direct solution especially in the

presence of very large number of steel nodes was adopted for the solution. Solution of the complete structure by the iterative method is achieved by deriving the interforces between the concrete and the steel and applying them in an iterative fashion. Solutions which are obtained for three practical reinforced concrete problems using linear stress/strain and bond/slip relationships in two dimensional analysis showed the following achievements of the method :

1) Concrete could be modelled quite separately from the steel. Finite element mesh of the concrete was designed solely to match the expected stress patterns in the concrete.

2) All reinforcement bars could be accurately and completely modelled regardless of their orientation and location with very little impact on the computer time needed for the solution.

3) Bond stiffness which must be represented in accurate modelling of reinforced concrete was included in the analysis and thus improved the overall modelling.

4) Thin concrete cover over reinforcement could be accommodated without influencing the finite element mesh representing the concrete.

5) Anchorage of bars could be easily modelled by two methods. Either by including a very high stiffness value or by applying an external force which is calculated based on a given development length.

6) Loads could be applied to either or both the concrete and the steel.

7) Detailed stress distributions computed for all bars ensured a more accurate modelling of bond and concrete behaviour.

The method was extended to accommodate a nonlinear bond model described by Allwood et al. (1984). Application of the nonlinear bond model to different pull-out test problems was compared to another solution using the same nonlinear bond model (i.e. the model by Allwood et al.) in conventional finite element analysis of reinforced concrete and where bond was represented by 6 noded shearing element. The method showed the following advantages:

1) Free end slip was much better predicted by the present model especially when using parameters to describe bond between deformed bars and the surrounding concrete.

2) Higher load needed to cause failure of bond was predicted by the present model which is nearer to experimental values.

3) Steel, bond and concrete stresses agree well with the earlier solution.

The following effects were studied : effect of bond stiffness value on main reinforcement showed higher loads are transferred between concrete and steel when higher bond stiffness value is used. Effect of mesh size and number of nodes showed no significant difference obtained in the solution of pull-out test.

Effect of the method of anchorage showed that anchorage can be equally done by the two methods mentioned earlier.

9.3 Difficulty and anticipated solutions

One common difficulty was faced in the solution of flexural problems and is the irregularities in the bond stress curves which coincides with the concrete element edges.

This was found to be due to the calculation of the concrete displacements at the bar level which are used along with the steel displacements to calculate the bond stresses. These concrete displacements at the bar level are obtained from the concrete nodes using the shape functions. The second differences of the concrete displacements at the bar level showed discrepancies at the boundaries of the concrete elements but smooth values from the boundaries. When calculating element stresses at points within an 8-noded element Hinton and Campbell (1974) showed that stresses derived from the shape functions were most accurate at the Gauss points and at their worst at the boundary edges and thus they recommended to interpolate through the Gauss point values. Therefore, the solution to this problem may be to use a similar smoothing process to improve the bond stresses calculated from the method presented in this thesis. The possibility of doing this needs further investigation.

It is noted that in this research concrete is modelled by 8 noded isoparametic quadralateral elements while steel is modelled by 2 noded bar elements. The error in compatability is reduced by dividing the steel into small segments because many steel nodes are usually used per concrete element (typically 7 to 10). Thus, there is only a little improvement in compatability to be gained using three noded bar elements for steel. This is expalined in section (3.4).

9.4 Recommendation for further work

The following extensions of the method presented in this research are recommended for further work :

1) Nonlinear behaviour of concrete must be included. This may be implemented in a similar manner to the nonlinear bond model.

2) Allowing for cracks to develop must be considered. This needs careful consideration since their existence could cause the left hand side, K_c , of the first equation in (equations 4.9) to become singular. Convergence of the method is expected to be much slower than in the linear solution. The matrix K_c is very flexible when extensive cracking takes place since stiffness of steel is not included in this matrix. Concrete deformations obtained in the first iteration in the linear solution were very high compared to the actual deformation in the concrete and so a damping factor was applied starting by the second iteration to reduce the concrete deformation nearer to the actual solution. In the

presence of cracks such deformations are expected to be much exaggerated and thus obtaining the final solution will need more iterations.

3) Extension to three-dimensional analysis should be considered. The potential of this method when applied to three dimensional reinforced concrete structures is substantial. The constraint imposed on the mesh of concrete elements by conventional methods of representing reinforcement steel is greater than for the two-dimensional problems discussed and the realistic inclusion of steel adds considerably to the cost of an analysis. The method described in this thesis will show real savings when analysing three dimensional problems.

5) Dowel action. The interforces have been calculated throughout this research by consideration of bond action only. Reinforcement also adds to the shear stiffness of concrete by dowel action. No extra degrees of freedom are necessary to include this effect, only the calculation of the interforces normal to the axis of a reinforcing bar generated by the shear distortion of the bar.

REFERENCES

REFERENCES

Abrams D. A. (1913) "Test of Bond between Concrete and Steel"., University of Illinois Bulletin. vol. XI, no.15, paper no. 71, 238 pp.

Ahmad S. H., Shah S. P. "Complete Triaxial Stress-Strain Curves for Concrete". ASCE, Journal of the Structural Division, vol. 108, no. ST4, April 82, pp 728-742.

Allwood R. J. (1980) "Reinforced Stresses in a reinforced concrete beam-column connection".Magazine of Concrete Research" vol. 32, No. 112. pp 143-146

Allwood R. J., Parsons S. D., Robins P. J. (1984) "New Bond Model for Reinforced Concrete". Proceedings of the International Conference on 'Computer-Aided Analysis and Design of Concrete Structures', Part 1. Split, Yugoslavia, 215-230.

Allwood R. J., Bajarwan A. A. (1989) "A New Method For Modelling Reinforcement And Bond In Finite Element Analyses Of Reinforced Concrete". Paper to be published in the International Journal For Numerical Methods In Engineering, vol. 28,

Bajarwan A. A. (1977) "Analysis of Continuous Plates by Finite Difference Method", M. Sc. Thesis, University of Petroleum and Minerals, Dhahran, 83pp.

Barots (1982) "Bond in Concrete", Proceedings of the International Conference on Bond in Concrete, Paisley College of Technology, Science Publishers, London, 466pp.

Bresler B., Bertero V. (1966) "Influence of Load History on Cracking in Reinforced Concrete"., Report to California Division of Highways, department of Civil Engineering, Division of Structural Engineering, University of California (Berkely), 20pp.

Balakarishnan S., Murray D. W. (1987) "Prediction of Response of Concrete Beams and Panels by Nonlinear Finite Element Analysis", Proceedings IABSE Colloquium Computational Mechanics of Concrete Structures, Delft Univ. Press, pp 393-404.

Chen A. C. T., Chen W (1975) "Constitutive Relations for Concrete". ASCE, Journal of the Engineering Mechanics Division, vol. 101, no. EM4, August 75, pp 465-481.

Clark A. P. (1946) "Comparative Bond Efficiency of Deformed Concrete Reinforcing Bars. Journal of the American Concrete Institute. Proceedings. vol. 46, no. 3, 161-184

Clark A. P. (1949) "Bond of Concrete Reinforcing bars"., Journal of the American Concrete Institute. Proceedings. vol.46, no.3, 161-184.

Dorr k., (1978) "Bond-Behaviour of Ribbed Reinforcement under Transversal Pressure". Proceedings of the International Association of Spatial Structures Symposium on Nonlinear Behaviour of Reinforced Concrete shell Structures. vol. 1, Dormstadt, Germany, July, 13-24.

Darwin D., Pecknold D. A. (1977) "Nonlinear Biaxial Stress-Strain Law for Concrete". ASCE, Journal of the Engineering Mechanics Division, vol. 103, no. EM2, April 77, pp 229-241.

Edwards A.D., Yannopoulos P.J., (1978) "Local Bond-Stress-Slip Relationships Under Repeated Loading". Magazine of Concrete Research, vol. 30, no. 103, 62-72.

Glanville, W. H. (1930) "Studies in Reinforced Concrete Bond Resistance", Building Research Technical Paper no. 10, Department of Scientific and Industrial Research, 37pp.

Hinton E., Scott F. C., Ricketts R. E. (1975) "Short Communications Local Least Squares Stress Smoothing for Parabolic Isoparametric Elements". International Journal for Numerical Methods in Engineering, vol. 9, no. 1, pp 235-238.

Hinton E., Campell J. S. (1974) "Local and Global Smoothing of Discontinuous Finite Element Functions Using A Least Squares Method". International Journal for Numerical Methods in Engineering, vol. 8, pp 461-480.

Houde J., Mirza M. (1972) "A Study of Bond Stress-Slip Relationship in Reinforced Concrete"., Structural Concrete Series No. 72-8 McGill University, Montreal.

Imbabi M. S., Cope R. J. (1984) "An Equivalent Elasto-Plastic Constitutive Model for Biaxially Loaded Concrete". Proceedings of the International Conference on Computer Aided Analysis and Design of Concrete Structures, Part 1, Yugoslavia 17-21, Sep. 84.

Kani G. N. J. (1969) "A Rational Theory for the function of Web Reinforcement". American Concrete institute. Proceedings. vol. 66 185-197.

Kupfer H. B., Gerstle K. H. (1973) "Behaviour of Concrete Under Biaxial Stresses". ASCE, Journal of the Engineering Mechanics Division, vol. 99, no. EM4, August 73, pp 853-865.

Labib F., Edwards A. D. (1978) "An analytical Investigation of Cracking in Concentric and Eccentric Reinforced Concrete Tension Members"., Proceedings of the Institution of Civil Engineers, Part 2, no. 65, 53-70.

Liu T. C., Nilson A. H., Slate F. O. (1972) "Biaxial Stress-Strain Relations for Concrete". ASCE, Journal of the Structural Division, vol. 98, no. ST5, May 72, pp 1025-1034.

Lutz L. A., Gergely P. (1967) "Mechanics of Bond and Slip of Deformed Bars in Concrete"., Journal of the American Concrete Institute, vol. 64, 711-721.

Lutz L. A. (1970) "Analysis of Stresses in Concrete Near a Reinforcing Bar Due to Bond and Transverse Cracking". Journal of The American Concrete Institute. Title No. 67-45, October 1970 pp 778-787.

Mains R. M. (1951) "Measurement of the Distribution of Tensile and Bond Stresses Along Reinforcing Bars", Proceedings, Journal of the American Concrete Institute, vol. 48, no. 3, 225-252.

Nilson A. H., (1972) "Internal Measurement of Bond Slip". Journal of the American Concrete Institute Proceedings. vol. 69, no.7, 439-654.

Nilson A. (1971) "Bond Stress-Slip Relation in Reinforced Concrete"., Report No. 345.

Nagatomo K., Kaku T. (1985) "Experimental and Analytical Study on Bond Characteristics of Reinforcing Bars With Only A Single Transverse Rib". Transactions of The Japan Concrete Institute, vol. 7. 333-340.

Ngo D., Scordelis A. C. (1967) "Finite Element Analysis of Reinforced Concrete Beams". Journal of the American Concrete Institute. Proceedings. vol. 64, no. 3, 152-163.

Nilson A. H. (1968) "Nonlinear Analysis of Reinforced Concrete by Finite Element Method". Proceedings. Journal of the American Concrete Institute, vol. 65, pp 757-766.

Phillips D. V., Zienkiewicz O. C. (1976) "Finite Element Non-Linear Analysis of Concrete Structures". Proceedings. Institution of Civil Engineers, Part 2, 1976, vol. 61, pp 59-88

Parsons S. D. (1984) "Representation of Bond in Finite Element Analysis of Reinforced Concrete Structures", Ph. D. Thesis, Loughborough University of Technology, 310pp.

Popvics S. (1970) "A Review of Stress-Strain Relationship for Concrete". Journal of the American Concrete Institute, vol. 67 pp 243-248

Peattie K. R., Pope J. A. (1956) "Effect of Age Of Concrete on Bond Resistance. Journal of the American Concrete Institute. Proceedings. vol. 27, 661-672.

Perry E.S., Thompson J.N. (1966) "Bond Stress Distribution in Reinforcing Steel in Beams And Pull Out Specimens" Journal of The American Concrete Institute. Proceedings. vol.63, no. 8, 865-875.

Parland H (1957) "Inelasticity of Bond between Steel and Concrete and distribution of stress in Steel and Concrete and Uncracked Structural Members. RILEM Symposium in Bond and Crack Formulation in Reinforced Concrete. Stockholm. vol.2, 307-316.

Regan P. E., Khan M. H. (1974). "Bent-Up Bars As Shear Reinforcement"., Shear in Reinforced Concrete, vol. 1, ACI Publication, SP 42-11, 249-265.

Robins P. J. (1971) " Reinforced Concrete Deep Beams Studied Experimentally and by the Finite Element Method"., Ph. D. Thesis. University of Nottingham.

Robins P. J., Standish I. G. (1982) "Effect of Lateral Pressure on Bond of Reinforcing Bars in Concrete". Proceedings of the International Conference on Bond in Concrete. Paisley, June 86, pp 262-271.

Ruhnau J. (1974) "Influence Of Repeated Loading On The Stirrup Stress Of Reinforced Concrete Beams"., Shear in Reinforced Concrete, vol. 1, ACI Publication, SP 42-7, 169-181.

Reinhardt H. W., Blaauwendraad J., Vos E. (1984) "Prediction of Bond Between Steel and Concrete by NUmerical Analysis", Material Construction Material Structure", vol. 17, no. 100, July-August 84, pp 311-320.

Scordelis D., Ngo D., Franklin H. A. (1974)."Finite Element Study Of Reinforced Concrete Beams With Diagonal Tension Cracks". Shear in Reinforced Concrete, vol. 1, aci Publication SP-42, pp 79-102.

Saenz L. P. (1964) "Discussion of Equation for the stress-strain Curve of Concrete by Desayi P. and Krishman S." Journal of the American Concrete Institute. Proceedings. vol.61. no.9, 1229-1235.

Standish I. G. (1982) "The Effect of Lateral Pressure on Anchorage Bond in Lightweight Aggregate Concrete. Ph. D. Thesis. Loughborough University of Technology. 256pp.

Spencer R. A., Panda A. K., Mindess S. (1982) "Bond of Deformed Bars in Plain Fibre Reinforced Concrete under Reversed Cyclic Loading. International Journal of Cement Composites and Lightweight Concrete"., vol.4, no.1, 3-16.

Tanner J. A. (1971) "An Experimental Determination of Bond Slip in reinforced Concrete. M.S. Dissertation. Cornell University, Ithaca.

Tassios T. P., Yannopoulos P.J. (1981) "Studies of Concrete Members under Cyclic Loading"., Journal of the American Concrete Institute. Proceedings. vol.78, no.3, 206-216.

Untrauer R. E., Henry R. L. (1965) "Influence of Normal Pressure on Bond Strength"., Journal of the American Concrete Institute. Proceedings. vol.62, no.5, 577-585.

Wang C. and Salmon C. G. (1985) "Reinforced Concrete Design", Harper & Row, New York,

Wahla H. I. (1970) "Direct Measurement of Bond Slip in Reinforced Concrete"., Ph. D. Thesis, Cornell University.

Wilkins R. J. (1951) "Some Experiments on the Load Distribution in Bond Tests"., Magazine of Concrete Research", vol.2, no.5, 65-72.

Yankelevesky D. (1985) "New Finite Element For Bond-Slip Analysis", ASCE, Journal of the Structural Engineering, vol. 111, no. 7, July 85 pp 1533-1542.

Zienkiewicz O. C. (1985) "The Finite Element Method", Third Edition, McGraw-Hill, London, 787pp.

BIBLIOGRAPHY

Bresler B., Scordelis A. C. (1974) "Shear Strength of REinforced Concrete Beams". Journal of the American Institute. Proceedings. vol.60, 51-73.

Buyukozturk, O. (1975) "Nonlinear Analysis of reinforced Concrete Structures".Computers & Structures Vol. 7 pp 149-156.

Bedard C., Kotsovos M. D. (1986) "Fracture Processes of Concrete for NLFEA Methods". ASCE, Journal of Structural Engineering, vol. 112, no. 3, March 86, pp 573-587.

Bashur F. K., Darwin D. (1978) "Nonlinear Model for Reinforced Concrete Slabs", ASCE, Journal of the Structural Division, vol. 104, no. ST1, 157-170.

Broms B. B. (1965) "Stress Distribution in Reinforced Concrete Members with Tension Cracks"., Journal of the American Concrete Institute, vol. 62, 1095-1111.

Burden R., Faires D., Reynolds A. (1981) "Numerical Analysis"., Prindle, Weber & Schmidt.

Chen W. F., Suzuki H. (1980) "Constitutive Models for Concrete". Computers and Structures vol. 12, pp 23-32.

Cope R. J., Vasudeva R. (1977) "Non-Linear Finite Element Analysis of Concrete Slab Structure". Proceedings. Institution of Civil Engineers, Part 2, 1977, 63, pp 159-179.

Domingo J., Carreira, Kuang-Han Chu (1986) "Stress-Strain Relationship for Reinforced Concrete in Tension". Journal of The American Concrete Institute, January-February 86. no.1 v.83.

Goto Y. (1971) "Cracks Formed in Concrete Around Deformed Tension Bars", Proceedings, Journal of the American Concrete Institute", vol. 68, no. 4, pp 244-251.

Ingraffea A. R., Gerstle W. H., Gergely P., Saouma V. (1984) "Fracture Mechanics of Bond in Reinforced Concrete". ASCE, Journal of Structural Engineering, vol. 110, no. 4, April 1984, pp 871-890.

Jennings, A. (1977) "Matrix Computation for Engineers snd Scientists", John Wiley & Sons.

Kabila A. and Authers, (1964) "Equations for the Stress-Strain Curve of Concrete". Journal of the American Concrete Institute, vol. 61 pp 1227-1239.

Kemp E. L. (1986) "Bond in Reinforced Concrete: Behaviour and Design Criteria". Proceedings, Journal of the American Concrete Institute, vol. 83, no. 1, January-February 86, pp 50-57.

Klink S. (1985) "Actual Poisson Ratio of Concrete", Proceedings, Journal of the American Concrete Institute, vol. 82, pp 813-817.

Kupfer H., Hilsdorf H. K. (1969) "Behavior of Concrete Under Biaxial Stresses", Journal of the American Concrete Institute, vol. 66, August 1969, 656-666.

Leibengood L. D., Darwin D., Dodds R. H. (1986) "Parameters Affecting FE Analysis of Concrete Structures". ASCE, Journal of Structural Engineering, vol. 112, no. 2, February 86, pp 326-341.

Morimoto H., and Others (1984) "Local Bond-Slip Behaviour Under Splitting Bond-Shear Failure Of R. C. Columns". Transactions of the Japan Concrete Institute, vol. 6, pp 469-476.

Smith I. M. (1982) "Programming the Finite Element Method", John Wiley, 351pp.

Stricklin J. A., Haisler W. E. (1977) "Formulations and Solution Procedures for Nonlinear Structural Analysis"., Computers and Structures, vol.7, pp. 125-136.

Suidan M., Schnobrich W. (1973) "Finite Element Analysis of Reinforced Concrete"., ASCE, Journal of the Structural Division, vol. 99, no. ST10. 2109-2122.

Scorensen H. C. (1974) "Efficiency of Bent-Up Bars as Shear Reinforcement"., Shear in Reinforced Concrete, vol. 1, ACI Publications, SP 42-11, 267-283.

Takahashi Y., Kakuta Y., Magishi T. (1985) "Effect of Transverse Reinforcement on the Bond Strength of Deformed Bars". Transactions of the Japan Concrete Institute, vol. 7, pp 341-346.

Ueda T., Lin I., Hawkins N. M. (1984) "Beam Bar Anchorage in Exterior Column-Beam Connections". Journal of the American Concrete Institute, vol. 83, no. 3, pp 412-422.

Weaver W. & Johnson P. (1984) "Finite Element for Structural Analysis"., Prentice-Hall, Inc., New Jersey.

Appendices

A. COMPUTER PROGRAM

A.1 General

Development of the computer program formed a major part of this research. The purpose was to construct an efficient computer program which represents the practical implementation of the new method discussed in chapter 3. The computer program was constructed based on the iterative method of solution presented in chapter 4 and then it was extended to accommodate the nonlinear method discussed in chapter 7. The program is written in Fortran IV language and is developed on the Honeywell Multics System. The finite element analysis is based on the displacement type of finite element formulation.

The computer program is built by the author to accommodate the method of solutions as explained above. The program gets advantage of the NAG (Natural Algorithm Group) finite element library subroutines which is available on the Honeywell Multics System at Loughborough University of Technology in the following parts of the program :

1) Constructing the stiffness matrix for concrete elements.

2) Assembling the global concrete stiffness matrix, K_c.

3) Reduction of the concrete global stiffness matrix, K_c, and the global matrix $[K_s+K_b]$ using Choleski's Method.

4) The back-substitution in the reduced form of the above two matrices.

A.2 Some highlights on the computer program

The following points are explained about the program :

1) Banded form of matrices

All stiffness matrices are assembled in the banded form. This includes $[K_c]$ and $[K_s+K_b]$.

The band width of the global stiffness matrix of concrete, $[K_c]$, depends on the efficiency of the numbering scheme of the nodes of the concrete elements.

However, $[K_s+K_b]$ matrix has a special form of being always a tridiagonal matrix. In the program the half band width of $[K_s+K_b]$ which is always equal to two is formed directly without the conventional method of assembly.

2) Reduction of matrices

In the program the above matrices are reduced into lower triangular matrices using Choleski's method before the iteration solution starts. Time needed for the reduction of $[K_s+K_b]$ is trivial because of its simple form.

3) Back substitution

In the iterative solution forward and backward substitution are performed on the reduced forms to produce concrete and reinforcement solutions.

4) Reinforcement nodes numbering

Among other informations entered in the input data about every reinforcement bar is the number of bar elements into which the reinforcement bar is to be divided and the coordinates of the first and the last nodes in the bar. The program then divides every reinforcement bar into a number of steel nodes, assign a global number for every node, obtain the global coordinates for the nodes and calculated the angle of inclination of the bar. The node numbering continues in sequential order for all steel nodes of all bars.

5) Local coordinates

The information of every reinforcement bar contains the number of concrete element which the bar passes through. This adds one step to the efficiency of the program because it is faster to identify the concrete elements in which every steel node lies and thus calculating the local coordinates of steel nodes.

Another step in this regard is to specify if the concrete elements edges are parallel to the global coordinates axis or if they are inclined. This also adds to the efficiency of the program because the number of calculation involved in obtaining the local coordinates of steel nodes within an inclined concrete elements is much more than if the concrete elements edges are parallel to the global axis.

6) Conditions of steel nodes

Steel nodes can be free, anchored or restrained. If a steel node to be anchored or restrained then this is indicated in the input data.

The information for nodes to be anchored by applying an external force contains: global node number, bar diameter and initial anchorage length.

For restrained nodes only global node number is required.

7) Loading

Loading can be applied to concrete and/or to steel. If load is applied to concrete then load size and the associated concrete degree of freedom is specified. If steel is loaded then load size and the associated steel node number is specified.

8) Units

Units can be either in imperial or in SI. Units have to be consistent as follows:

SI units

Stress in N/mm^2

Load in N

Length in mm

Initial bond stiffness N/mm^3

Imperial units:

Stress in lb/in^2

Load in lb

Length in inch

Initial bond stiffness in lb/in^3.

The unit type is specified in the nonlinear solution so that the appropriate value for Δu and q_0 is selected.

9) Scratch tapes

To reduce the memory storage needed for the large number of matrices needed in the solution some of the matrices are left as element related matrices and are written on a scratch tape. The information contained are read again whenever needed.

A.3 Calculations of concrete and steel stresses

Calculations of the concrete stresses at the concrete element nodes and at the steel nodes are done as follows

Concrete stresses at element nodes

The stress at the concrete element nodes are obtained from the four quadrature points for all concrete element using Least square smoothing method discussed in chapter 7. Once this is done for all concrete elements then the average values at the nodes are obtained by knowing the number of the concrete elements which the concrete node shares. The program takes care of that.

Steel stress

Axial stress in steel at the nodes is simply calculated from axial steel displacements by finite difference method. Central, Forward and Backward differences are used as needed e.g. Bajarwan (1977).

A.4 Testing the program

As part of the testing of the computer program the following problem was solved. The beam problem shown in figure (A.1a) was solved twice once being in the normal position as shown in figure (A.1a) and another time by rotating the whole problem an angle φ to the global coordinates as shown in figure (A.1b).

The solution obtained for the two problems is exactly the same. Concrete stress and displacements are transformed in the horizontal plane using the angle of inclination φ to make comparison possible. Steel displacements and stress are compared directly since they are given along the bar axis.

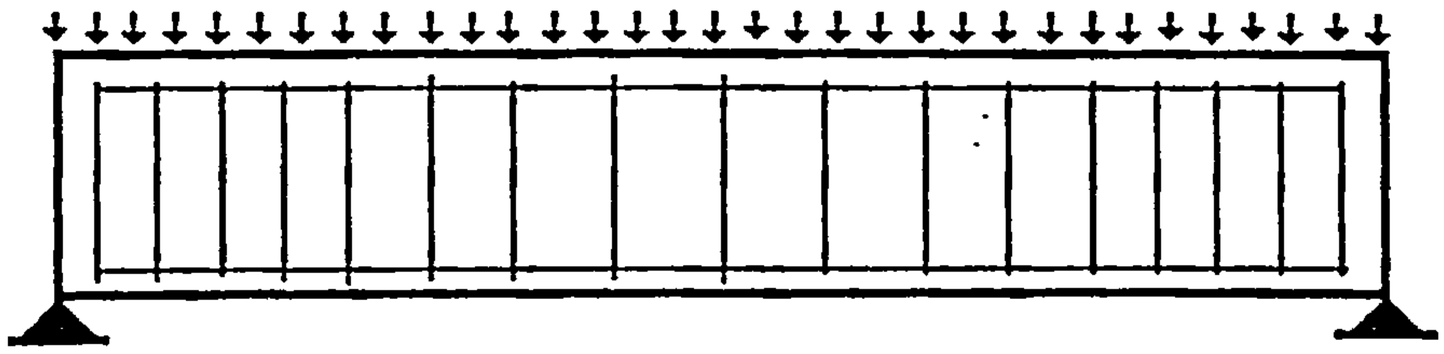

(a) - Normal position

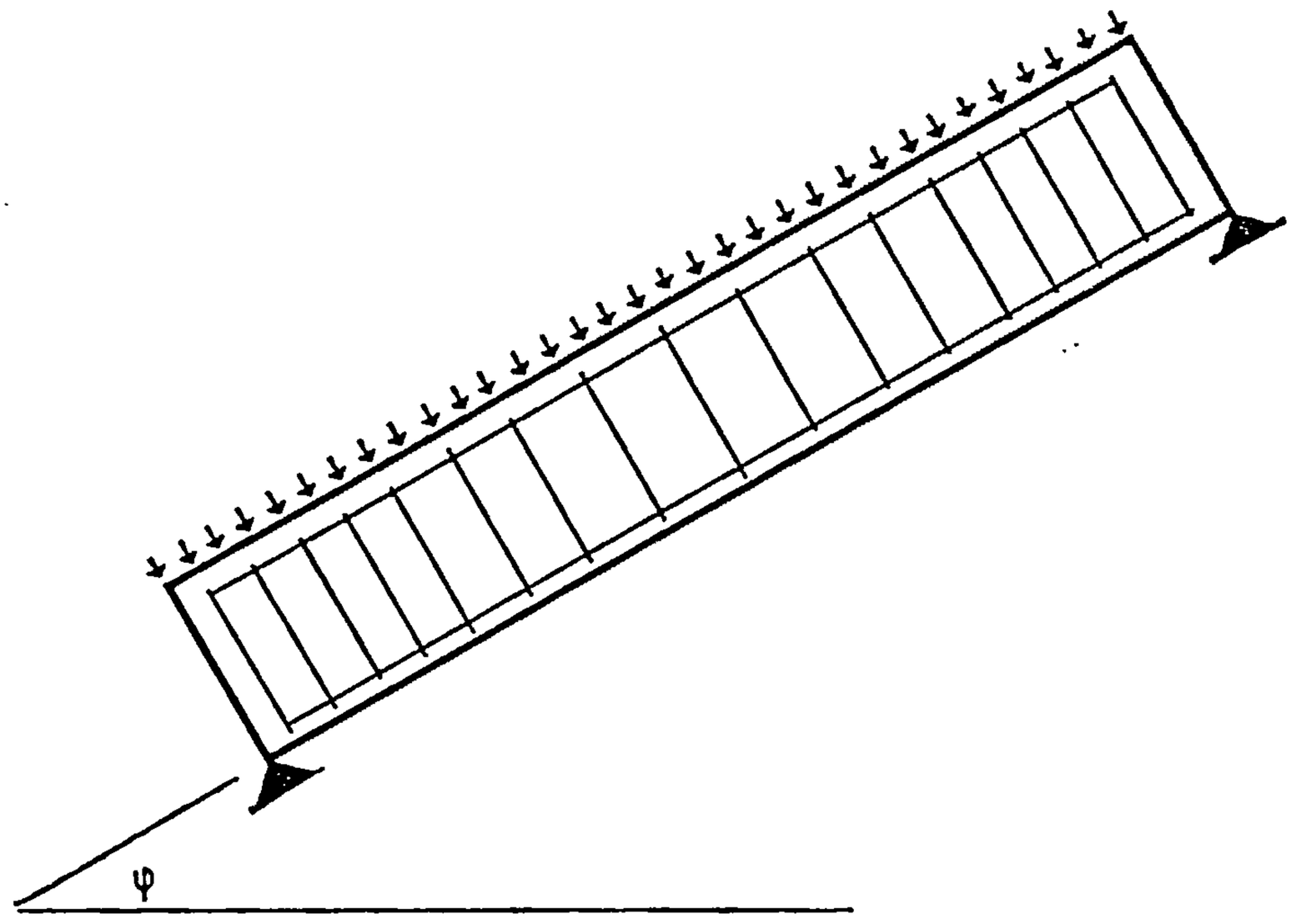

(b) - Inclined position

Figure (A.1) - Beam used for testing the program.

B. OUTPUT OF THE PROGRAM

The program output consist of two parts. First it feeds back the input data and then the solution.

The solution given contains detailed solution at every steel node which includes node coordinates, displacement, stress in steel, bond stress etc.

Examples of computer output is given in the next three figures. Figure (B.1) shows part of the output feeding back the input data for steel in the linear analysis of the cantilever. Figure (B.2) shows part of the output showing the solution for the same problem. Figure (B.3) shows part of the output for the nonlinear case solution.

INPUT DATA FOR REINFORECEMENT

NO. OF GROUPS OF STEEL BARS = 29
Es = 0.290000D+05 Kb = 0.200000D+03

gr. no.	no. Bars	Dia./Bar	no. Segts	X(first)	Y(first)	X(last)	Y(last)	no. Elem	Concrete Elements Along the Bar
1	2	1.0000	96	0.000	120.000	192.000	120.000	9	5 15 25 31 33 35 37 39 41
2	1	1.0000	47	0.000	120.000	94.000	120.000	5	5 15 25 31 33
3	2	0.3750	22	50.000	102.000	180.000	102.000	6	32 34 36 38 40 42
4	2	0.3750	4	50.000	101.438	50.000	120.875	2	32 31
5	2	0.3750	4	60.000	101.438	60.000	120.875	2	32 31
6	2	0.3750	4	70.000	101.438	70.000	120.875	2	32 31
7	2	0.3750	4	80.000	101.438	80.000	120.875	2	34 33
8	2	0.3750	4	90.000	101.438	90.000	120.875	2	34 33
9	2	0.3750	4	100.000	101.438	100.000	120.875	2	36 35
10	2	0.3750	4	110.000	101.438	110.000	120.875	2	36 35
11	2	0.3750	4	120.000	101.438	120.000	120.875	2	36 35
12	2	0.3750	4	130.000	101.438	130.000	120.875	2	38 37
13	2	0.3750	4	140.000	101.438	140.000	120.875	2	38 37
14	2	0.3750	4	150.000	101.438	150.000	120.875	2	40 39
15	2	0.3750	4	160.000	101.438	160.000	120.875	2	40 39
16	2	0.3750	4	170.000	101.438	170.000	120.875	2	42 41
17	2	0.3750	4	180.000	101.438	180.000	120.875	2	42 41
18	2	1.0000	30	2.500	0.000	2.500	232.000	10	10 9 8 7 6 5 4 3 2 1
19	2	1.0000	30	45.500	0.000	45.500	232.000	10	30 29 28 27 26 25 24 23 22 21
20	2	0.3750	4	1.625	8.000	46.375	8.000	3	10 20 30
21	2	0.3750	4	1.625	32.000	46.375	32.000	3	9 19 29
22	2	0.3750	4	1.625	56.000	46.375	56.000	3	9 19 29
23	2	0.3750	4	1.625	80.000	46.375	80.000	3	7 17 27
24	2	0.3750	4	1.625	104.000	46.375	104.000	3	6 16 26
25	2	0.3750	4	1.625	128.000	46.375	128.000	3	4 14 24
26	2	0.3750	4	1.625	152.000	46.375	152.000	3	3 13 23
27	2	0.3750	4	1.625	176.000	46.375	176.000	3	2 12 22
28	2	0.3750	4	1.625	200.000	46.375	200.000	3	2 12 22
29	2	0.3750	4	1.625	224.000	46.375	224.000	3	1 11 21

anchorage input (node no., bar dia, anchorage length)
1 2.000 12.000
58 1.000 12.000

Figure (B.1) - Part of the output feeding back the input data.

Problem Title :
Linear Solution to the Cantilever Problem(42 concrete elements,33 steel groups)

The Average of the Absolute Values of all degrees of freedom is:

Iter.	Conc. Displ.	Steel Displ.	Fbs(stress)	Fbc(Force)	Tolerence
1	0.32963D-01	0.37872D-01	0.24829D-01	0.00000D+00	0.10000D+01
2	0.29442D-01	0.34087D-01	0.21013D-01	0.40141D+00	0.12507D+00
3	0.29969D-01	0.34253D-01	0.21247D-01	0.34295D+00	0.69656D-02
4	0.29933D-01	0.34238D-01	0.21227D-01	0.34594D+00	0.59983D-03
5	0.29936D-01	0.34238D-01	0.21228D-01	0.34562D+00	0.39596D-04

The value of alpha = 0.90351

Reinforecement Solution

Output for Anchorage : (node no., dif(Ds-Dc), anchorage length)

1	0.765223D-08	10.86528
98	0.765227D-08	10.86529

BAR	NODE		X-COORD	Y-COORD	DISPLACEMENT	BAR-STRESS	BOND-STRESS	Kb	ds-dc
1	1	1	0.00000D+00	0.12000D+03	0.16852D-02	0.26279D+00	0.15304D-05	0.20000D+03	0.76522D-08
1	2	2	0.20000D+01	0.12000D+03	0.17038D-02	0.27649D+00	0.17125D-02	0.20000D+03	0.85623D-05
1	3	3	0.40000D+01	0.12000D+03	0.17233D-02	0.29577D+00	0.31061D-02	0.20000D+03	0.15531D-04
1	4	4	0.60000D+01	0.12000D+03	0.17446D-02	0.32554D+00	0.43363D-02	0.20000D+03	0.21682D-04
1	5	5	0.80000D+01	0.12000D+03	0.17682D-02	0.36504D+00	0.55388D-02	0.20000D+03	0.27694D-04
1	6	6	0.10000D+02	0.12000D+03	0.17949D-02	0.41458D+00	0.68463D-02	0.20000D+03	0.34231D-04
1	7	7	0.12000D+02	0.12000D+03	0.18254D-02	0.47558D+00	0.84029D-02	0.20000D+03	0.42015D-04
1	8	8	0.14000D+02	0.12000D+03	0.18605D-02	0.55071D+00	0.10381D-01	0.20000D+03	0.51903D-04
1	9	9	0.16000D+02	0.12000D+03	0.19014D-02	0.64422D+00	0.12998D-01	0.20000D+03	0.64988D-04
1	10	10	0.18000D+02	0.12000D+03	0.19494D-02	0.76614D+00	0.17481D-01	0.20000D+03	0.87403D-04
1	11	11	0.20000D+02	0.12000D+03	0.20071D-02	0.92226D+00	0.21552D-01	0.20000D+03	0.10776D-03
1	12	12	0.22000D+02	0.12000D+03	0.20766D-02	0.11111D+01	0.25659D-01	0.20000D+03	0.12830D-03
1	13	13	0.24000D+02	0.12000D+03	0.21603D-02	0.13348D+01	0.30257D-01	0.20000D+03	0.15129D-03
1	14	14	0.26000D+02	0.12000D+03	0.22607D-02	0.15992D+01	0.35853D-01	0.20000D+03	0.17927D-03
1	15	15	0.28000D+02	0.12000D+03	0.23809D-02	0.19149D+01	0.43064D-01	0.20000D+03	0.21532D-03

Figure (B.2) - Example of output solution for the linear case.

Problem Title :
Pull-Out Test (150mm cube) Using 16mm plain bar.

Load increment number 1
Load increment applied = 0.1000 of the total load
Total load applied so far = 0.1000 of the total load

The Average of the Absolute Values of all degrees of freedom is:

Iter.	Conc. Displ.	Steel Displ.	Fbc(Force)	Tolerence
1	0.616730-04	0.151100-02	0.149670+02	0.100000+01
2	0.608480-04	0.150900-02	0.148940+02	0.175340-01
3	0.608730-04	0.150900-02	0.148940+02	0.433680-03
4	0.608730-04	0.150900-02	0.148940+02	0.166090-04
5	0.340210-05	0.174330-03	0.194740+01	0.100000+01
6	0.328370-05	0.174180-03	0.194450+01	0.296330-01
7	0.328720-05	0.174190-03	0.194450+01	0.113550-02
8	0.328710-05	0.174190-03	0.194450+01	0.421920-04
9	0.590690-06	0.386260-04	0.440130+00	0.100000+01
10	0.567740-06	0.385970-04	0.439680+00	0.329500-01
11	0.568470-06	0.385980-04	0.439690+00	0.124710-02
12	0.568450-06	0.385980-04	0.439690+00	0.464760-04

Iter.	q(actual)	q(nonlinear)	q(ultimate)	Max(qa-qn)/
1	0.268500+00	0.233900+00	0.195600+01	0.287450+0
2	0.267190+00	0.259600+00	0.195340+01	0.399620-0
3	0.267060+00	0.265320+00	0.195300+01	0.828620-0

BAR	NODE		X-COORD	Y-COORD	DISPLACEMENT	BAR-STRESS	BOND-STRESS	Kb	ds-dc	Qultimate
1	1	1	0.750000+02	0.000000+00	0.910400-03	-0.779800-04	0.131930+00	0.179190+03	0.696870-03	0.198150+01
1	2	2	0.750000+02	0.500000+01	0.912470-03	0.165600+00	0.132050+00	0.179170+03	0.697550-03	0.198170+01
1	3	3	0.750000+02	0.100000+02	0.918680-03	0.331870+00	0.133000+00	0.179030+03	0.702850-03	0.198300+01
1	4	4	0.750000+02	0.150000+02	0.929060-03	0.499960+00	0.134780+00	0.178760+03	0.712780-03	0.198530+01
1	5	5	0.750000+02	0.200000+02	0.943670-03	0.670610+00	0.137390+00	0.178360+03	0.727410-03	0.198850+01
1	6	6	0.750000+02	0.250000+02	0.962590-03	0.845180+00	0.140850+00	0.177840+03	0.746810-03	0.198260+01
1	7	7	0.750700+02	0.300000+02	0.985930-03	0.102460+01	0.145160+00	0.177180+03	0.771110-03	0.198270+01

Figure (B.3) - Example of output solution for the nonlinear case.